MICROCOPY RESOLUTION TEST CHART
NATIONAL BUREAU OF STANDARDS-1963-A

THE APPLICATION OF A SUPERCONDUCTING
QUANTUM INTERFERENCE DEVICE SECOND-ORDER
GRADIOMETER TO MEASURE VISUAL EVOKED
RESPONSES

THESIS

AFIT/GE/EE/83D-50

ROBERT D. MURRAY
CAPT.   USAF

DTIC

MAR 1   1984

A

DEPARTMENT OF THE AIR FORCE

AIR UNIVERSITY (ATC)

AIR FORCE INSTITUTE OF TECHNOLOGY

Wright-Patterson Air Force Base, Ohio

84 02 29 052

AFIT/GE/EE/83D-50

THE APPLICATION OF A SUPERCONDUCTING
QUANTUM INTERFERENCE DEVICE SECOND-ORDER
GRADIOMETER TO MEASURE VISUAL EVOKED
RESPONSES

THESIS

AFIT/GE/EE/83D-50

ROBERT D. MURRAY
CAPT.   USAF

i

AFIT/GE/EE/83D-50

THE APPLICATION OF A SUPERCONDUCTING QUANTUM INTERFERENCE

DEVICE SECOND-ORDER GRADIOMETER TO MEASURE VISUAL

EVOKED RESPONSES

THESIS

Presented to the Faculty of the School of Engineering

of the Air Force Institute of Technology,

Air University

in Partial Fulfillment of the

Requirements for the Degree of

Master of Science in Electrical Engineering

by

ROBERT D. MURRAY

CAPT.   USAF

Graduates Electrical Engineering

December 1983

A-1

ii

PREFACE

For many years, I have been fascinated with the profound, yet mysterious capabilities of the brain. This marvelous mass of tissue is able to perform complicated tasks involving the combination of sight, touch, hearing, taste, and smelling, while automatically performing life sustaining functions. Although, these tasks are often complex, many of them can be performed by young children. Yet, how the brain is able to perform these tasks is still much of a mystery.

For many years, researchers in the area of brain and central nervous system research, have used two methods to attempt to unlock the mysteries of the brain. The first method was the use of a standard electroenphalographic (EEG) machine, using scalp electrodes, to measure the gross electrical activity of the brain as measured on the surface of the scalp. The second method used to gain some insights into the operation of the brain was the meticulous, and painstaking measurements of the responses of individuals brain cells to specific sensory stimulus, via the use of microelectrodes, a extremely slender glass or metal electrodes which are inserted into the individual cells.

It was late in the 1960's before advancements in cryogenics, and in the technology of superconducting semiconductors devices, brought about a new, and powerful tool to be used in the quest for understanding of the brain. This powerful tool is the Superconducting Quantum Interference Device (SQUID) Gradiometer. This device allows us for the first time to measure extremely small magnetic field, as those

iii

bioengineering classes motivated me to quest further knowledge in these areas. Also, I would like to thank him for support, and encouragement in my thesis effort.

Another special thanks goes to my thesis advisor, Dr. Charles P. Hatsell for his expert support, guidance, and technical advice. His expert knowledge in the areas of engineering and medicine, and his high degree of professionalism, sets a high standard for a researcher to follow.

Finally, I would like to express my sincere, and equally important gratitude to my wife, Sherry Murray, and our sons, Robert D. Jr., and John N. Murray, for their patience and understanding during the long work hours, both at home and away from home.

Robert D. Murray

TABLE of CONTENTS

CONTENTS

List of Figures

List of Figures

(Continued)

List of Tables

x

List of Equations

ABSTRACT

The acquisition of a Superconducting Quantum Interference Device (SQUID) gradiometer, by the Air Force Aerospace Medical Research Laboratory, along with the previous research conducted at the Air Force Institute of Technology which led to the first cortical implant of a multiplexed multi-electrode semiconductor brain electrode, motivated the use of the SQUID second-order gradiometer to measure visual evoked responses (VER) from humans, and from the canine which had previously had the AFIT brain electrode implanted and removed. Some discussion of the current dipole model for the fields measured from the brain is presented. The human visual evoked responses picked up by gradiometer were compared to previous human electroencephalograph visual evoked responses, and were found to have similar latencies. The canine visual evoked responses which were measured by the gradiometer had similar initial waveform and latencies, but then dampen out more rapidly than the waveforms measured by the AFIT brain chip. Conclusions about the use of a SQUID gradiometer in measuring visual evoked reponses, along with comparisons been the EEG and AFIT brain chip data versus the SQUID data is discussed. Recommendations for further research with the SQUID gradiometer by itself, and it in conjuction with the AFIT brain chip are discussed.

CHAPTER I

INTRODUCTION

BACKGROUND

Ever since the discovery of the electrical properties of nerves in the eighteenth century, scientists have been studying this phenomenon in the hope that with its understanding, they would be better able to understand how the central nervous system functions (Ref. 1:2). This quest to understand the central nervous system, and especial.y the brain, gave birth to the modern science of neurology, which is the branch of medicine which deals with the nervous system and its diseases, and to the modern science of neurophysiology, which is the branch of medicine which deals with the physiology of the nervous structure of the body. Even though, through the years, many new tools were developed for neural researchers, these tools were usually improved versions of their predecessors, rather than new innovations.

Ever since Hans Berger discovered human brain waves in 1924, after he placed small metal strips on the scalps of his subjects and ran wires from these strips to a sensitive galvanometer, the electroencephalograph (EEG) has been a major tool used by researchers to study brain activity (Ref. 1:98). Many improvements have been made to the standard electroencephalograph over the years, but still the basic concept of the EEG is measurement of electrical potentials on the subjects scalp via "gross electrodes" placed at specific locations on the scalp, and then interpreting these

1

measurements in the hope that detailed information about mental processes, and the mental and physiological condition of the subject might be realized. A good example of the use of the EEG as a diagnostic tool is shown in Figure 1-1, which shows an EEG record taken during a brief epileptic fit -- note the spiky waves during the attack (starting at the arrow marked a) and the return of the alpha rhythm after eye closure (arrow marked b)" (Ref. 2:148). For more background in the use of EEG, see references 3,4,5,6,7, and 8.
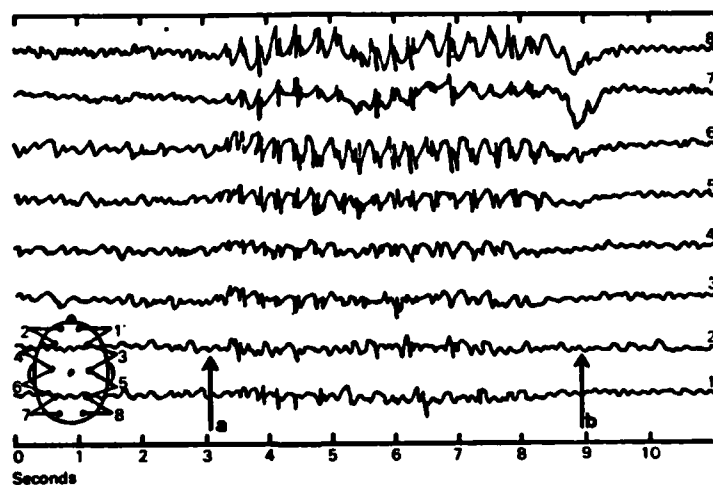
FIGURE 1-1

EEG RECORD OF BRIEF EPILEPTIC FIT
(Ref. 2:148)

Another tool which researchers have used to study brain activity, is the microelectrode. The basic microelectrode is usually a extremely slender glass or metal electrode which is inserted into or near an individual neuron. Once again, it is electrical potentials which are measured, but this time the firing rates of action potentials of the neurons are analyzed.

2

This tool has been used in many, and varied research in neuron activity. Figure 1-2 shows nerve fiber activity signals which were taken by a microelectrode inserted into the hand of a subject lying at rest (Ref. 9:141).

A Cold Sweat Diagrammed
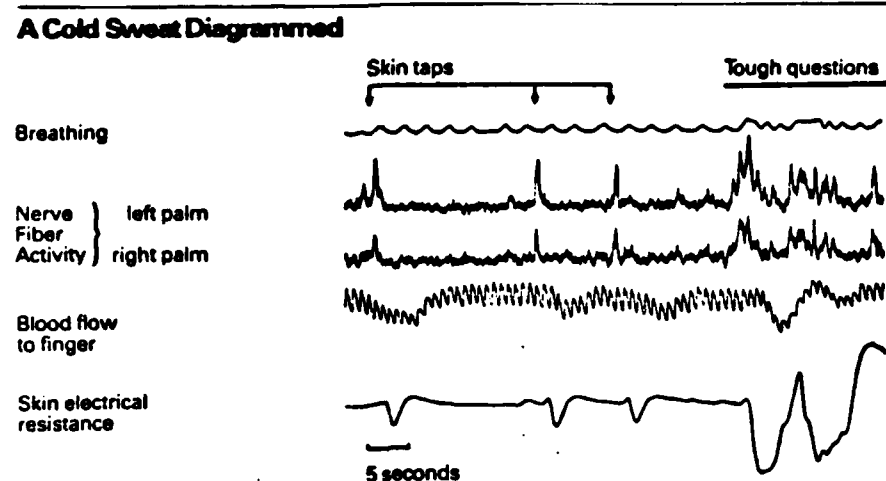
Nerve fiber activity underlies breathing, blood flow and skin responses to disturbances of a subject lying at rest. Adapted from Ludberg, Wallin/Psychophysiology. ©1981 The Soc. for Psychophysiological Res.

FIGURE 1-2

EXAMPLE OF NERVE FIBER ACTIVITY
TAKEN WITH A MICROELECTRODE
(Ref. 9:141)

For more background in the applications of microelectrodes in neural research see references 9 thru 16.

Although, both the use of the electroencephalograph and the use of the microelectrode has provided us with valuable information in the study of the central nervous system, and related electrical phenomenon, two newer innovations have provided additional understanding of neural activity. These two advance measurement devices are AFIT Cortical Implant and

3

the Superconducting Quantum Interference Device (SQUID)
Gradiometer.
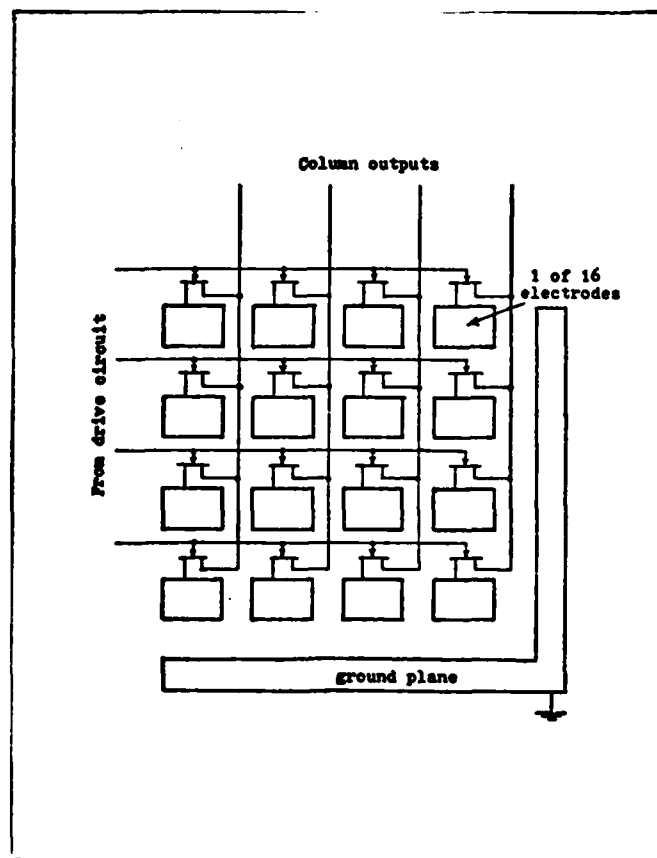
FIGURE 1-3

AFIT MULTIELECTRODE ARRAY
(REF 18:55)

In October, 1982, the first cortical implant of a
multiplexed multi-electrode semiconductor brain electrode was
successfully implanted on the brain of a laboratory beagle
(Canis familiaris) (Ref. 17 and Ref. 18). It is an X-Y
addressable, 16 electrode (4 X 4 array) multiplexed

4

switching electrode based on contemporary silicon computer chip technology (Ref 17). The circuit diagram for the electrode is shown in Figure 1-3.

The development of the AFIT implant is important, since it allows us to measure potentials directly from a very small area of the cortex of the brain; the electrodes were spaced 30 microns apart in one direction and 100 microns in the orthogonal direction.

Now that we have a device which can measure potentials directly from the surface of the cortex of the brain, we can look at other approaches to the measurement of brain activity. The relatively new approach to the measurement of brain activity is the use of a SQUID gradiometer to measure the magnetic fields emanating from the brain. This approach was slow in coming because we didn't have the technological advancements necessary to take these measurements until relatively recent years. These advancements were made in the fields of cryogenics, and the very low temperature superconducting semiconductor physics, which developed Josephson Junction electronic devices to be used in the Superconducting Quantum Interference Device. A discussion of the theory involved in the operation of a SQUID gradiometer will be later (Chapter 2).

Having now, both the AFIT cortical implant electrode research continuing, and research at the Air Force Aerospace Medical Research Laboratory with a second-order SQUID gradiometer, I decided to take a series of magnetic measurements with the SQUID gradiometer, and compare the results with

5

predicted values, and with measurements taken by the AFIT cortical implant electrode.

STATEMENT OF THE PROBLEM

The primary emphasis of this research is the comparison of measurements taking with a second-order SQUID gradiometer to waveforms either predicted mathematically, or to waveforms measured in the past with an EEG or a AFIT cortical implant electrode.

The first area of investigation was comparing the predicted mathematical magnetic and potential fields waveform emanating from a current dipole submerged in a saline solution.

Next, magnetoencephalographic visual evoked responses were measured from several human subjects, and compared with the basic EEG visual evoked response waveform.

Finally, magnetoencephalographic visual evoked responses were measured from the same laboratory beagle which had had electroencephalographic visual evoked responses measured by the AFIT cortical implant electrode.

SCOPE

When the dewar which held the liquid helium for the SQUID gradiometer failed to maintain superconducting temperatures, the ensuing downtime, along with the growing interest to measure magnetoencephalographic visual evoked responses from the same laboratory beagle which had had electroencephalographic visual evoked responses measured by the AFIT

cortical implant electrode, I decided to place my primary emphasis in taking measurements with the SQUID gradiometer. I especially placed my emphasis on measuring visual evoked responses from the laboratory beagle, instead of doing a feasibility study of simultaneous or near simultaneous electroencephalographic and magnetoencephalographic measurements from a brain.

The problem with the SQUID gradiometer downtime also reduced the amount of time I had to collect data, but sufficient data was collected to make conclusions possible.

APPROACH AND PRESENTATION

This research is presented in essentially chronological order, with each chapter representing a phase of research.

Chapter II gives a brief discussion into the theory behind the SQUID gradiometer, along with some of it proposed applications.

Chapter III gives a look at the basic current dipole model for the brain, along with the predicted and measured results for a current dipole submerged in a saline solution.

Next, Chapter IV discusses some basic theory behind visual evoked response measurements, along with human magneto-encephalographic visual evoked responses waveforms compared to the standard EEG waveform for a visual evoked response.

Chapter V details the magnetoencephalographic measurement of the laboratory beagle's visual evoked response, along with the comparison of the magnetoencephalographic visual evoked response to the electroencephalographic visual evoked

response.

Chapter VI draws conclusions about the use of the SQUID gradiometer to measure magnetoencephalographic visual evoked responses, and summarizes the results of this research.

Finally, Chapter VII makes recommendations for further experiments using the SQUID gradiometer.

CHAPTER II

SQUID GRADIOMETER THEORY

THEORY

SQUID is an acronym of "superconducting quantum interference device." In this chapter I will first discuss general SQUID theory, and then I will discuss some parameters and details of the specific SQUID gradiometer which I used in measuring the visual evoked responses.

First lets look at the SQUID gradiometer as a black box to see how it behaves when magnetic flux crosses perpendicular to the input detection coil. The input to this black box is the current which the external magnetic flux cutting the input detection coil induced into the detection loop. The output of the black box is a voltage which is proportional to the amount of magnetic flux which has perpendicularly penetrated the effective area of the input loops. So, we can say that it simply behaves like a current-to-voltage converter. It offers very high gain, extremely low noise, wide dynamic range, excellent linearity, and a wide bandwidth, extending down to dc. The current-to-voltage conversion factor for a SQUID gradiometer is usually approximately 10^7 V/A (Ref. 26:70).

Well, we see from the black box outlook, the SQUID gradiometer can give us a voltage which is proportional to a small magnetic flux detected by its input detection coil. This is an interesting conclusion, but what is the significance of the SQUID gradiometer which makes it the major tool in the area of biomagnetic measurement? It is the SQUID gradiometer's

capability to detect a magnetic field as weak as 10^{-15} Tesla which makes it so attractive in many areas of research. That weak magnetic field is over 10^{10} times smaller than the magnetic field of the earth.

Now that we have an idea of some of the capabilities of a SQUID gradiometer, lets discuss in greater detail the attributes of a SQUID gradiometer which gives it those capabilities. First, let us start by disecting the acronym "SQUID" into its components. The "S" stands for superconducting. This device uses a special semiconductor device which operates at superconducting temperatures, that is, temperatures usually below 20° Kelvin. This special device is called a superconducting insulator-barrier junction, or more commonly as a Josephson junction, after the Noble-prize-winning English gratuate student, Brian Josephson, who predicted the junctions properties in 1962 (Ref 27:42). In the literature, the Josephson junction is referred to as a "weak link" device. Josephson junctions which we find in SQUID gradiometers many times rely on the oxide at the surface of a sharp niobium point where it presses against a flat niobium surface. They are called "point contact" Josephson junctions. The superconducting transition temperature for niobium, that is, the temperature at which niobium resistance drops dramatically to approach zero resistance, is 9.2° Kelvin. The resistance of the superconducting material is not exactly zero, since you still have some molecular motion even at 9.2° Kelvin. To get zero resistance, the superconducting material must be at 0° Kelvin. Even though the resistance is not

exactly equal to zero for superconductors operating at 9.2°

Kelvin, by using rings with very low inductance and a very

long measurement time, together with a high sensitivity

current detector, it has been possible to demonstrate that the

residual resistivity of a superconductor is at least 10^{17}

smaller than the resistivity of copper at room temperaure.

Therefore, for all practical purposes, we can consider that

the superconducting material has zero resistances (Ref.

26:72). To insure that the SQUID remains superconducting, it

is usually immerged in a bath of liquid helium. The 4.2

degrees Kelvin temperature of the liquid helium bath is

adequate to keep the SQUID superconducting (Ref. 26:69).

But what effects of this superconducting Josephson

junction allows it to be used in a SQUID gradiometer? First

lets review the Meissner effect of a superconductor. Back in

1933 in Berlin, two men, Meissner and Ochsenfeld, found that

the interior of a superconducting material is free of magnetic

flux independent of whether the magneic field is applied above

or below T_c, the superconducting transition temperature. This

property is now commonly known as the Meissner effect. In the

presence of a magnetic field, a current in a very thin surface

layer is generated in such a way that its field compensates

the field inside. This is distinctly different that for an

ideal case of Lenz's law, since the expulsion of flux from the

Meissner effect occurs even in a constant field as a sample is

cooled through its transition temperature. The superconductor

behaves as an ideal diamagnetic material with susceptibility

equal to -1 (Ref. 26:72).

The "QU" and the "I" in the acronym comes once again from the effects of a Josephson junction operating at superconducting temperatures. The "QU", as mention above, stands for quantum, and the "I" stands for interference. And finally, the "D" just stand for device. Thus the name "superconducting quantum interference device" derives from the fact that quantum interference phenomena can be observed with SQUIDs on a macroscopic scale. For example, the current through a two-junction dc-SQUID varies periodically in a manner which is analogous to the optical interference pattern from two slits. At the Josephson junction insulating barrier, the amplitude of the "wave function" describing the wavelike-properties of the superconducting electrons cannot drop abruptly to zero, because then according to quantum theory the electrons would have an enormously high kinetic energy, which is not permitted. Instead, the wave function penetrates into the wall a short distance as it decays smoothly toward zero. However, if the barrier is sufficiently thin, with superconducting electrons on both sides, the decaying wave functions from the two sides overlap appreciable, and this overlap implies that superconducting electrons can flow through the insulator without any resistance. This effect is known as tunnelling because the electrons penetrate through a potential energy barrier, where by the classical laws of physics they are forbidden to go (Ref. 26:74). But how did the electrons manage to penetrate through the potential energy barrier? Well, this phenomena can be explained by the microscopic theory of the superconducting

state which was published by Cooper and Shrieffr in 1957. The basis for this theory is the consideration that at very low temperature a weak attractive force between electrons becomes more important than the disordering effect of thermal agitation, and they bind together in pairs called Cooper pairs. It is these Cooper pairs which can tunnel through the barrier as a unit. The Cooper pairs are not scattered in a superconductor whereby wave coherence is conserved over infinitely long distances. Interference effects can thus be observed on a macroscopic scale. It can be shown that the magnetic flux Φ_1 passing through the area of the weak link can be taken in account when calculating J_c, the critical current density for the junction. J_c becomes the periodic function shown in Equation 2-1.

$$J_c = J_c(0) * \frac{|\sin(PI * \Phi_j/\Phi_o)|}{PI * \Phi_j/\Phi_o}$$

where

J_c is the critical current density

PI is 3.1415926

Φ_j is the magnetic flux passing
through the weak link

Φ_o is the flux quantum which is equal
to $2.07 * 10^{-15}$ Weber

EQUATION 2-1

13

This formula has the same form as the optical Fraunhofer diffraction from a slit. Because ϕ_j is much smaller than ϕ, the magnetic flux threading through the superconducting loop, the interference pattern from a SQUID is modulated by "diffraction" occurring at the weak link.

If wires are connected to each side of the weak link, the voltage measured will be proportional to the externally applied magnetic flux.
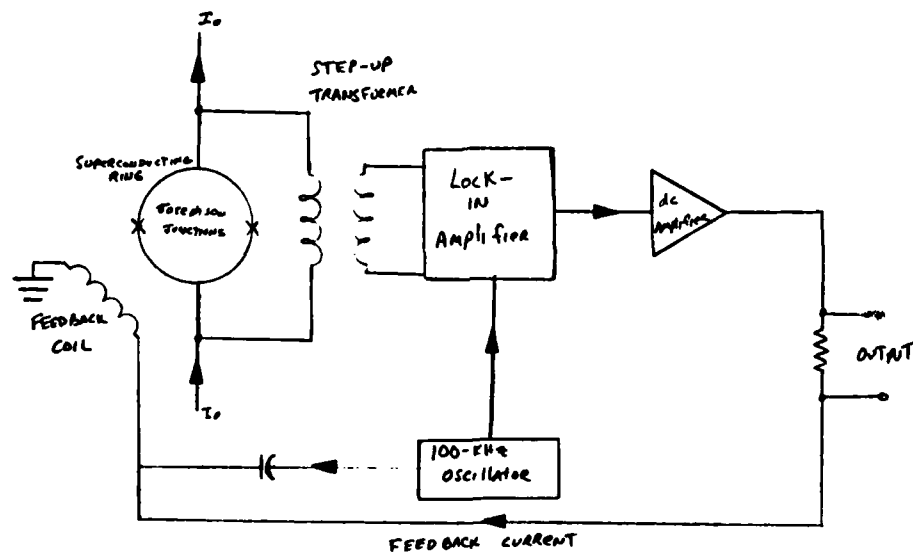
FIGURE 2-1

DC SQUID MAGNETOMETER

Now that we have discussed how a Josephson junction can be used as a weak link in a superconducting ring so as to detect small magnetic fields, lets talk about the rest of a

SQUID gradiometer. There are two types of SQUID gradiometers.
The first type of SQUID gradiometer which I will discuss is
the DC SQUID gradiometer. Figure 2-1 shows a diagram of a DC
SQUID gradiometer.

The DC SQUID gradiometer consist of a superconducting
ring interrupted by two Josephson junctions. the name follows
from the fact that in operating this two-junction SQUID only a
dc bias current is necessary. The voltage is taken off of the
superconducting ring and passed through a step-up transformer
to the lock in amplifier and then amplified by a dc amplifier.
Part of the output is sent by to a feedback coil too provide
the feedback necessary to allow the lock-in amplifier to
maintain flux-locked mode. Flux-lock mode and the lock-in
amplifier will be covered later.
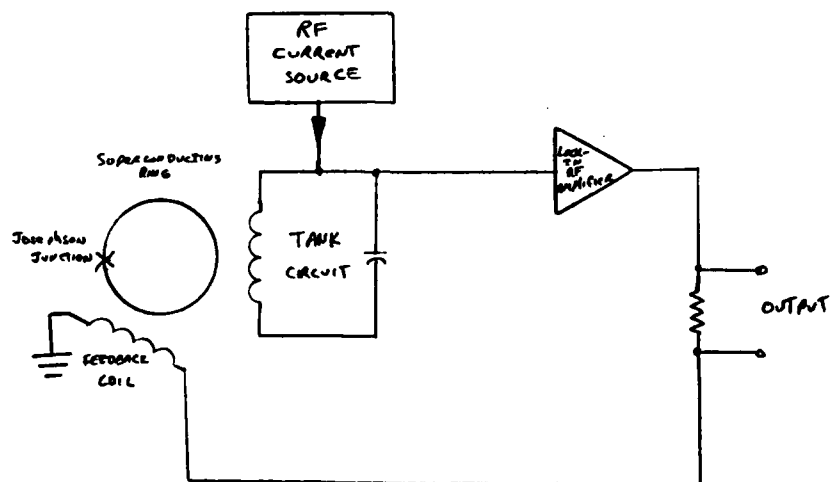
FIGURE 2-2

RF SQUID MAGNETOMETER

15

The second type of SQUID gradiometer is the RF SQUID gradiometer. A diagram of a RF SQUID gradiometer is shown in Figure 2-2. Once again a SQUID loop is used, but this time only one Josephson junction is used. The RF SQUID gradiometer is the type usually commercially produced. In this case, the SQUID loop is weakly coupled to a resonant tank circuit tuned to a sinusoidal pump current in the radio frequency range. The rf current source supplies a "pumping" current to a resonant tank circuit. The current flowing between the inductor and capacitor of the tank circuit exceeds the pumping current by the quality factor "Q" of the tank circuit. This circulating current generates an rf voltage across the parallel combination of the inductor and capacitor which is usually enhanced by a preamplifier, rectified by an rf detector, and then smoothed by a low-pass filter (usually a resistor and capacitor) to produce an average voltage that is proportional to the amplitude of the tank circuit's rf voltage. Note that the voltage is affected by the state of the SQUID, because the inductor of the tank circuit is magnetically coupled to the SQUID. The changing field of the inductor induces a current that flows around hte SQUID loop, and this rf current is superimposed on a second current representing the input signal that results from the field applied by the input coil. In the simplest case, the non-linear response of the junction has the effect of changing the inductance of the SQUID due to the presence of this signal current. This change in SQUID inductance slightly alters the inductance in the tank circuit to which it is magnetically coupled, and thereby it affects

16

the tank voltage. This is a parametric effect (Ref. 26:78).

Note that the diagrams in Figure 2-1 and Figure 2-2 are magnetometers, and not gradiometers. For a magnetometer to become a gradiometer, it must have a specific coil configuration. Figure 2-3 shows four coil configurations.

$\sim B_z$ $\sim L\frac{\partial B_z}{\partial z}$ $\sim L\frac{\partial B_x}{\partial z}$ $\sim L^2\frac{\partial^2 B_z}{\partial z^2}$

a)   b)   c)
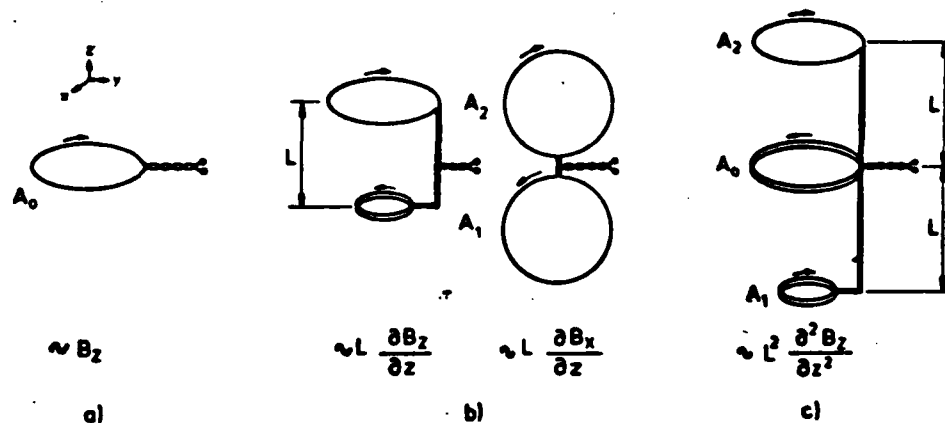
FIGURE 2-3

COIL CONFIGURATIONS

The coil in Figure 2-3(a) is a magnetometer coil for measuring the average flux density over the area of the coil. Both coils ih Figure 2-3(b) are used in first order gradiometers, that is , with gradiometers which will measure flux differences of approximately one component of the field gradient. They allow measurements of local biomagnetic fields in the presence of much stronger but uniform fields from distant sources, since for distant sources the change in the

17

partial derivative of the magnetic field with respect to distance in the "z" direction is approximately equal to zero. The last coil configuration which is shown in Figure 2-3 is the second-order gradiometer configuration which is better suited to measure extremely small local magnetic fields while in the presence of higher noise levels, since not only are the uniform fields rejected, but also the first-order fields are rejected.

Because of its ability to select specific magnetic fields out of a noisy background, the second-order SQUID gradiometer is normally used to take biomagnetic measurements, including all the measurements reported in this report.

The second-order SQUID gradiometer can also be used to analyze heart activity by producing a magnetocardiogram (MCG), analyze muscle activity by producing a magnetomyogram (MMG), and monitoring movement of the eye by producing a magnetooculogram (MOG).

Before leaving this chapter, I will discuss the operation of the SQUID gradiometer in "Flux-lock mode", and some information on the particular SQUID gradiometer which I used to take measurements for this report. To use the SQUID in practical instruments, a linearization circuit is necessary to minimize the nonlinearity and also maximize the dynamic range by avoiding the periodicity of the SQUID responce. For this reason, the SQUID normally is used as a null detector in a feedback loop. Usually, an audio frequency generator introduces a modulation flux into the SQUID. The amplitude of the modulation is approximately one-fourth of a flux quantum.

The choice of the modulation frequency depends on the desired bandwidth for a measurement, because this frequency has to be higher than the highest frequency component of the signal to be measured. Usually it is chosen to be about 50 kHz or higher. A phase-sensitive detector (PSD) extracts the portion of the SQUID electronics output at this modulation frequency and rectifies it; and this rectified output of the PSD goes to an integrator (low-pass filter). The PSD and integrator comprise what is known as a "lock-in" amplifier. Figure 2-4 showns a block diagram of a lock-in amplifier (Ref. 28:597).
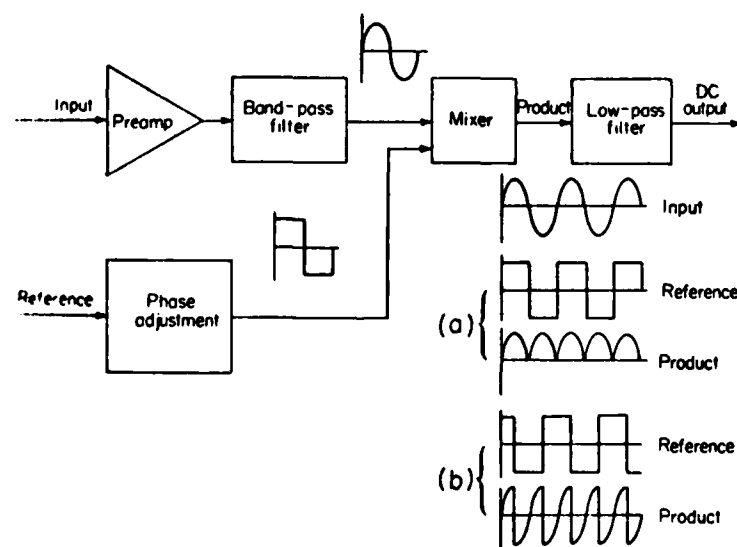
FIGURE 2-4

DIAGRAM OF A LOCK-IN AMPLIFIER

Finally, I will discuss the S.H.E. Corporation System 330X Second-Order SQUID gradiometer, which I used in collecting data for this report.

As shown in Figure 2-5, the Model 330 RF Unit uses a single weak link made from niobium. Its rf coil requires one microamp to change flux by one flux quantum. Its input coil has a current sensitivity of .1 microamp per flux quantum. It uses a RF bias frequency of 19 MHz with a 50 kHz square wave modulation. The input has an overall gain of 83 db.
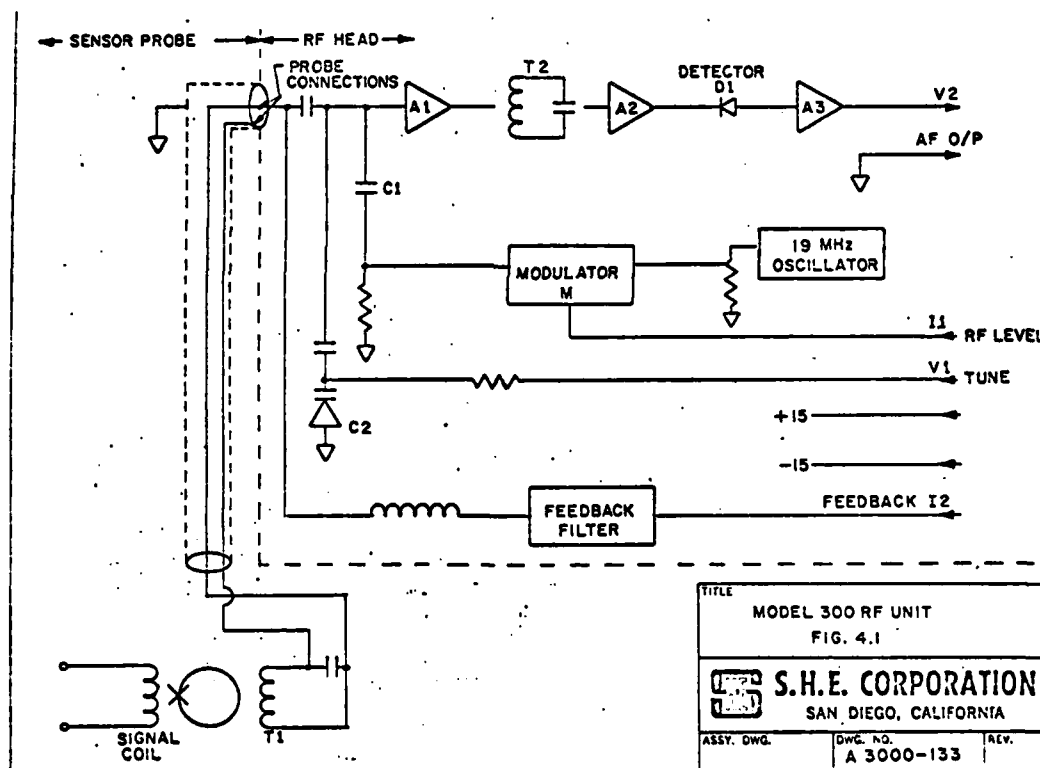
FIGURE 2-5

DIAGRAM OF S.H.E. MODEL 300 RF UNIT

Its bandwidth is plus and minus 150 kHz at carrier

frequency. The SQUID is immerged in a liquid helium bath inside of a superinsulated dewar similar to the arrangement shown in Figure 2-6.
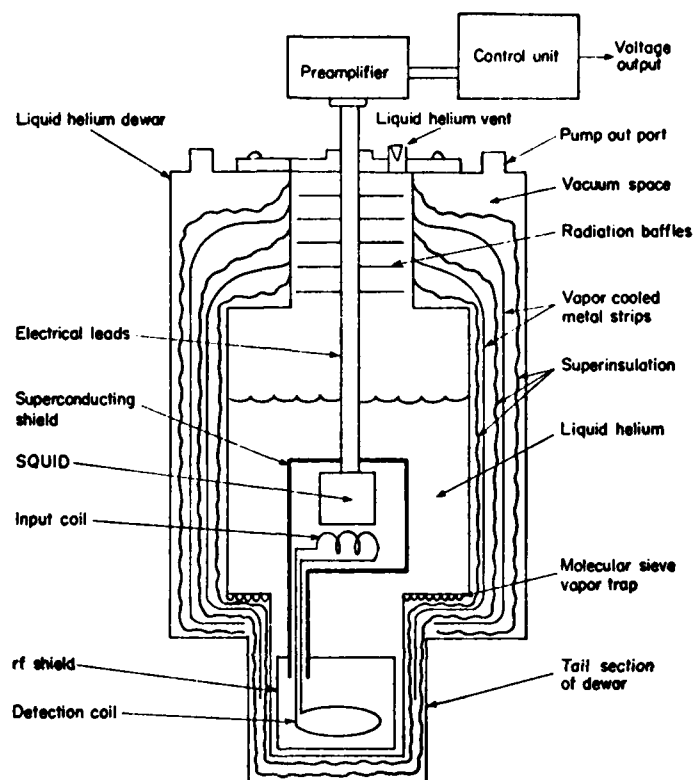
FIGURE 2-6

SQUID SYSTEM MOUNTED IN LIQUID HELIUM BATH

CHAPTER III

DIPOLE MODEL WITH TESTING

BACKGROUND

In this chapter, I will first discuss the dipole theory as the source of electrical activity in the brain. Next, I will discuss the single dipole model. In this case, it has been placed in a bowl immerged in a saline solution. The predicted values for the magnetic field emanating from the dipole are plotted, and compared with the plot of the measurements taken by the second-order SQUID gradiometer. Finally, the surface potential predicted values are plotted, and compared with the plot of the potentials measured off the surface of the saline solution, by using an oscilloscope with input differential amplifiers.

DIPOLE MODEL FOR THE BRAIN

With approximately 60 to 75 percent of cortical neurons oriented perpendicular to the cortical surface, and a large number of interconnections, it then appears that the scalp potentials are due to current dipole layers occupying various surface areas of the cortex (Ref. 5:273). For more background in reference to the dipole model for the brain see references 5,6, and 21 thru 24.

SINGLE DIPOLE

For this part of my research, I immerged a .5 cm. current dipole in a solution of .464 percent saline. Figure

3-1 shows a diagram of the current dipole experiment apparatus, while Figure 3-2 shows a picture of the apparatus. This apparatus included two 48 cm. by 31 cm. by 1 cm. pieces of plexiglas, an approximately 3 liter glass bowl, a 2 cm. by 2 cm. by 3 cm. block of lucite, and a 3 meter piece of shielded wire. I made a 1/2 cm. current dipole on one end of the wire, and connected the other end of the wire thru a 1000 ohm resister to a BNC connector. On one of the large pieces of plexiglass I etched a 40 cm. by 25 cm. grid. This grid was graduated in 1 cm. increments. From the top left-hand corner of this grid, I marked the origin for the cartesian coordinate system to be down 12 cm. and right 20 cm. From the origin of this cartesian coordinate system, I chose the direction to the right to be the positive "y" direction, and the direction down to be the positive "x" direction. The positive "z" direction was in the direction above the apparatus. This piece of plexiglass became the bottom of my apparatus, and was used to correctly align the apparatus to the desired measurement point. For example, to align the apparatus to the "x,y" coordinate (3,-5), the point on the grid corresponding to the intersection of the "x" equal to positive 3 line and the "y" equal to negative 5 line is placed on top of a center of measurement point which was initially determined before the dipole apparatus was placed under the SQUID gradiometer. This initial center of measurement point was determined by placing the SQUID gradiometer in its vertical position and placing a mark at the point on the measurement table at which the line projecting from the center of the SQUID gradiometer detection

23

coil down to the table would enter the table.

TOP

BOTTOM
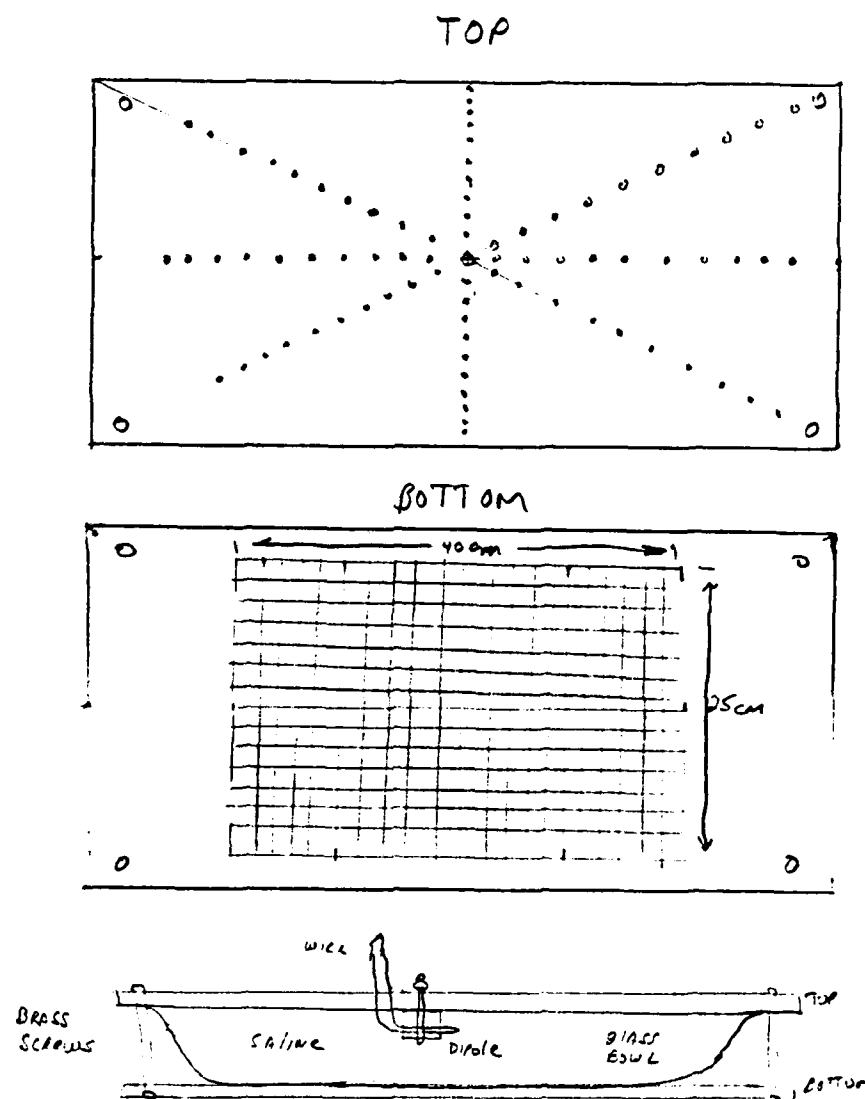
FIGURE 3-1

DIAGRAM OF DIPOLE EXPERIMENT APPARATUS

24

The other piece of plexiglass became the top of the apparatus, and the mount for the dipole. From the picture shown in Figure 3-2, we see that the top has a hole drilled into it at the point corresponding to the origin of the cartesian coordinate system. Also, there are ten holes drilled into the top of this apparatus in each of eight directions. These series of holes all start at the origin, and they are placed 1 cm. apart. The first direction that these holes were placed was in the positive "y" direction. The rest of the series of holes are then placed every 45°. There was also a hole drilled at the approximate "x,y" coordinate of (1,-2). This hole was used to mount the lucite block which held the dipole under the surface of the saline solution, at a position directly over the origin and pointing in the positive "y" direction.
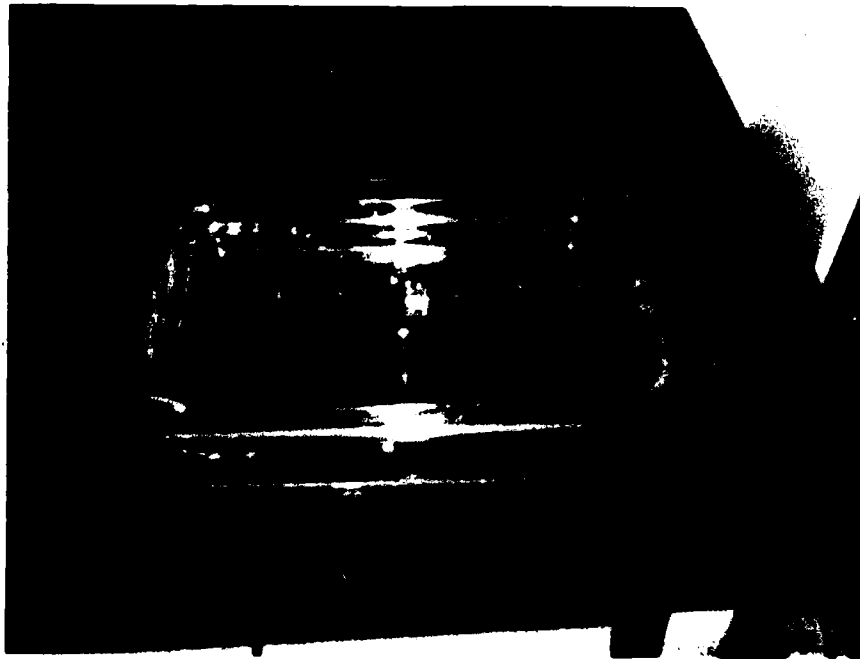
FIGURE 3-2

DIPOLE EXPERIMENT APPARATUS

25

The bowl was filled with the .464 percent saline solution and placed between the pieces of plexiglass. Four brass screws with wingnuts were used to fasten the bowl in place. The center of this glass bowl was determined and marked. This mark was placed on top of the origin mark on the bottom piece of plexiglas so that the dipole would be centered in the cartesian coordinate system.

Before the apparatus was completely built, I calculated mathematically the predicted values of the magnetic field strength (H) using the equation derived by Cuffin and Cohen in there paper, "Magnetic Fields of a Dipole in Special Volume Conductor Shapes. (Ref. 24:374)" Equation 3-1 shows the formula for H_z.

$$H_z = \frac{X*Py}{4*PI*(X*X + Y*Y +(D+Z)*(D+Z))^{3/2}}$$

where

Py = dipole moment = current * dipole length

PI = 3.14159

X = distance in the X direction

Y = distance in the Y direction

Z = distance in the Z direction

D = depth dipole is below surface

EQUATION 3-1

26

For my experiment, $Py = (.008)*(.005) = .00004$ and the value of D was .015 meters. To calulate the magnetic flux density (B), I used Equation 3-2.

$$B_z = \mu_o * H$$

where

B_z = magnetic flux density

$\mu_o = 4*PI*10^{-7}$

H_z = magnetic field strength

EQUATION 3-2

The calculated magnetic flux density (B) values for the plus and minus 10 cm. grid is located in Appendix A, along with Table A-1 which shows a subset of the measurements which were taken, and their associated predicted value. As I was analyzing the calculated values versus the measured data I was looking for an isofield contour shape to correlate to each other. Figure 3-3 shows a current dipole with its associated magnetic field B and volume current density J^v Figure 3-4 shows the plot of the calculated magnetic field for the dipole. Note that the calculated magnetic fields isofield contours forms two lobes. One lobe is pointed in the positive "x" direction, and the other lobe is pointed in the negative "x" direction.
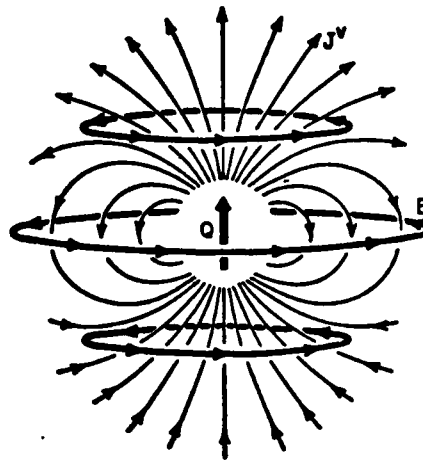
FIGURE 3-3

CURRENT DIPOLE

Also note that the positive "y" direction, that is, the direction which the dipole is pointing, is to the right, and the positive "x" direction is toward the bottom of the plot. This plot was then compared to the plot obtained by plotting the data measured by the SQUID gradiometer. This plot is shown in Figure 3-5. Although, the plot differs in absolute isofield value, and the wave shape is distorted, we can still see that it is still directly correlated to the calculated field plot. There are several factors involved in the distortion of the isofield contour lines in the measured magnetic field plot. First, we must remember that the calculated isofield contour plot did not take into account the edge effects which are introduced into the measurements since the bowl sides restricts the medium to a finite distance in the "x" and "y" directions, even though the calculations are based on an

28

infinite medium in the "x" and "y" directions.

CALCULATED DIPOLE MAGNETIC FIELD
PLOT NO.   4   DATE 11/10/83   TIME 20:41:44
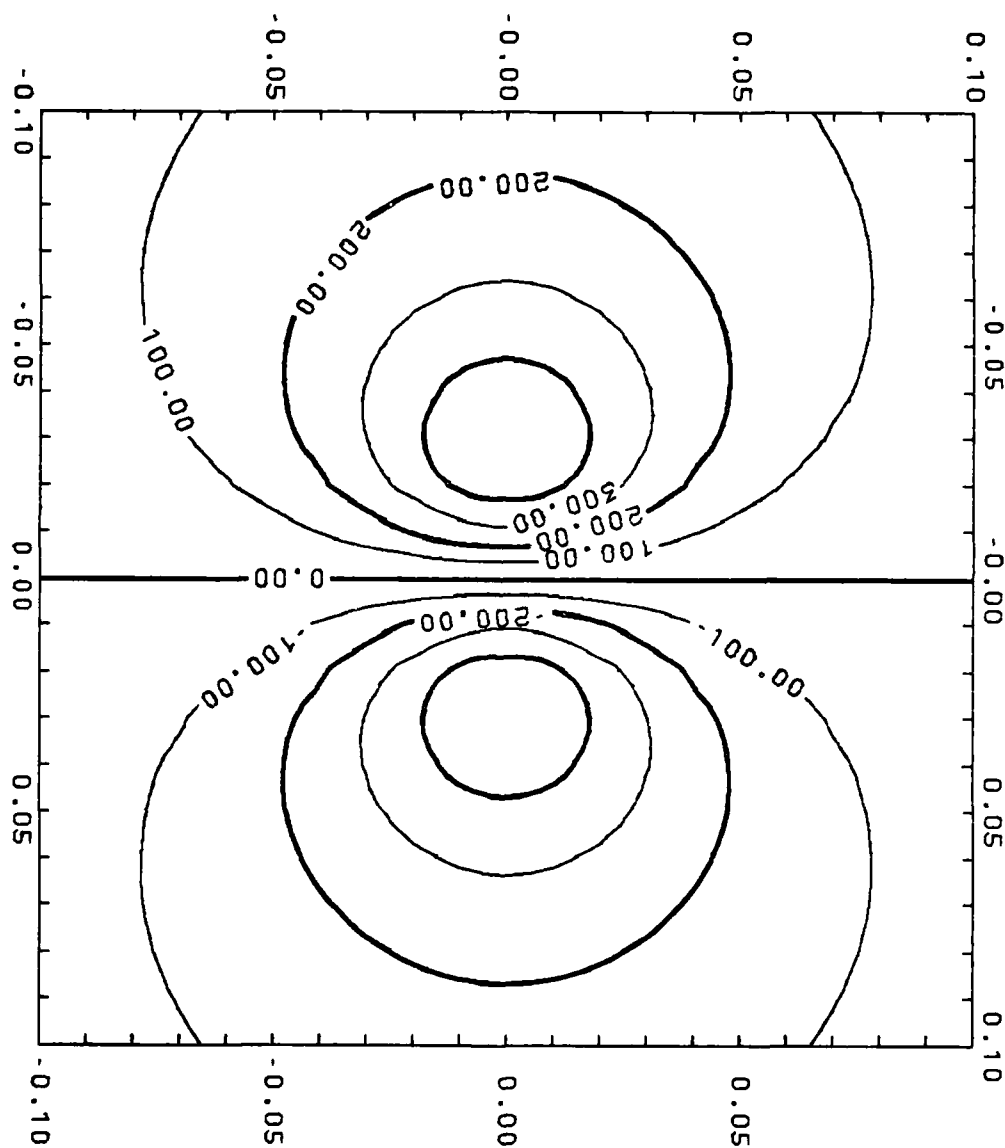
FIGURE 3-4

CALCULATED DIPOLE MAGNETIC FIELD ISOFIELDS

29

MEASURED DIPOLE MAGNETIC FIELD

PLOT NO.   2   DATE 11/10/83   TIME 22:13:25
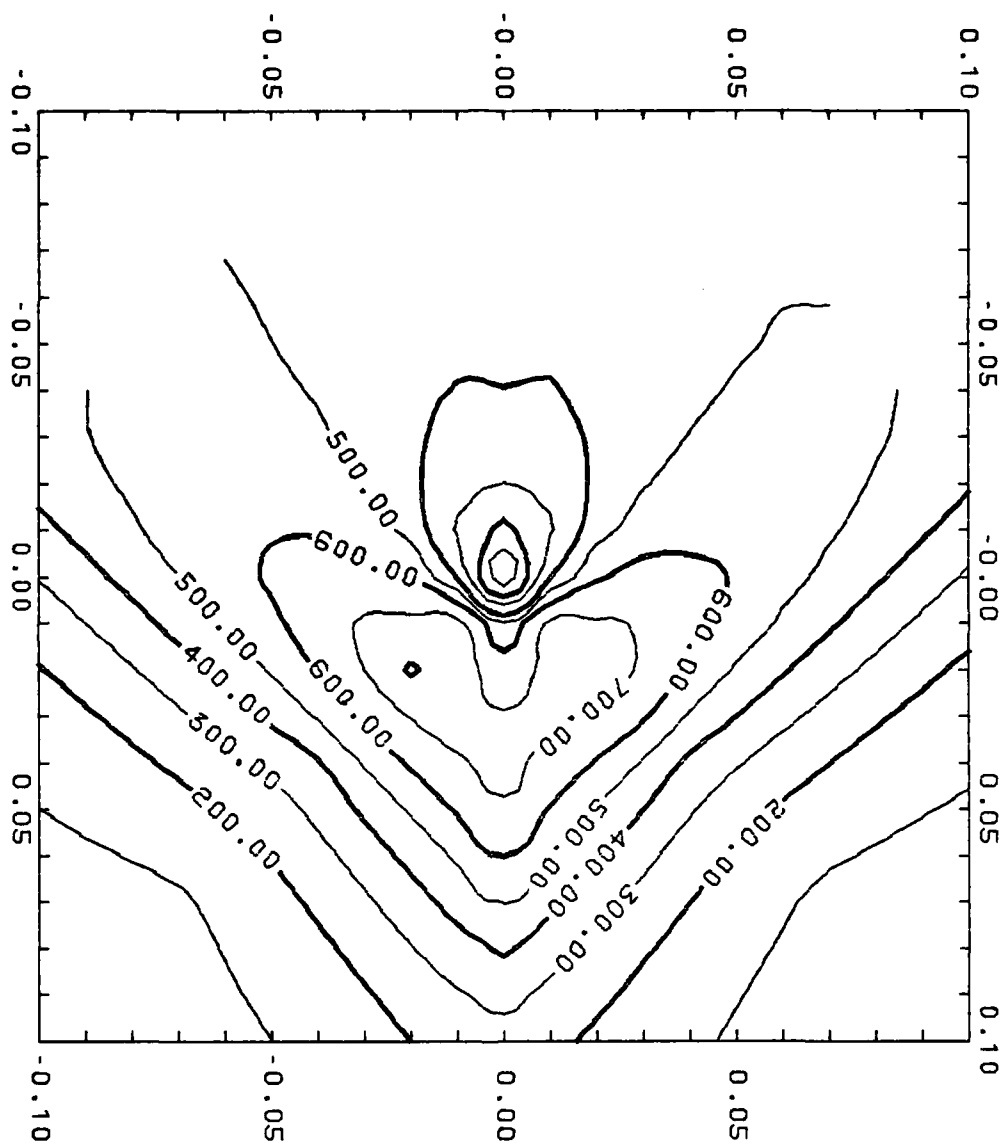
FIGURE 3-5

MEASURED DIPOLE MAGNETIC FIELD ISOFIELDS

Also, the lower lobe is greatly distorted, as expected, because of the lucite block which is used to mount the dipole is at the negative side of the dipole, so the volume are forced to go around this block and in doing so get distorted. The difference in the absolute value of the calculated magnetic field versus the measured magnetic field is partially due to the edge effects introduced into the measurements, and also the possible inaccuracies in the positioning of the apparatus with respect to the SQUID gradiometer.

Since later in this report I will be comparing magneto-encephalographic measurements of visual evoked responses to electroencephalographic measurements of visual evoked responses, my single dipole experiment would not be complete without predicting the surface electrical potential of the saline solution, and then compare the predicted values to the values I obtain from measuring the surface potential using a Tektronix 7A22 Differential Amplifier plugged into a Tektronix 7623A Oscilloscope. As for all of the experiments with the single dipole apparatus, the Textronix 503 Function Generater supplied the 8 milliamps of current to the dipole.

In order to solve for the surface potential caused by a dipole which is submerged a depth "d" below the surface of the solution, let us first consider the case shown in Figure 3-6. In Figure 3-6, you see a single dipole of length 2 "e". The dipole is centered at the origin, but pointing in the "y" direction. For this case, the conductivity is the same throughout the medium. Once we choose an arbitrary point, say P, we can apply the potential function for a dipole to

31

determine the potential at point P due to the dipole.
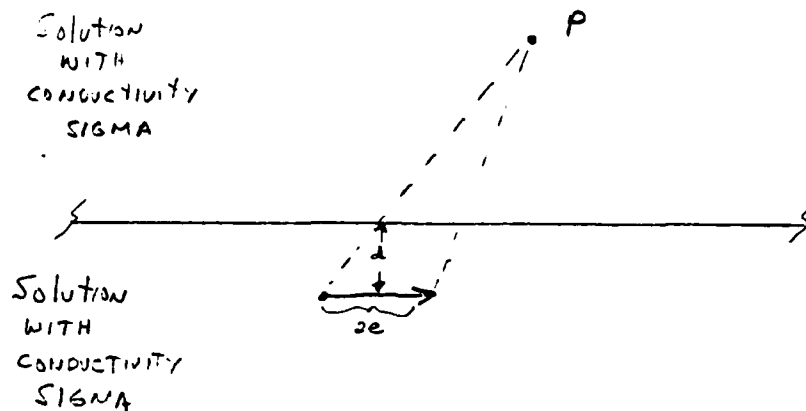
FIGURE 3-6

SINGLE DIPOLE MODEL

The potential at point P due to the dipole can be written in the form shown in Equation 3-3:

$$\Phi_d = \frac{p/e}{4*PI*SIGMA} * \left[\frac{1}{R_+} - \frac{1}{R_-} \right]$$

EQUATION 3-3

where

    p = dipole moment

    e = half the length of the dipole

32

PI = 3.14159

$R_+ = (\ X*X+(Y-e)*(Y-e)+Z*Z)^{1/2}$

$R_- = (\ X*X+(Y+e)*(Y+e)+Z*Z)^{1/2}$

Φ_d = potential at point P due to the dipole

SIGMA = the conductivity of the medium

If we take the limit of the expression above as "e" goes to zero, and do some algebra, we get the expression shown below in Equation 3-4:

$$\Phi_d = \frac{2*P*Y}{4*PI*SIGMA*R^3}$$

EQUATION 3-4

So now we have an equation for the potential at an arbitrary point P due to a single dipole in a infinite medium. Now we can use the above equation, and the superposition principle to develop the equation for the potential at an arbitrary point P due to two dipoles. Figure 3-7 shows the new problem we are working, that is, two dipoles are separated by 2 "d", but they are orientated in the same direction. Using the superposition principle, we get Equation 3-5, which is shown below, as the solution to the problem of two dipoles placed 2 "d" apart and with the same orientation.

The calculated potentials are located in Appendix B, along with Table B-1, which contains a subset of the measurements which were taken, and their associated predicted value.

33

$$\Phi_d = \frac{p*y}{2*PI*SIGMA} * \left[\frac{1}{R_+} - \frac{1}{R_-} \right]$$

EQUATION 3-5

where

p = dipole moment

PI = 3.14159

$R_+ = (\ X*X+Y*Y+(Z-D)*(Z-D)\ )^{3/2}$

$R_- = (\ X*X+Y*Y+(Z+D)*(Z+D)\ )^{3/2}$

Φ_d = potential at point P due to the dipoles

SIGMA = conductivity of the medium

Once again, we will analyze the plot of the calculated dipole surface potential shown in Figure 3-8, along with the plot of the measured dipole surface potential shown in Figure 3-9. Once again, the positive "y" direction is toward the right of the plot, and the positive "x" direction is toward the bottom of the plot. In Figure 3-8, we see two lobes as we saw in the calculated magnetic field plot of Figure 3-4, but this time the lobes are pointing in the plus and minus "y" direction instead of the plus and minus "x" direction. Once again, we see that the lobe associated with the positive "y" direction is present, but that the lucite block effects is once again present.

34

CONDUCTIVITY
SIGMA
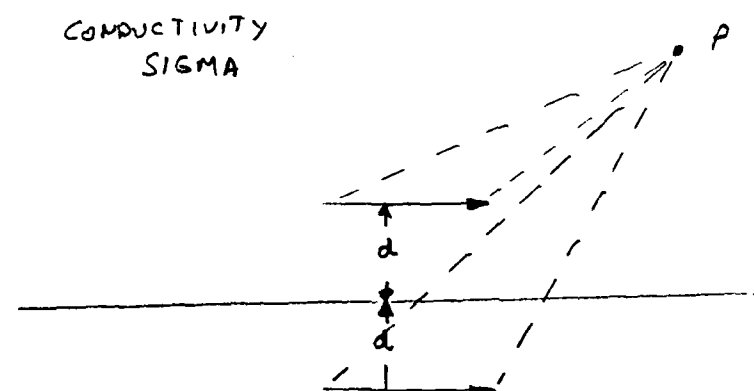
FIGURE 3-7

TWO DIPOLE MODEL

CALCULATED DIPOLE SURFACE POTENTIAL

PLOT NO. 2   DATE 11/10/83   TIME 20:21:15
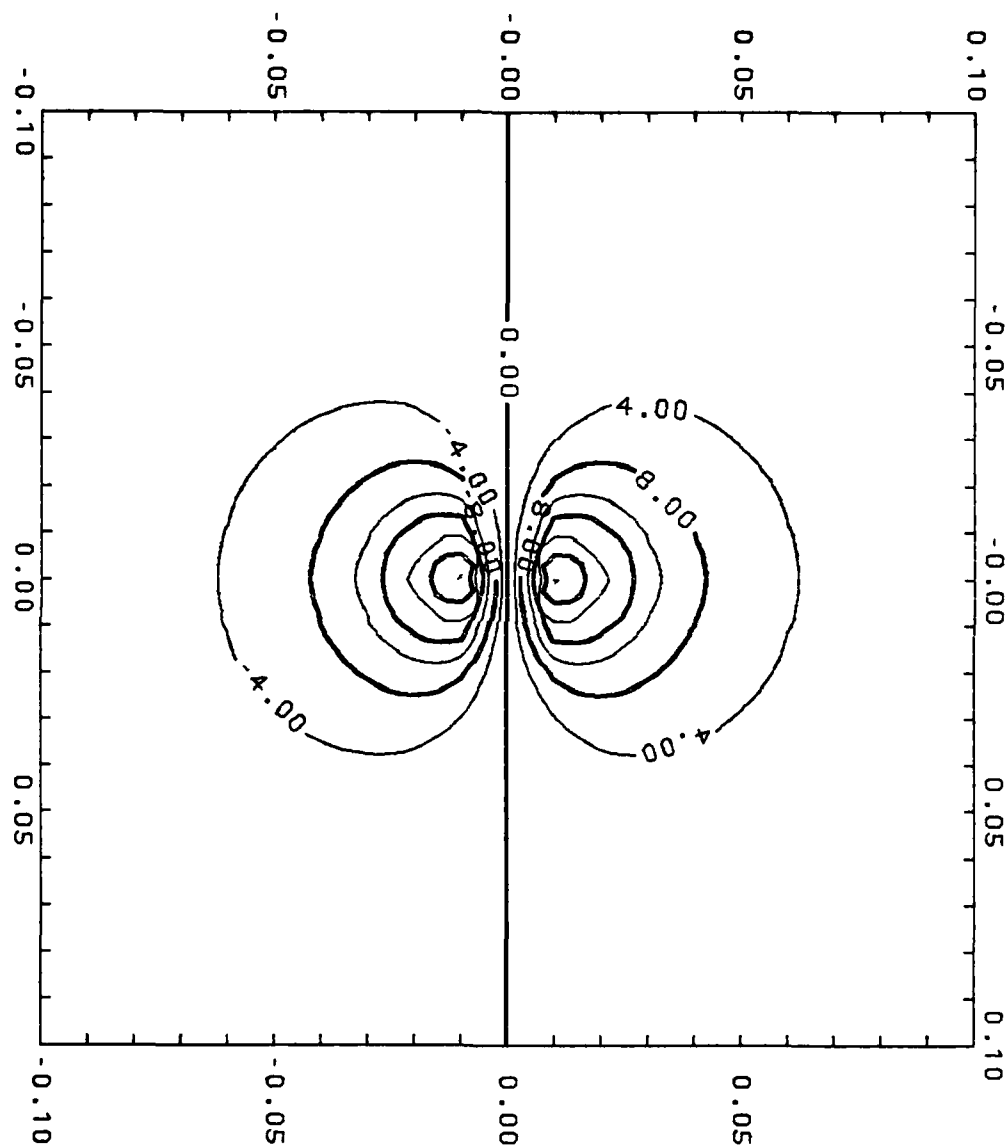
FIGURE 3-8

CALCULATED DIPOLE SURFACE POTENTIAL

36

MEASURED DIPOLE SURFACE POTENTIAL

PLOT NO.   4   DATE 11/10/83   TIME 19:03:39
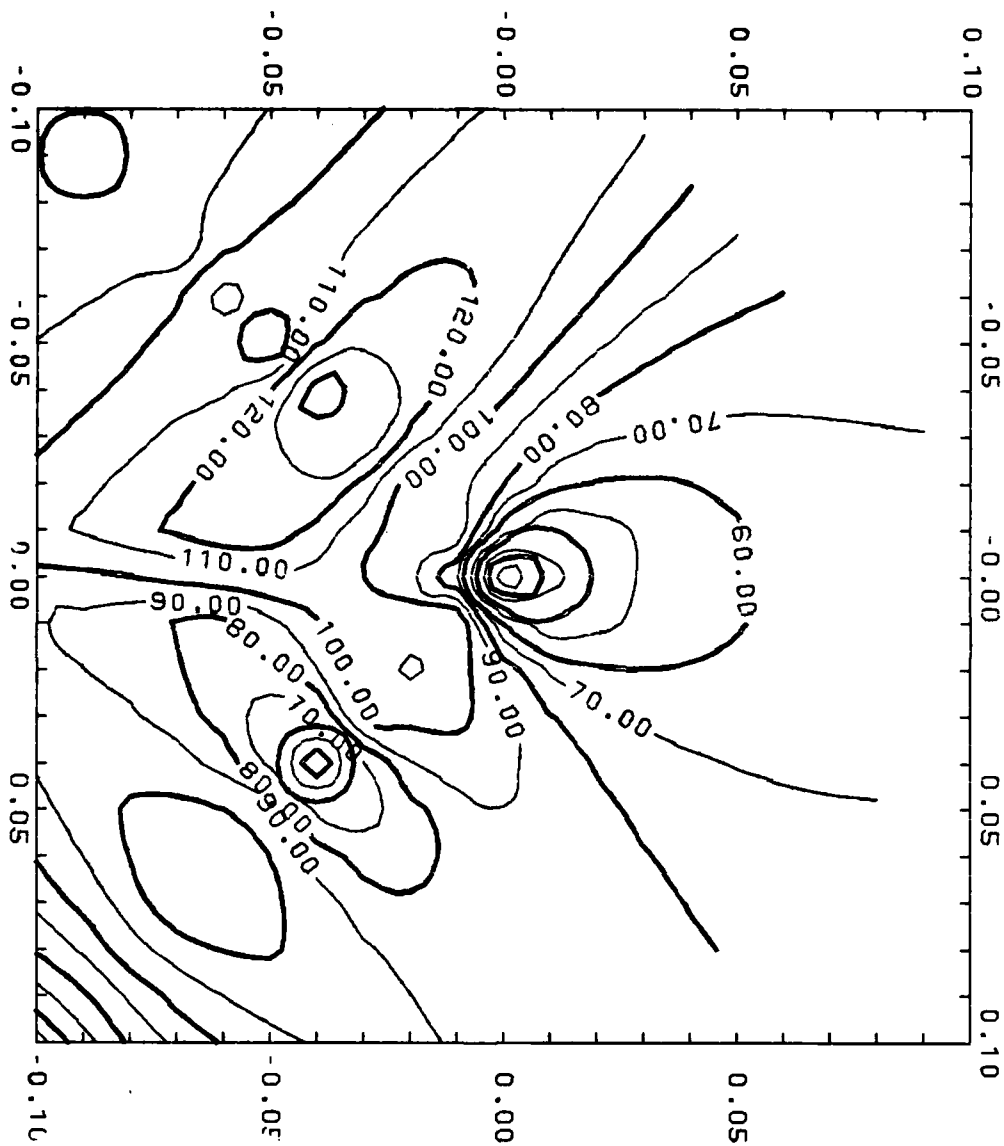
FIGURE 3-9

MEASURED DIPOLE SURFACE POTENTIAL

Some of the inaccuracies in both the wave shape and the absolute value of the measured data versus the calculated values is due to, once again, the edge effects of having a finite volume, rather than a semi-infinite volume. Also, positioning of the measurement probe may have had some affects. And finally, as shown in Equation 3-5, some inaccuracies may have been introduced by using an estimated value for SIGMA, the conductivity of the saline solution.

CHAPTER IV

HUMAN VISUAL EVOKED RESPONSE

BACKGROUND

Human brain waves were discovered in 1924 by Hans
Berger of the University of Jena, Ausria (Ref. 1:98). Since
then many techniques have been developed to study brain
activity. One major advancement in the area of brain research
was the development of the electroencephalograph. Through the
years, the electroencephalograph has had many applications,
including its use to measure visual evoked responses. The
theory behind the technique of taking visual evoked responses,
is that the chances of detecting some very small transient
electromagnetic field may be enhanced by synchronizing the
sample timing so that 50 to a 100 of these synchronized data
sampling windows can been added together, and then averaged.
Most of the noise signals when averaged will add to zero, but
if there is a good signal from the brain which is hiding, it
will grow bigger, since it will be synchronized.

The electroencephalograph is not the only piece of
equipment which can detect visual evoked responses, SQUID
gradiometer can also detect them. In this chapter, we will
look at some visual evoked responses which were taken with the
SQUID gradiometer, along with a comparison of some electro-
encephalographic visual evoked responses verses magnetoen-
cephalographic visual evoked responses. For further research
into visual evoked responses look at references 3,4,23,24, and
25.

Before continuing, lets look at the plot shown in Figure 4-1, to determine what information can be derived from its symbols and text, and then I'll talk about the experiment setup.

HEATHER MEG.002
10 Hz NOTCH   1.15-03 V   VLN
22-SEP-83   T
          0.07812 SEC

A
R
TSU
50
AT

2.0A   10. A -B/16   SEC   0.4
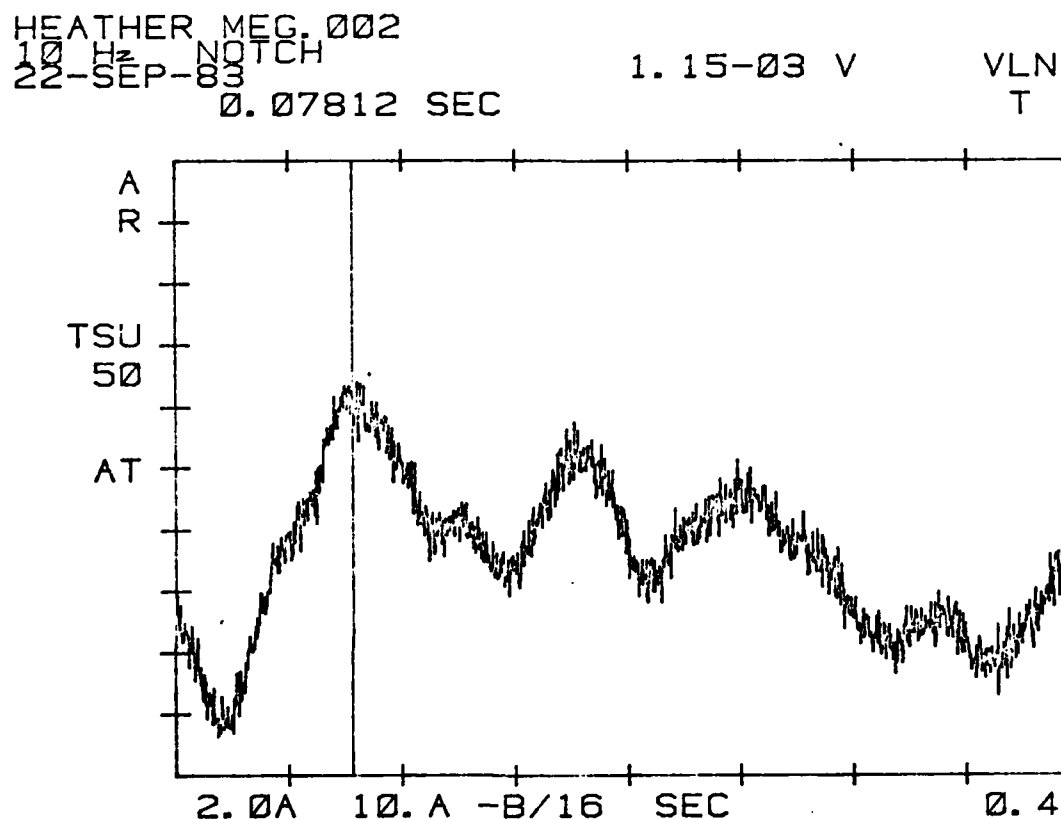
FIGURE 4-1

EXAMPLE OF A MVER

This plot was taken from the Nicolet Scientific Corporation Model 660B Dual-Channel FFT Analyzer, which is shown in Figures 4-2 and 4-3.

HEATHER is the name of the subject. MEG.002 is the name of the disk file which contains the data for this plot. To the right of the disk file name will sometimes be other information. For example, the position at which the measurement was taken and any other information about the

40
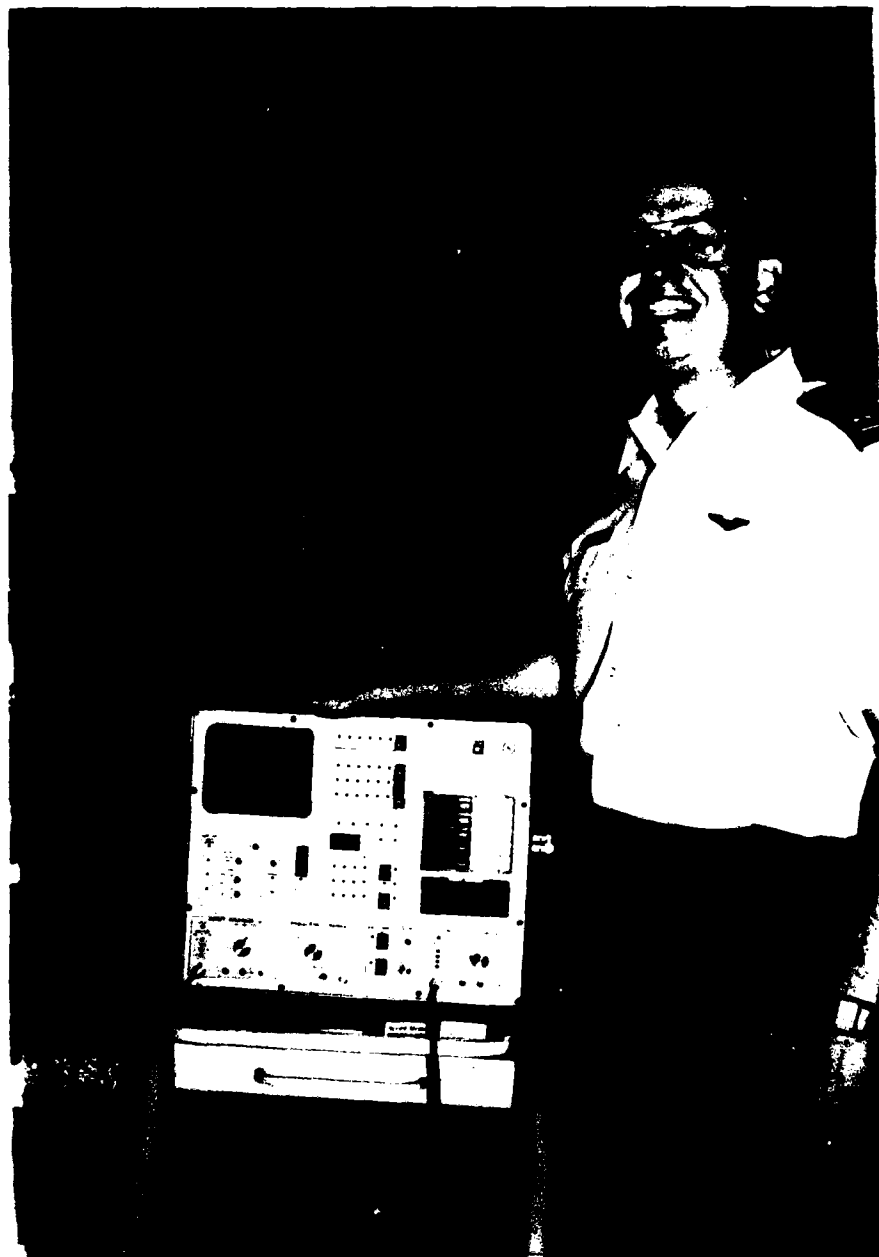
FIGURE 4-2

THE AUTHOR WITH THE FFT ANALYZER

41
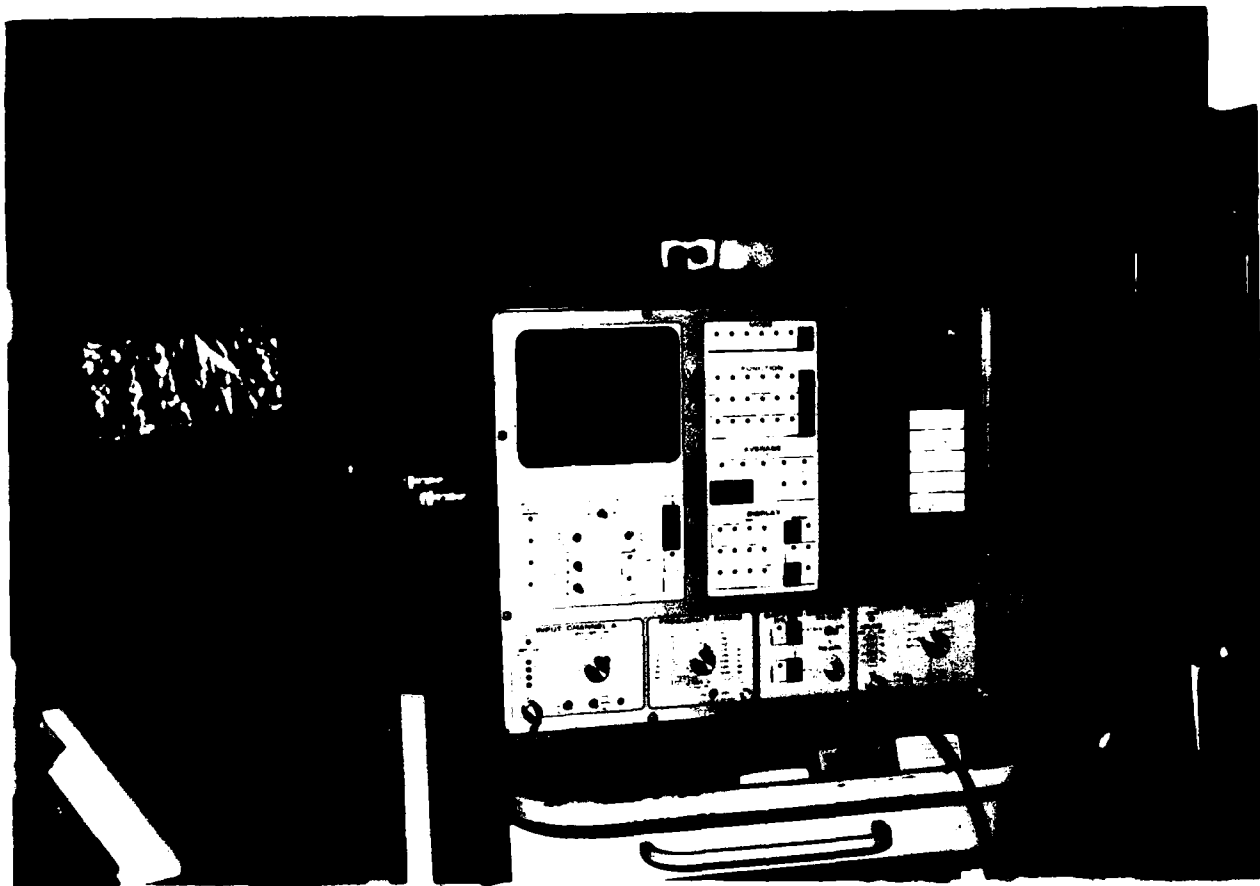
FIGURE 4-3

NICOLET MODEL 660B FFT ANALYZER

measurement environment may be there. On the second line, the 10 Hz and Notch is telling us that the 10 Hz low pass filter was used, along with the 60 Hz notch filter. Further to the right of the filter information is the value of the voltage at the cursor location. Still further to the right is the vertical scale mode. VLN stands for the vertical scale

is in linear volts, while a VLG would indicate the use of a logarithmic scale. On the third line, I have placed the date the measurement was taken. Sometimes, especially on the later plots, I entered information about the stimulus on this line and to the right of the date. Clear to the far right of the third line will be a "T" or a "C". For all of the measurements in this report, a "T" will be to the far right of the third line to indicate that the capture control setting was on transient. If I wanted to take measurements with the capture control setting in the continuous mode, a "C" would have replaced the "T". On the fourth line you will find the cursor position as determined by the horizontal scale units selected for the measurement. In this case, the cursor position is in time, that is, seconds. Now going down the left side of the plotted box, we see that the "A" tells us that the input of the top trace is was on channel A, while the "R" tells us that the format of that trace is real, versus a "P" if the format was phase, or a "M" if the format was magnitude, or "I" if the format was imaginary. The "TSU" is telling us what type of averaging, while the "50" is telling us the number of averages which were taken. In this case, the "T" stands for transient averaging, while the "SU" tells us the sum is being average. Other possible types of averaging are "PK" for peak, "EX" for expontential, "DF" for difference, and "SW" for sweep. Continuing down the left side, the "AT" tells us what function was performed. In this case, averaging by time was selected, but other types of function could have been selected. For example, a "TF" would indicate a transfer function was

43

selected, while a "RS" would indicate that a RMS spectrum function was selected. Two more types of functions are "COH" for coherence, and "IT" for instantaneous time. If we were using the dual trace capability of this FFT analyzer, simular information on the input channel and format of the second trace would be next to the lower left side of the box. Now, going across the bottom of the box from left to right we see the "2.0A" and the "10. A" which tells us the maximum setting for channels A and B, respectively. In this case, the maximum setting for channel A is 2 volts ac, while the maximum setting for channel B is 10 volts ac. A "D" instead of a "A" would have indicated the values were dc voltages instead of ac voltages. The "B/16" indicates that the transient trigger source is channel B, and the trigger level is set on channel B full scale divided by 16. Next, the "SEC" indicates that the horizontal scale is in time, that is, seconds. The horizontal scale may also be "HZ" if the horizontal scale is in frequency, that is, hertz. The last item at the far right of the bottom line is the horizontal full scale value. In this case, the horizontal full scale value is .4 second, or 400 milliseconds.

Now that we known how to interpret the information of the plot, lets discuss how the measurements were taken, that is, the experimental setup for the human magnetoencephalo-graphic visual evoked response experiment. The subject sat in a wooden chair beneath the SQUID gradiometer. Pictures of the SQUID gradiometer will be shown in the next chapter. The SQUID gradiometer mount is adjusted so that the SQUID detection

coil, that is, the bottom of the dewar, is perpendicular to, and nearly touching the place on the subjects head at which the measurement is to be taken. A Grass Model PS22A Photo-stimulator was used to trigger a bright strobe light at random intervals. This flash was used as the stimulus. The signal used to fire the strobe was also used to trigger the Nicolet 660B FFT Analyzer. For the visual evoked responses measured from humans, the FFT analyzer did the time average of the sum of 50 measurements, each of a 400 millisecond window starting at the time the stimulus was triggered. The measurement stored at the end of the 50 measurements was then stored on an 8 inch disk via a Intel 80/20 computer. Later, the disk files were plotted out on a HP digital plotter.

HUMAN VER

In Figure 4-1, is an example of a human visual evoked response taking with a second-order SQUID gradiometer. You will find this plot, and other human visual evoked response plots in Appendix C. This plot is a typical human magnetoen-cephalographic visual evoked response, since you can see a 78 millisecond peak, and 180 millisecond peak. These latencies are related to the time it takes the signals produced in the eye to be conducted via the optic nerve, pass the optic chiasm, through the lateral geniculate nucleus, and finally to the primary visual cortex.

As you look thru the five examples of human magneto-encephalographic visual evoked responses which are contained in Appendix C, note that all five different human visual

45

evoked response plots had an initial peak around 80 milli-seconds. This component of the magnetoencephalographic visual evoked response seems to be consistent.

Figure 4-4 shows us the EEG profile of a visual evoked response.

COMPONENTS OF THE VISUAL EVOKED RESPONSE
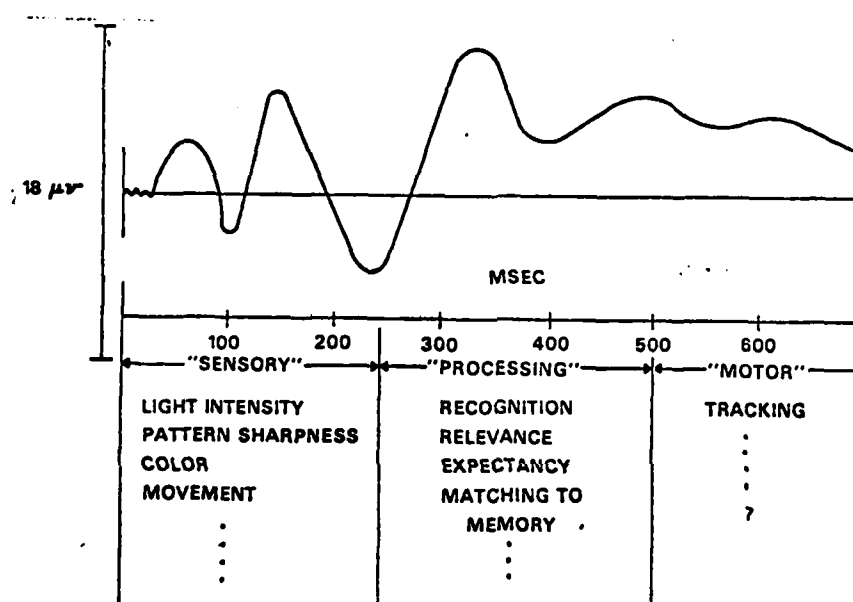
HE-75-12-17

FIGURE 4-4

STANDARD EEG VER

Note, that the electroencephalographic visual evoked response also contains a peak with a latency off approximately 80 miliseconds, along with a peak with a latency off approximately 180 milliseconds.

CHAPTER V

DOG VISUAL EVOKED RESPONSE

BACKGROUND

During the late part of September and early part of October of this year, we got the opportunity to run some magnetoencephalographic visual evoked responses experiments on "Ricky", the laboratory beagle in which the first cortical brain chip was implanted. Appendix D has a number of plots of "Ricky's" magnetoencephalographic visual evoked response. We also had the chance to take some magnetoencephalographic auditory evoked responses from Ricky. The plots of Ricky's auditory evoked responses, along with some discussion of auditory evoked responses are contained in Appendix E.

EXPERIMENT SETUP

The experiment setup for the Ricky's magnetoencephalographic visual evoked response measurements were similar to the setup used to measure the human magnetoencephalographic visual evoked responses. For example, once again the subject is placed beneath the SQUID gradiometer, and the SQUID gradiometer mount is adjusted so that the SQUID detection coil, that is, the bottom of the dewar, is perpendicular to, and nearly touching the place on the subjects head at which the measurement is to be taken. Once again, a Grass Model PS22A Photostimulator was used to trigger a strobe light at random intervals. This flash was used as the stimulus. The signal

47

used to fire the strobe was once again used to trigger the FFT analyzer. Once again, the Intel 80/20 computer was used to store the average of the 50 measurements on a 8 inch disk, which was used later to recovery the data so that it could be plotted out. The major difference in the experiment setup for Ricky, versus the experiment setup for the humans is that the beagle, Ricky, was lightly anesthetized to prevent him from too much movement. Pictures of the experiment setup are shown at the end of this chapter.

VER COMPARISON

In Figures 5-1 and 5-2 are two of the magnetoencephalo-graphic visual evoked response which were taken from the laboratory beagle, Ricky. While, Figure 5-3 is the electroencephalographic visual evoked response taken off of the visual cortex of Ricky by the AFIT Semiconductor Multielectrode Array, which was implanted on his brain. We expected to see a magnetoencephalographic visual evoked response with approximately the same latencies as the latencies measured by the AFIT array. Also, as we move the position at which the SQUID gradiometer is measuring the visual evoked response, we expected to see a phase reversal. It turns out that we did get approximately the same latencies as did the AFIT array. Also, we were able to get the phase reversal. We see that MEG.022 shown in Figure 5-1, and MEG.045 shown in Figure 5-2 could possibly be a phase reversal, but the best example of a phase reversal is from two of the plots in Appendix D. These two plots are MEG.057 and MEG.059.

```
RICKY        MEG.Ø22        RT-OC     LIGHTS-ON
1ØCPS AND NOTCH FILTERS  12.7-Ø3 V        VLN
26-SEP-83      Ø.Ø2598 SEC                       T

A
R

TSU
5Ø

AT

1.ØA    1Ø.A    B/16   SEC              Ø.2
```
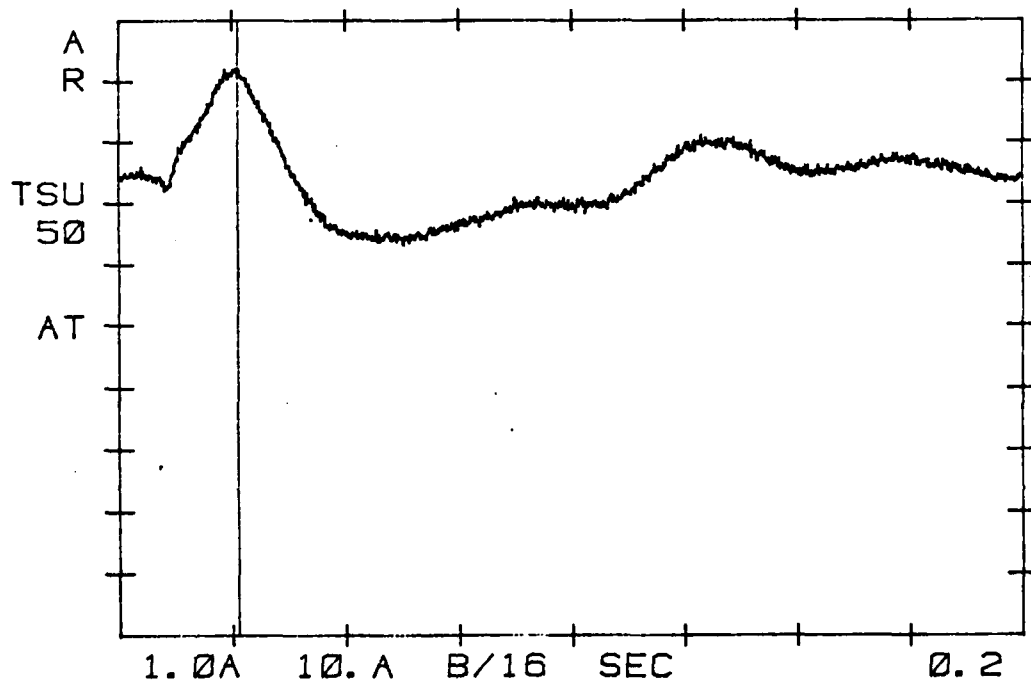
FIGURE 5-1

Ricky's VER

Figures 5-4 through Figure 5-11 shows several different
pictures taken of the dog experiment.

49

A
R

TSU
50

AT

5.0A   5.0D   B/2   SEC   0.2
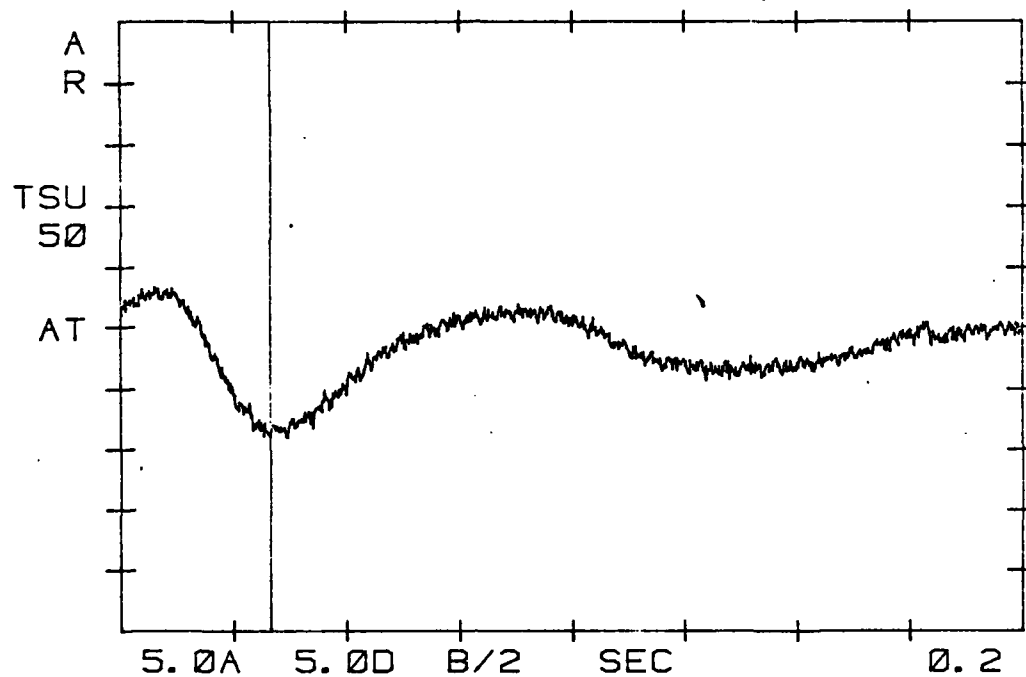
FIGURE 5-2

Ricky's VER

FIGURE 5-3

EEG VER

50
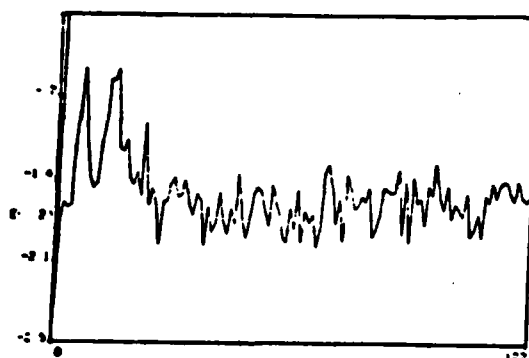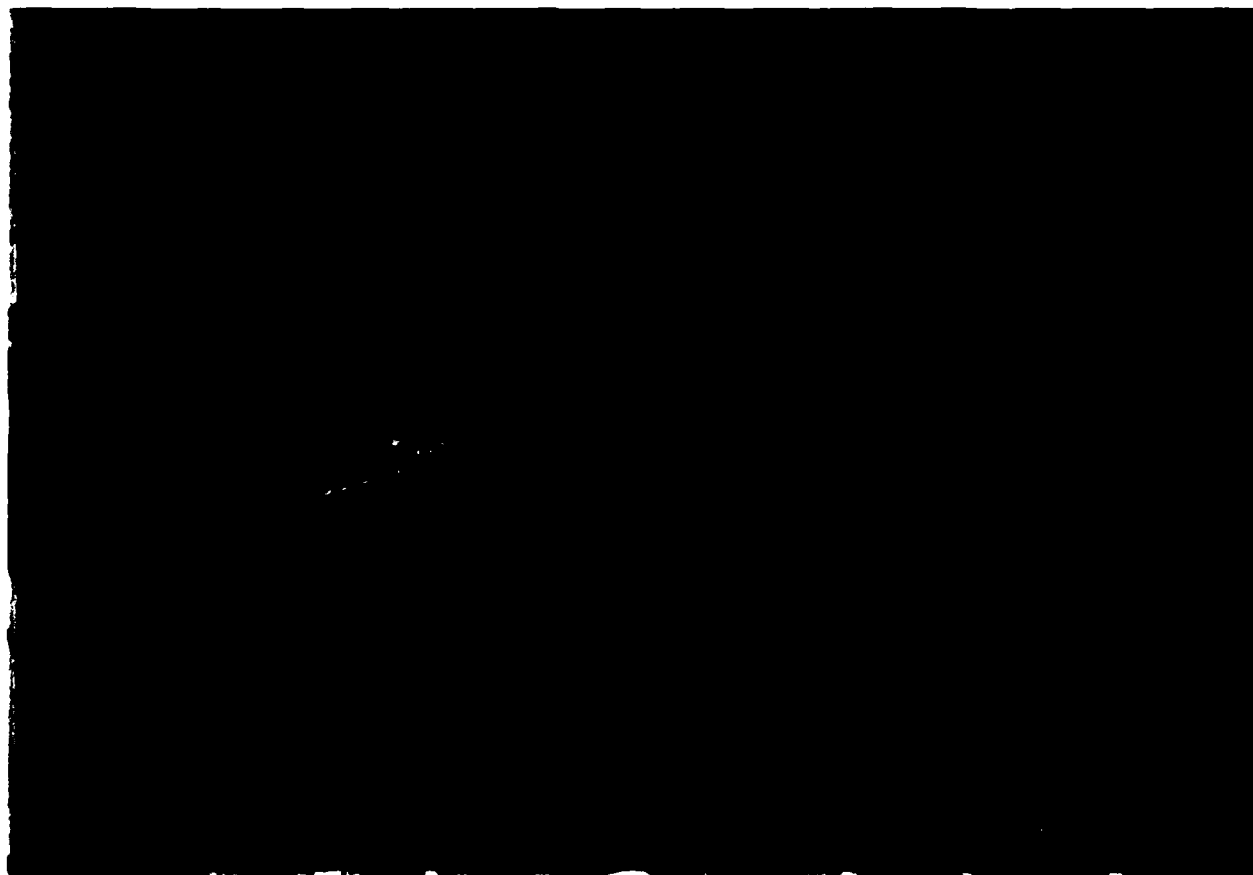
FIGURE 5-4

AUTHOR WITH EQUIPMENT

FIGURE 5-5

SQUID GRADIOMETER AND RICKY

52

FIGURE 5-6

SQUID, MOUNT, AND RICKY

53

FIGURE 5-7

SQUID POSITIONING EXAMPLE

54

FIGURE 5-8

BARB McFAWN WITH STROBE LIGHT
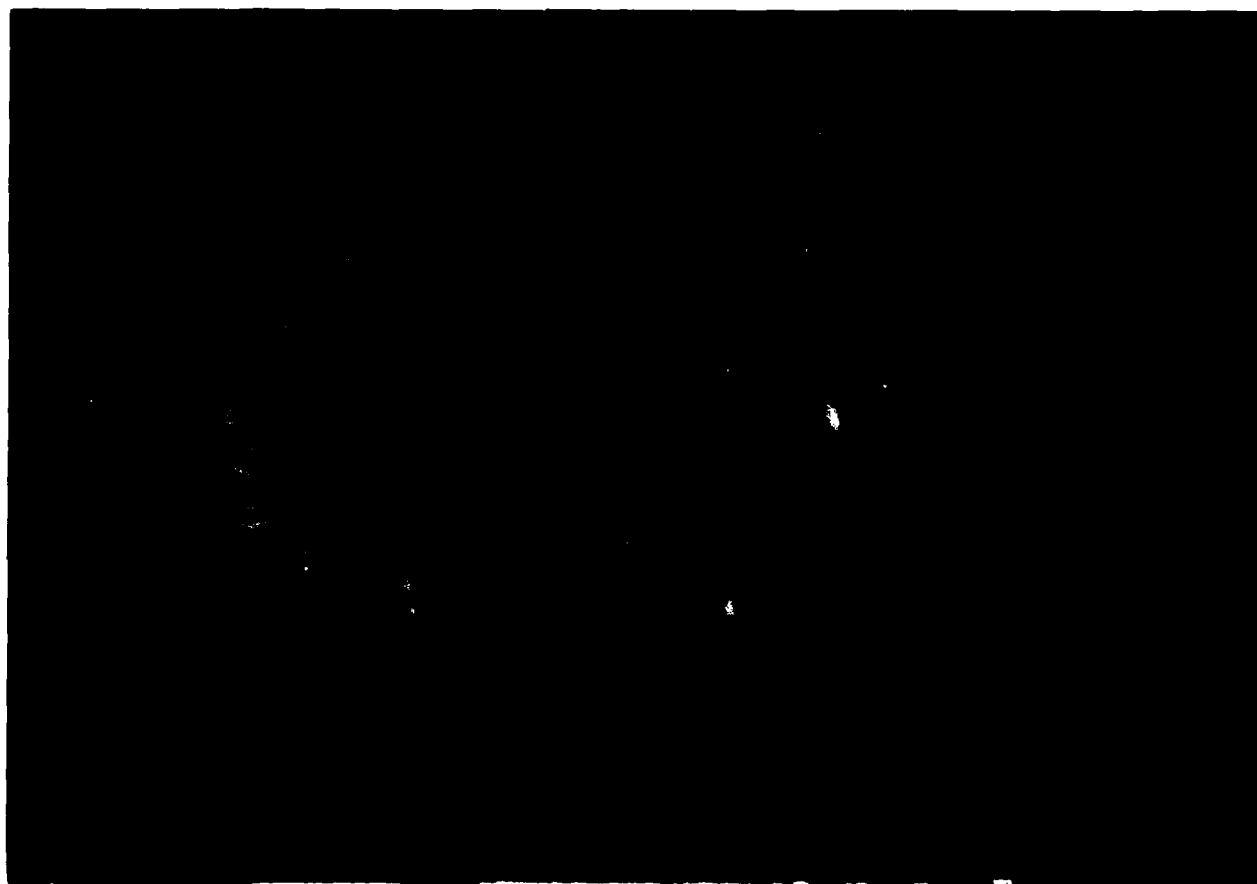
FIGURE 5-9

ALVA KARL MONITORING RICKY

<u>FIGURE 5-10</u>

DR. KABRISKY CHECKING A POSITION

57

FIGURE 5-11

DR. HATSELL POSITIONING RICKY

58

CHAPTER VI

CONCLUSION

DIPOLE MODEL

We saw that the predicted values in both the magnetic field and the surface potential had differences, especially in absolute value in relation to their measured values, but the wave shape of the measure magnetic field or surface potential correlated well with the calculated wave shape, except for distortions believed to be due to such factors as edge effects, the finite volume, and the lucite mounting block. Also, the conductivity of the saline solution may have been a factor in the surface potential case.

HUMAN VER

We saw some excellent plots of visual evoked responses in humans, long with some discussion into VER theory. Also, we saw that the 80 millisecond component of the visual evoked response taken by electroencephalographic means, also shows up in the magnetoencephalographic visual evoked response.

DOG VER

Once again we saw some good plots of visual evoked responses in a dog. We also conclude that the latency of the visual evoked response as measured by the AFIT implant is approximately the same as the latency measured by the SQUID gradiometer. This conclusion would tend to prove that the AFIT array seems to work.

CHAPTER VII

RECOMMENDATIONS

I recommend that further research be planned especially with a researcher looking into the feasibility of simultaneous magnetoencephalographic and electroencephalographic measurement. Also, more research be done in the area of determining means by which the SQUID gradiometer can be used as a diagnostic tool. For example, could a change in latencies of various evoked responses indicate deterioration of the visual system, or the onset of Multiple Sclerosis (MS) or Alzheimer's disease?

BIBLIOGRAPHY

1. Wooldridge, D. E. _The Machinery of the Brain_. New York: McGraw-Hill Book Company, 1963.

2. Lewis, P. and Rubenstein, D. _The Human Body_. New York: Bantam Book Company, 1971.

3. Callaway, E., Tuetius, P., and Koslow, S. _Event-Related Brain Potentials in Man_. New York: Academic Press, Inc, 1978.

4. Regan, D. _Evoked Potential in Psychology, Sensory Physiology, and Clinical Medicine_. London: Chapman and Hall, LTD. 1972.

5. Nuney, P. L. "A Study of Origin of the Time Dependencies of Scalp EEG: I -- Theoretical Basis," _IEEE Transaction on Biomedical Engineering, Vol. BME-28, No. 3_, 271-280. March 1981.

6. Nuney, P. L. "A Study of Origin of the Time Dependencies of Scalp EEG: II -- Experimental Support of Theory" _IEEE Transaction on Biomedical Engineering, Vol. BME-28, No. 3_, 281-293. March 1981.

7. Guyton, A. C. _Textbook of Medical Physiology_ (sixth edition). Philadephia: W. B. Saunders Company. 675-683, 1981.

8. Perry, N. W., Jr. and Childers, D. G. _The Human Visual Evoked Response_, Springfield, Illinois: Charles C. Thomas, Publisher, 1969.

9. Miller, J. A. "Wiretap on the Nervous System," _Science News, Vol 123_. 140-143.

10. Ratliff, F. "Inhibitory Interaction and the Detection and Enhancement of Contours," 183-203. The Rockefeller Institute.

11. Werblin, F. S. "The Control of Sensitivity of the Retina," _Scienitific American_. 71-79. January, 1973.

12. Lettvin, H. R. _et al_. "What the Frog's Eyes tells the Frog's Brain," _Processings of the IRE_. 1940-1951. November, 1959.

13. Lettvin, H. R. _et al_. "Two Remarks on the Visual System," _Sensory Communication_. 1962.

14. Peterson, E. L. "Visual Processing in the Leech Central Nervous System," _Nature Vol 303_. 240-242. 19 May 1983.

15.   Maffei, L. and Fiorentini, A.   "The Visual Cortex as a
        Spatial Frequency Analyser," Vision   Res   Vol 13.
        1255-1267, Pergamon Press, 1973.

16.   Glezer, V. D., Ivanoff, V.A., and Tscherlasch, T. A.
        "Investigation of Complex and Hypercomplex Receptive
        Fields of Visual Cortex of the Cat as Spatial Frequency
        Filters," Vision Res, Vol 13 1875-1904, Pergamon Press,
        1973.

17.   Kabrisky, M. et al "The First Cortical Implant of a
        Multiplexed   Multi-Electrode   Semiconductor   Brain
        Electrode," AIAA (Day/Cin) 83-1. 9-4-1 -- 9-4-3.

18.   Tatman, J. 1979. A Two-Dimensional Multielectrode
        Microprobe for the Visual Cortex, M.S.E.E. Thesis, Air
        Force   Institute   of   Technology,   AFIT/GE/EE/79-37,
        December, 1979.

19.   Duzer, V. and Turner, C. Principles of Superconductive
        Devices and Circuits. New York: Elsevier.

20.   ------."Low-Frequency Applications of Superconducting
        Quantum Interference Devices," Proceedings of the IEEE
        Vol 61, No. 1, January, 1973.

21.   Heringa, A. and et al. "Solution Methods of Electrical
        Field Problem in Physiology," IEEE Transactions on
        Biomedical Engineering, Vol 29, No. 1. 34-42. January,
        1982.

22.   Barr, R., et al. "Determining Surfaces Potentials from
        Current Dipoles with Application to Electrocardiography
        IEEE Transaction on Biomedical Engineering, Vol BME-13
        No. 2, 88-92. April, 1982.

23.   Williamson, S. and Kaufman, L. "Magnetic Fields of the
        Cerebral Cortex," Proceedings of the Third Interna-
        tional Workshop on Biomagnetism, Berlin (West) May
        1980.

24.   Cuffin, N. and Cohen, D. "Magnetic Fields of a Dipole
        in Special Volume Conductor Shapes," IEEE Transaction
        on Biomedical Engineering, Vol BME 24, No. 4 , 372-381.
        July, 1971.

25.   Cohen, D. and Cuffin, N. "Demostration of Useful
        Differences Between magnetoencephalogram and electro-
        encephalogram," Electroencephalography and Clinical
        Neurophysiology, Vol 56, 38-51, 1983.

26.   Erne, S. N. "SQUID Sensors," Biomagnetism: An
        Interdisciplinary Approach, New York: Plenum Press,
        69-84, 1983.

27. Zimmerman, J. E. "Magnetic Quantiies, Units, Materials, and Measurements," <u>Biomagnetism: An Interdisciplinary Approach</u>, New York: Plenum Press, 17-42, 1983.

28. Lehmann, H. P. "Signal Processing," <u>Biomagnetism: An Interdisciplinary Approach</u>, New York: Plenum Press, 591-624, 1983.

APPENDIX A

SINGLE DIPOLE MAGNETIC DATA

```
5 REM
10 REM   THESIS DIPOLE FIELD CALCULATION PROGRAM
20 REM   BFIELD AND VOLTAGE ( X100 )
30 REM   BY BOB MURRAY
40 REM
50 LPRINT CHR$(12)
60 INPUT "ENTER Z";Z
70 LPRINT TAB(15);"Z = ";Z
80 LPRINT TAB(15);"I = 8 MILLIAMPS"
90 LPRINT TAB(15);"L = .005 METERS":LPRINT
100 FOR I=-10 TO 10
110 FOR J=-10 TO 10
120 X=I/100
130 Y=J/100
140 T=4.D-12*X
150 F=0.0
160 B=((X[2+Y[2+(.015+Z)[2)[1.5)
170 F=-T/B
180 VF=(4.9D9)*F
190 LPRINT TAB(15);"B(";I;",";J;")=";F,TAB(15);"V(";I;",";J;")=";VF
200 NEXTJ
210 NEXTI
220 LPRINT CHR$(12)
230 INPUT"ANOTHER RUN";ANS$
240 IF(ANS$="Y") GOTO60
250 END
```

```
Z = .022
I = 8 MILLIAMPS
L = .005 METERS

B(-10 ,-10 )= 1.28051E-10          V(-10 ,-10 )= .627451
B(-10 ,-9 )= 1.47246E-10           V(-10 ,-9 )= .721507
B(-10 ,-8 )= 1.68875E-10           V(-10 ,-8 )= .827488
B(-10 ,-7 )= 1.92761E-10           V(-10 ,-7 )= .944528
B(-10 ,-6 )= 2.18409E-10           V(-10 ,-6 )= 1.0702
B(-10 ,-5 )= 2.44902E-10           V(-10 ,-5 )= 1.20002
B(-10 ,-4 )= 2.70832E-10           V(-10 ,-4 )= 1.32708
B(-10 ,-3 )= 2.94338E-10           V(-10 ,-3 )= 1.44226
B(-10 ,-2 )= 3.13293E-10           V(-10 ,-2 )= 1.53514
B(-10 ,-1 )= 3.25665E-10           V(-10 ,-1 )= 1.59576
B(-10 , 0 )= 3.29972E-10           V(-10 , 0 )= 1.61686
B(-10 , 1 )= 3.25665E-10           V(-10 , 1 )= 1.59576
B(-10 , 2 )= 3.13293E-10           V(-10 , 2 )= 1.53514
B(-10 , 3 )= 2.94338E-10           V(-10 , 3 )= 1.44226
B(-10 , 4 )= 2.70832E-10           V(-10 , 4 )= 1.32708
B(-10 , 5 )= 2.44902E-10           V(-10 , 5 )= 1.20002
B(-10 , 6 )= 2.18409E-10           V(-10 , 6 )= 1.0702
B(-10 , 7 )= 1.92761E-10           V(-10 , 7 )= .944528
B(-10 , 8 )= 1.68875E-10           V(-10 , 8 )= .827488
B(-10 , 9 )= 1.47246E-10           V(-10 , 9 )= .721507
B(-10 , 10 )= 1.28051E-10          V(-10 , 10 )= .627451
B(-9 ,-10 )= 1.32522E-10           V(-9 ,-10 )= .649356
B(-9 ,-9 )= 1.5459E-10             V(-9 ,-9 )= .757492
B(-9 ,-8 )= 1.80085E-10            V(-9 ,-8 )= .882418
B(-9 ,-7 )= 2.09008E-10            V(-9 ,-7 )= 1.02414
B(-9 ,-6 )= 2.40957E-10            V(-9 ,-6 )= 1.18069
B(-9 ,-5 )= 2.74926E-10            V(-9 ,-5 )= 1.34714
B(-9 ,-4 )= 3.09129E-10            V(-9 ,-4 )= 1.51473
B(-9 ,-3 )= 3.40955E-10            V(-9 ,-3 )= 1.67068
B(-9 ,-2 )= 3.67192E-10            V(-9 ,-2 )= 1.79924
B(-9 ,-1 )= 3.84594E-10            V(-9 ,-1 )= 1.88451
B(-9 , 0 )= 3.90703E-10            V(-9 , 0 )= 1.91444
B(-9 , 1 )= 3.84594E-10            V(-9 , 1 )= 1.88451
B(-9 , 2 )= 3.67192E-10            V(-9 , 2 )= 1.79924
B(-9 , 3 )= 3.40955E-10            V(-9 , 3 )= 1.67068
B(-9 , 4 )= 3.09129E-10            V(-9 , 4 )= 1.51473
B(-9 , 5 )= 2.74926E-10            V(-9 , 5 )= 1.34714
B(-9 , 6 )= 2.40957E-10            V(-9 , 6 )= 1.18069
B(-9 , 7 )= 2.09008E-10            V(-9 , 7 )= 1.02414
B(-9 , 8 )= 1.80085E-10            V(-9 , 8 )= .882418
B(-9 , 9 )= 1.5459E-10             V(-9 , 9 )= .757492
B(-9 , 10 )= 1.32522E-10           V(-9 , 10 )= .649356
B(-8 ,-10 )= 1.351E-10             V(-8 ,-10 )= .66199
B(-8 ,-9 )= 1.60076E-10            V(-8 ,-9 )= .784371
B(-8 ,-8 )= 1.89732E-10            V(-8 ,-8 )= .929687
B(-8 ,-7 )= 2.24407E-10            V(-8 ,-7 )= 1.09959
B(-8 ,-6 )= 2.63977E-10            V(-8 ,-6 )= 1.29349
B(-8 ,-5 )= 3.07509E-10            V(-8 ,-5 )= 1.50679
B(-8 ,-4 )= 3.52866E-10            V(-8 ,-4 )= 1.72904
B(-8 ,-3 )= 3.96457E-10            V(-8 ,-3 )= 1.94264
B(-8 ,-2 )= 4.33408E-10            V(-8 ,-2 )= 2.1237
B(-8 ,-1 )= 4.58428E-10            V(-8 ,-1 )= 2.2463
B(-8 , 0 )= 4.67307E-10            V(-8 , 0 )= 2.2898
B(-8 , 1 )= 4.58428E-10            V(-8 , 1 )= 2.2463
B(-8 , 2 )= 4.33408E-10            V(-8 , 2 )= 2.1237
B(-8 , 3 )= 3.96457E-10            V(-8 , 3 )= 1.94264
B(-8 , 4 )= 3.52866E-10            V(-8 , 4 )= 1.72904
B(-8 , 5 )= 3.07509E-10            V(-8 , 5 )= 1.50679
B(-8 , 6 )= 2.63977E-10            V(-8 , 6 )= 1.29349
B(-8 , 7 )= 2.24407E-10            V(-8 , 7 )= 1.09959
B(-8 , 8 )= 1.89732E-10            V(-8 , 8 )= .929687
```

```
B(-8 , 9 )= 1.60076E-10          V(-8 , 9 )= .784371
B(-8 , 10 )= 1.351E-10           V(-8 , 10 )= .66199
B(-7 ,-10 )= 1.34933E-10         V(-7 ,-10 )= .661169
B(-7 ,-9 )= 1.62562E-10          V(-7 ,-9 )= .796552
B(-7 ,-8 )= 1.96356E-10          V(-7 ,-8 )= .962145
B(-7 ,-7 )= 2.37212E-10          V(-7 ,-7 )= 1.16234
B(-7 ,-6 )= 2.85594E-10          V(-7 ,-6 )= 1.39941
B(-7 ,-5 )= 3.40983E-10          V(-7 ,-5 )= 1.67082
B(-7 ,-4 )= 4.01124E-10          V(-7 ,-4 )= 1.96551
B(-7 ,-3 )= 4.61286E-10          V(-7 ,-3 )= 2.2603
B(-7 ,-2 )= 5.14123E-10          V(-7 ,-2 )= 2.5192
B(-7 ,-1 )= 5.50873E-10          V(-7 ,-1 )= 2.69928
B(-7 , 0 )= 5.64106E-10          V(-7 , 0 )= 2.76412
B(-7 , 1 )= 5.50873E-10          V(-7 , 1 )= 2.69928
B(-7 , 2 )= 5.14123E-10          V(-7 , 2 )= 2.5192
B(-7 , 3 )= 4.61286E-10          V(-7 , 3 )= 2.2603
B(-7 , 4 )= 4.01124E-10          V(-7 , 4 )= 1.96551
B(-7 , 5 )= 3.40983E-10          V(-7 , 5 )= 1.67082
B(-7 , 6 )= 2.85594E-10          V(-7 , 6 )= 1.39941
B(-7 , 7 )= 2.37212E-10          V(-7 , 7 )= 1.16234
B(-7 , 8 )= 1.96356E-10          V(-7 , 8 )= .962145
B(-7 , 9 )= 1.62562E-10          V(-7 , 9 )= .796552
B(-7 , 10 )= 1.34933E-10         V(-7 , 10 )= .661169
B(-6 ,-10 )= 1.31045E-10         V(-6 ,-10 )= .642123
B(-6 ,-9 )= 1.60638E-10          V(-6 ,-9 )= .787125
B(-6 ,-8 )= 1.97983E-10          V(-6 ,-8 )= .970116
B(-6 ,-7 )= 2.44794E-10          V(-6 ,-7 )= 1.19949
B(-6 ,-6 )= 3.02563E-10          V(-6 ,-6 )= 1.48256
B(-6 ,-5 )= 3.71807E-10          V(-6 ,-5 )= 1.82185
B(-6 ,-4 )= 4.50778E-10          V(-6 ,-4 )= 2.20881
B(-6 ,-3 )= 5.33783E-10          V(-6 ,-3 )= 2.61554
B(-6 ,-2 )= 6.10058E-10          V(-6 ,-2 )= 2.98928
B(-6 ,-1 )= 6.65009E-10          V(-6 ,-1 )= 3.25855
B(-6 , 0 )= 6.85185E-10          V(-6 , 0 )= 3.35741
B(-6 , 1 )= 6.65009E-10          V(-6 , 1 )= 3.25855
B(-6 , 2 )= 6.10058E-10          V(-6 , 2 )= 2.98928
B(-6 , 3 )= 5.33783E-10          V(-6 , 3 )= 2.61554
B(-6 , 4 )= 4.50778E-10          V(-6 , 4 )= 2.20881
B(-6 , 5 )= 3.71807E-10          V(-6 , 5 )= 1.82185
B(-6 , 6 )= 3.02563E-10          V(-6 , 6 )= 1.48256
B(-6 , 7 )= 2.44794E-10          V(-6 , 7 )= 1.19949
B(-6 , 8 )= 1.97983E-10          V(-6 , 8 )= .970116
B(-6 , 9 )= 1.60638E-10          V(-6 , 9 )= .787125
B(-6 , 10 )= 1.31045E-10         V(-6 , 10 )= .642123
B(-5 ,-10 )= 1.22451E-10         V(-5 ,-10 )= .60001
B(-5 ,-9 )= 1.52737E-10          V(-5 ,-9 )= .748409
B(-5 ,-8 )= 1.92193E-10          V(-5 ,-8 )= .941746
B(-5 ,-7 )= 2.4356E-10           V(-5 ,-7 )= 1.19344
B(-5 ,-6 )= 3.09839E-10          V(-5 ,-6 )= 1.51821
B(-5 ,-5 )= 3.9348E-10           V(-5 ,-5 )= 1.92805
B(-5 ,-4 )= 4.94502E-10          V(-5 ,-4 )= 2.42306
B(-5 ,-3 )= 6.0728E-10           V(-5 ,-3 )= 2.97567
B(-5 ,-2 )= 7.17036E-10          V(-5 ,-2 )= 3.51348
B(-5 ,-1 )= 7.9985E-10           V(-5 ,-1 )= 3.91926
B(-5 , 0 )= 8.31059E-10          V(-5 , 0 )= 4.07219
B(-5 , 1 )= 7.9985E-10           V(-5 , 1 )= 3.91926
B(-5 , 2 )= 7.17036E-10          V(-5 , 2 )= 3.51348
B(-5 , 3 )= 6.0728E-10           V(-5 , 3 )= 2.97567
B(-5 , 4 )= 4.94502E-10          V(-5 , 4 )= 2.42306
B(-5 , 5 )= 3.9348E-10           V(-5 , 5 )= 1.92805
B(-5 , 6 )= 3.09839E-10          V(-5 , 6 )= 1.51821
B(-5 , 7 )= 2.4356E-10           V(-5 , 7 )= 1.19344
B(-5 , 8 )= 1.92193E-10          V(-5 , 8 )= .941746
B(-5 , 9 )= 1.52737E-10          V(-5 , 9 )= .748409
B(-5 , 10 )= 1.22451E-10         V(-5 , 10 )= .60001
B(-4 ,-10 )= 1.08333E-10         V(-4 ,-10 )= .530831
```

```
B(-4 ,-9 )= 1.37391E-10        V(-4 ,-9 )= .673214
B(-4 ,-8 )= 1.76433E-10        V(-4 ,-8 )= .864522
B(-4 ,-7 )= 2.29214E-10        V(-4 ,-7 )= 1.12315
B(-4 ,-6 )= 3.00518E-10        V(-4 ,-6 )= 1.47254
B(-4 ,-5 )= 3.95602E-10        V(-4 ,-5 )= 1.93845
B(-4 ,-4 )= 5.1807E-10         V(-4 ,-4 )= 2.53854
B(-4 ,-3 )= 6.64847E-10        V(-4 ,-3 )= 3.25775
B(-4 ,-2 )= 8.18217E-10        V(-4 ,-2 )= 4.00926
B(-4 ,-1 )= 9.41075E-10        V(-4 ,-1 )= 4.61127
B(-4 , 0 )= 9.89019E-10        V(-4 , 0 )= 4.84619
B(-4 , 1 )= 9.41075E-10        V(-4 , 1 )= 4.61127
B(-4 , 2 )= 8.18217E-10        V(-4 , 2 )= 4.00926
B(-4 , 3 )= 6.64847E-10        V(-4 , 3 )= 3.25775
B(-4 , 4 )= 5.1807E-10         V(-4 , 4 )= 2.53854
B(-4 , 5 )= 3.95602E-10        V(-4 , 5 )= 1.93845
B(-4 , 6 )= 3.00518E-10        V(-4 , 6 )= 1.47254
B(-4 , 7 )= 2.29214E-10        V(-4 , 7 )= 1.12315
B(-4 , 8 )= 1.76433E-10        V(-4 , 8 )= .864522
B(-4 , 9 )= 1.37391E-10        V(-4 , 9 )= .673214
B(-4 , 10 )= 1.08333E-10       V(-4 , 10 )= .530831
B(-3 ,-10 )= 8.83014E-11       V(-3 ,-10 )= .432677
B(-3 ,-9 )= 1.13652E-10        V(-3 ,-9 )= .556894
B(-3 ,-8 )= 1.48671E-10        V(-3 ,-8 )= .72849
B(-3 ,-7 )= 1.97694E-10        V(-3 ,-7 )= .968701
B(-3 ,-6 )= 2.66892E-10        V(-3 ,-6 )= 1.30777
B(-3 ,-5 )= 3.64368E-10        V(-3 ,-5 )= 1.7854
B(-3 ,-4 )= 4.98635E-10        V(-3 ,-4 )= 2.44331
B(-3 ,-3 )= 6.72663E-10        V(-3 ,-3 )= 3.29605
B(-3 ,-2 )= 8.70279E-10        V(-3 ,-2 )= 4.26437
B(-3 ,-1 )= 1.04072E-09        V(-3 ,-1 )= 5.09952
B(-3 , 0 )= 1.11027E-09        V(-3 , 0 )= 5.44033
B(-3 , 1 )= 1.04072E-09        V(-3 , 1 )= 5.09952
B(-3 , 2 )= 8.70279E-10        V(-3 , 2 )= 4.26437
B(-3 , 3 )= 6.72663E-10        V(-3 , 3 )= 3.29605
B(-3 , 4 )= 4.98635E-10        V(-3 , 4 )= 2.44331
B(-3 , 5 )= 3.64368E-10        V(-3 , 5 )= 1.7854
B(-3 , 6 )= 2.66892E-10        V(-3 , 6 )= 1.30777
B(-3 , 7 )= 1.97694E-10        V(-3 , 7 )= .968701
B(-3 , 8 )= 1.48671E-10        V(-3 , 8 )= .72849
B(-3 , 9 )= 1.13652E-10        V(-3 , 9 )= .556894
B(-3 , 10 )= 8.83014E-11       V(-3 , 10 )= .432677
B(-2 ,-10 )= 6.26586E-11       V(-2 ,-10 )= .307027
B(-2 ,-9 )= 8.15981E-11        V(-2 ,-9 )= .399831
B(-2 ,-8 )= 1.08352E-10        V(-2 ,-8 )= .530924
B(-2 ,-7 )= 1.46892E-10        V(-2 ,-7 )= .719772
B(-2 ,-6 )= 2.03353E-10        V(-2 ,-6 )= .996428
B(-2 ,-5 )= 2.86814E-10        V(-2 ,-5 )= 1.40539
B(-2 ,-4 )= 4.09109E-10        V(-2 ,-4 )= 2.00463
B(-2 ,-3 )= 5.80186E-10        V(-2 ,-3 )= 2.84291
B(-2 ,-2 )= 7.91955E-10        V(-2 ,-2 )= 3.88058
B(-2 ,-1 )= 9.90093E-10        V(-2 ,-1 )= 4.85145
B(-2 , 0 )= 1.07522E-09        V(-2 , 0 )= 5.26858
B(-2 , 1 )= 9.90093E-10        V(-2 , 1 )= 4.85145
B(-2 , 2 )= 7.91955E-10        V(-2 , 2 )= 3.88058
B(-2 , 3 )= 5.80186E-10        V(-2 , 3 )= 2.84291
B(-2 , 4 )= 4.09109E-10        V(-2 , 4 )= 2.00463
B(-2 , 5 )= 2.86814E-10        V(-2 , 5 )= 1.40539
B(-2 , 6 )= 2.03353E-10        V(-2 , 6 )= .996428
B(-2 , 7 )= 1.46892E-10        V(-2 , 7 )= .719772
B(-2 , 8 )= 1.08352E-10        V(-2 , 8 )= .530924
B(-2 , 9 )= 8.15981E-11        V(-2 , 9 )= .399831
B(-2 , 10 )= 6.26586E-11       V(-2 , 10 )= .307027
B(-1 ,-10 )= 3.25665E-11       V(-1 ,-10 )= .159576
B(-1 ,-9 )= 4.27327E-11        V(-1 ,-9 )= .20939
B(-1 ,-8 )= 5.73035E-11        V(-1 ,-8 )= .280787
B(-1 ,-7 )= 7.86961E-11        V(-1 ,-7 )= .385611
```

```
B(-1 ,-6 )= 1.10835E-10          V(-1 ,-6 )= .543091
B(-1 ,-5 )= 1.5997E-10           V(-1 ,-5 )= .783852
B(-1 ,-4 )= 2.35269E-10          V(-1 ,-4 )= 1.15282
B(-1 ,-3 )= 3.46906E-10          V(-1 ,-3 )= 1.69984
B(-1 ,-2 )= 4.95046E-10          V(-1 ,-2 )= 2.42573
B(-1 ,-1 )= 6.43614E-10          V(-1 ,-1 )= 3.15371
B(-1 , 0 )= 7.1044E-10           V(-1 , 0 )= 3.48116
B(-1 , 1 )= 6.43614E-10          V(-1 , 1 )= 3.15371
B(-1 , 2 )= 4.95046E-10          V(-1 , 2 )= 2.42573
B(-1 , 3 )= 3.46906E-10          V(-1 , 3 )= 1.69984
B(-1 , 4 )= 2.35269E-10          V(-1 , 4 )= 1.15282
B(-1 , 5 )= 1.5997E-10           V(-1 , 5 )= .783852
B(-1 , 6 )= 1.10835E-10          V(-1 , 6 )= .543091
B(-1 , 7 )= 7.86961E-11          V(-1 , 7 )= .385611
B(-1 , 8 )= 5.73035E-11          V(-1 , 8 )= .280787
B(-1 , 9 )= 4.27327E-11          V(-1 , 9 )= .20939
B(-1 , 10 )= 3.25665E-11         V(-1 , 10 )= .159576
B( 0 ,-10 )= 0     V( 0 ,-10 )= 0
B( 0 ,-9 )= 0      V( 0 ,-9 )= 0
B( 0 ,-8 )= 0      V( 0 ,-8 )= 0
B( 0 ,-7 )= 0      V( 0 ,-7 )= 0
B( 0 ,-6 )= 0      V( 0 ,-6 )= 0
B( 0 ,-5 )= 0      V( 0 ,-5 )= 0
B( 0 ,-4 )= 0      V( 0 ,-4 )= 0
B( 0 ,-3 )= 0      V( 0 ,-3 )= 0
B( 0 ,-2 )= 0      V( 0 ,-2 )= 0
B( 0 ,-1 )= 0      V( 0 ,-1 )= 0
B( 0 , 0 )= 0      V( 0 , 0 )= 0
B( 0 , 1 )= 0      V( 0 , 1 )= 0
B( 0 , 2 )= 0      V( 0 , 2 )= 0
B( 0 , 3 )= 0      V( 0 , 3 )= 0
B( 0 , 4 )= 0      V( 0 , 4 )= 0
B( 0 , 5 )= 0      V( 0 , 5 )= 0
B( 0 , 6 )= 0      V( 0 , 6 )= 0
B( 0 , 7 )= 0      V( 0 , 7 )= 0
B( 0 , 8 )= 0      V( 0 , 8 )= 0
B( 0 , 9 )= 0      V( 0 , 9 )= 0
B( 0 , 10 )= 0     V( 0 , 10 )= 0
B( 1 ,-10 )=-3.25665E-11         V( 1 ,-10 )=-.159576
B( 1 ,-9 )=-4.27327E-11          V( 1 ,-9 )=-.20939
B( 1 ,-8 )=-5.73035E-11          V( 1 ,-8 )=-.280787
B( 1 ,-7 )=-7.86961E-11          V( 1 ,-7 )=-.385611
B( 1 ,-6 )=-1.10835E-10          V( 1 ,-6 )=-.543091
B( 1 ,-5 )=-1.5997E-10           V( 1 ,-5 )=-.783852
B( 1 ,-4 )=-2.35269E-10          V( 1 ,-4 )=-1.15282
B( 1 ,-3 )=-3.46906E-10          V( 1 ,-3 )=-1.69984
B( 1 ,-2 )=-4.95046E-10          V( 1 ,-2 )=-2.42573
B( 1 ,-1 )=-6.43614E-10          V( 1 ,-1 )=-3.15371
B( 1 , 0 )=-7.1044E-10           V( 1 , 0 )=-3.48116
B( 1 , 1 )=-6.43614E-10          V( 1 , 1 )=-3.15371
B( 1 , 2 )=-4.95046E-10          V( 1 , 2 )=-2.42573
B( 1 , 3 )=-3.46906E-10          V( 1 , 3 )=-1.69984
B( 1 , 4 )=-2.35269E-10          V( 1 , 4 )=-1.15282
B( 1 , 5 )=-1.5997E-10           V( 1 , 5 )=-.783852
B( 1 , 6 )=-1.10835E-10          V( 1 , 6 )=-.543091
B( 1 , 7 )=-7.86961E-11          V( 1 , 7 )=-.385611
B( 1 , 8 )=-5.73035E-11          V( 1 , 8 )=-.280787
B( 1 , 9 )=-4.27327E-11          V( 1 , 9 )=-.20939
B( 1 , 10 )=-3.25665E-11         V( 1 , 10 )=-.159576
B( 2 ,-10 )=-6.26586E-11         V( 2 ,-10 )=-.307027
B( 2 ,-9 )=-8.15981E-11          V( 2 ,-9 )=-.399831
B( 2 ,-8 )=-1.08352E-10          V( 2 ,-8 )=-.530924
B( 2 ,-7 )=-1.46892E-10          V( 2 ,-7 )=-.719772
B( 2 ,-6 )=-2.03353E-10          V( 2 ,-6 )=-.996428
B( 2 ,-5 )=-2.86814E-10          V( 2 ,-5 )=-1.40539
B( 2 ,-4 )=-4.09109E-10          V( 2 ,-4 )=-2.00463
```

```
B( 2 ,-3 )=-5.80186E-10        V( 2 ,-3 )=-2.84291
B( 2 ,-2 )=-7.91955E-10        V( 2 ,-2 )=-3.88058
B( 2 ,-1 )=-9.90093E-10        V( 2 ,-1 )=-4.85145
B( 2 , 0 )=-1.07522E-09        V( 2 , 0 )=-5.26858
B( 2 , 1 )=-9.90093E-10        V( 2 , 1 )=-4.85145
B( 2 , 2 )=-7.91955E-10        V( 2 , 2 )=-3.88058
B( 2 , 3 )=-5.80186E-10        V( 2 , 3 )=-2.84291
B( 2 , 4 )=-4.09109E-10        V( 2 , 4 )=-2.00463
B( 2 , 5 )=-2.86814E-10        V( 2 , 5 )=-1.40539
B( 2 , 6 )=-2.03353E-10        V( 2 , 6 )=-.996428
B( 2 , 7 )=-1.46892E-10        V( 2 , 7 )=-.719772
B( 2 , 8 )=-1.08352E-10        V( 2 , 8 )=-.530924
B( 2 , 9 )=-8.15981E-11        V( 2 , 9 )=-.399831
B( 2 , 10 )=-6.26586E-11       V( 2 , 10 )=-.307027
B( 3 ,-10 )=-8.83014E-11       V( 3 ,-10 )=-.432677
B( 3 ,-9 )=-1.13652E-10        V( 3 ,-9 )=-.556894
B( 3 ,-8 )=-1.48671E-10        V( 3 ,-8 )=-.72849
B( 3 ,-7 )=-1.97694E-10        V( 3 ,-7 )=-.968701
B( 3 ,-6 )=-2.66892E-10        V( 3 ,-6 )=-1.30777
B( 3 ,-5 )=-3.64368E-10        V( 3 ,-5 )=-1.7854
B( 3 ,-4 )=-4.98635E-10        V( 3 ,-4 )=-2.44331
B( 3 ,-3 )=-6.72663E-10        V( 3 ,-3 )=-3.29605
B( 3 ,-2 )=-8.70279E-10        V( 3 ,-2 )=-4.26437
B( 3 ,-1 )=-1.04072E-09        V( 3 ,-1 )=-5.09952
B( 3 , 0 )=-1.11027E-09        V( 3 , 0 )=-5.44033
B( 3 , 1 )=-1.04072E-09        V( 3 , 1 )=-5.09952
B( 3 , 2 )=-8.70279E-10        V( 3 , 2 )=-4.26437
B( 3 , 3 )=-6.72663E-10        V( 3 , 3 )=-3.29605
B( 3 , 4 )=-4.98635E-10        V( 3 , 4 )=-2.44331
B( 3 , 5 )=-3.64368E-10        V( 3 , 5 )=-1.7854
B( 3 , 6 )=-2.66892E-10        V( 3 , 6 )=-1.30777
B( 3 , 7 )=-1.97694E-10        V( 3 , 7 )=-.968701
B( 3 , 8 )=-1.48671E-10        V( 3 , 8 )=-.72849
B( 3 , 9 )=-1.13652E-10        V( 3 , 9 )=-.556894
B( 3 , 10 )=-8.83014E-11       V( 3 , 10 )=-.432677
B( 4 ,-10 )=-1.08333E-10       V( 4 ,-10 )=-.530831
B( 4 ,-9 )=-1.37391E-10        V( 4 ,-9 )=-.673214
B( 4 ,-8 )=-1.76433E-10        V( 4 ,-8 )=-.864522
B( 4 ,-7 )=-2.29214E-10        V( 4 ,-7 )=-1.12315
B( 4 ,-6 )=-3.00518E-10        V( 4 ,-6 )=-1.47254
B( 4 ,-5 )=-3.95602E-10        V( 4 ,-5 )=-1.93845
B( 4 ,-4 )=-5.1807E-10         V( 4 ,-4 )=-2.53854
B( 4 ,-3 )=-6.64847E-10        V( 4 ,-3 )=-3.25775
B( 4 ,-2 )=-8.18217E-10        V( 4 ,-2 )=-4.00926
B( 4 ,-1 )=-9.41075E-10        V( 4 ,-1 )=-4.61127
B( 4 , 0 )=-9.89019E-10        V( 4 , 0 )=-4.84619
B( 4 , 1 )=-9.41075E-10        V( 4 , 1 )=-4.61127
B( 4 , 2 )=-8.18217E-10        V( 4 , 2 )=-4.00926
B( 4 , 3 )=-6.64847E-10        V( 4 , 3 )=-3.25775
B( 4 , 4 )=-5.1807E-10         V( 4 , 4 )=-2.53854
B( 4 , 5 )=-3.95602E-10        V( 4 , 5 )=-1.93845
B( 4 , 6 )=-3.00518E-10        V( 4 , 6 )=-1.47254
B( 4 , 7 )=-2.29214E-10        V( 4 , 7 )=-1.12315
B( 4 , 8 )=-1.76433E-10        V( 4 , 8 )=-.864522
B( 4 , 9 )=-1.37391E-10        V( 4 , 9 )=-.673214
B( 4 , 10 )=-1.08333E-10       V( 4 , 10 )=-.530831
B( 5 ,-10 )=-1.22451E-10       V( 5 ,-10 )=-.60001
B( 5 ,-9 )=-1.52737E-10        V( 5 ,-9 )=-.748409
B( 5 ,-8 )=-1.92193E-10        V( 5 ,-8 )=-.941746
B( 5 ,-7 )=-2.4356E-10         V( 5 ,-7 )=-1.19344
B( 5 ,-6 )=-3.09839E-10        V( 5 ,-6 )=-1.51821
B( 5 ,-5 )=-3.9348E-10         V( 5 ,-5 )=-1.92805
B( 5 ,-4 )=-4.94502E-10        V( 5 ,-4 )=-2.42306
B( 5 ,-3 )=-6.0728E-10         V( 5 ,-3 )=-2.97567
B( 5 ,-2 )=-7.17036E-10        V( 5 ,-2 )=-3.51348
B( 5 ,-1 )=-7.9985E-10         V( 5 ,-1 )=-3.91926
```

```
B( 5 , 0 )=-8.31059E-10        V( 5 , 0 )=-4.07219
B( 5 , 1 )=-7.9985E-10         V( 5 , 1 )=-3.91926
B( 5 , 2 )=-7.17036E-10        V( 5 , 2 )=-3.51348
B( 5 , 3 )=-6.0728E-10         V( 5 , 3 )=-2.97567
B( 5 , 4 )=-4.94502E-10        V( 5 , 4 )=-2.42306
B( 5 , 5 )=-3.9348E-10         V( 5 , 5 )=-1.92805
B( 5 , 6 )=-3.09839E-10        V( 5 , 6 )=-1.51821
B( 5 , 7 )=-2.4356E-10         V( 5 , 7 )=-1.19344
B( 5 , 8 )=-1.92193E-10        V( 5 , 8 )=-.941746
B( 5 , 9 )=-1.52737E-10        V( 5 , 9 )=-.748409
B( 5 , 10 )=-1.22451E-10       V( 5 , 10 )=-.60001
B( 6 ,-10 )=-1.31045E-10       V( 6 ,-10 )=-.642123
B( 6 ,-9 )=-1.60638E-10        V( 6 ,-9 )=-.787125
B( 6 ,-8 )=-1.97983E-10        V( 6 ,-8 )=-.970116
B( 6 ,-7 )=-2.44794E-10        V( 6 ,-7 )=-1.19949
B( 6 ,-6 )=-3.02563E-10        V( 6 ,-6 )=-1.48256
B( 6 ,-5 )=-3.71807E-10        V( 6 ,-5 )=-1.82185
B( 6 ,-4 )=-4.50778E-10        V( 6 ,-4 )=-2.20881
B( 6 ,-3 )=-5.33783E-10        V( 6 ,-3 )=-2.61554
B( 6 ,-2 )=-6.10058E-10        V( 6 ,-2 )=-2.98928
B( 6 ,-1 )=-6.65009E-10        V( 6 ,-1 )=-3.25855
B( 6 , 0 )=-6.85185E-10        V( 6 , 0 )=-3.35741
B( 6 , 1 )=-6.65009E-10        V( 6 , 1 )=-3.25855
B( 6 , 2 )=-6.10058E-10        V( 6 , 2 )=-2.98928
B( 6 , 3 )=-5.33783E-10        V( 6 , 3 )=-2.61554
B( 6 , 4 )=-4.50778E-10        V( 6 , 4 )=-2.20881
B( 6 , 5 )=-3.71807E-10        V( 6 , 5 )=-1.82185
B( 6 , 6 )=-3.02563E-10        V( 6 , 6 )=-1.48256
B( 6 , 7 )=-2.44794E-10        V( 6 , 7 )=-1.19949
B( 6 , 8 )=-1.97983E-10        V( 6 , 8 )=-.970116
B( 6 , 9 )=-1.60638E-10        V( 6 , 9 )=-.787125
B( 6 , 10 )=-1.31045E-10       V( 6 , 10 )=-.642123
B( 7 ,-10 )=-1.34933E-10       V( 7 ,-10 )=-.661169
B( 7 ,-9 )=-1.62562E-10        V( 7 ,-9 )=-.796552
B( 7 ,-8 )=-1.96356E-10        V( 7 ,-8 )=-.962145
B( 7 ,-7 )=-2.37212E-10        V( 7 ,-7 )=-1.16234
B( 7 ,-6 )=-2.85594E-10        V( 7 ,-6 )=-1.39941
B( 7 ,-5 )=-3.40983E-10        V( 7 ,-5 )=-1.67082
B( 7 ,-4 )=-4.01124E-10        V( 7 ,-4 )=-1.96551
B( 7 ,-3 )=-4.61286E-10        V( 7 ,-3 )=-2.2603
B( 7 ,-2 )=-5.14123E-10        V( 7 ,-2 )=-2.5192
B( 7 ,-1 )=-5.50873E-10        V( 7 ,-1 )=-2.69928
B( 7 , 0 )=-5.64106E-10        V( 7 , 0 )=-2.76412
B( 7 , 1 )=-5.50873E-10        V( 7 , 1 )=-2.69928
B( 7 , 2 )=-5.14123E-10        V( 7 , 2 )=-2.5192
B( 7 , 3 )=-4.61286E-10        V( 7 , 3 )=-2.2603
B( 7 , 4 )=-4.01124E-10        V( 7 , 4 )=-1.96551
B( 7 , 5 )=-3.40983E-10        V( 7 , 5 )=-1.67082
B( 7 , 6 )=-2.85594E-10        V( 7 , 6 )=-1.39941
B( 7 , 7 )=-2.37212E-10        V( 7 , 7 )=-1.16234
B( 7 , 8 )=-1.96356E-10        V( 7 , 8 )=-.962145
B( 7 , 9 )=-1.62562E-10        V( 7 , 9 )=-.796552
B( 7 , 10 )=-1.34933E-10       V( 7 , 10 )=-.661169
B( 8 ,-10 )=-1.351E-10         V( 8 ,-10 )=-.66199
B( 8 ,-9 )=-1.60076E-10        V( 8 ,-9 )=-.784371
B( 8 ,-8 )=-1.89732E-10        V( 8 ,-8 )=-.929687
B( 8 ,-7 )=-2.24407E-10        V( 8 ,-7 )=-1.09959
B( 8 ,-6 )=-2.63977E-10        V( 8 ,-6 )=-1.29349
B( 8 ,-5 )=-3.07509E-10        V( 8 ,-5 )=-1.50679
B( 8 ,-4 )=-3.52866E-10        V( 8 ,-4 )=-1.72904
B( 8 ,-3 )=-3.96457E-10        V( 8 ,-3 )=-1.94264
B( 8 ,-2 )=-4.33408E-10        V( 8 ,-2 )=-2.1237
B( 8 ,-1 )=-4.58428E-10        V( 8 ,-1 )=-2.2463
B( 8 , 0 )=-4.67307E-10        V( 8 , 0 )=-2.2898
B( 8 , 1 )=-4.58428E-10        V( 8 , 1 )=-2.2463
B( 8 , 2 )=-4.33408E-10        V( 8 , 2 )=-2.1237
```

```
B( 8 , 3 )=-3.96457E-10          V( 8 , 3 )=-1.94264
B( 8 , 4 )=-3.52866E-10          V( 8 , 4 )=-1.72904
B( 8 , 5 )=-3.07509E-10          V( 8 , 5 )=-1.50679
B( 8 , 6 )=-2.63977E-10          V( 8 , 6 )=-1.29349
B( 8 , 7 )=-2.24407E-10          V( 8 , 7 )=-1.09959
B( 8 , 8 )=-1.89732E-10          V( 8 , 8 )=-.929687
B( 8 , 9 )=-1.60076E-10          V( 8 , 9 )=-.784371
B( 8 , 10 )=-1.351E-10           V( 8 , 10 )=-.66199
B( 9 ,-10 )=-1.32522E-10         V( 9 ,-10 )=-.649356
B( 9 ,-9 )=-1.5459E-10           V( 9 ,-9 )=-.757492
B( 9 ,-8 )=-1.80085E-10          V( 9 ,-8 )=-.882418
B( 9 ,-7 )=-2.09008E-10          V( 9 ,-7 )=-1.02414
B( 9 ,-6 )=-2.40957E-10          V( 9 ,-6 )=-1.18069
B( 9 ,-5 )=-2.74926E-10          V( 9 ,-5 )=-1.34714
B( 9 ,-4 )=-3.09129E-10          V( 9 ,-4 )=-1.51473
B( 9 ,-3 )=-3.40955E-10          V( 9 ,-3 )=-1.67068
B( 9 ,-2 )=-3.67192E-10          V( 9 ,-2 )=-1.79924
B( 9 ,-1 )=-3.84594E-10          V( 9 ,-1 )=-1.88451
B( 9 , 0 )=-3.90703E-10          V( 9 , 0 )=-1.91444
B( 9 , 1 )=-3.84594E-10          V( 9 , 1 )=-1.88451
B( 9 , 2 )=-3.67192E-10          V( 9 , 2 )=-1.79924
B( 9 , 3 )=-3.40955E-10          V( 9 , 3 )=-1.67068
B( 9 , 4 )=-3.09129E-10          V( 9 , 4 )=-1.51473
B( 9 , 5 )=-2.74926E-10          V( 9 , 5 )=-1.34714
B( 9 , 6 )=-2.40957E-10          V( 9 , 6 )=-1.18069
B( 9 , 7 )=-2.09008E-10          V( 9 , 7 )=-1.02414
B( 9 , 8 )=-1.80085E-10          V( 9 , 8 )=-.882418
B( 9 , 9 )=-1.5459E-10           V( 9 , 9 )=-.757492
B( 9 , 10 )=-1.32522E-10         V( 9 , 10 )=-.649356
B( 10 ,-10 )=-1.28051E-10        V( 10 ,-10 )=-.627451
B( 10 ,-9 )=-1.47246E-10         V( 10 ,-9 )=-.721507
B( 10 ,-8 )=-1.68875E-10         V( 10 ,-8 )=-.827488
B( 10 ,-7 )=-1.92761E-10         V( 10 ,-7 )=-.944528
B( 10 ,-6 )=-2.18409E-10         V( 10 ,-6 )=-1.0702
B( 10 ,-5 )=-2.44902E-10         V( 10 ,-5 )=-1.20002
B( 10 ,-4 )=-2.70832E-10         V( 10 ,-4 )=-1.32708
B( 10 ,-3 )=-2.94338E-10         V( 10 ,-3 )=-1.44226
B( 10 ,-2 )=-3.13293E-10         V( 10 ,-2 )=-1.53514
B( 10 ,-1 )=-3.25665E-10         V( 10 ,-1 )=-1.59576
B( 10 , 0 )=-3.29972E-10         V( 10 , 0 )=-1.61686
B( 10 , 1 )=-3.25665E-10         V( 10 , 1 )=-1.59576
B( 10 , 2 )=-3.13293E-10         V( 10 , 2 )=-1.53514
B( 10 , 3 )=-2.94338E-10         V( 10 , 3 )=-1.44226
B( 10 , 4 )=-2.70832E-10         V( 10 , 4 )=-1.32708
B( 10 , 5 )=-2.44902E-10         V( 10 , 5 )=-1.20002
B( 10 , 6 )=-2.18409E-10         V( 10 , 6 )=-1.0702
B( 10 , 7 )=-1.92761E-10         V( 10 , 7 )=-.944528
B( 10 , 8 )=-1.68875E-10         V( 10 , 8 )=-.827488
B( 10 , 9 )=-1.47246E-10         V( 10 , 9 )=-.721507
B( 10 , 10 )=-1.28051E-10        V( 10 , 10 )=-.627451
```

TABLE A-1

Comparison of Predicted Versus Measured Magnetic Field

Coordinates (x,y)	Predicted mV	Measured mV	Factor
-10,-10	0.627	.042	14.9
-9,-9	0.757	.049	15.4
-8,-8	0.929	.063	14.7
-7,-7	1.162	.081	14.3
-6,-6	1.483	.126	11.8
-5,-5	1.928	.234	8.2
-4,-4	2.539	.371	6.8
-3,-3	3.296	.61	5.4
-2,-2	3.881	.788	4.9
-1,-1	3.154	.72	4.4
0,0	0.000	.4	-----
1,1	3.154-	.731	4.3
2,2	3.881-	.811	4.8
3,3	3.296-	.633	5.2
4,4	2.539-	.387	6.6
5,5	1.928-	.251	7.7
6,6	1.483-	.147	10.1
7,7	1.162-	.088	13.2
8,8	0.929-	.067	13.9
9,9	0.757	.051	14.8
10,10	0.627	.043	14.6

APPENDIX B

SINGLE DIPOLE SURFACE POTENTIAL DATA

```
10 REM
20 REM PROGRAM PHIB/BAS
30 REM CALCULATES SURFACE POTENTIAL FOR A DIPOLE
40 REM SUBMERGED IN A .464% NACL SOLUTION
50 REM I = 8 MILLIAMPS
60 REM LENGTH OF DIPOLE = .005 METERS
70 REM CAPT. ROBERT D. MURRAY
80 REM
90 P=.008*.005
100 PI=3.14159
110 D=.015
120 SIGMA=.7624
130 FOR X=-.1 TO .1 STEP .01
140 FOR Y=-.1 TO .1 STEP .01
150 R1=((X*X+Y*Y+D*D)[1.5)
160 R2=((X*X+Y*Y+D*D)[1.5)
170 K=P/(2*PI*SIGMA)
180 PHI = ((K*Y)*((1/R1)+(1/R2)))
190 LPRINT"PHI(";INT(100*(.005+X));",";INT(100*(.005+Y));") = ";PHI
200 NEXTY
210 NEXTX
```

```
PHI(-10 ,-10 ) = -5.80624E-04
PHI(-10 ,-9 ) = -6.05905E-04
PHI(-10 ,-8 ) = -6.23268E-04
PHI(-10 ,-7 ) = -6.28467E-04
PHI(-10 ,-6 ) = -6.16426E-04
PHI(-10 ,-5 ) = -5.81716E-04
PHI(-10 ,-4 ) = -5.195E-04
PHI(-10 ,-3 ) = -4.26971E-04
PHI(-10 ,-2 ) = -3.04975E-04
PHI(-10 ,-1 ) = -1.59182E-04
PHI(-10 , 0 ) = -2.40687E-10
PHI(-10 , 1 ) =  1.59181E-04
PHI(-10 , 2 ) =  3.04975E-04
PHI(-10 , 3 ) =  4.26971E-04
PHI(-10 , 4 ) =  5.195E-04
PHI(-10 , 5 ) =  5.81716E-04
PHI(-10 , 6 ) =  6.16426E-04
PHI(-10 , 7 ) =  6.28467E-04
PHI(-10 , 8 ) =  6.23269E-04
PHI(-10 , 9 ) =  6.05905E-04
PHI(-10 , 10 ) =  5.80623E-04
PHI(-9 ,-10 ) = -6.73227E-04
PHI(-9 ,-9 ) = -7.14023E-04
PHI(-9 ,-8 ) = -7.47712E-04
PHI(-9 ,-7 ) = -7.68656E-04
PHI(-9 ,-6 ) = -7.69469E-04
PHI(-9 ,-5 ) = -7.41405E-04
PHI(-9 ,-4 ) = -6.75604E-04
PHI(-9 ,-3 ) = -5.65457E-04
PHI(-9 ,-2 ) = -4.09836E-04
PHI(-9 ,-1 ) = -2.1596E-04
PHI(-9 , 0 ) = -3.27621E-10
PHI(-9 , 1 ) =  2.15959E-04
PHI(-9 , 2 ) =  4.09835E-04
PHI(-9 , 3 ) =  5.65456E-04
PHI(-9 , 4 ) =  6.75603E-04
PHI(-9 , 5 ) =  7.41405E-04
PHI(-9 , 6 ) =  7.69469E-04
PHI(-9 , 7 ) =  7.68656E-04
PHI(-9 , 8 ) =  7.47712E-04
PHI(-9 , 9 ) =  7.14023E-04
PHI(-9 , 10 ) =  6.73227E-04
PHI(-8 ,-10 ) = -7.79085E-04
PHI(-8 ,-9 ) = -8.41176E-04
PHI(-8 ,-8 ) = -8.98774E-04
PHI(-8 ,-7 ) = -9.44853E-04
PHI(-8 ,-6 ) = -9.69134E-04
PHI(-8 ,-5 ) = -9.57962E-04
PHI(-8 ,-4 ) = -8.95537E-04
PHI(-8 ,-3 ) = -7.67519E-04
PHI(-8 ,-2 ) = -5.67268E-04
PHI(-8 ,-1 ) = -3.02824E-04
PHI(-8 , 0 ) = -4.61497E-10
PHI(-8 , 1 ) =  3.02823E-04
PHI(-8 , 2 ) =  5.67267E-04
PHI(-8 , 3 ) =  7.67518E-04
PHI(-8 , 4 ) =  8.95537E-04
PHI(-8 , 5 ) =  9.57962E-04
PHI(-8 , 6 ) =  9.69134E-04
PHI(-8 , 7 ) =  9.44853E-04
PHI(-8 , 8 ) =  8.98775E-04
PHI(-8 , 9 ) =  8.41176E-04
PHI(-8 , 10 ) =  7.79086E-04
PHI(-7 ,-10 ) = -8.9781E-04
```

```
PHI(-7 ,-9 ) = -9.88272E-04
PHI(-7 ,-8 ) = -1.07983E-03
PHI(-7 ,-7 ) = -1.16466E-03
PHI(-7 ,-6 ) = -1.22951E-03
PHI(-7 ,-5 ) = -1.25412E-03
PHI(-7 ,-4 ) = -1.21129E-03
PHI(-7 ,-3 ) = -1.07131E-03
PHI(-7 ,-2 ) = -8.13316E-04
PHI(-7 ,-1 ) = -4.42179E-04
PHI(-7 , 0 ) = -6.78276E-10
PHI(-7 , 1 ) =  4.42178E-04
PHI(-7 , 2 ) =  8.13315E-04
PHI(-7 , 3 ) =  1.07131E-03
PHI(-7 , 4 ) =  1.21129E-03
PHI(-7 , 5 ) =  1.25412E-03
PHI(-7 , 6 ) =  1.22951E-03
PHI(-7 , 7 ) =  1.16466E-03
PHI(-7 , 8 ) =  1.07983E-03
PHI(-7 , 9 ) =  9.88272E-04
PHI(-7 , 10 ) =  8.9781E-04
PHI(-6 ,-10 ) = -1.02738E-03
PHI(-6 ,-9 ) = -1.1542E-03
PHI(-6 ,-8 ) = -1.29218E-03
PHI(-6 ,-7 ) = -1.43442E-03
PHI(-6 ,-6 ) = -1.56615E-03
PHI(-6 ,-5 ) = -1.65999E-03
PHI(-6 ,-4 ) = -1.67181E-03
PHI(-6 ,-3 ) = -1.54257E-03
PHI(-6 ,-2 ) = -1.21623E-03
PHI(-6 ,-1 ) = -6.79155E-04
PHI(-6 , 0 ) = -1.05196E-09
PHI(-6 , 1 ) =  6.79153E-04
PHI(-6 , 2 ) =  1.21623E-03
PHI(-6 , 3 ) =  1.54257E-03
PHI(-6 , 4 ) =  1.67181E-03
PHI(-6 , 5 ) =  1.65999E-03
PHI(-6 , 6 ) =  1.56615E-03
PHI(-6 , 7 ) =  1.43442E-03
PHI(-6 , 8 ) =  1.29218E-03
PHI(-6 , 9 ) =  1.1542E-03
PHI(-6 , 10 ) =  1.02738E-03
PHI(-5 ,-10 ) = -1.16343E-03
PHI(-5 ,-9 ) = -1.33453E-03
PHI(-5 ,-8 ) = -1.53274E-03
PHI(-5 ,-7 ) = -1.75576E-03
PHI(-5 ,-6 ) = -1.99199E-03
PHI(-5 ,-5 ) = -2.21089E-03
PHI(-5 ,-4 ) = -2.3486E-03
PHI(-5 ,-3 ) = -2.29555E-03
PHI(-5 ,-2 ) = -1.91198E-03
PHI(-5 ,-1 ) = -1.11224E-03
PHI(-5 , 0 ) = -1.74943E-09
PHI(-5 , 1 ) =  1.11224E-03
PHI(-5 , 2 ) =  1.91198E-03
PHI(-5 , 3 ) =  2.29555E-03
PHI(-5 , 4 ) =  2.3486E-03
PHI(-5 , 5 ) =  2.2109E-03
PHI(-5 , 6 ) =  1.99199E-03
PHI(-5 , 7 ) =  1.75576E-03
PHI(-5 , 8 ) =  1.53274E-03
PHI(-5 , 9 ) =  1.33453E-03
PHI(-5 , 10 ) =  1.16343E-03
PHI(-4 ,-10 ) = -1.29875E-03
PHI(-4 ,-9 ) = -1.52011E-03
PHI(-4 ,-8 ) = -1.79107E-03
PHI(-4 ,-7 ) = -2.11976E-03
```

```
PHI(-4 ,-6 ) = -2.50772E-03
PHI(-4 ,-5 ) = -2.93574E-03
PHI(-4 ,-4 ) = -3.3327E-03
PHI(-4 ,-3 ) = -3.52208E-03
PHI(-4 ,-2 ) = -3.18245E-03
PHI(-4 ,-1 ) = -1.97734E-03
PHI(-4 , 0 ) = -3.19193E-09
PHI(-4 , 1 ) =  1.97734E-03
PHI(-4 , 2 ) =  3.18245E-03
PHI(-4 , 3 ) =  3.52208E-03
PHI(-4 , 4 ) =  3.3327E-03
PHI(-4 , 5 ) =  2.93575E-03
PHI(-4 , 6 ) =  2.50772E-03
PHI(-4 , 7 ) =  2.11976E-03
PHI(-4 , 8 ) =  1.79107E-03
PHI(-4 , 9 ) =  1.52011E-03
PHI(-4 , 10 ) =  1.29875E-03
PHI(-3 ,-10 ) = -1.42324E-03
PHI(-3 ,-9 ) = -1.69637E-03
PHI(-3 ,-8 ) = -2.04672E-03
PHI(-3 ,-7 ) = -2.49971E-03
PHI(-3 ,-6 ) = -3.08515E-03
PHI(-3 ,-5 ) = -3.82592E-03
PHI(-3 ,-4 ) = -4.6961E-03
PHI(-3 ,-3 ) = -5.49808E-03
PHI(-3 ,-2 ) = -5.60857E-03
PHI(-3 ,-1 ) = -3.89514E-03
PHI(-3 , 0 ) = -6.59506E-09
PHI(-3 , 1 ) =  3.89514E-03
PHI(-3 , 2 ) =  5.60858E-03
PHI(-3 , 3 ) =  5.49808E-03
PHI(-3 , 4 ) =  4.69611E-03
PHI(-3 , 5 ) =  3.82592E-03
PHI(-3 , 6 ) =  3.08515E-03
PHI(-3 , 7 ) =  2.49971E-03
PHI(-3 , 8 ) =  2.04672E-03
PHI(-3 , 9 ) =  1.69637E-03
PHI(-3 , 10 ) =  1.42324E-03
PHI(-2 ,-10 ) = -1.52488E-03
PHI(-2 ,-9 ) = -1.84426E-03
PHI(-2 ,-8 ) = -2.26907E-03
PHI(-2 ,-7 ) = -2.8466E-03
PHI(-2 ,-6 ) = -3.6487E-03
PHI(-2 ,-5 ) = -4.77994E-03
PHI(-2 ,-4 ) = -6.3649E-03
PHI(-2 ,-3 ) = -8.41286E-03
PHI(-2 ,-2 ) = -.0101782
PHI(-2 ,-1 ) = -8.555E-03
PHI(-2 , 0 ) = -1.59267E-08
PHI(-2 , 1 ) =  8.55499E-03
PHI(-2 , 2 ) =  .0101782
PHI(-2 , 3 ) =  8.41287E-03
PHI(-2 , 4 ) =  6.36492E-03
PHI(-2 , 5 ) =  4.77994E-03
PHI(-2 , 6 ) =  3.64871E-03
PHI(-2 , 7 ) =  2.84661E-03
PHI(-2 , 8 ) =  2.26907E-03
PHI(-2 , 9 ) =  1.84426E-03
PHI(-2 , 10 ) =  1.52488E-03
PHI(-1 ,-10 ) = -1.59182E-03
PHI(-1 ,-9 ) = -1.94364E-03
PHI(-1 ,-8 ) = -2.42259E-03
PHI(-1 ,-7 ) = -3.09525E-03
PHI(-1 ,-6 ) = -4.07493E-03
PHI(-1 ,-5 ) = -5.56121E-03
PHI(-1 ,-4 ) = -7.90935E-03
```

```
PHI(-1 ,-7 ) = -.0114984
PHI(-1 ,-2 ) = -.01711
PHI(-1 ,-1 ) = -.0190609
PHI(-1 , 0 ) = -4.24739E-08
PHI(-1 , 1 ) =  .0190609
PHI(-1 , 2 ) =  .01711
PHI(-1 , 3 ) =  .0116854
PHI(-1 , 4 ) =  7.90936E-03
PHI(-1 , 5 ) =  5.56122E-03
PHI(-1 , 6 ) =  4.07492E-03
PHI(-1 , 7 ) =  3.09526E-03
PHI(-1 , 8 ) =  2.42259E-03
PHI(-1 , 9 ) =  1.94364E-03
PHI(-1 , 10 ) =  1.59182E-03
PHI( 0 ,-10 ) = -1.61522E-03
PHI( 0 ,-9 ) = -1.97876E-03
PHI( 0 ,-8 ) = -2.47764E-03
PHI( 0 ,-7 ) = -3.18629E-03
PHI( 0 ,-6 ) = -4.23576E-03
PHI( 0 ,-5 ) = -5.87013E-03
PHI( 0 ,-4 ) = -8.56826E-03
PHI( 0 ,-3 ) = -.0132776
PHI( 0 ,-2 ) = -.0213765
PHI( 0 ,-1 ) = -.0285038
PHI( 0 , 0 ) = -7.3735E-08
PHI( 0 , 1 ) =  .0285038
PHI( 0 , 2 ) =  .0213766
PHI( 0 , 3 ) =  .0132776
PHI( 0 , 4 ) =  8.56828E-03
PHI( 0 , 5 ) =  5.87013E-03
PHI( 0 , 6 ) =  4.23576E-03
PHI( 0 , 7 ) =  3.18629E-03
PHI( 0 , 8 ) =  2.47764E-03
PHI( 0 , 9 ) =  1.97876E-03
PHI( 0 , 10 ) =  1.61522E-03
PHI( 1 ,-10 ) = -1.59182E-03
PHI( 1 ,-9 ) = -1.94364E-03
PHI( 1 ,-8 ) = -2.42259E-03
PHI( 1 ,-7 ) = -3.09525E-03
PHI( 1 ,-6 ) = -4.07493E-03
PHI( 1 ,-5 ) = -5.56122E-03
PHI( 1 ,-4 ) = -7.90936E-03
PHI( 1 ,-3 ) = -.0116854
PHI( 1 ,-2 ) = -.01711
PHI( 1 ,-1 ) = -.019061
PHI( 1 , 0 ) = -4.2474E-08
PHI( 1 , 1 ) =  .019061
PHI( 1 , 2 ) =  .01711
PHI( 1 , 3 ) =  .0116854
PHI( 1 , 4 ) =  7.90936E-03
PHI( 1 , 5 ) =  5.56122E-03
PHI( 1 , 6 ) =  4.07492E-03
PHI( 1 , 7 ) =  3.09526E-03
PHI( 1 , 8 ) =  2.42259E-03
PHI( 1 , 9 ) =  1.94364E-03
PHI( 1 , 10 ) =  1.59182E-03
PHI( 2 ,-10 ) = -1.52488E-03
PHI( 2 ,-9 ) = -1.84426E-03
PHI( 2 ,-8 ) = -2.26907E-03
PHI( 2 ,-7 ) = -2.84661E-03
PHI( 2 ,-6 ) = -3.6487E-03
PHI( 2 ,-5 ) = -4.77994E-03
PHI( 2 ,-4 ) = -6.36491E-03
PHI( 2 ,-3 ) = -8.41287E-03
PHI( 2 ,-2 ) = -.0101782
PHI( 2 ,-1 ) = -8.55503E-03
```

```
PHI( 2 , 0 ) = -1.59268E-08
PHI( 2 , 1 ) =  8.55501E-03
PHI( 2 , 2 ) =  .0101782
PHI( 2 , 3 ) =  8.41288E-03
PHI( 2 , 4 ) =  6.36492E-03
PHI( 2 , 5 ) =  4.77994E-03
PHI( 2 , 6 ) =  3.64871E-03
PHI( 2 , 7 ) =  2.84661E-03
PHI( 2 , 8 ) =  2.26907E-03
PHI( 2 , 9 ) =  1.84426E-03
PHI( 2 , 10 ) =  1.52488E-03
PHI( 3 ,-10 ) = -1.42324E-03
PHI( 3 ,-9 ) = -1.69637E-03
PHI( 3 ,-8 ) = -2.04672E-03
PHI( 3 ,-7 ) = -2.49971E-03
PHI( 3 ,-6 ) = -3.08515E-03
PHI( 3 ,-5 ) = -3.82592E-03
PHI( 3 ,-4 ) = -4.69611E-03
PHI( 3 ,-3 ) = -5.49809E-03
PHI( 3 ,-2 ) = -5.60858E-03
PHI( 3 ,-1 ) = -3.89515E-03
PHI( 3 , 0 ) = -6.59507E-09
PHI( 3 , 1 ) =  3.89514E-03
PHI( 3 , 2 ) =  5.60859E-03
PHI( 3 , 3 ) =  5.49809E-03
PHI( 3 , 4 ) =  4.69611E-03
PHI( 3 , 5 ) =  3.82592E-03
PHI( 3 , 6 ) =  3.08515E-03
PHI( 3 , 7 ) =  2.49971E-03
PHI( 3 , 8 ) =  2.04672E-03
PHI( 3 , 9 ) =  1.69637E-03
PHI( 3 , 10 ) =  1.42324E-03
PHI( 4 ,-10 ) = -1.29875E-03
PHI( 4 ,-9 ) = -1.52011E-03
PHI( 4 ,-8 ) = -1.79107E-03
PHI( 4 ,-7 ) = -2.11976E-03
PHI( 4 ,-6 ) = -2.50772E-03
PHI( 4 ,-5 ) = -2.93575E-03
PHI( 4 ,-4 ) = -3.33271E-03
PHI( 4 ,-3 ) = -3.52208E-03
PHI( 4 ,-2 ) = -3.18246E-03
PHI( 4 ,-1 ) = -1.97734E-03
PHI( 4 , 0 ) = -3.19193E-09
PHI( 4 , 1 ) =  1.97734E-03
PHI( 4 , 2 ) =  3.18246E-03
PHI( 4 , 3 ) =  3.52208E-03
PHI( 4 , 4 ) =  3.3327E-03
PHI( 4 , 5 ) =  2.93575E-03
PHI( 4 , 6 ) =  2.50772E-03
PHI( 4 , 7 ) =  2.11976E-03
PHI( 4 , 8 ) =  1.79108E-03
PHI( 4 , 9 ) =  1.52011E-03
PHI( 4 , 10 ) =  1.29875E-03
PHI( 5 ,-10 ) = -1.16343E-03
PHI( 5 ,-9 ) = -1.33453E-03
PHI( 5 ,-8 ) = -1.53274E-03
PHI( 5 ,-7 ) = -1.75576E-03
PHI( 5 ,-6 ) = -1.99199E-03
PHI( 5 ,-5 ) = -2.2109E-03
PHI( 5 ,-4 ) = -2.3486E-03
PHI( 5 ,-3 ) = -2.29555E-03
PHI( 5 ,-2 ) = -1.91198E-03
PHI( 5 ,-1 ) = -1.11225E-03
PHI( 5 , 0 ) = -1.74944E-09
PHI( 5 , 1 ) =  1.11224E-03
PHI( 5 , 2 ) =  1.91198E-03
```

B-7

```
PHI( 5 , 3 ) =  2.29555F-03
PHI( 5 , 4 ) =  2.3486E-03
PHI( 5 , 5 ) =  2.2109E-03
PHI( 5 , 6 ) =  1.99199E-03
PHI( 5 , 7 ) =  1.75576E-03
PHI( 5 , 8 ) =  1.53274E-03
PHI( 5 , 9 ) =  1.33453E-03
PHI( 5 , 10 ) =  1.16343E-03
PHI( 6 ,-10 ) = -1.02738E-03
PHI( 6 ,-9 ) = -1.1542E-03
PHI( 6 ,-8 ) = -1.29218E-03
PHI( 6 ,-7 ) = -1.43442E-03
PHI( 6 ,-6 ) = -1.56615E-03
PHI( 6 ,-5 ) = -1.65999E-03
PHI( 6 ,-4 ) = -1.67181E-03
PHI( 6 ,-3 ) = -1.54258E-03
PHI( 6 ,-2 ) = -1.21624E-03
PHI( 6 ,-1 ) = -6.79155E-04
PHI( 6 , 0 ) = -1.05196E-09
PHI( 6 , 1 ) =  6.79153E-04
PHI( 6 , 2 ) =  1.21624E-03
PHI( 6 , 3 ) =  1.54257E-03
PHI( 6 , 4 ) =  1.67181E-03
PHI( 6 , 5 ) =  1.66E-03
PHI( 6 , 6 ) =  1.56615E-03
PHI( 6 , 7 ) =  1.43442E-03
PHI( 6 , 8 ) =  1.29218E-03
PHI( 6 , 9 ) =  1.1542E-03
PHI( 6 , 10 ) =  1.02738E-03
PHI( 7 ,-10 ) = -8.9781E-04
PHI( 7 ,-9 ) = -9.88272E-04
PHI( 7 ,-8 ) = -1.07983E-03
PHI( 7 ,-7 ) = -1.16466E-03
PHI( 7 ,-6 ) = -1.22951E-03
PHI( 7 ,-5 ) = -1.25412E-03
PHI( 7 ,-4 ) = -1.21129E-03
PHI( 7 ,-3 ) = -1.07131E-03
PHI( 7 ,-2 ) = -8.13317E-04
PHI( 7 ,-1 ) = -4.4218E-04
PHI( 7 , 0 ) = -6.78277E-10
PHI( 7 , 1 ) =  4.42179E-04
PHI( 7 , 2 ) =  8.13316E-04
PHI( 7 , 3 ) =  1.07131E-03
PHI( 7 , 4 ) =  1.21129E-03
PHI( 7 , 5 ) =  1.25412E-03
PHI( 7 , 6 ) =  1.22951E-03
PHI( 7 , 7 ) =  1.16466E-03
PHI( 7 , 8 ) =  1.07983E-03
PHI( 7 , 9 ) =  9.88272E-04
PHI( 7 , 10 ) =  8.9781E-04
PHI( 8 ,-10 ) = -7.79086E-04
PHI( 8 ,-9 ) = -8.41176E-04
PHI( 8 ,-8 ) = -8.98775E-04
PHI( 8 ,-7 ) = -9.44853E-04
PHI( 8 ,-6 ) = -9.69134E-04
PHI( 8 ,-5 ) = -9.57963E-04
PHI( 8 ,-4 ) = -8.95538E-04
PHI( 8 ,-3 ) = -7.67519E-04
PHI( 8 ,-2 ) = -5.67269E-04
PHI( 8 ,-1 ) = -3.02824E-04
PHI( 8 , 0 ) = -4.61497E-10
PHI( 8 , 1 ) =  3.02823E-04
PHI( 8 , 2 ) =  5.67268E-04
PHI( 8 , 3 ) =  7.67519E-04
PHI( 8 , 4 ) =  8.95538E-04
PHI( 8 , 5 ) =  9.57962E-04
```

```
PHI( 8 , 6 ) =  9.69135E-04
PHI( 8 , 7 ) =  9.44853E-04
PHI( 8 , 8 ) =  8.98775E-04
PHI( 8 , 9 ) =  8.41177E-04
PHI( 8 , 10 ) =  7.79086E-04
PHI( 9 ,-10 ) = -6.73228E-04
PHI( 9 ,-9 ) = -7.14023E-04
PHI( 9 ,-8 ) = -7.47712E-04
PHI( 9 ,-7 ) = -7.68656E-04
PHI( 9 ,-6 ) = -7.6947E-04
PHI( 9 ,-5 ) = -7.41405E-04
PHI( 9 ,-4 ) = -6.75604E-04
PHI( 9 ,-3 ) = -5.65457E-04
PHI( 9 ,-2 ) = -4.09836E-04
PHI( 9 ,-1 ) = -2.1596E-04
PHI( 9 , 0 ) = -3.27621E-10
PHI( 9 , 1 ) =  2.1596E-04
PHI( 9 , 2 ) =  4.09835E-04
PHI( 9 , 3 ) =  5.65456E-04
PHI( 9 , 4 ) =  6.75604E-04
PHI( 9 , 5 ) =  7.41405E-04
PHI( 9 , 6 ) =  7.6947E-04
PHI( 9 , 7 ) =  7.68656E-04
PHI( 9 , 8 ) =  7.47713E-04
PHI( 9 , 9 ) =  7.14023E-04
PHI( 9 , 10 ) =  6.73227E-04
PHI( 10 ,-10 ) = -5.80624E-04
PHI( 10 ,-9 ) = -6.05905E-04
PHI( 10 ,-8 ) = -6.23269E-04
PHI( 10 ,-7 ) = -6.28467E-04
PHI( 10 ,-6 ) = -6.16426E-04
PHI( 10 ,-5 ) = -5.81716E-04
PHI( 10 ,-4 ) = -5.19501E-04
PHI( 10 ,-3 ) = -4.26972E-04
PHI( 10 ,-2 ) = -3.04975E-04
PHI( 10 ,-1 ) = -1.59182E-04
PHI( 10 , 0 ) = -2.40687E-10
PHI( 10 , 1 ) =  1.59181E-04
PHI( 10 , 2 ) =  3.04975E-04
PHI( 10 , 3 ) =  4.26971E-04
PHI( 10 , 4 ) =  5.195E-04
PHI( 10 , 5 ) =  5.81716E-04
PHI( 10 , 6 ) =  6.16427E-04
PHI( 10 , 7 ) =  6.28467E-04
PHI( 10 , 8 ) =  6.23269E-04
PHI( 10 , 9 ) =  6.05905E-04
PHI( 10 , 10 ) =  5.80624E-04
```

TABLE B-1

Comparison of Predicted Versus Measured Surface

Potential

Coordinates (x,y)	Predicted mV	Measured mV	Factor
-10,-10	0.581-	90.0	155.
-9,-9	0.714-	70.0	98.0
-8,-8	0.898-	90.0	100.
-7,-7	1.165-	84.0	72.0
-6,-6	1.566-	114.	73.0
-5,-5	2.211-	92.0	42.0
-4,-4	3.333-	144.	43.0
-3,-3	5.498-	140.	25.0
-2,-2	10.18-	94.0	9.0
-1,-1	19.06-	98.0	5.0
0,0	0.000	00.0	0.0
1,1	19.06	110.	6.0
2,2	10.18	112.	11.0
3,3	5.498	102.	19.0
4,4	3.333	29.0	9.0
5,5	2.211	96.0	43.0
6,6	1.566	110.	70.0
7,7	1.165	108.	93.0
8,8	0.898	86.0	96.0
9,9	0.714	58.0	81.0
10,10	0.581	25.0	43.0

END
FILMED
4
DTIC
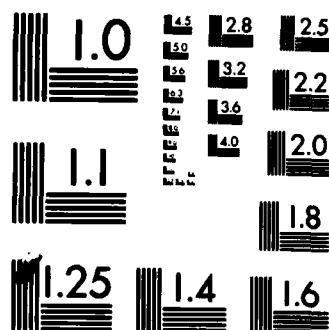
MICROCOPY RESOLUTION TEST CHART

NATIONAL BUREAU OF STANDARDS-1963-A

APPENDIX C

HUMAN VISUAL EVOKED RESPONSE PLOTS

HEATHER MEG. 002
10 Hz NOTCH
22-SEP-83

0.07812 SEC

1.15-03 V   VLN
            T

0.07812 SEC

A
R

TSU
50

AT

2.0A   10.A -B/16 SEC   0.4

C

O

C
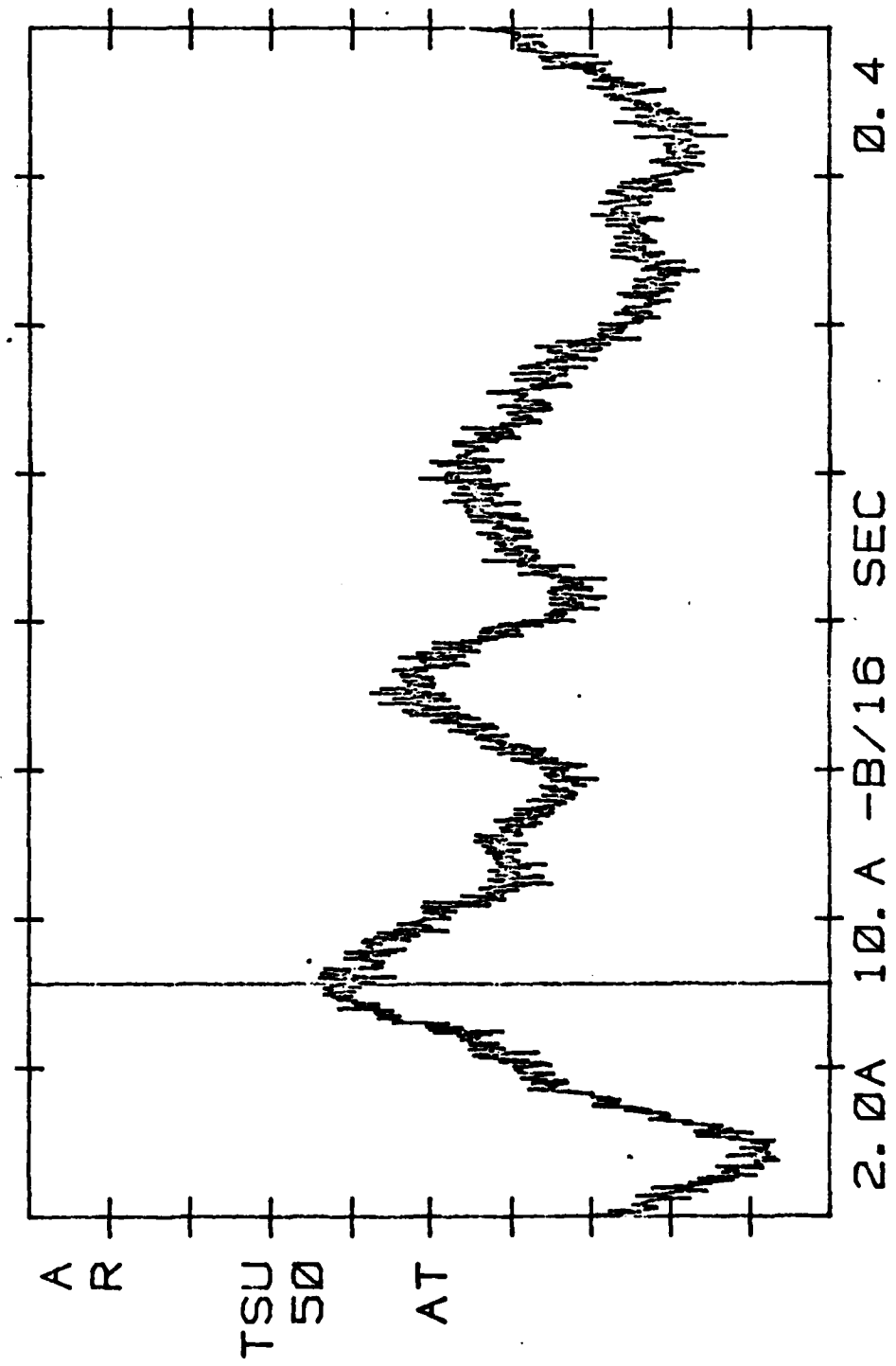
SHERRY MEG. 010
10 HZ NOTCH
22-SEP-83 0.08086 SEC

-332.-06 V VLN T

ARTSU 50 AT

2.0A   10. A -B/16 SEC   0.4

C

ROBBY   MEG. 011
10 Hz   NOTCH   −532. −06 V   VLN
22-SEP-83   T
          0.07539 SEC

A
R

TSU
50

AT

2.0A   10.A −B/16 SEC   0.4
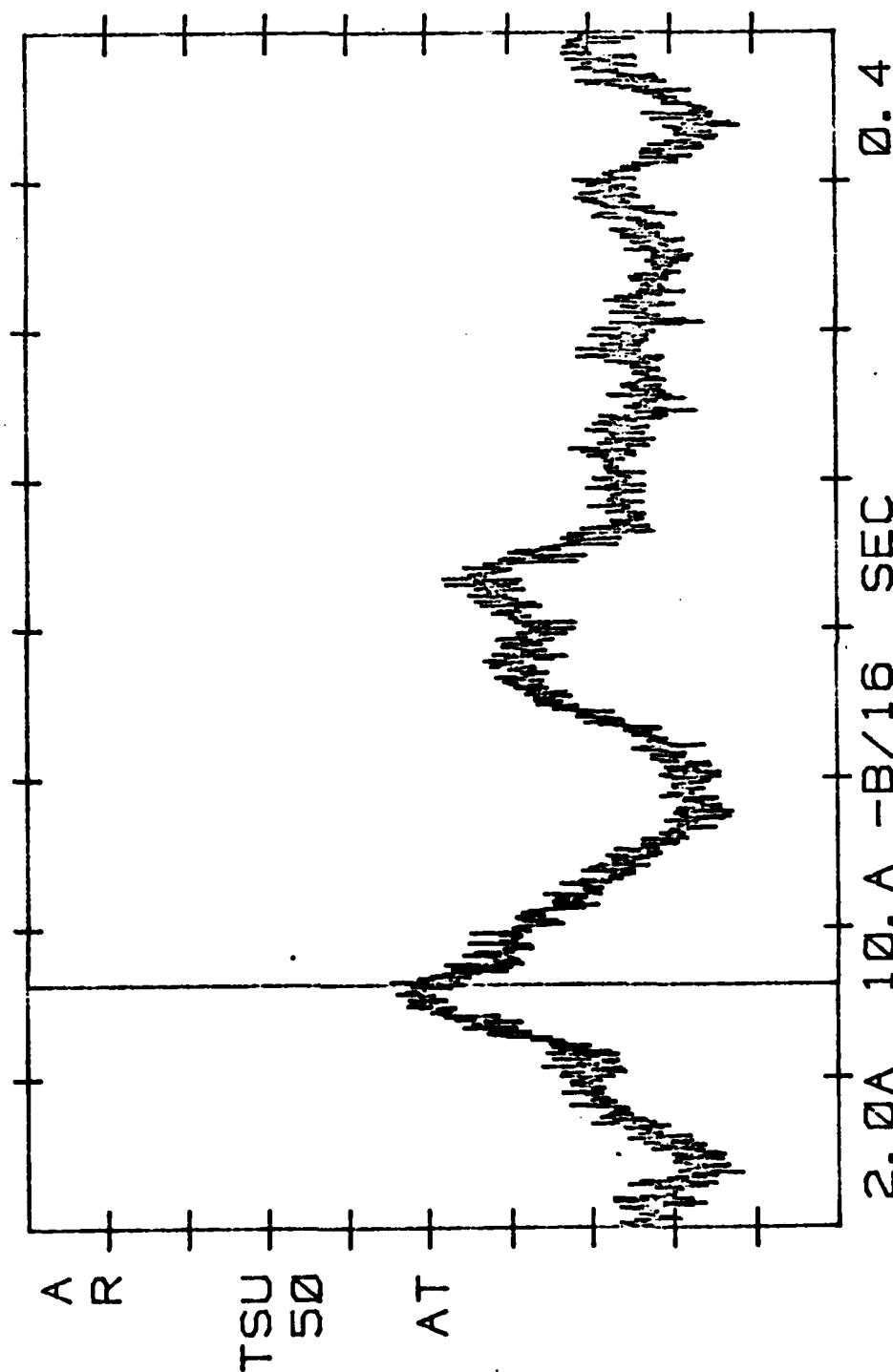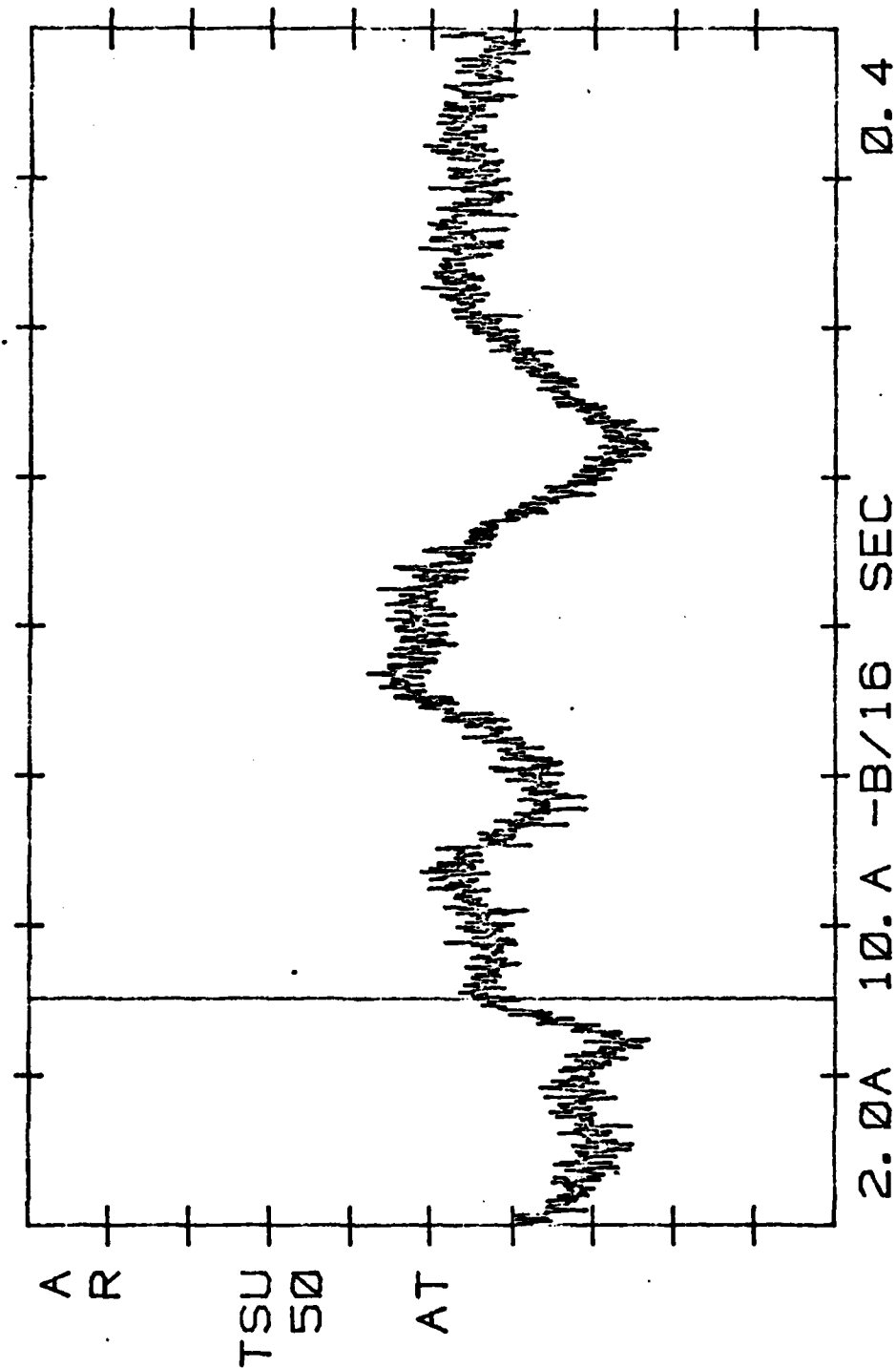
JOHN   MEG. 012
10. Hz NOTCH
22-SEP-83   0.07539 SEC

410. -06 V   VLN
                T

A
R

TSU
50

AT

2.0A   10. A -B/16 SEC   0.4

BOB   MEG.018
10 Hz NOTCH
22-SEP-83

-1.60-03 V   VLN
                 T
0.07695 SEC

A
R

TSU
50

AT

2.0A   10. A -B/16 SEC   0.4
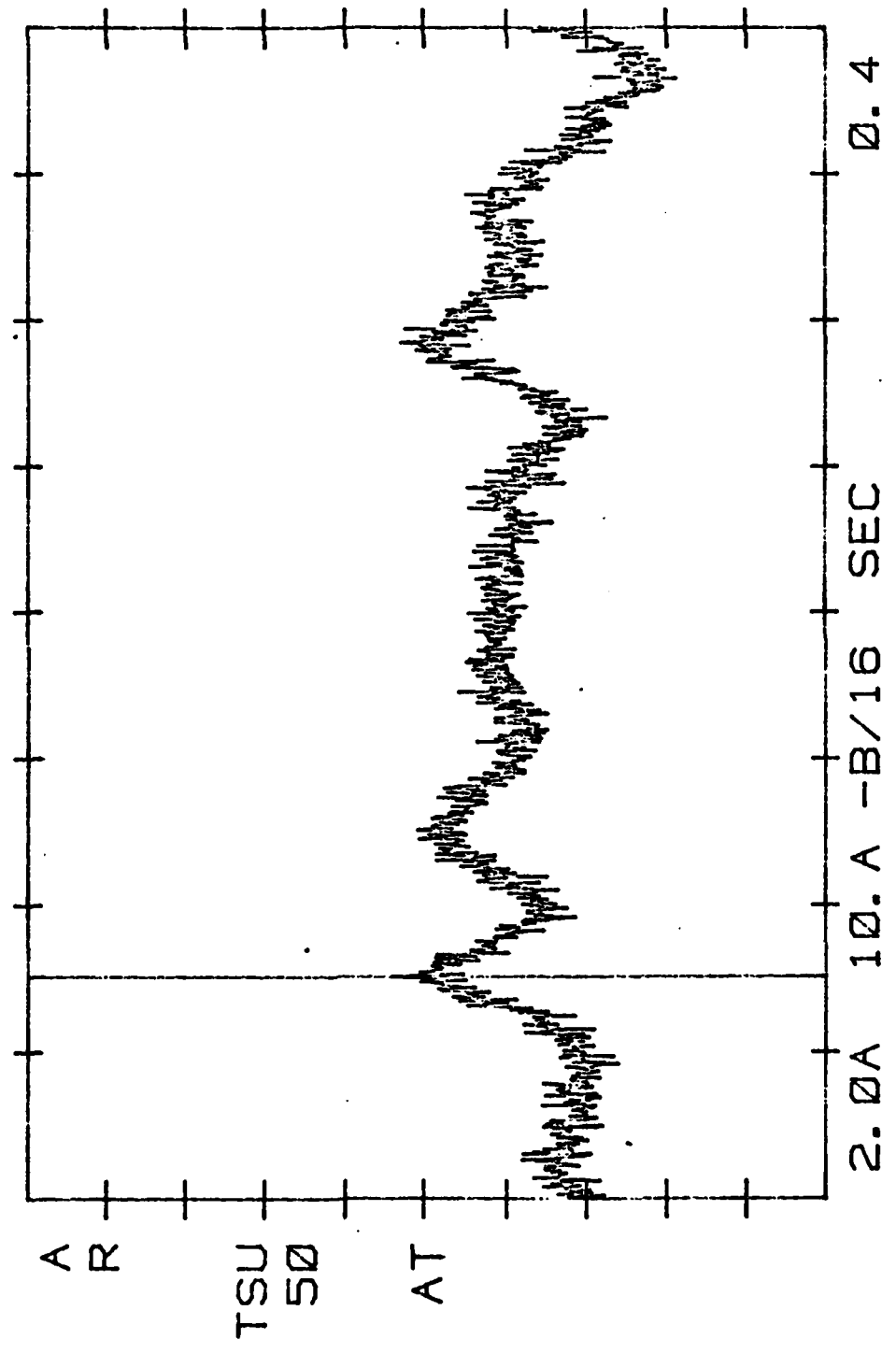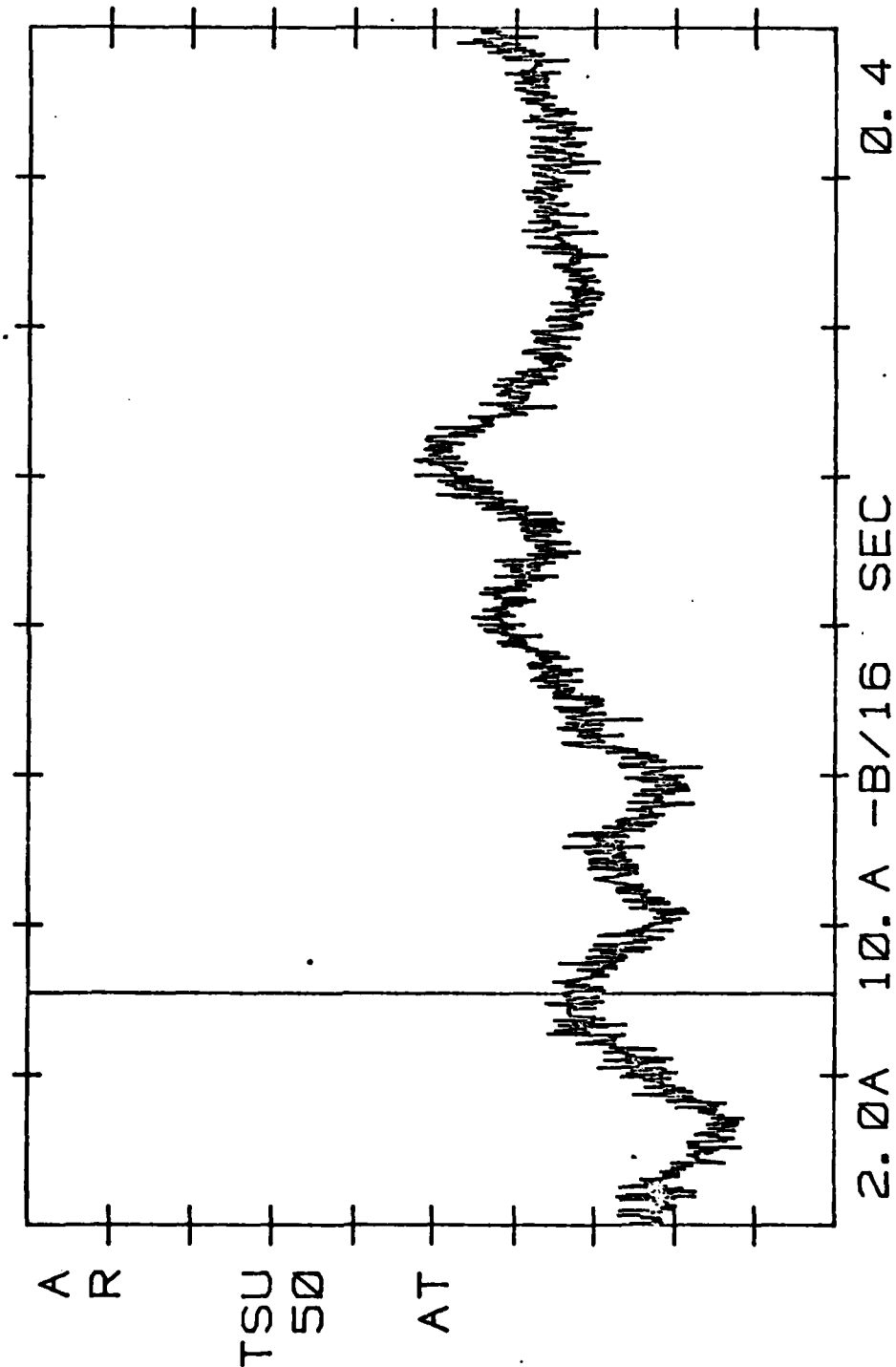
APPENDIX D

DOG VISUAL EVOKED RESPONSE PLOTS

RICKY MEG.022 RT-OC LIGHTS-ON
10CPS AND NOTCH FILTERS 12.7-03 V VLN
26-SEP-83 0.02598 SEC T

0.02598 SEC

A
R

TSU
50

AT

1.0A 10.A 10.A B/16 SEC 0.2
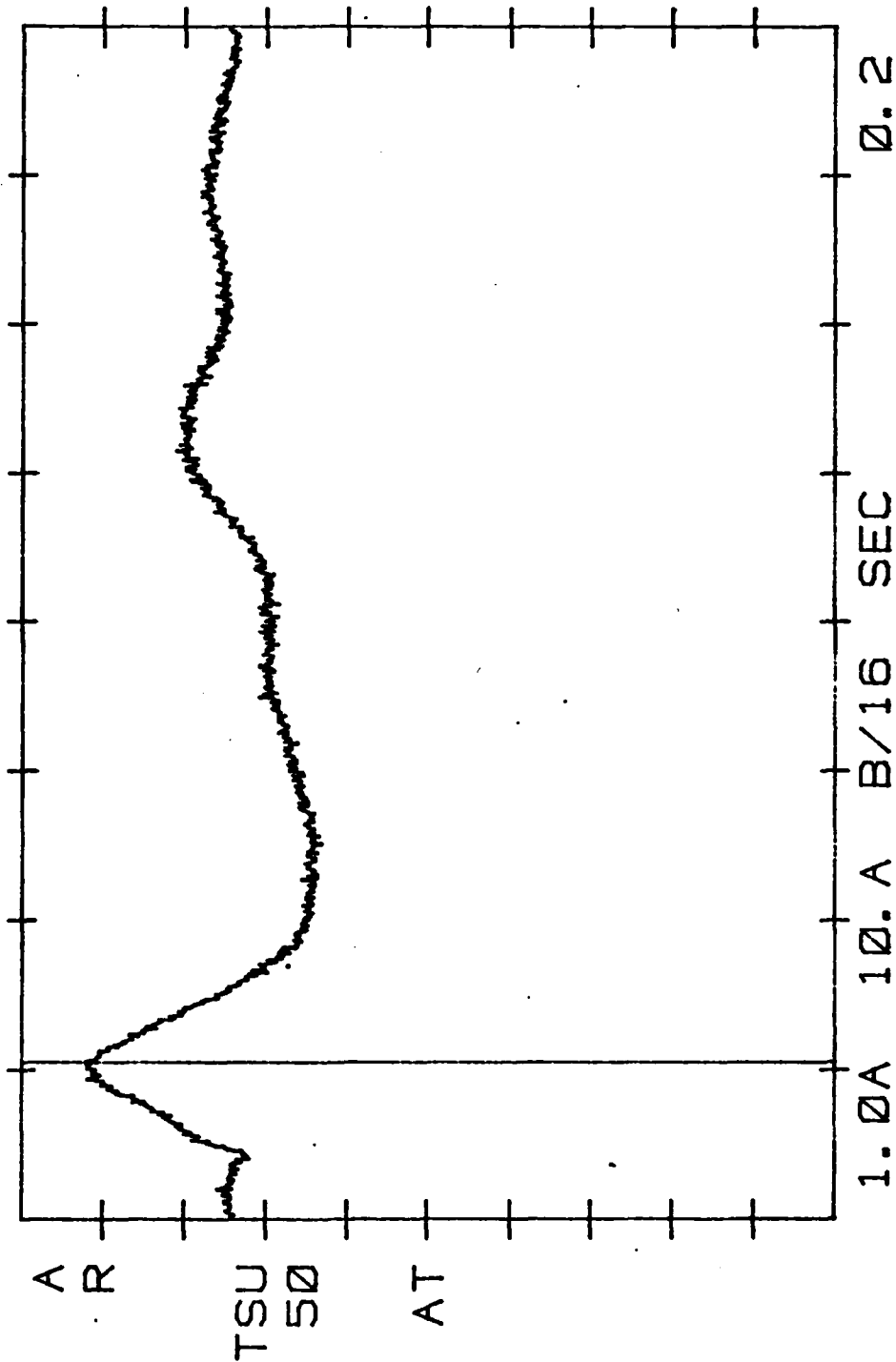
RICKY MEG.023 RT-OC LIGHTS-OFF
10CPS AND NOTCH FILTERS 3.31-03 V VLN
26-SEP-83 0.02598 SEC T

A R

TSU 50

AT

1.0A   10.A B/16 SEC   0.2
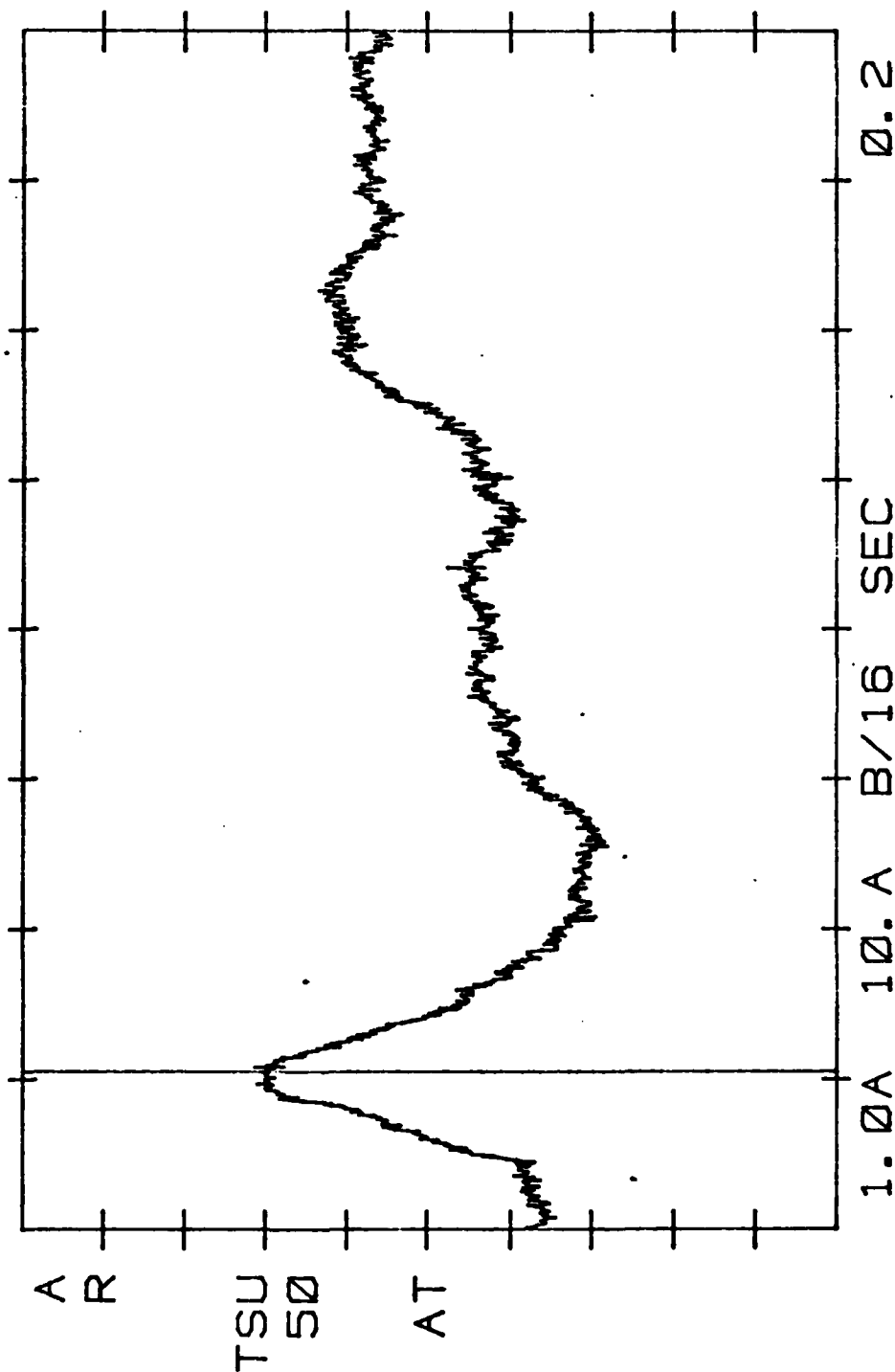
RICKY MEG.024 RT-OC LIGHTS-ON
10CPS AND NOTCH FILTERS 13.1-03 V VLN
26-SEP-83 0.02344 SEC

T

A
R

TSU
50

AT

1.0A   10.A   B/16 SEC   0.8
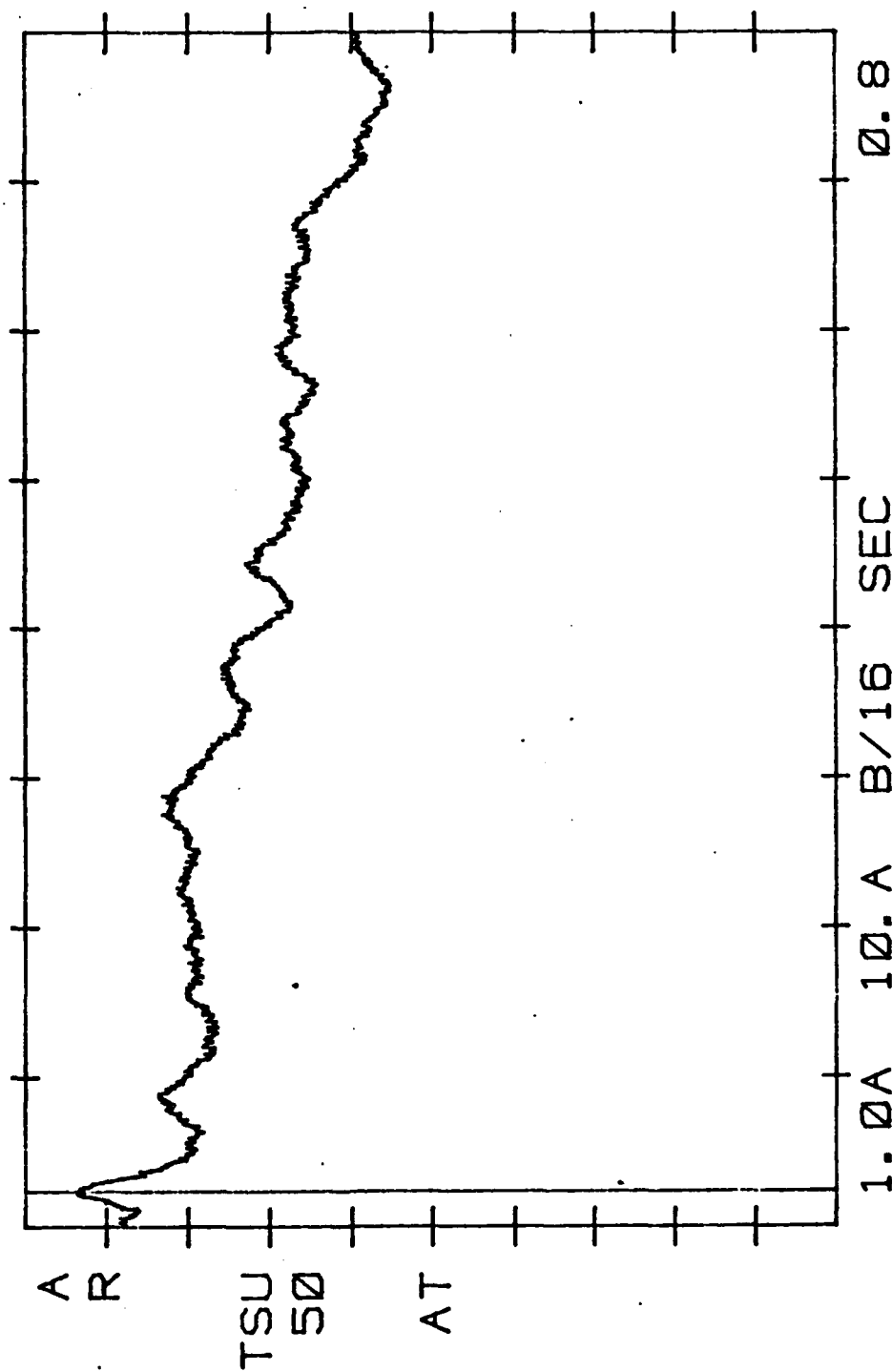
RICKY   MEG. 042 RT-OC   LIGHTS-ON
10CPS AND NOTCH FILTERS 9. 47-03 V   VLN
29-SEP-83   STROBE   R-N GEN   T
           0. 01230 SEC

A
R

TSU
50

AT

5.2   5.0A   5.0D   B/2   SEC   0.2
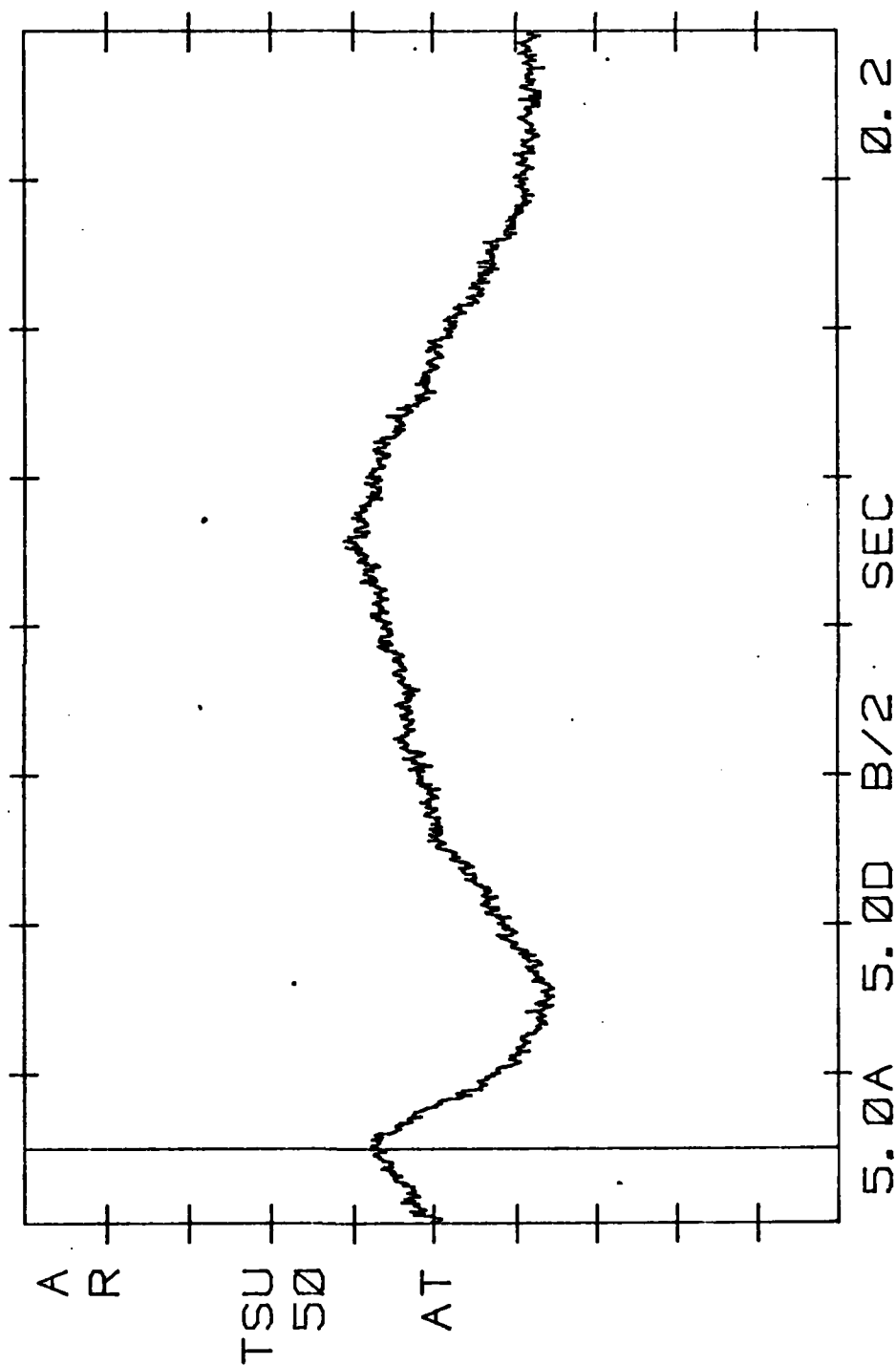
RICKY

MEG. 042 RT-OC   LIGHTS-ON
10CPS AND NOTCH FILTERS_17.5-03 V   VLN
29-SEP-83 STROBE   R-N GEN   T
0.03789 SEC

A
R

TSU
50

AT

5.0A   5.0D B/2 SEC   0.2
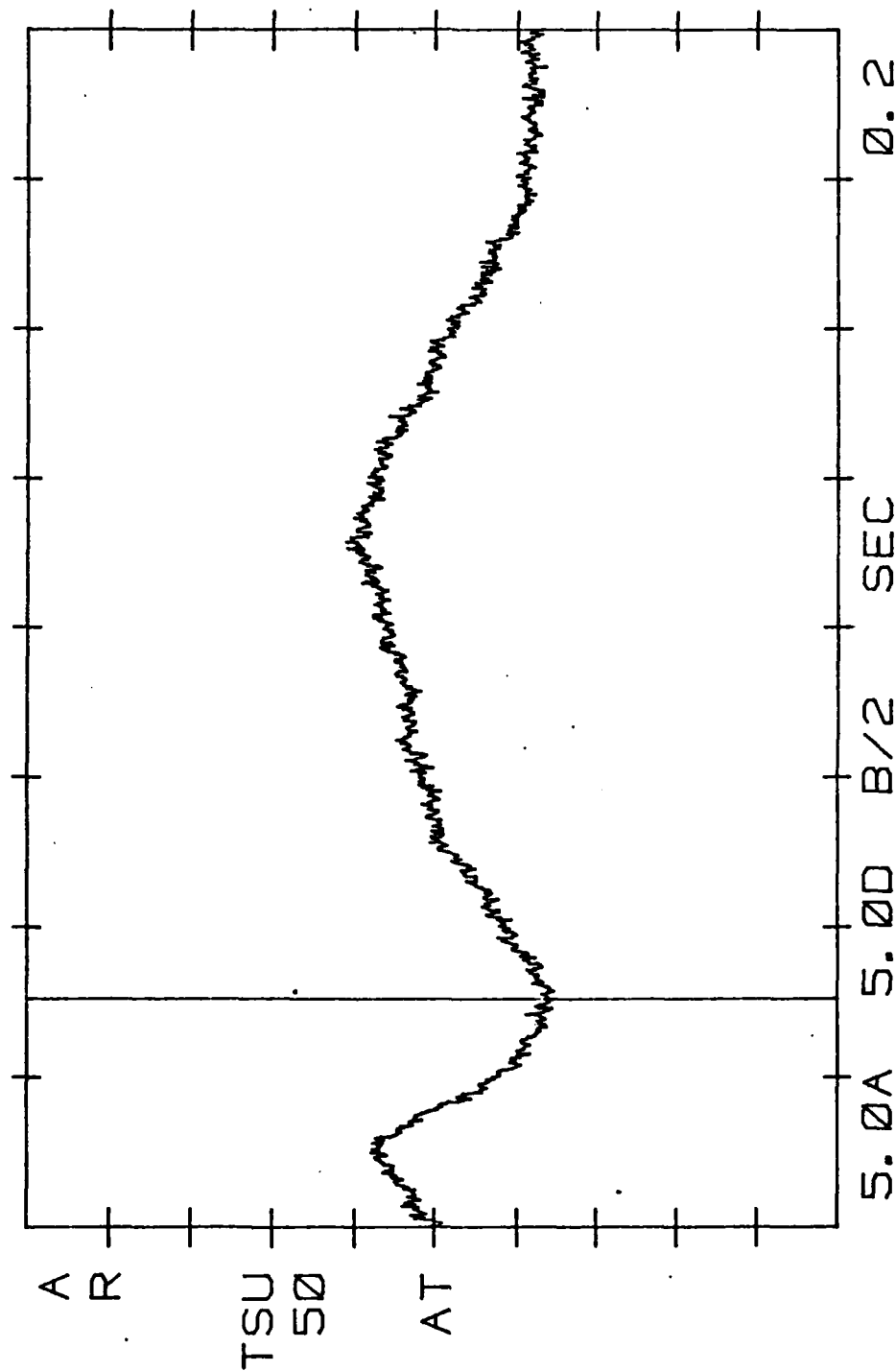
RICKY MEG.0043 RT-OC-NEW LIGHTS-ON
10CPS AND NOTCH FILTERS_3.88-03 V VLN
29-SEP-83 STROBE R-N GEN T
0.007003 SEC

A
R

TSU
50

AT

5.0A 5.0D B/2 SEC 0.2

SEC
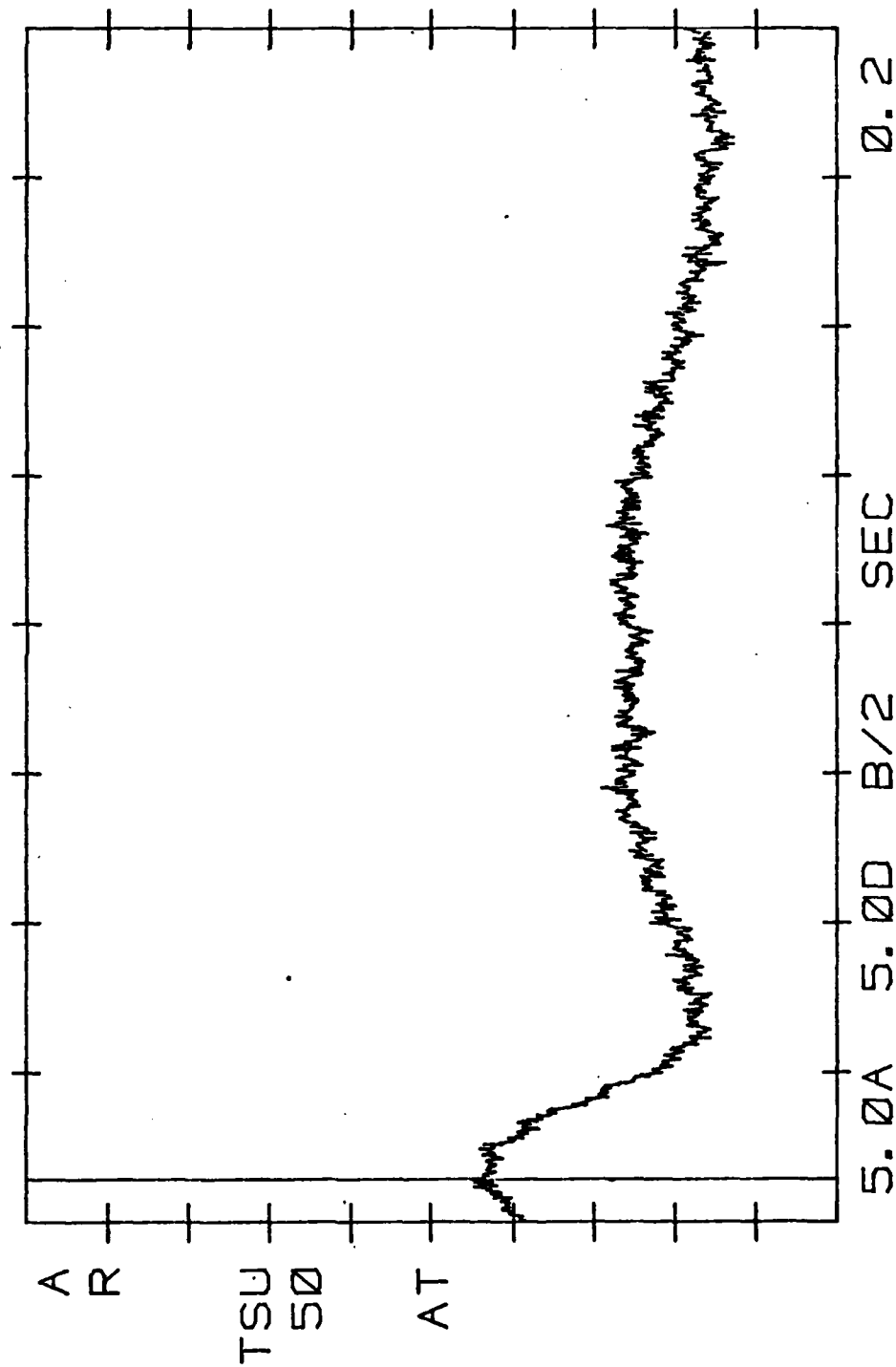
RICKY | MEG.0043 RT-OC-NEW LIGHTS-ON
10CPS AND NOTCH FILTERS_27.4-03 V VLN
29-SEP-83 STROBE R-N GEN T
0.03203 SEC
0.03203 SEC

A
R

TSU
50

AT

5.0A 5.0D B/2 SEC 0.2

RICK-BR MEG.044 RT-OC-SAME LIGHTS-ON
10CPS AND NOTCH FILTERS_23.9-03 V VLN
29-SEP-83 STROBE R-N GEN T
0.00762 SEC

A
R

TSU
50

AT

5.0A 5.0D B/2 SEC 0.2
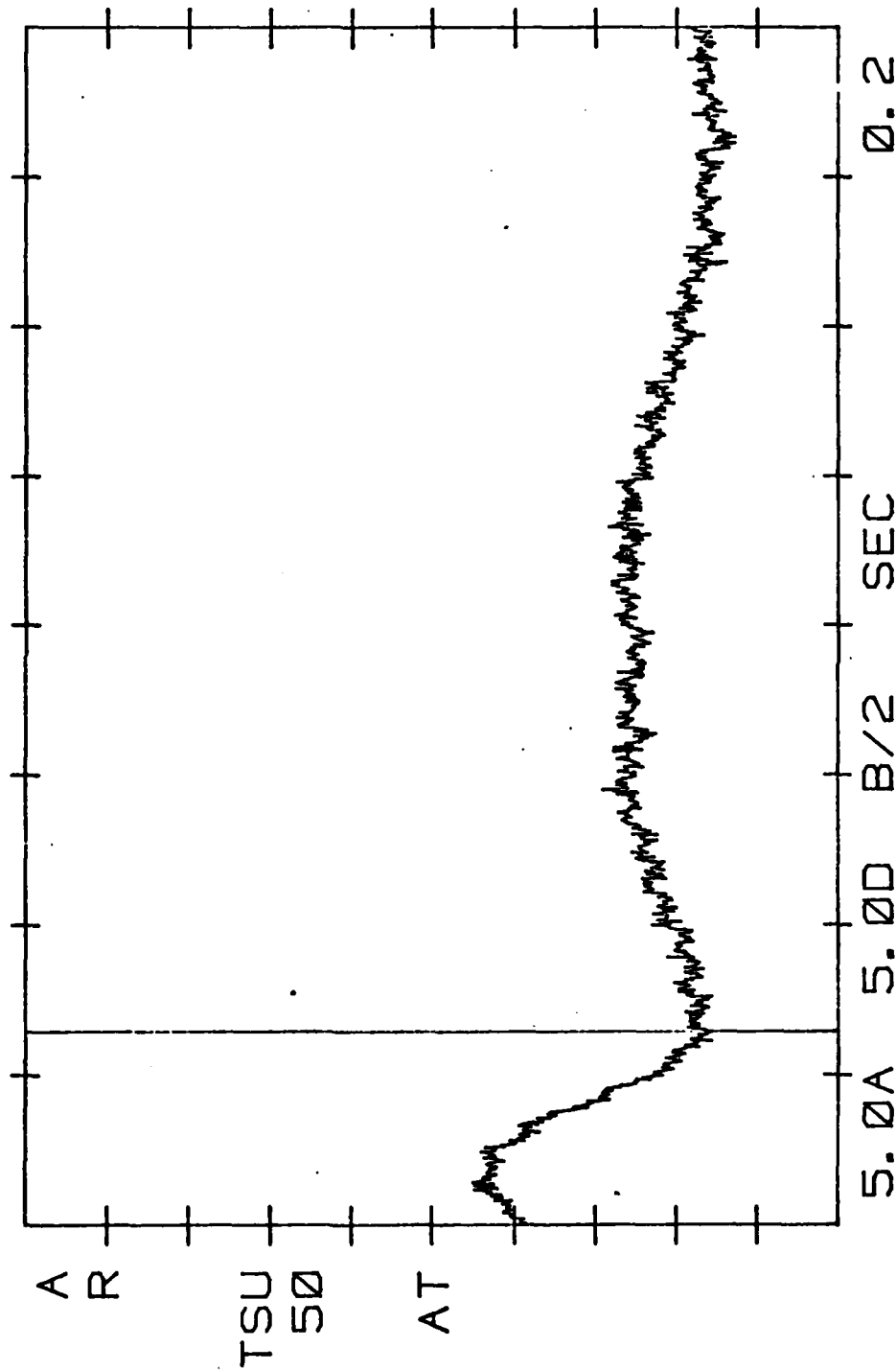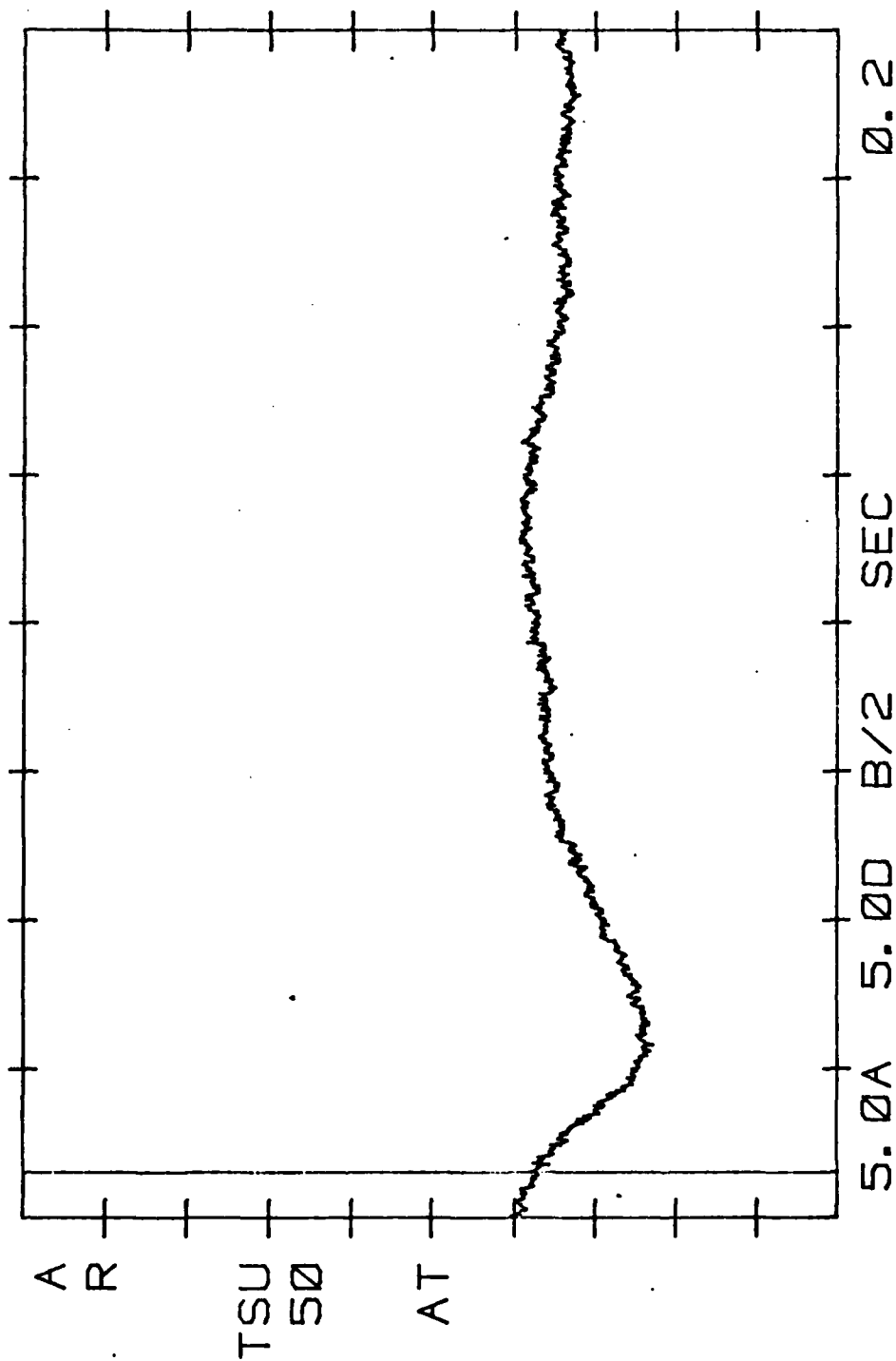
RICKY-BR MEG.044 RT-OC-SAME LIGHTS-ON
10CPS AND NOTCH FILTERS_54.1-03 V VLN
29-SEP-83 STROBE R-N GEN T
0.02910 SEC

A
R

TSU
50

AT

5.2   5.0A   5.0D   B/2   SEC   0.2
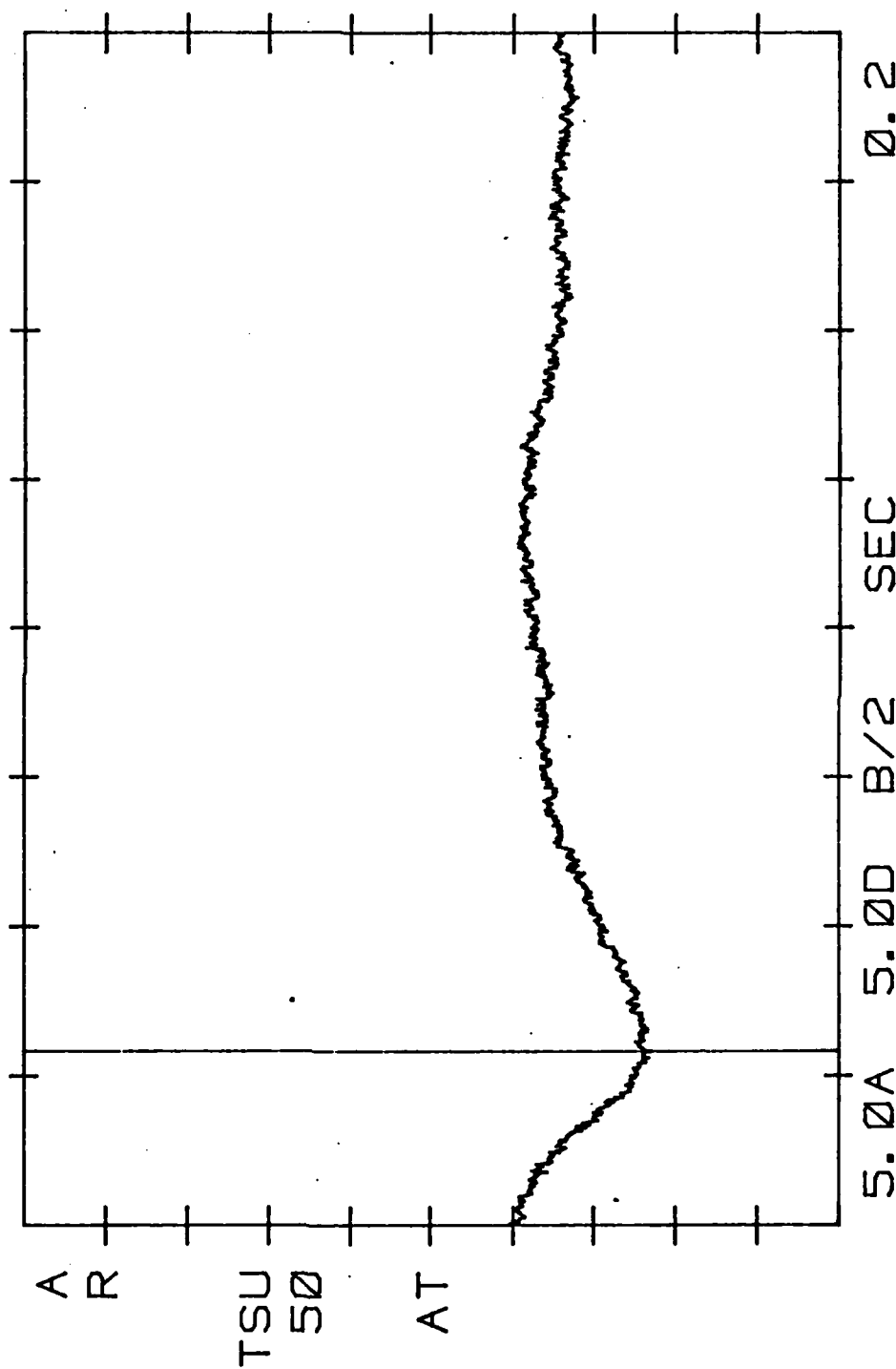
RICKY   MEG.045   RT-OC-SAME   LIGHTS-ON
CPS AND NOTCH FILTERS 8.05-03 V   VLN
29-SEP-83 STROBE   R-N GEN   T
0.00762 SEC
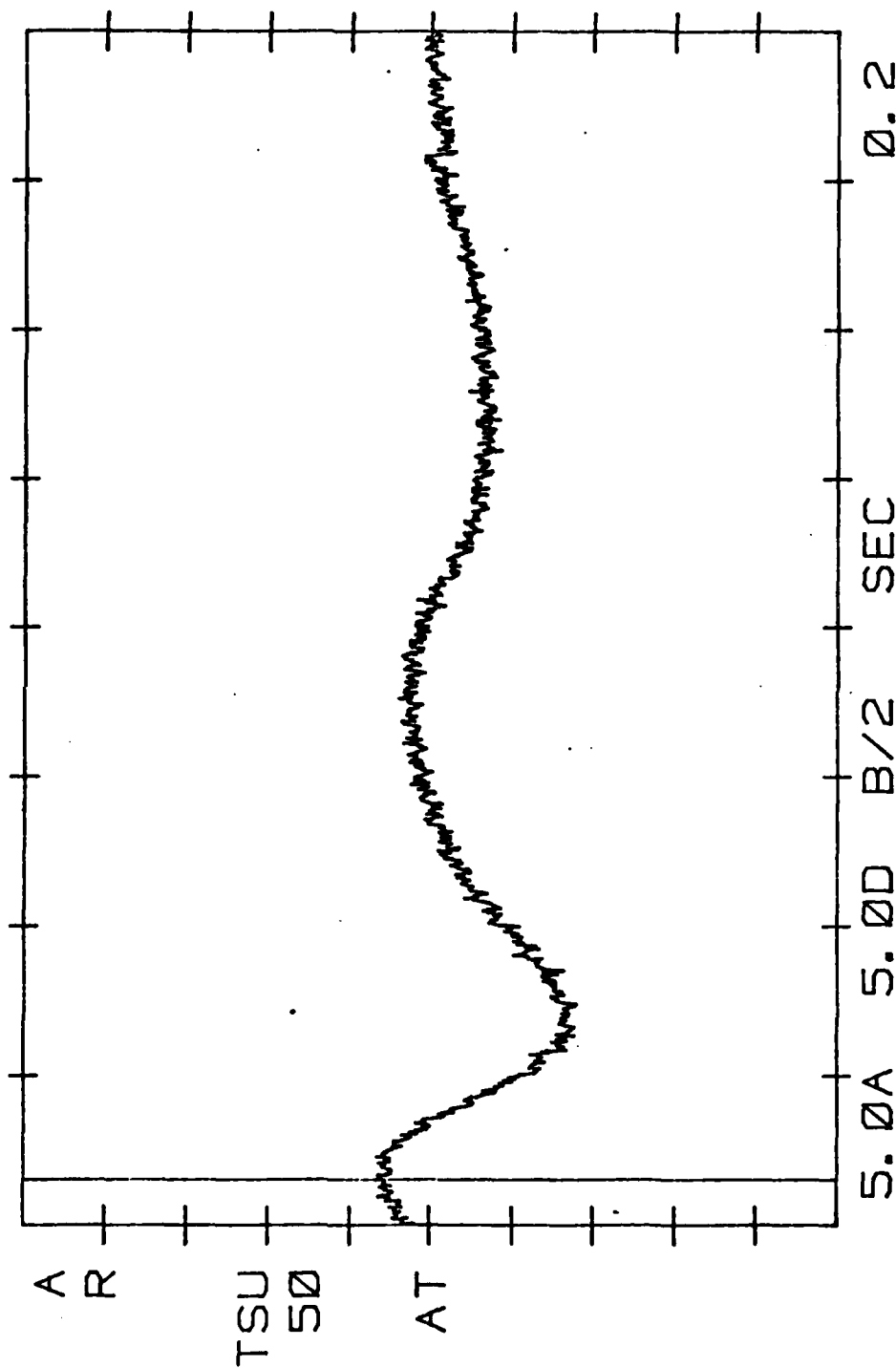
A
R
TSU
50
AT

5.0A   5.0D B/2   SEC   0.2

RICKY
MEG.045 RT-OC-SAME LIGHTS-ON
10CPS AND NOTCH FILTERS_21.4-03 V VLN
29-SEP-83 STROBE R-N GEN T
0.03301 SEC

A
R

TSU
50

AT

5.0A   5.0D B/2 SEC   0.2
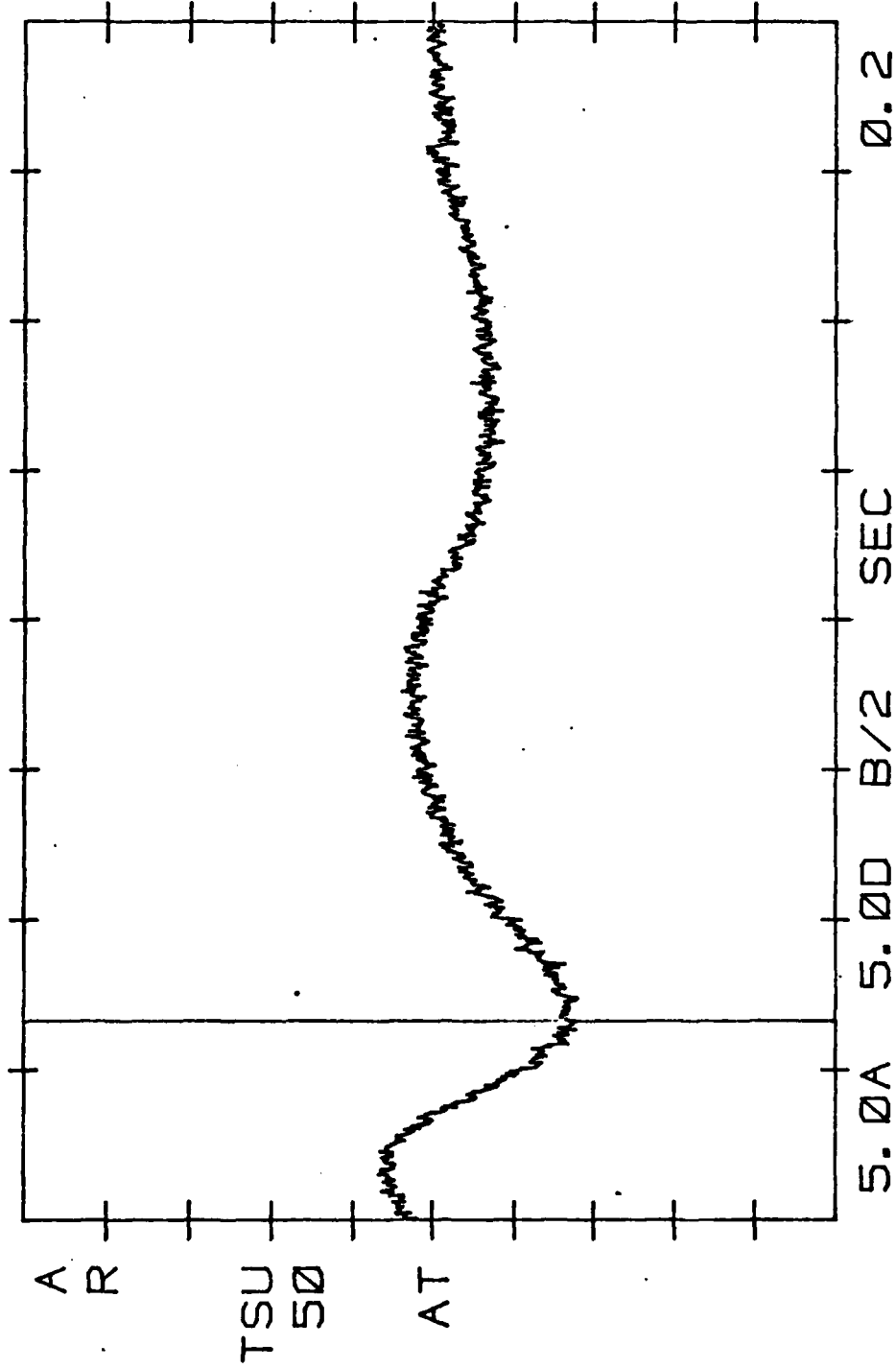
RICKY MEG 046 RT-QC-SAME LIGHTS-OFF
10CPS AND NOTCH FILTERS_14.9-03 V VLN
29-SEP-83 STROBE R-N GEN T
0.01504 SEC
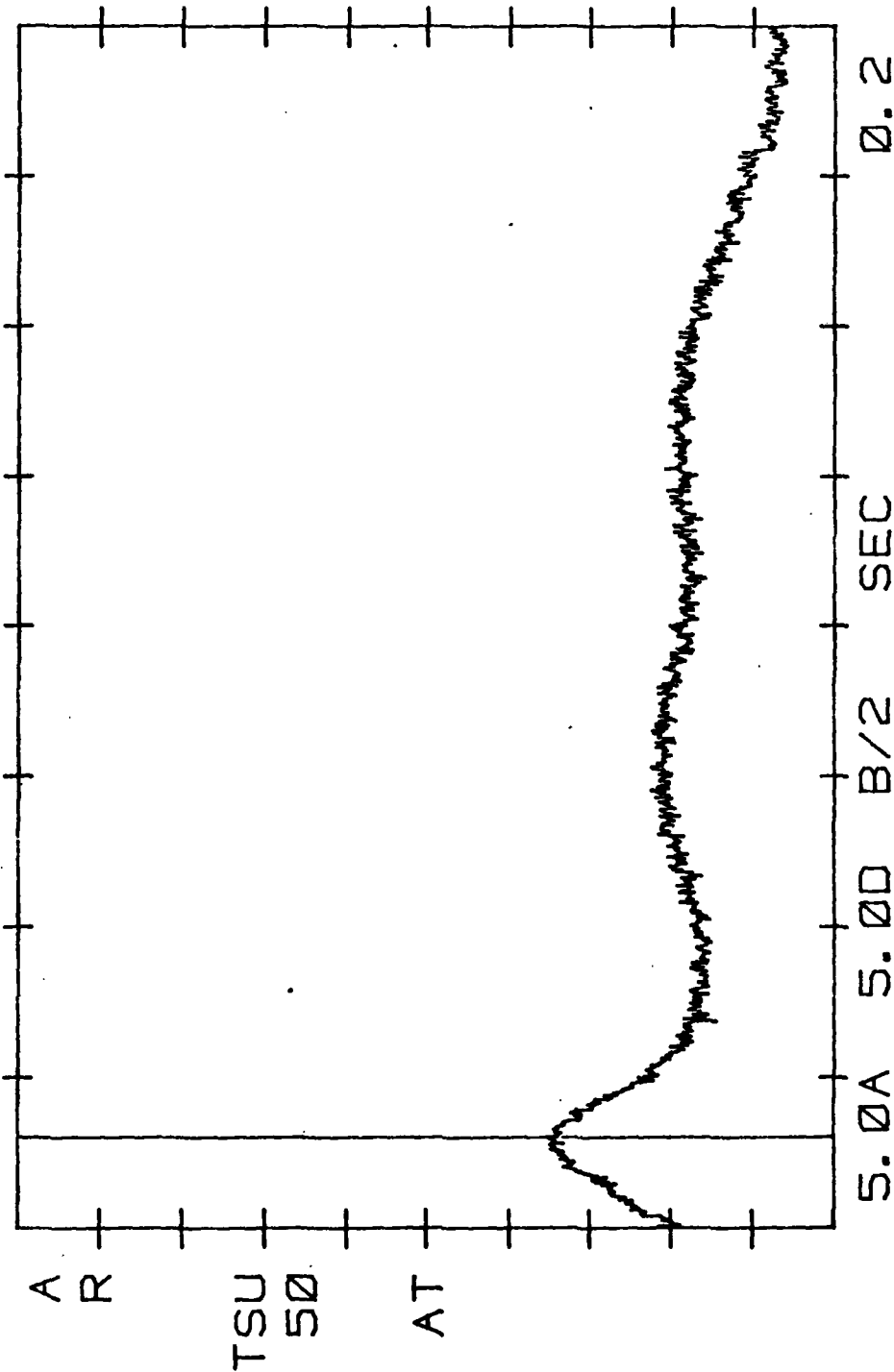
A
R

TSU
50

AT

5.0A 5.0D B/2 SEC 0.2

RICKY MEG.046 RT-QC-SAME LIGHTS-OFF
10CPS AND NOTCH FILTERS-35.5-03 V VLN
29-SEP-83 STROBE R-N GEN T
0.03437 SEC

A
R

TSU
50

AT

5.0A   5.0D B/2   SEC   0.2

RICKY MEG.047 RT-FR-NEW LIGHTS-OFF
10CPS AND NOTCH FILTERS 16.7-03 V VLN
29-SEP-83 STROBE R-N GEN T
0.01699 SEC

A
R

TSU
50

AT

5.0A   5.0D   B/2   SEC   0.2
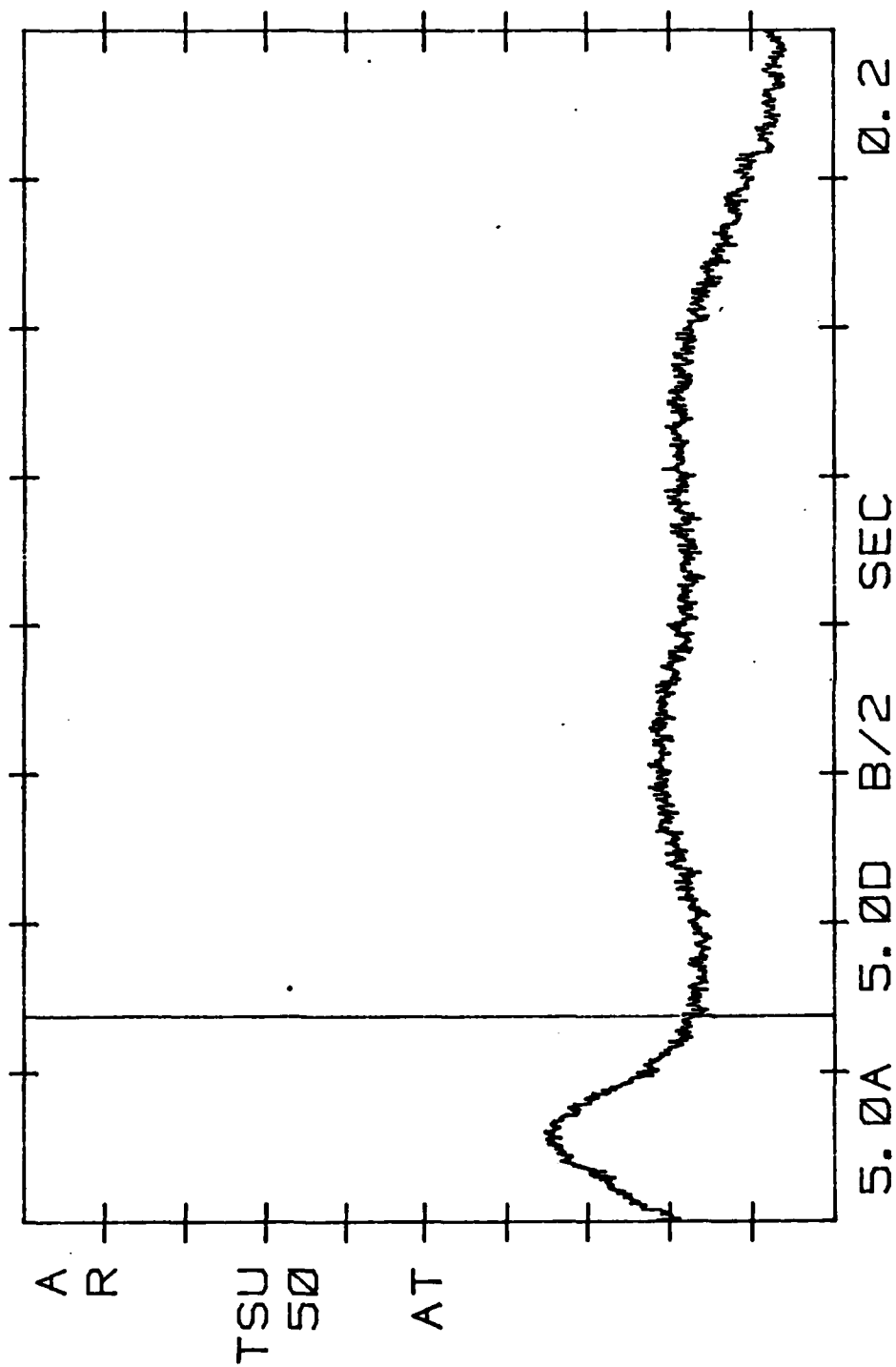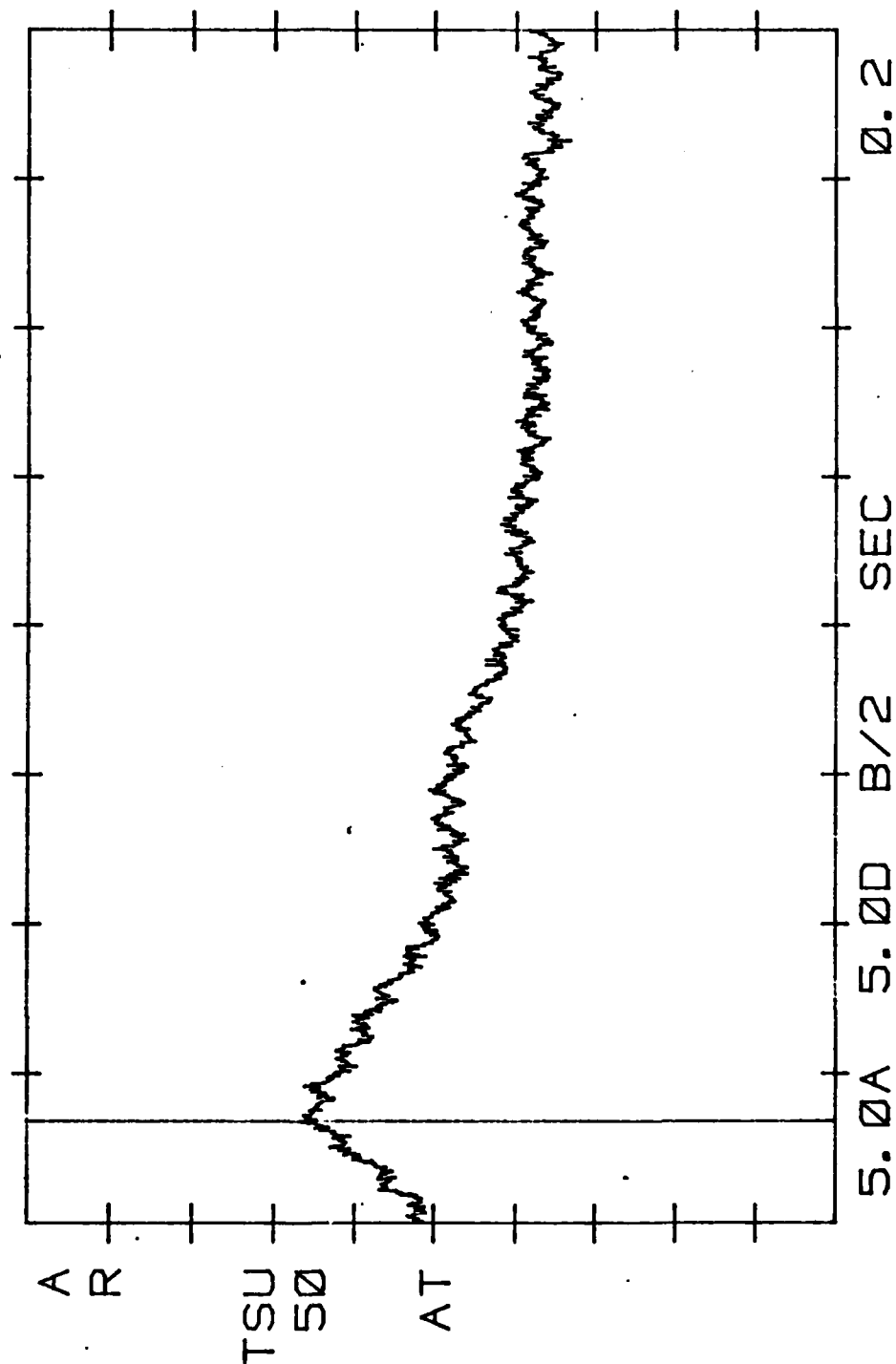
RICKY MEG.047 RT-FR-NEW LIGHTS-OFF
10CPS AND NOTCH FILTERS_1.22-03 V VLN
29-SEP-83 STROBE R-N GEN T
0.05508 SEC

AR
TSU
50
AT

5.0A   5.0D   5.0   B/2   SEC   0.2
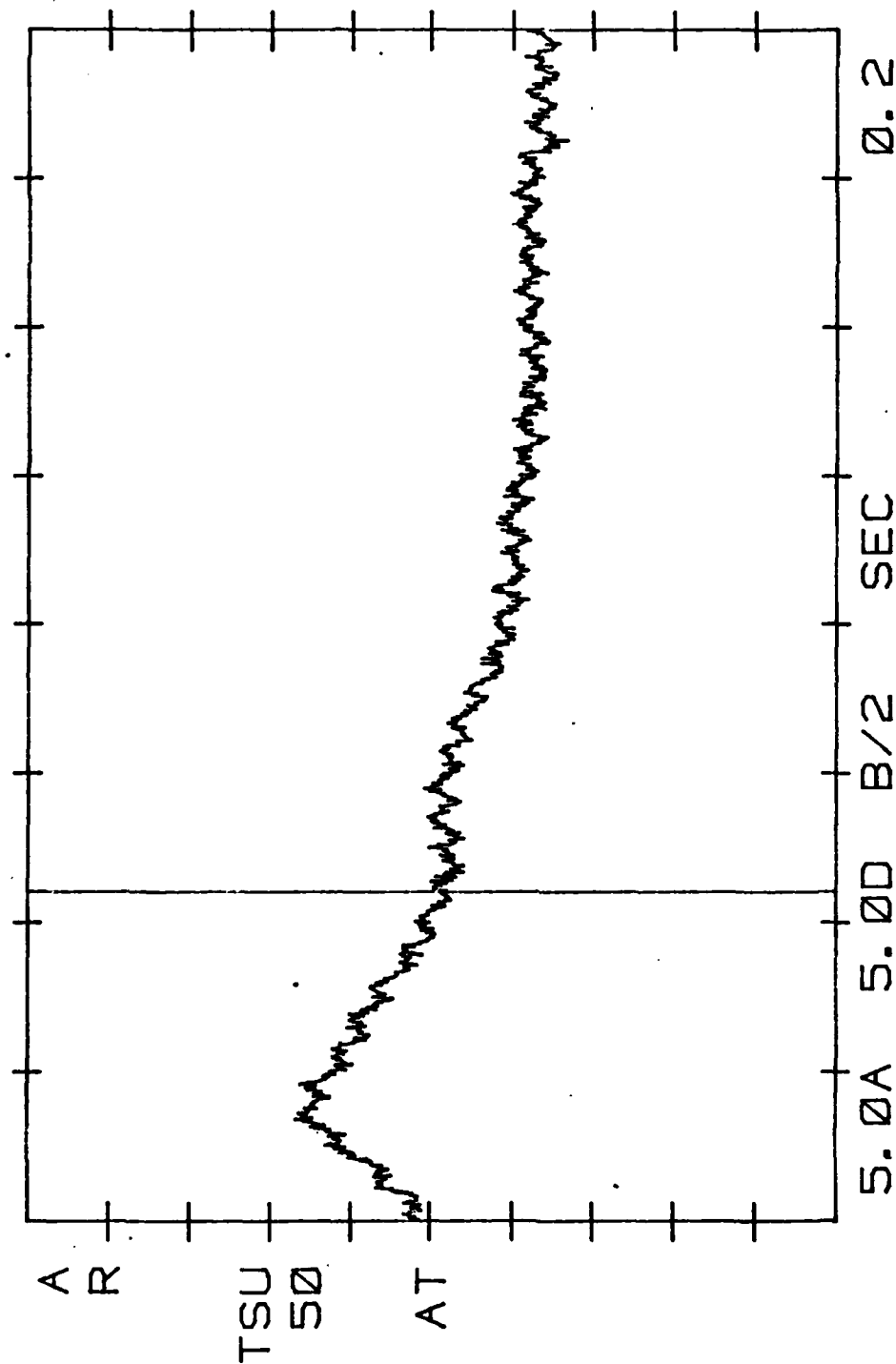
RICKY

MEG 048   RT-FR-SAME LIGHTS-OFF

10CPS AND NOTCH FILTERS 9.52-03 V   VLN

29-SEP-83 STROBE   R-N GEN   T

0.01699 SEC

A
R

TSU
50

AT

5.0A   5.0D   5/2   SEC   0.2
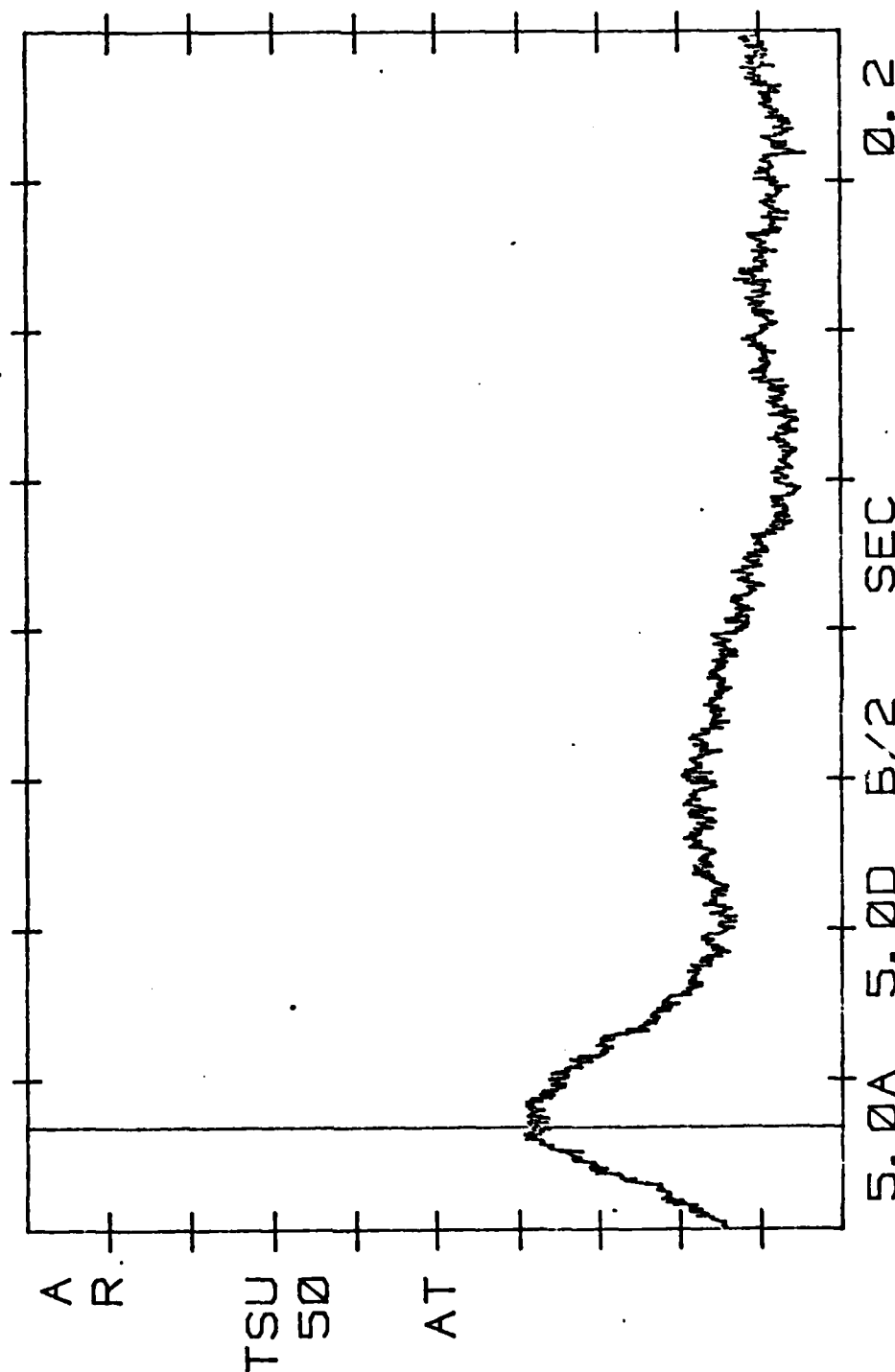
RICKY MEG.048 RT-FR-SAME LIGHTS-OFF
10CPS AND NOTCH FILTERS_28.9-03 V VLN
29-SEP-83 STROBE R-N GEN T
0.04609 SEC
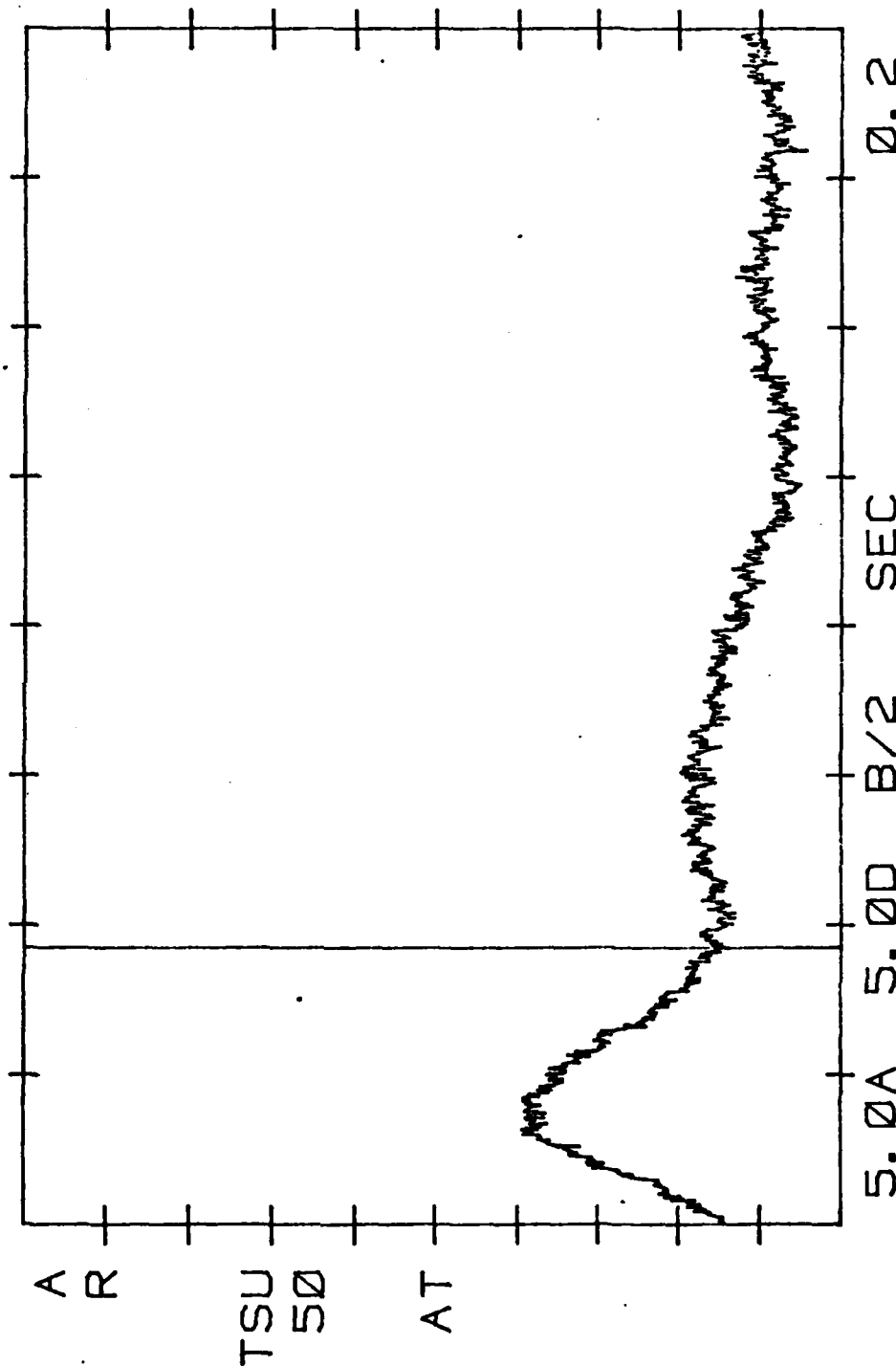
A
R

TSU
50

AT

5.2   5.0A   5.0D B/2   SEC   0.2

RICKY-BR MEG.049 RT-FR-SAME LIGHTS-OFF
CPS AND NOTCH FILTERS 3.22-03 V VLN
10CPS STROBE R-N GEN T
29-SEP-83
0.01875 SEC

A
R

TSU
50

AT

5.0A   5.0D B/2   SEC

0.2
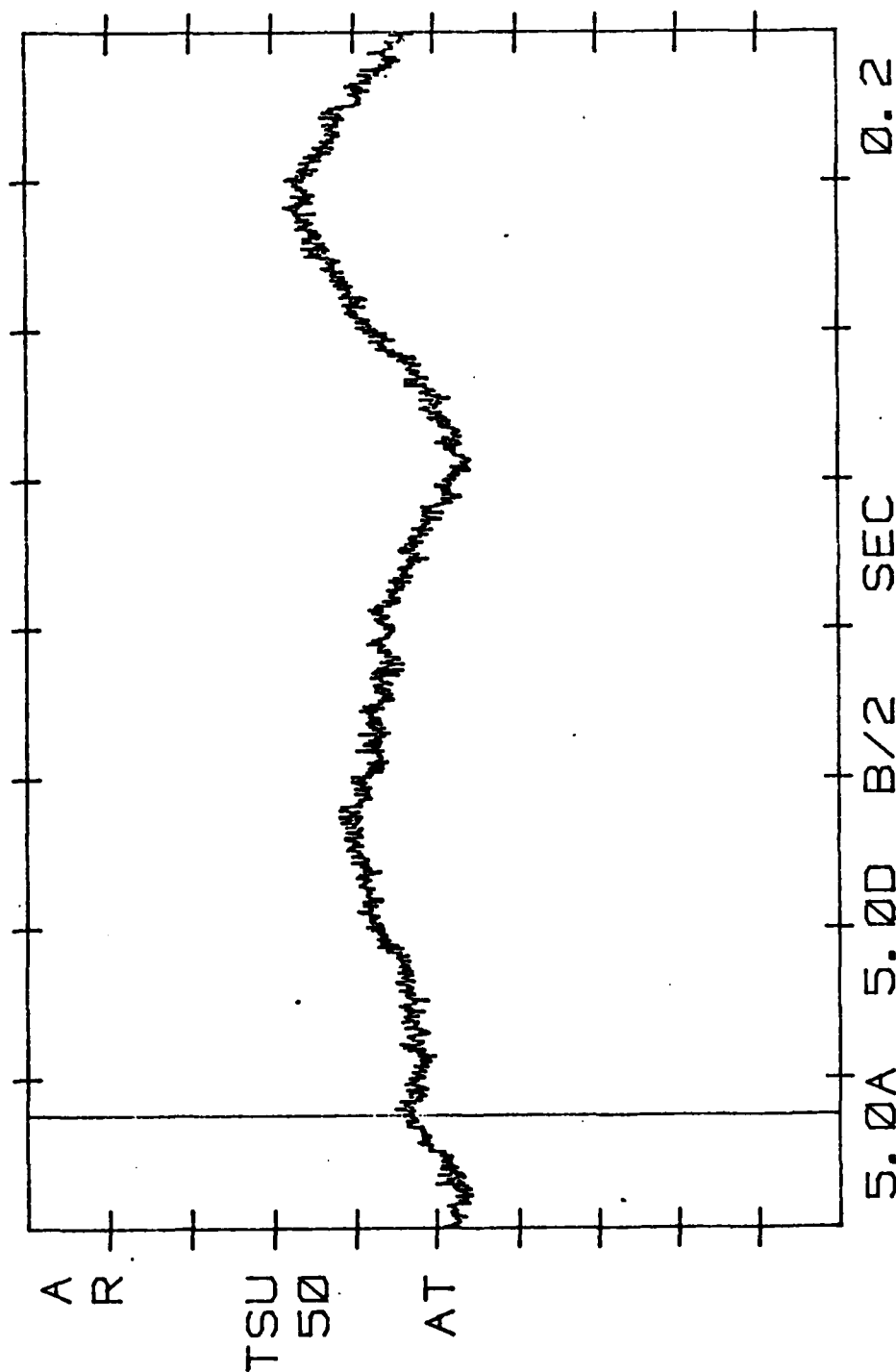
RICKY-BR MEG.049 RT-FR-SAME LIGHTS-OFF
10CPS AND NOTCH FILTERS 2.59-03 V VLN
29-SEP-83 STROBE R-N GEN T
0.03926 SEC
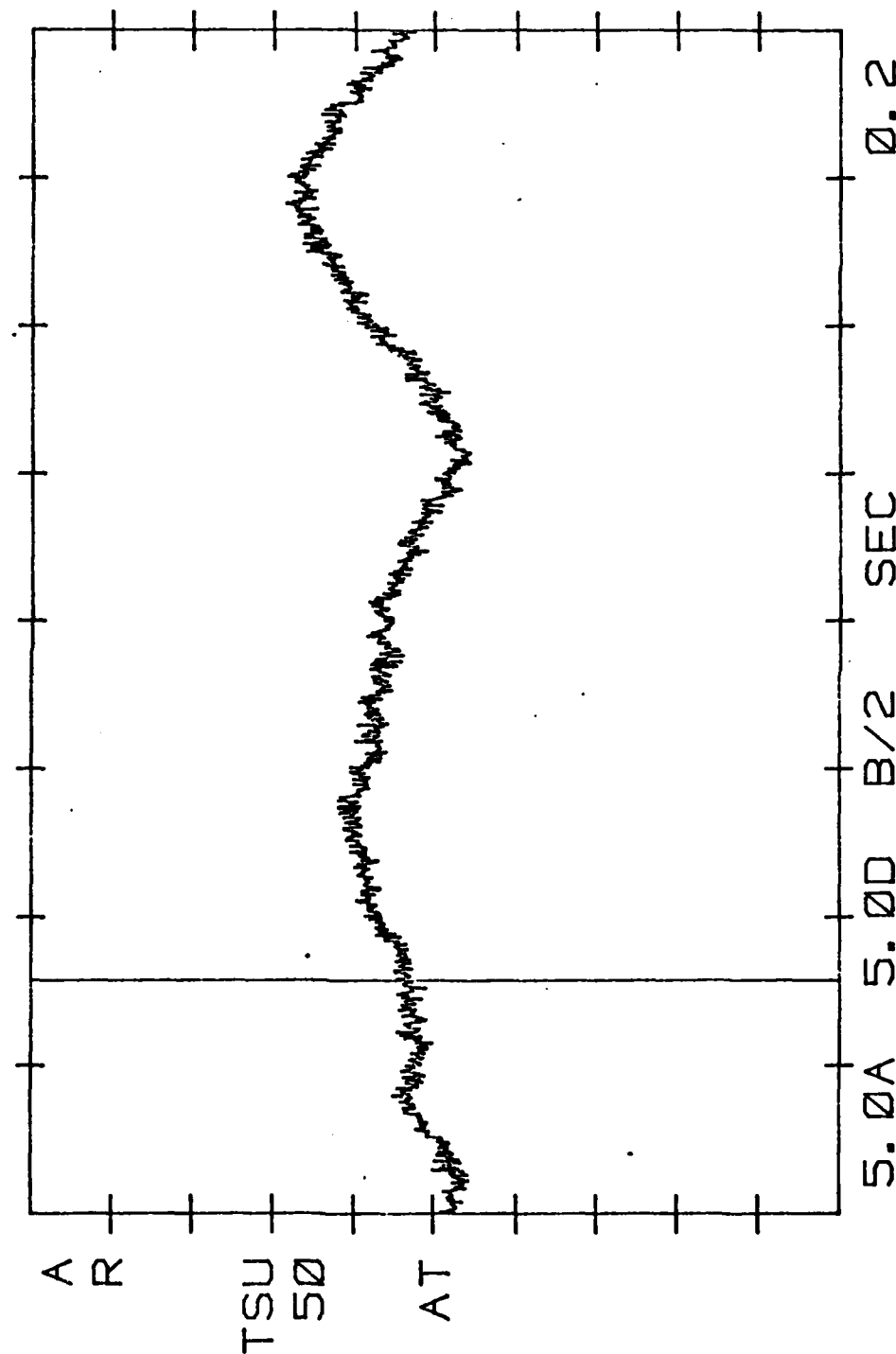
A
R

TSU
50

AT

5.0A 5.0D B/2 SEC 0.2
      5.0D B/2 SEC

RICKY MEG. Ø5Ø LT-QC-NEW LIGHTS-OFF
1ØCPS AND NOTCH FILTERS 83.3-Ø3 V VLN
29-SEP-83 STROBE R-N GEN T
Ø.Ø1348 SEC

5.ØA 5.ØD B/2 SEC Ø.2
5.2

A R TSU 5Ø AT
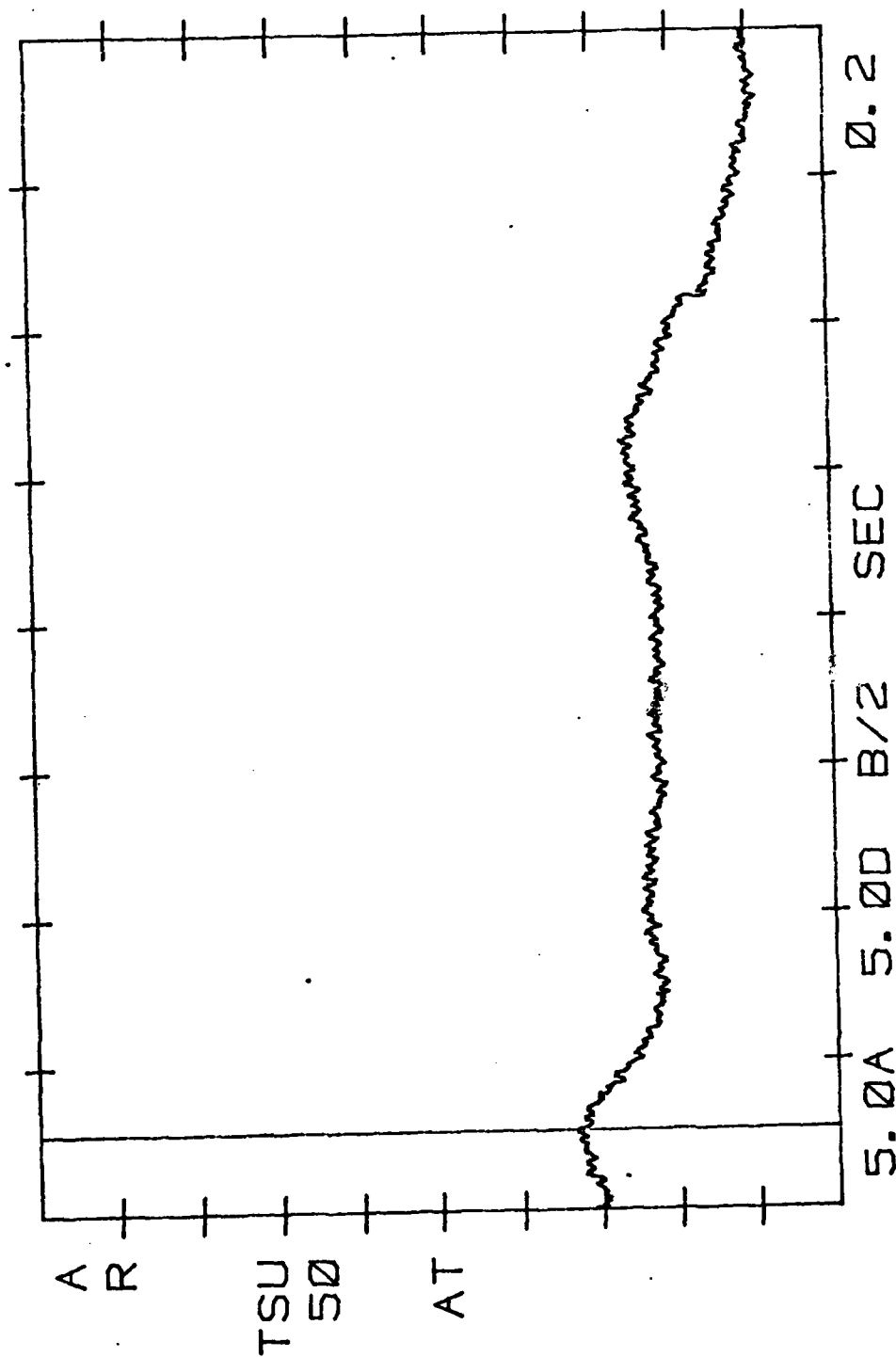
RICKY MEG.050 LT-QC-NEW LIGHTS-OFF
10CPS AND NOTCH FILTERS 141.-03 V VLN
29-SEP-83 STROBE R-N GEN T
0.03848 SEC

A
R

TSU
50

AT

5.0A 5.0D 5.0D B/2 SEC 0.2

D-22
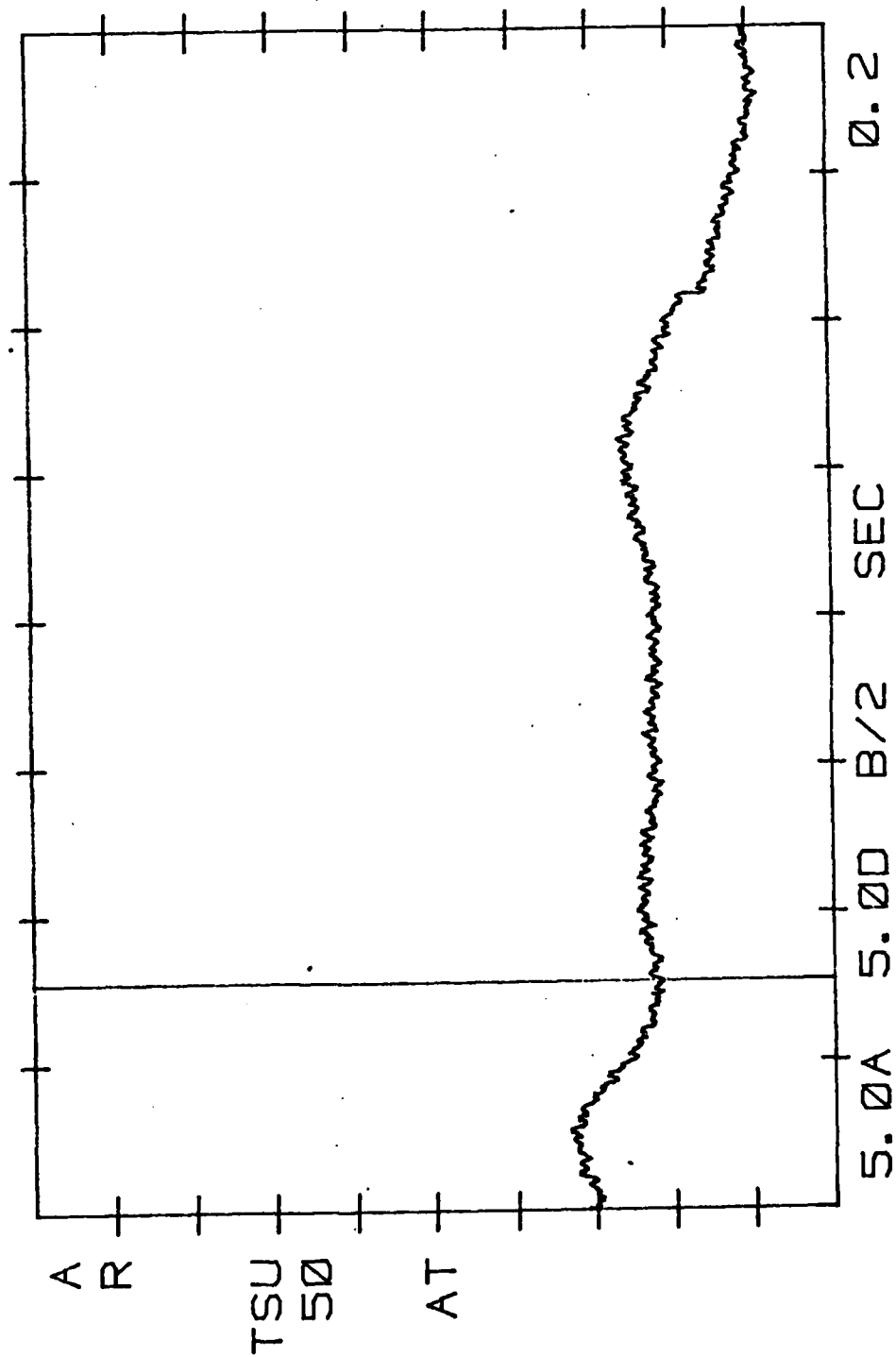
RICKY MEG.051 LT-OC-SAME LIGHTS-OFF
10CPS AND NOTCH FILTERS 42.6-03 V VLN
29-SEP-83 STROBE R-N GEN T
0.01387 SEC

A
R
TSU
50
AT

5.0A   5.0D   B/2   SEC
5.2   0.2

RICKY
MEG 051   LT-OC-SAME   LIGHTS-OFF
10CPS AND NOTCH FILTERS_83.1-03 V   VLN
29-SEP-83   STROBE   R-N GEN   T
0.03203 SEC

A
R

TSU
50

AT

5.0A   5.0D   B/2   SEC   0.2
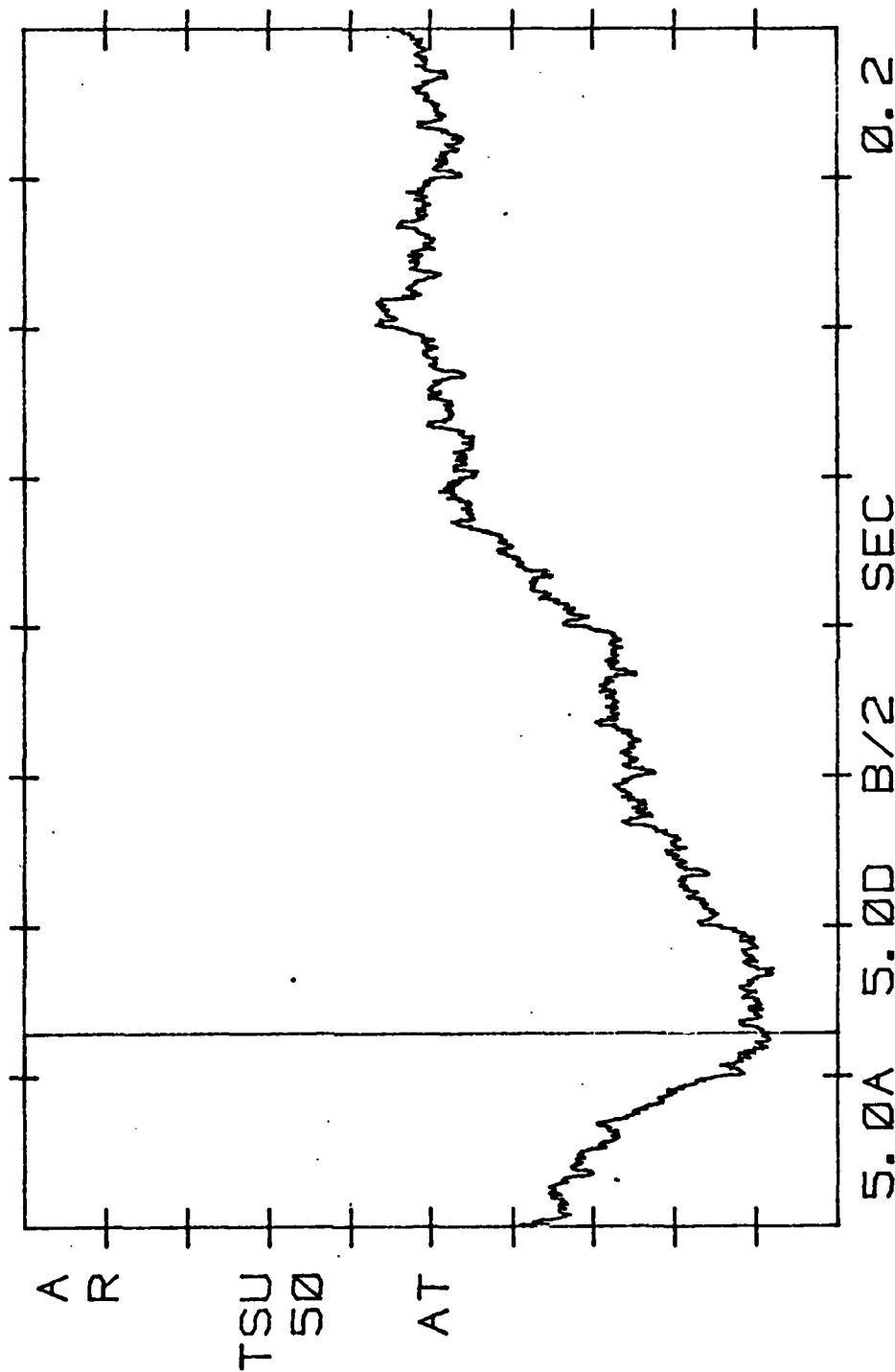
RICKY   MEG.052 ⌐T─GC─SAME   LIGHTS─OFF
  10CPS AND NOTCH FILTERS 16.0─03 V   VLN
  29─SEP─83   STROBE   R─N GEN   T
                  0.01074 SEC

A
R

TSU
50

AT

        5.0A 5.0D B/2 SEC   0.2

D─25
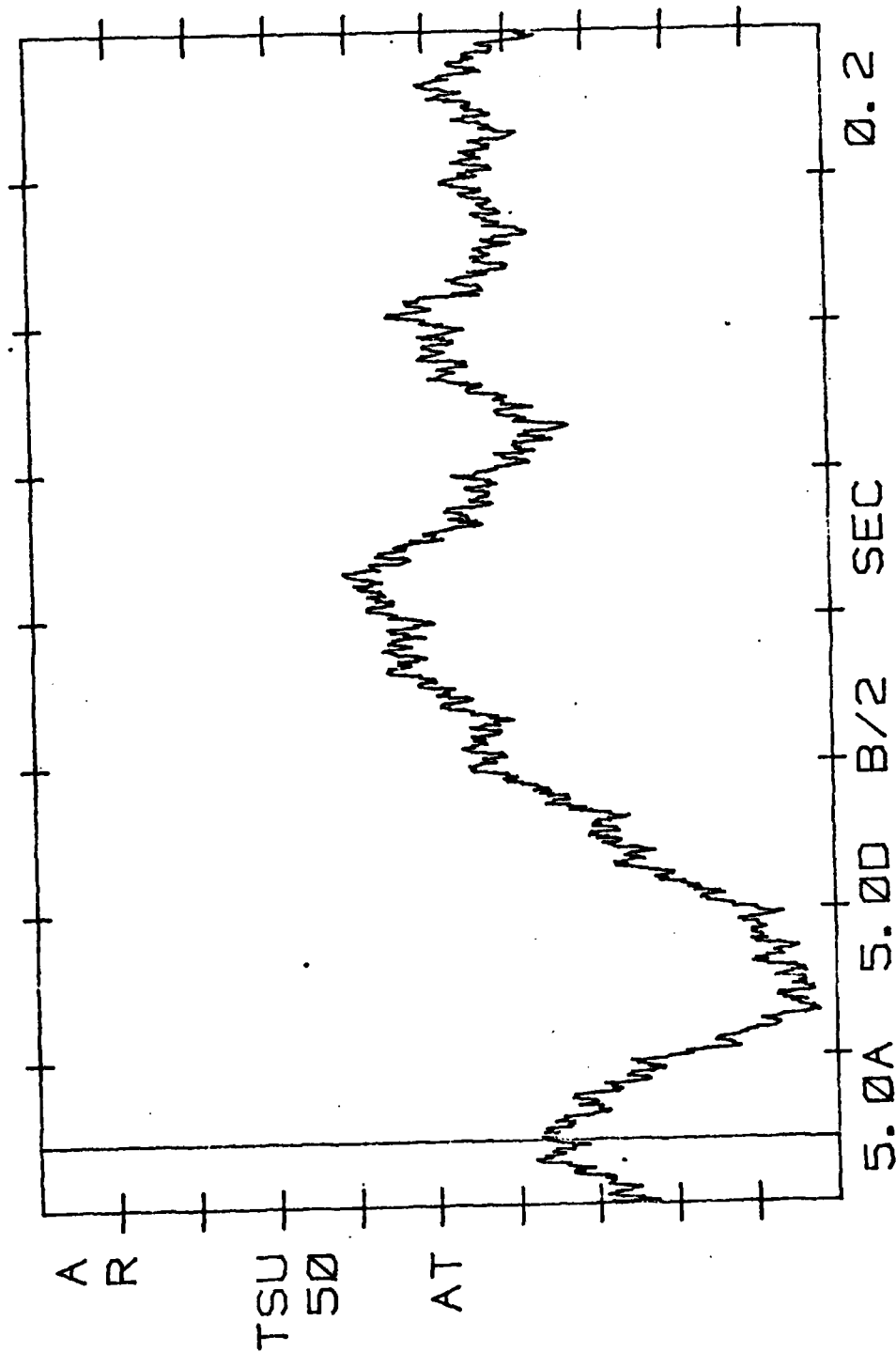
RICKY MEG 052 LT-QC-SAME LIGHTS-OFF
10CPS AND NOTCH FILTERS 57.2-03 V VLN
29-SEP-83 STROBE R-N GEN T
0.03223 SEC

A
R

TSU
50

AT

5.0A   5.0D   B/2   SEC   0.2

RICKY MEG.053 LT-OC-NEW LIGHTS-OFF
10CPS AND NOTCH FILTERS 16.7-03 V VLN
29-SEP-83 STROBE R-N GEN T
0.01016 SEC

A
R

TSU
50

AT

5.0A 5.0D B/2 SEC 0.2

5.0
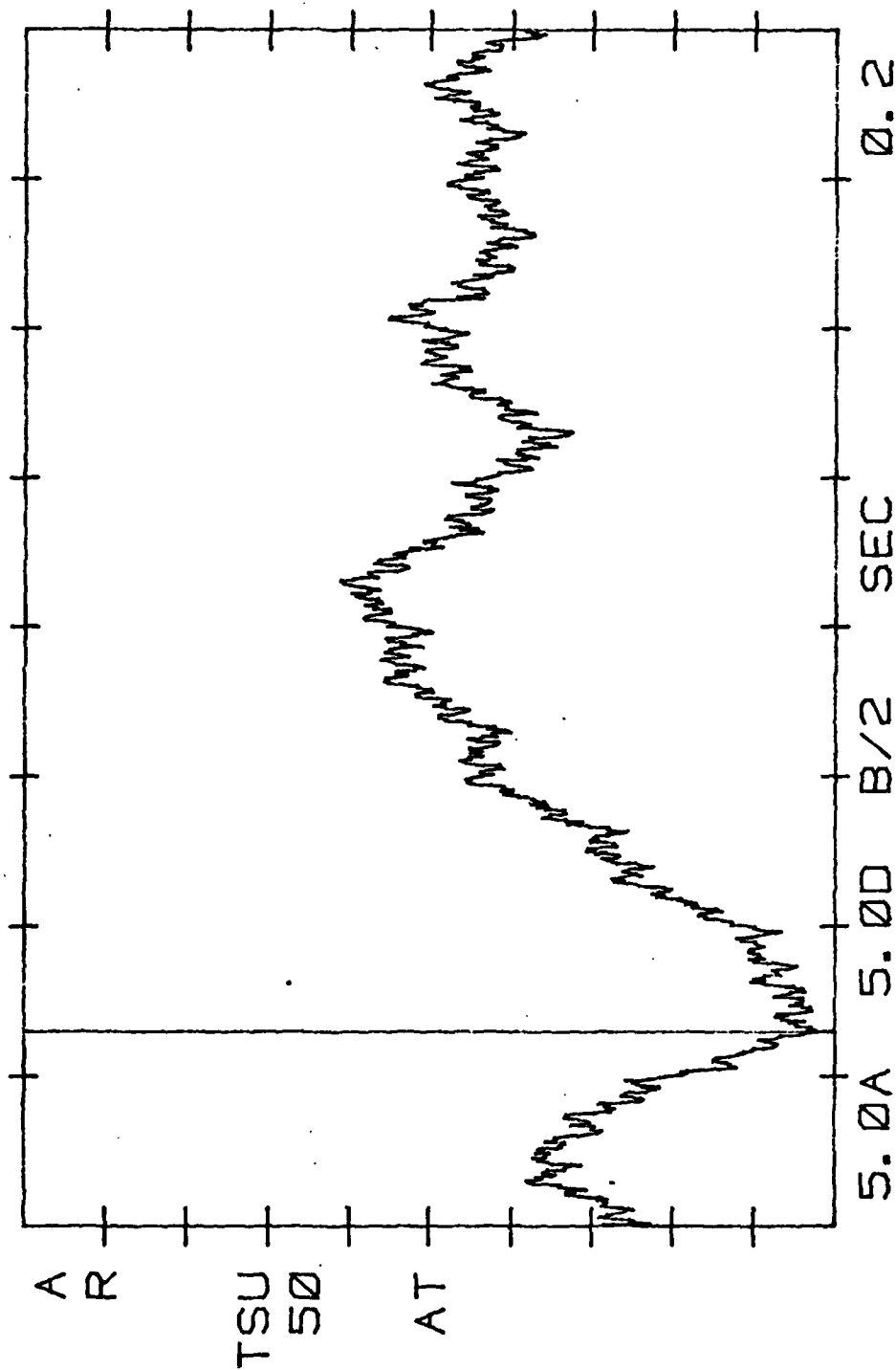
RICKY MEG.053 LT-QC-NEW LIGHTS-OFF
10CPS AND NOTCH FILTERS 52.6-03 V VLN
29-SEP-83 STROBE R-N GEN T
0.04160 SEC

A
R

TSU
50

AT

5.0A 5.0D B/2 SEC 0.2

RICKY   LIGHT-OFF
MEG.054   RT-OC
10CPS AND NOTCH FILTERS 200.-06 V   VLN
20-OCT-83 STROBE   T
0.02383 SEC

AR

TSU
50

AT

0.1A   10.A   B/16 SEC   0.2
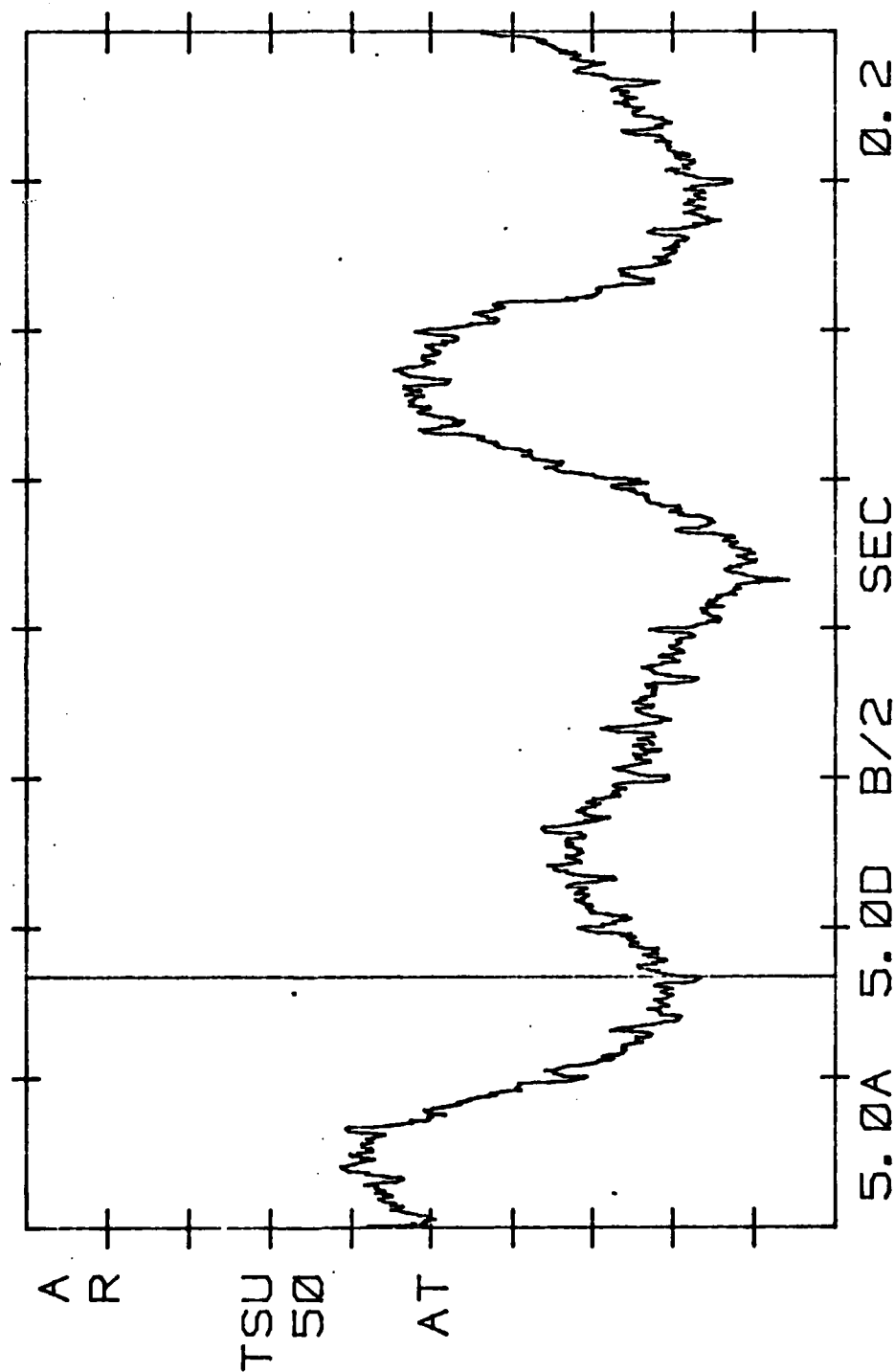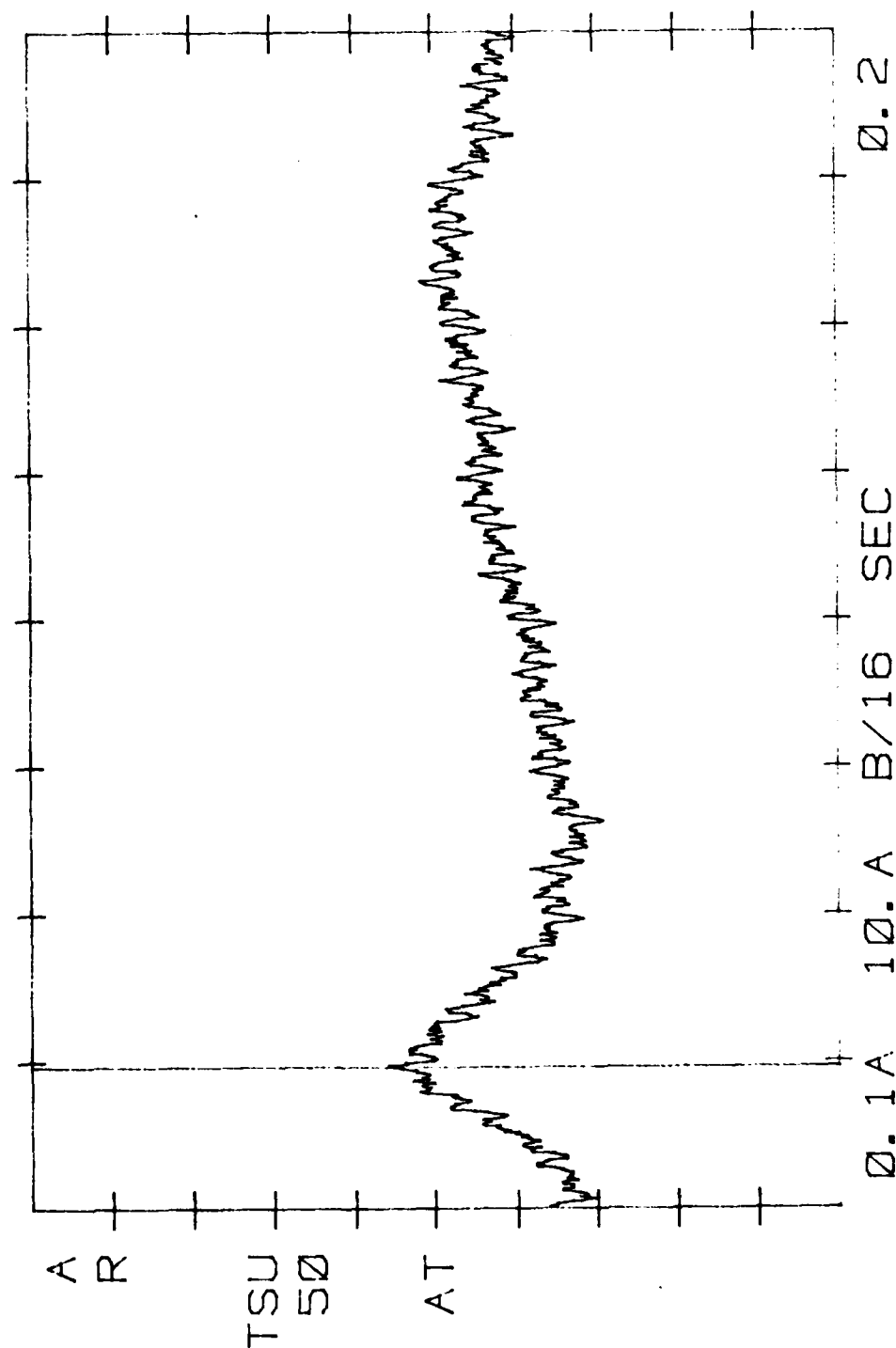
RICKY   MEG.054   RT-OC   LIGHT-OFF
10CPS   AND   NOTCH FILTERS_591.-06 V   VLN
20-OCT-83   STROBE   T
               0.00000 SEC

A
R

TSU
50

AT

0.1A   10.A   B/16   SEC   0.2

0.2

VLN
T
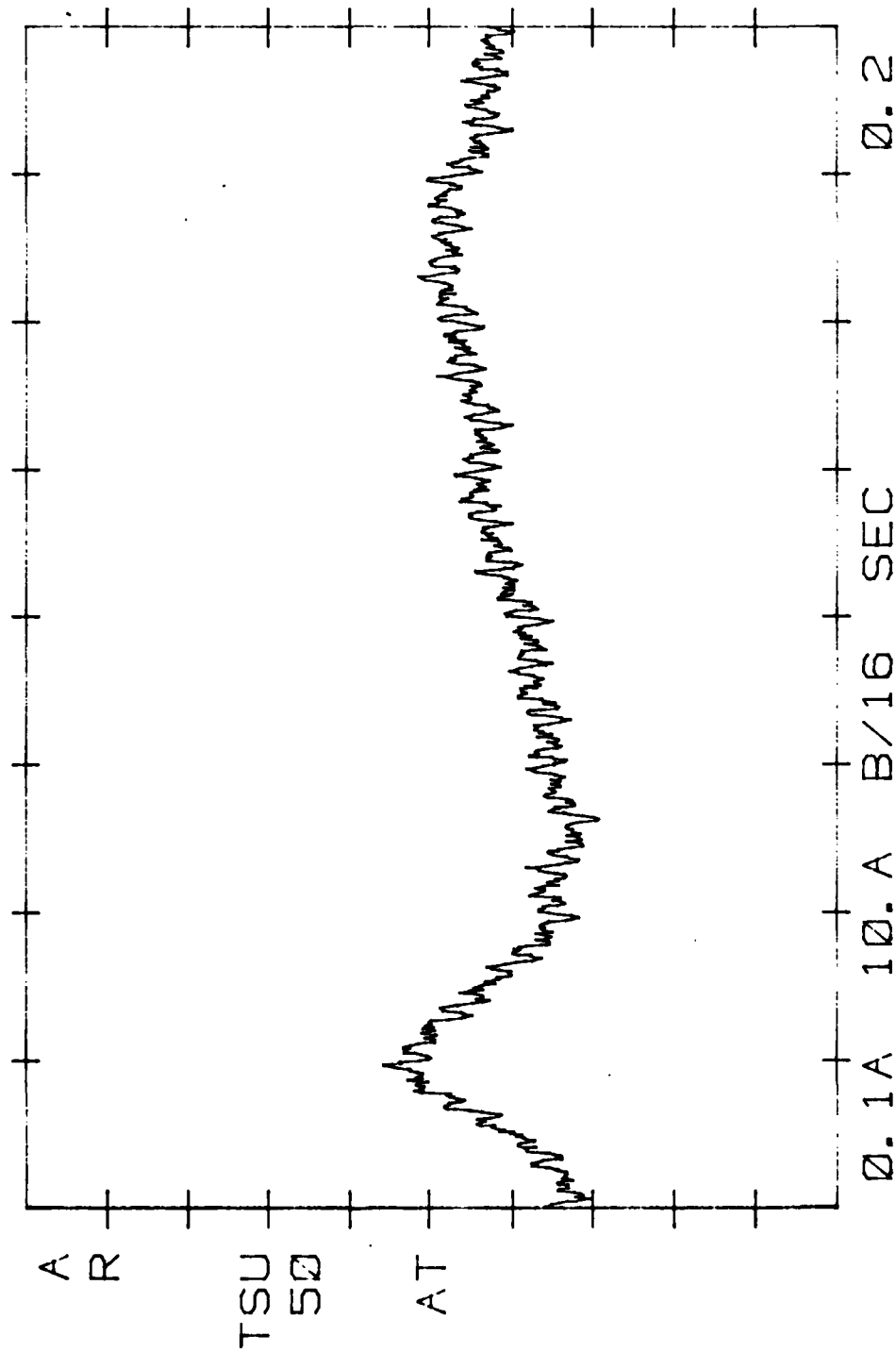
RICKY MEG.055 RT-OC LIGHT-OFF
10CPS AND NOTCH FILTERS 1.42-03 V VLN
20-OCT-83 STROBE 0.01426 SEC T
0.01426 SEC

A
R

TSU
50

AT

Ø.2

Ø.1A 10.A B/16 SEC

Ø.1A 10.A B/16 SEC

Ø.2
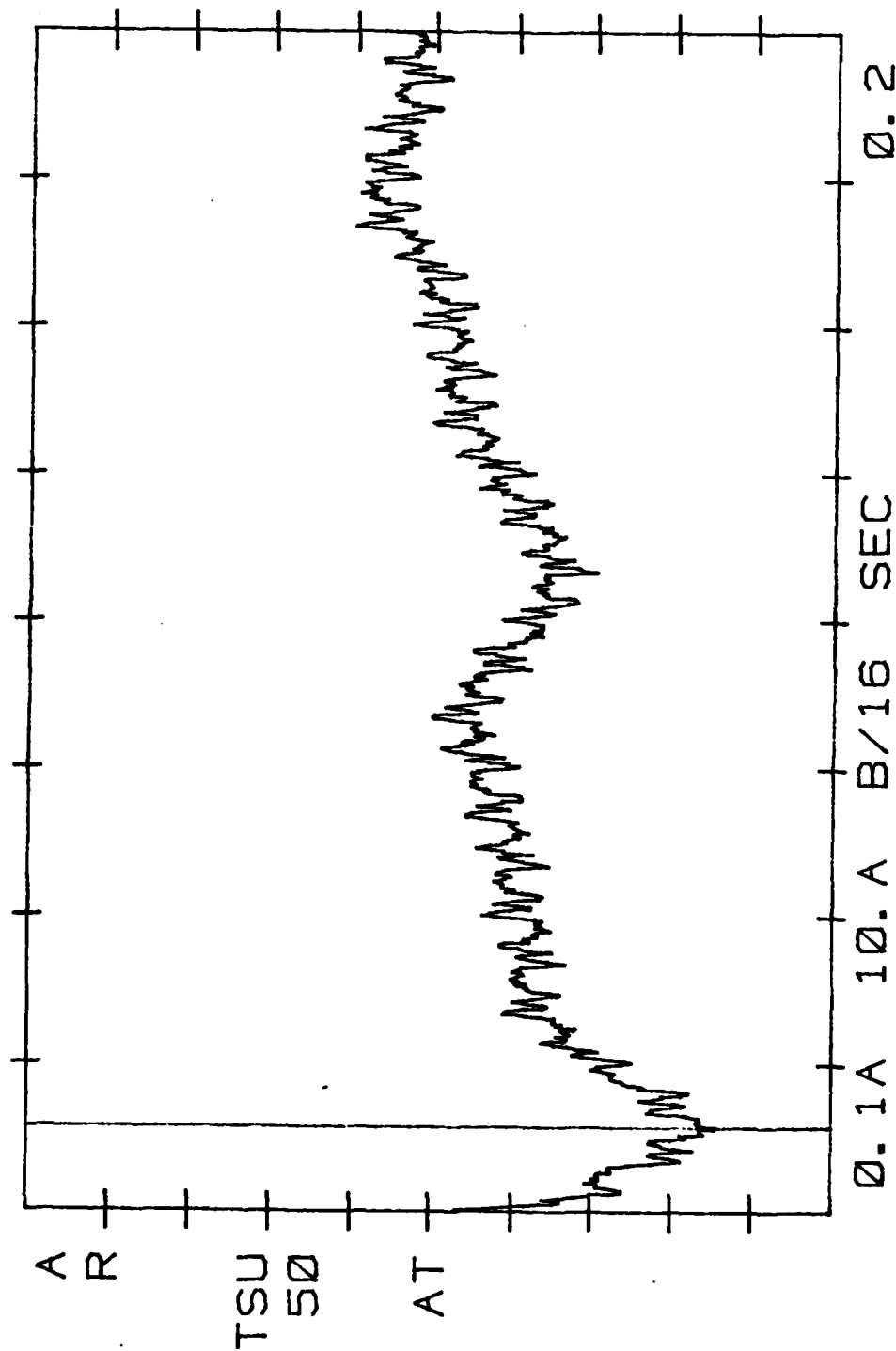
RICKY   MEG.055   RT-OC   LIGHT-OFF
10CPS AND NOTCH FILTERS 120. -06 V   VLN
20-OCT-83   STROBE   T
            0.00000 SEC

A
R

TSU
50

AT

0.1A   10.A   B/16 SEC

0.2   0.2
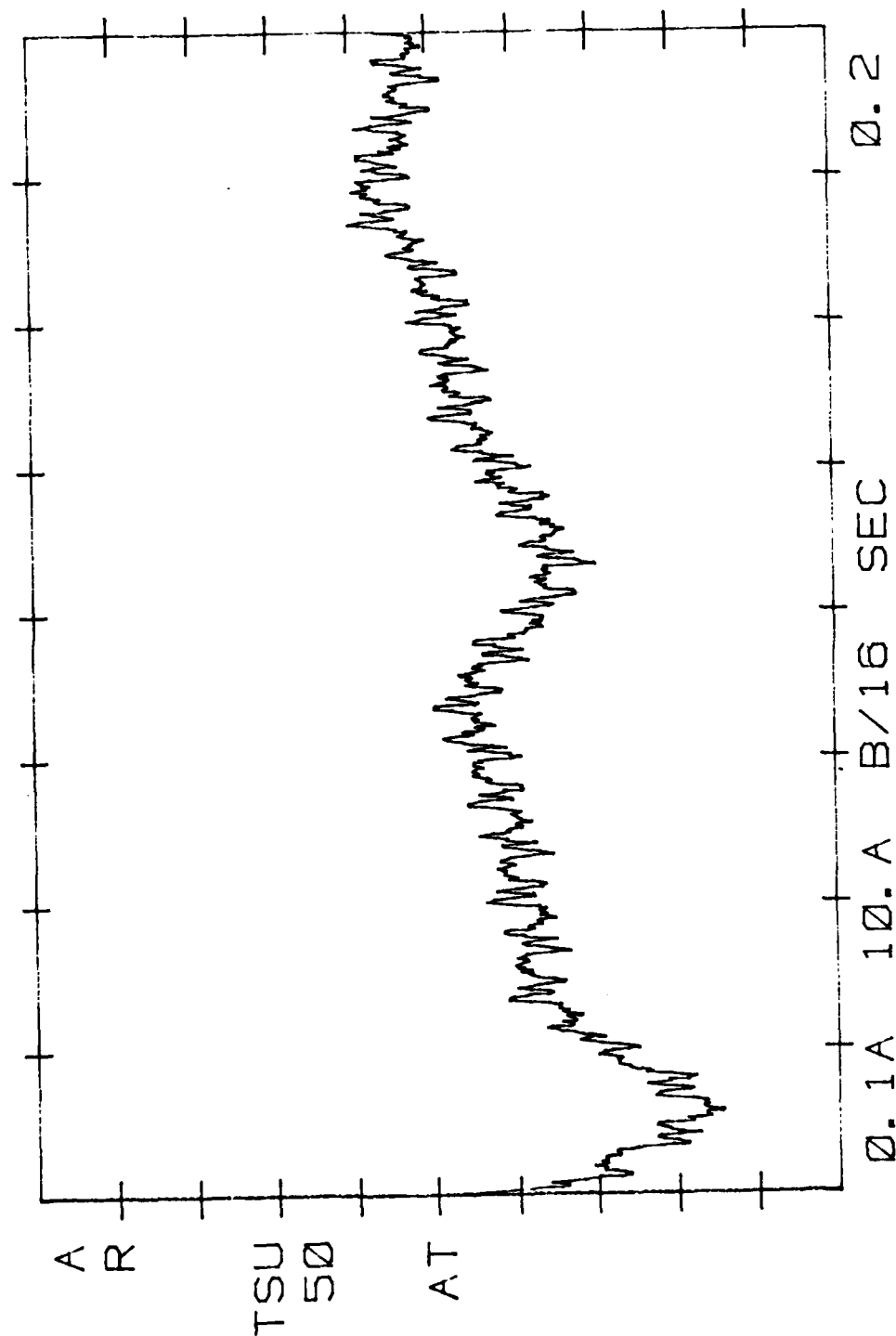
RICKY MEG.056 RT-OC-NEW LIGHT-OFF
10CPS AND NOTCH FILTERS 7.64-03 V VLN
28-OCT-83 STROBE 0.02012 SEC
0.02012 SEC
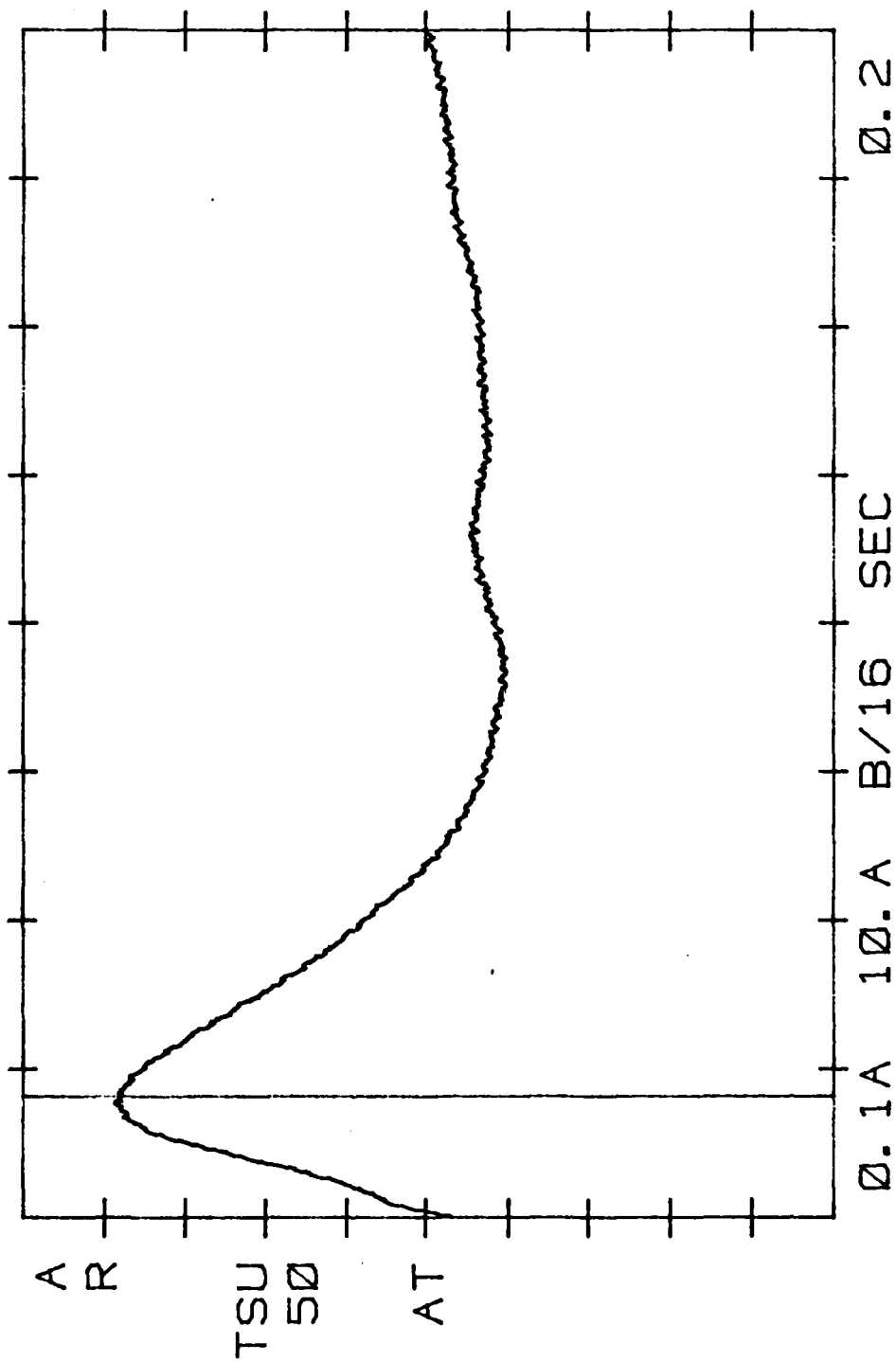
RICKY
10CPS AND NOTCH FILTERS_583. -06 V VLN
20-OCT-83 STROBE 0.00000 SEC
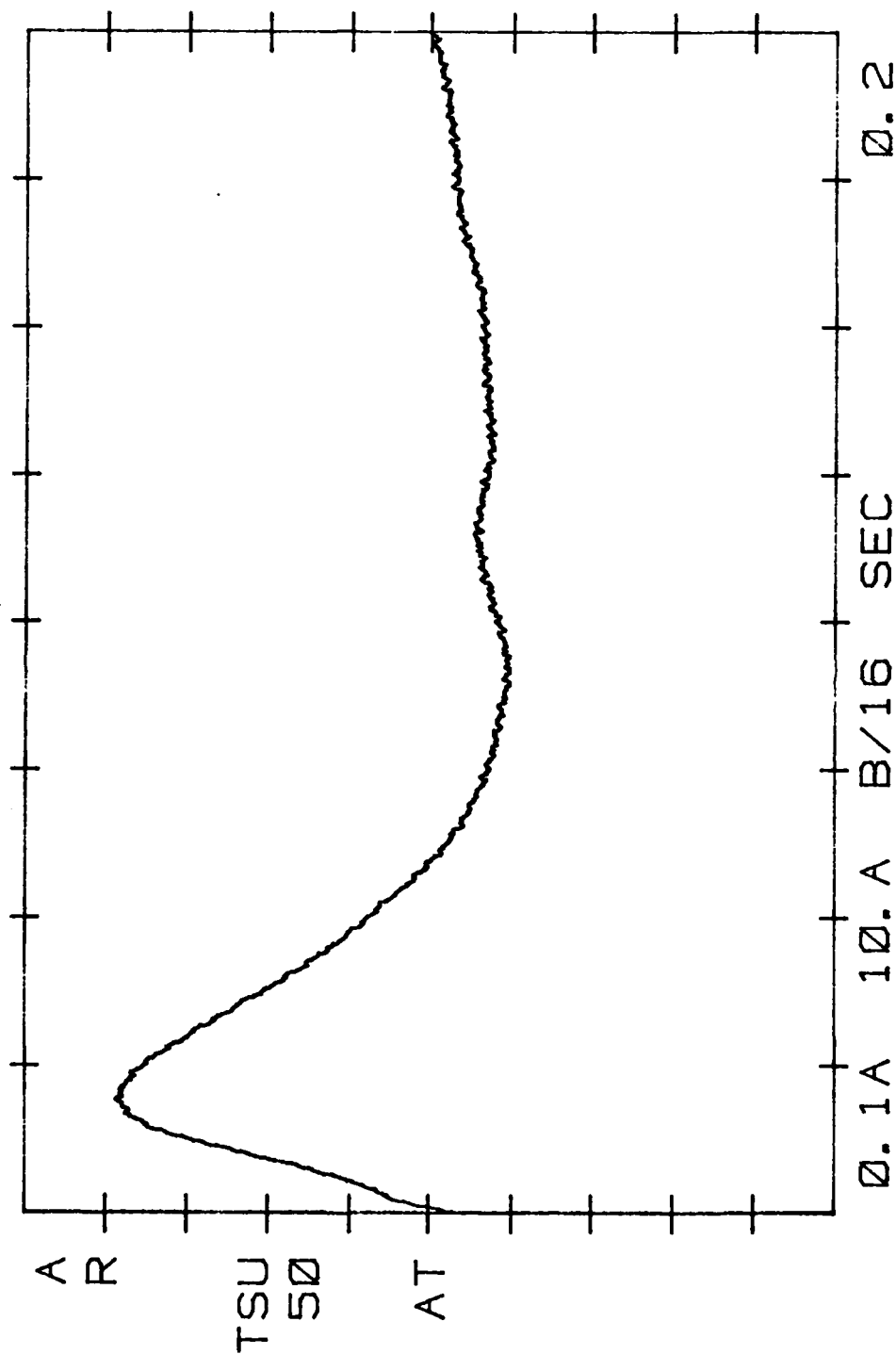
MEG.056 RT-OC-NEW LIGHT-OFF
V T
VLN
T

A
R

TSU
50

AT

Ø.1A   1Ø.A B/16 SEC   Ø.2

RICKY   MEG.Ø57 RT-OC-SAME LIGHT-OFF
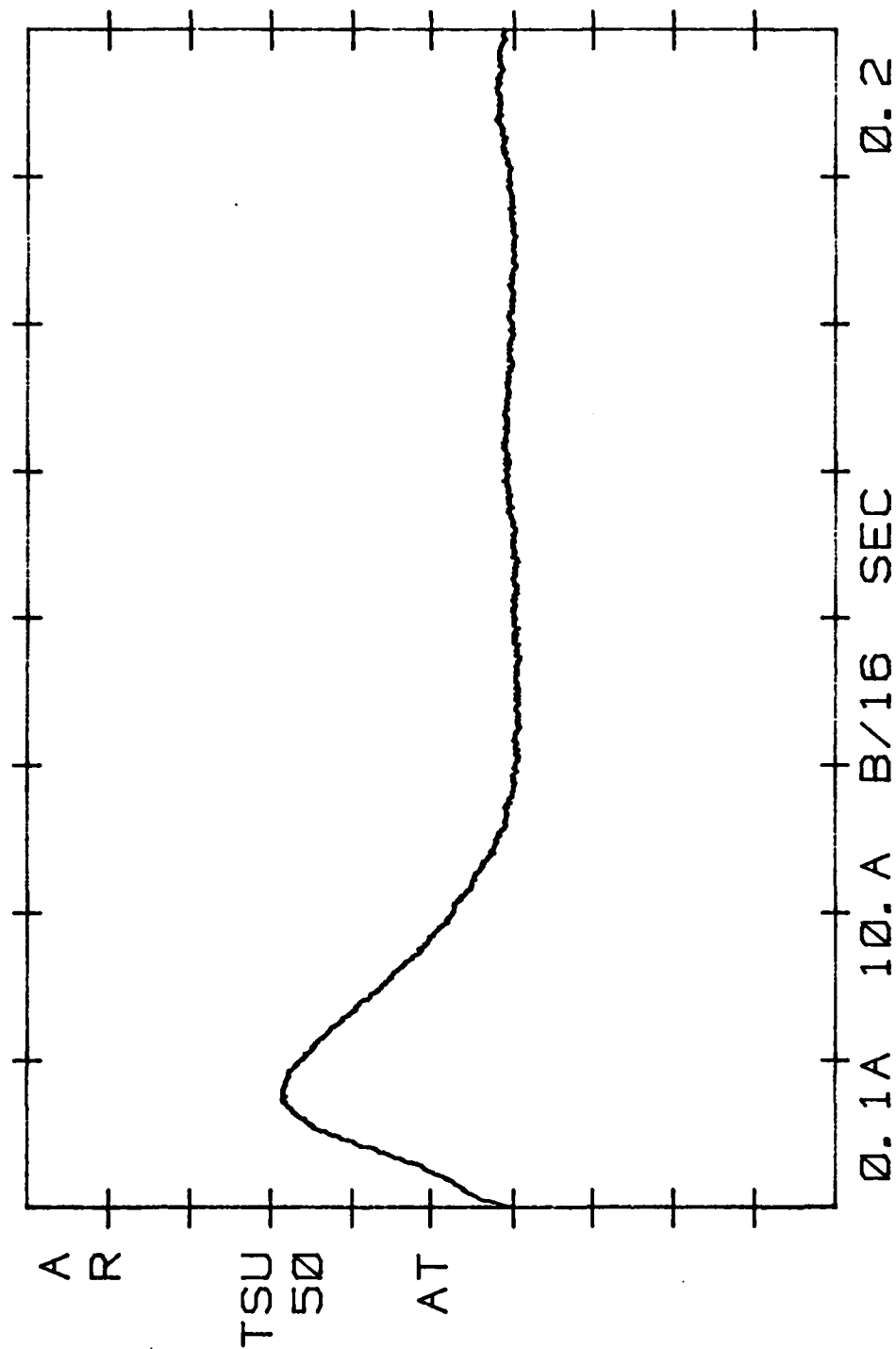
1ØCPS AND NOTCH FILTERS 3.69-Ø3 V VLN

2Ø-OCT-83 STROBE V T

Ø.Ø1953 SEC

A
R

TSU
5Ø

AT

Ø.1A   1Ø.A B/16 SEC   Ø.2

RICKY   MEG.057   RT-OC-SAME LIGHT-OFF
10CPS AND NOTCH FILTERS_2.01-03 V   VLN
20-OCT-83 STROBE   T
           0.00000 SEC

A
R

TSU
50

AT

0.1A   10.A B/16 SEC   0.2

RICKY-8R MEG.Ø58 RT-OC-SAME LIGHT-OFF
1ØCPS AND NOTCH FILTERS 246.-Ø6 V VLN
2Ø-OCT-83 STROBE Ø.Ø2559 SEC T

RICKY-BR   MEG.058   RT-OC-SAME   LIGHT-OFF
10CPS AND NOTCH FILTERS 487.-06 V   VLN
20-OCT-83   STROBE
            0.00000 SEC

0.1A 10.A B/16 SEC
0.2   0.2

A
R
TSU
50
AT

D-38

RICKY MEG.05g RT-OC-NEW LIGHT-OFF
CPS AND NOTCH FILTERS_5.92-03 V VLN
20-OCT-83 STROBE T
0.018836 SEC

A
R

TSU
50

AT

0.1A   10.A B/16 SEC   0.2
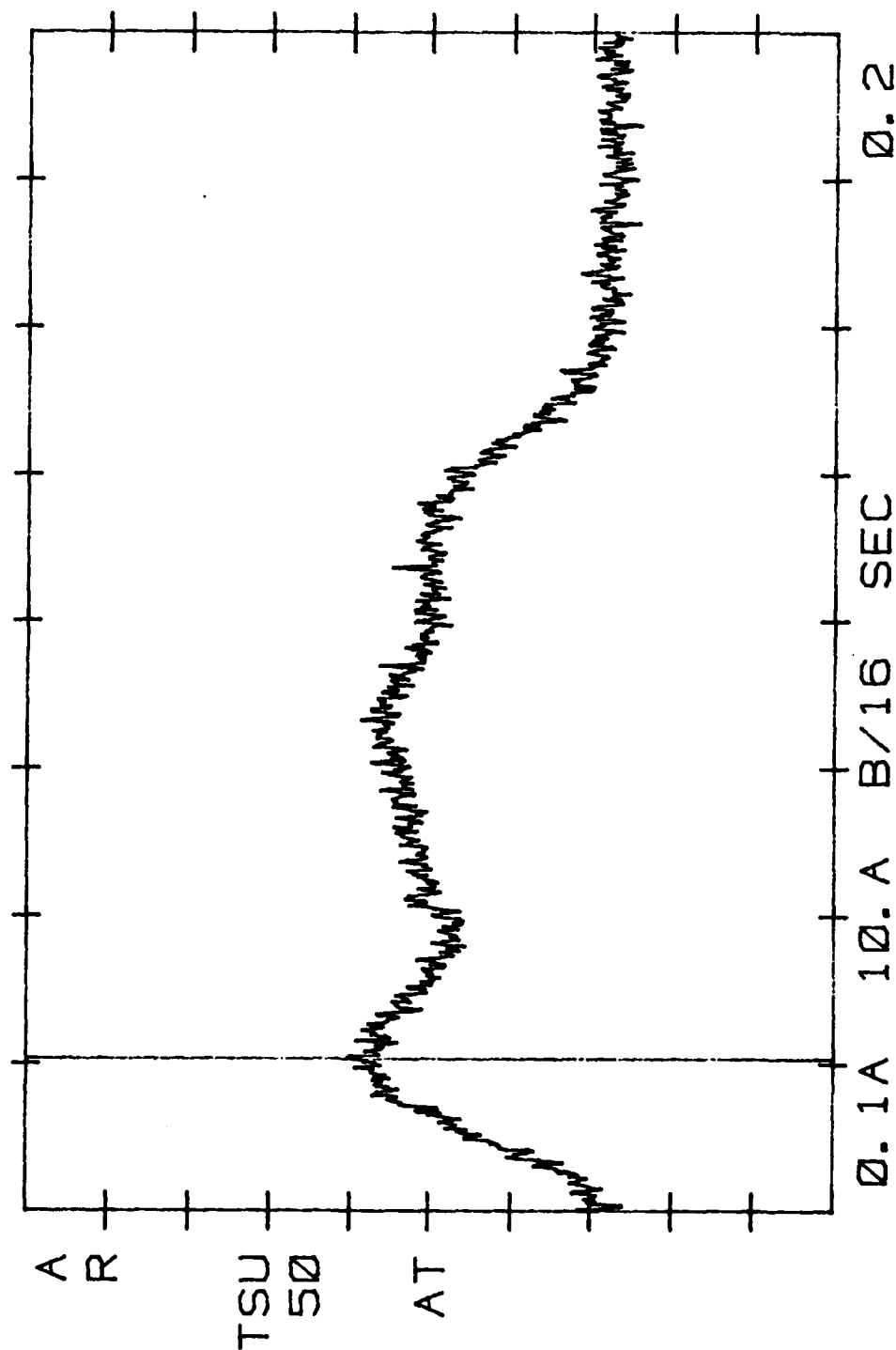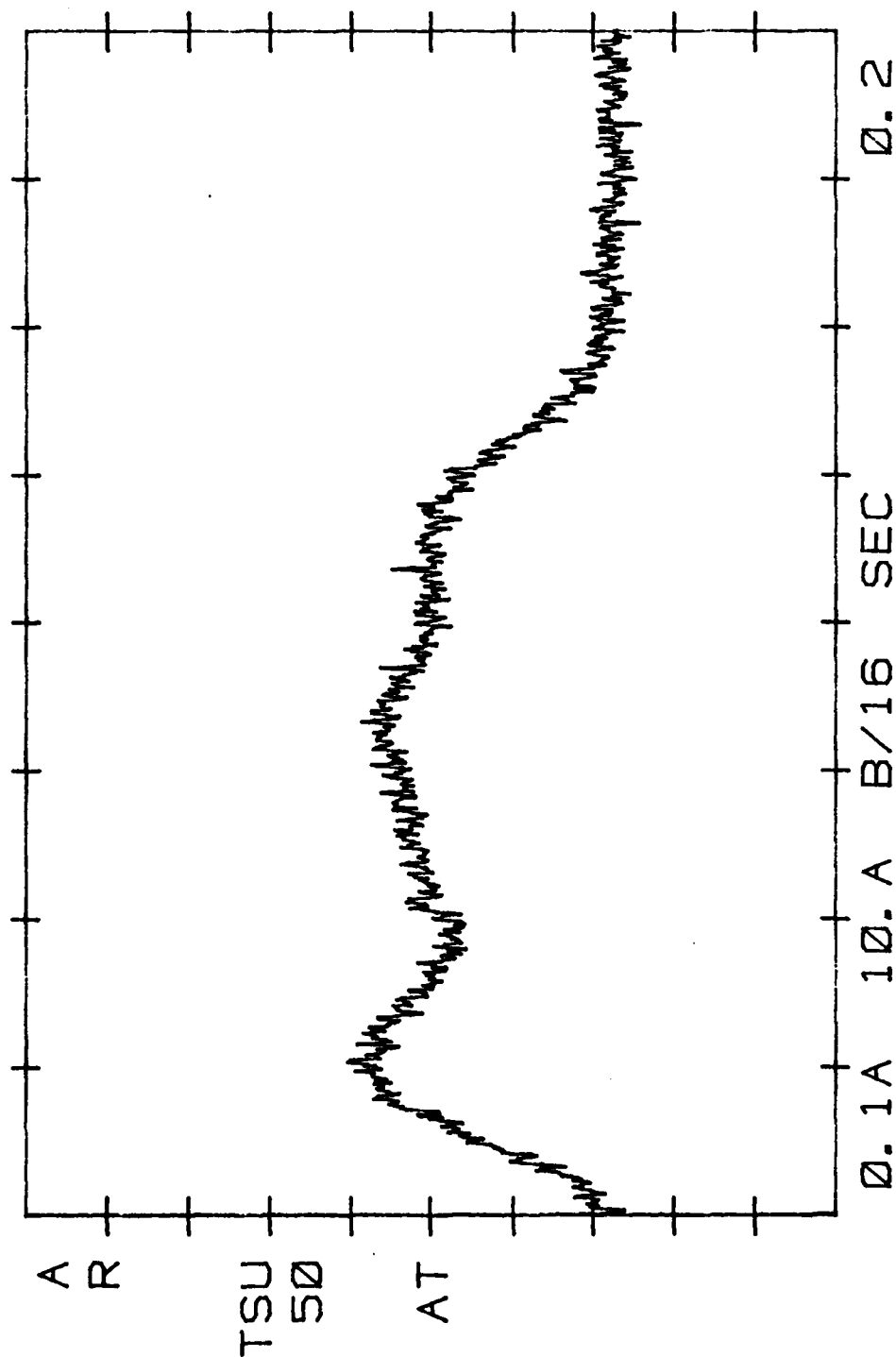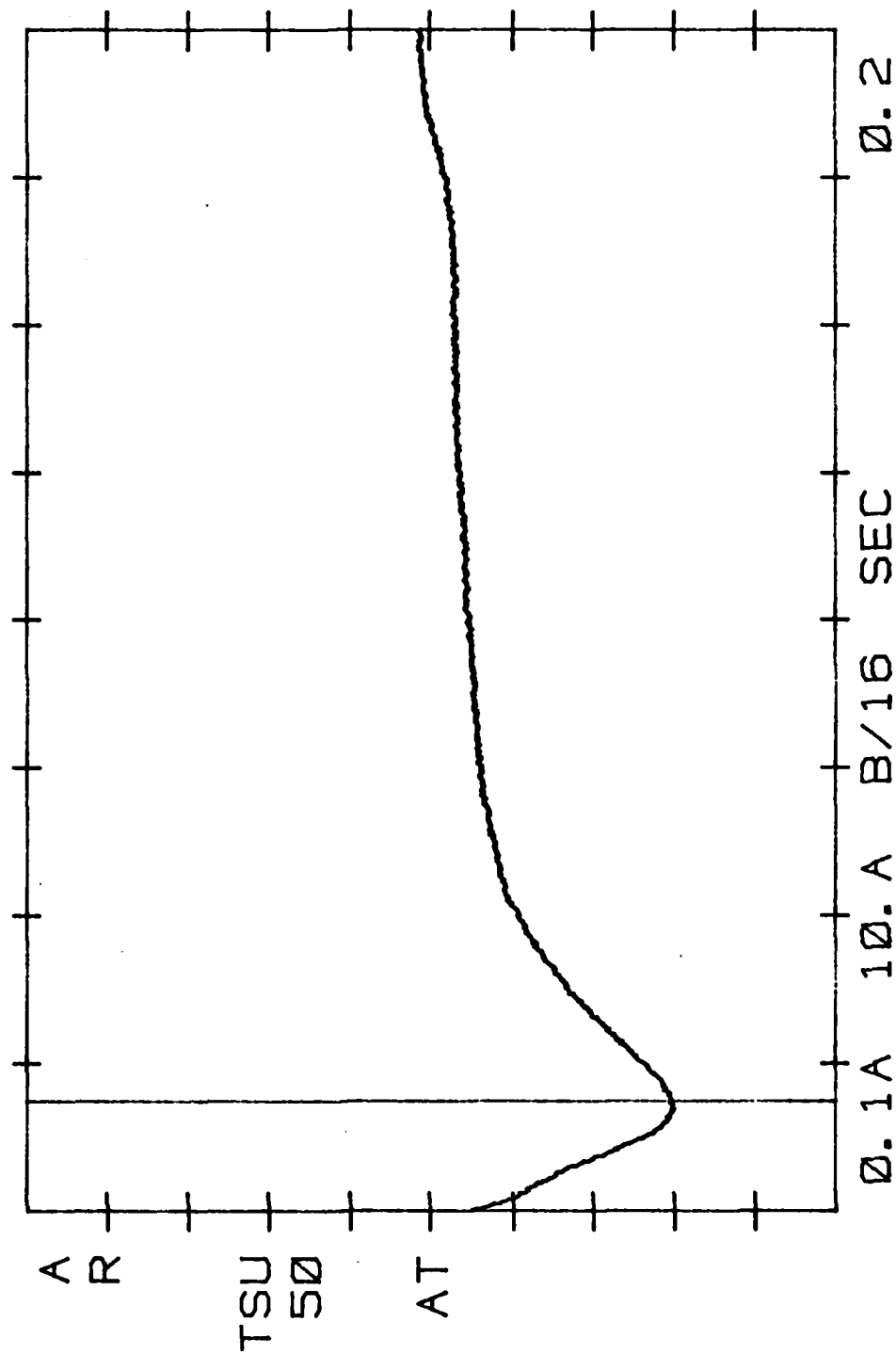
RICKY   MEG.059   RT-OC-NEW   LIGHT-OFF
10CPS AND NOTCH FILTERS_971.-06 V VLN
20-OCT-83 STROBE   V   T
        0.00000 SEC
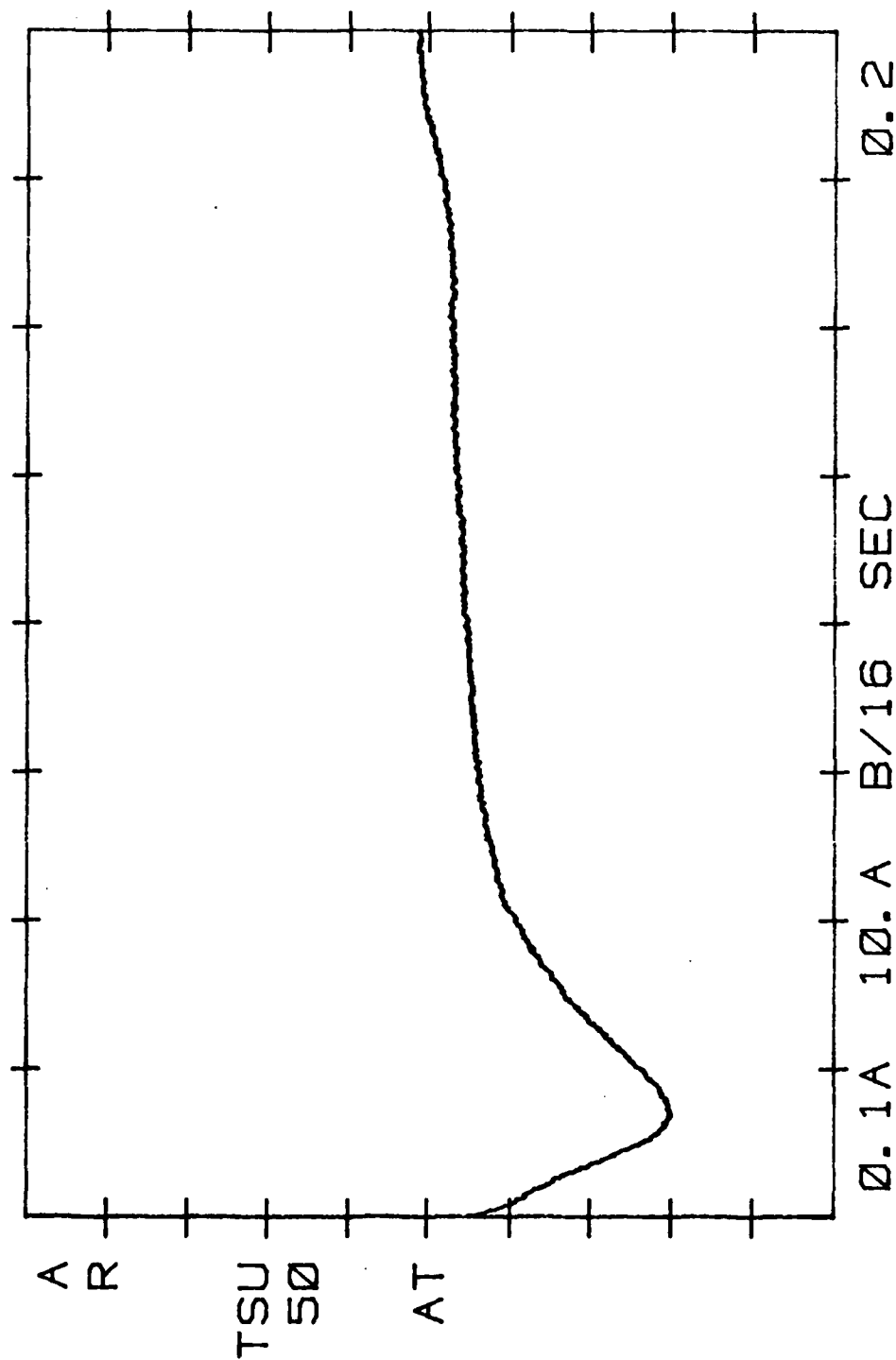
A
R

TSU
50

AT

0.1A   10.A   B/16 SEC
              0.2

RICKY   MEG.060   LT-FR-NEW   LIGHT-OFF
10CPS AND NOTCH FILTERS 5.75-03 V   VLN
20-OCT-83 STROBE   V   T
Ø.01836 SEC
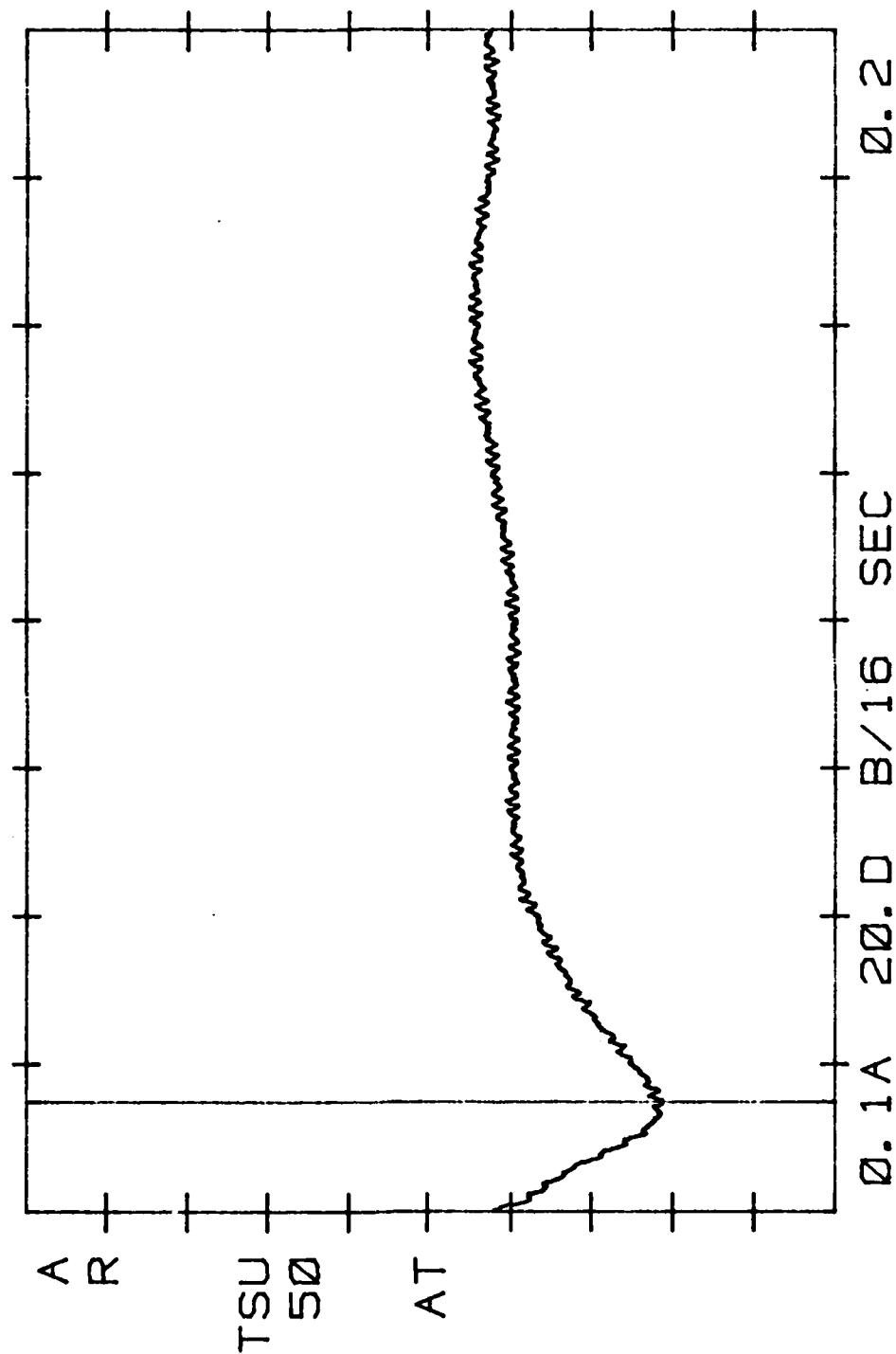
A
R

TSU
5Ø

AT

Ø.1A   20.0 20.D B/16 SEC   Ø.2   Ø.2

RICKY   MEG.060 LT-FR-NEW   LIGHT-OFF
CPS AND NOTCH FILTERS_1.60-03 V   VLN
20-OCT-83 STROBE 0.00000 SEC   T
           0.00000 SEC

A
R

TSU
50

AT

0.2   0.1A   20.D B/16 SEC   0.2

RICKY
MEG.Ø61 LT-FR-SAME LIGHT-OFF
1ØCPS AND NOTCH FILTERS_3.61-Ø3 V VLN
2Ø-OCT-83 STROBE T
Ø.Ø1758 SEC

A
R

TSU
5Ø

AT

Ø.1A   2Ø.D B/16 SEC   Ø.2
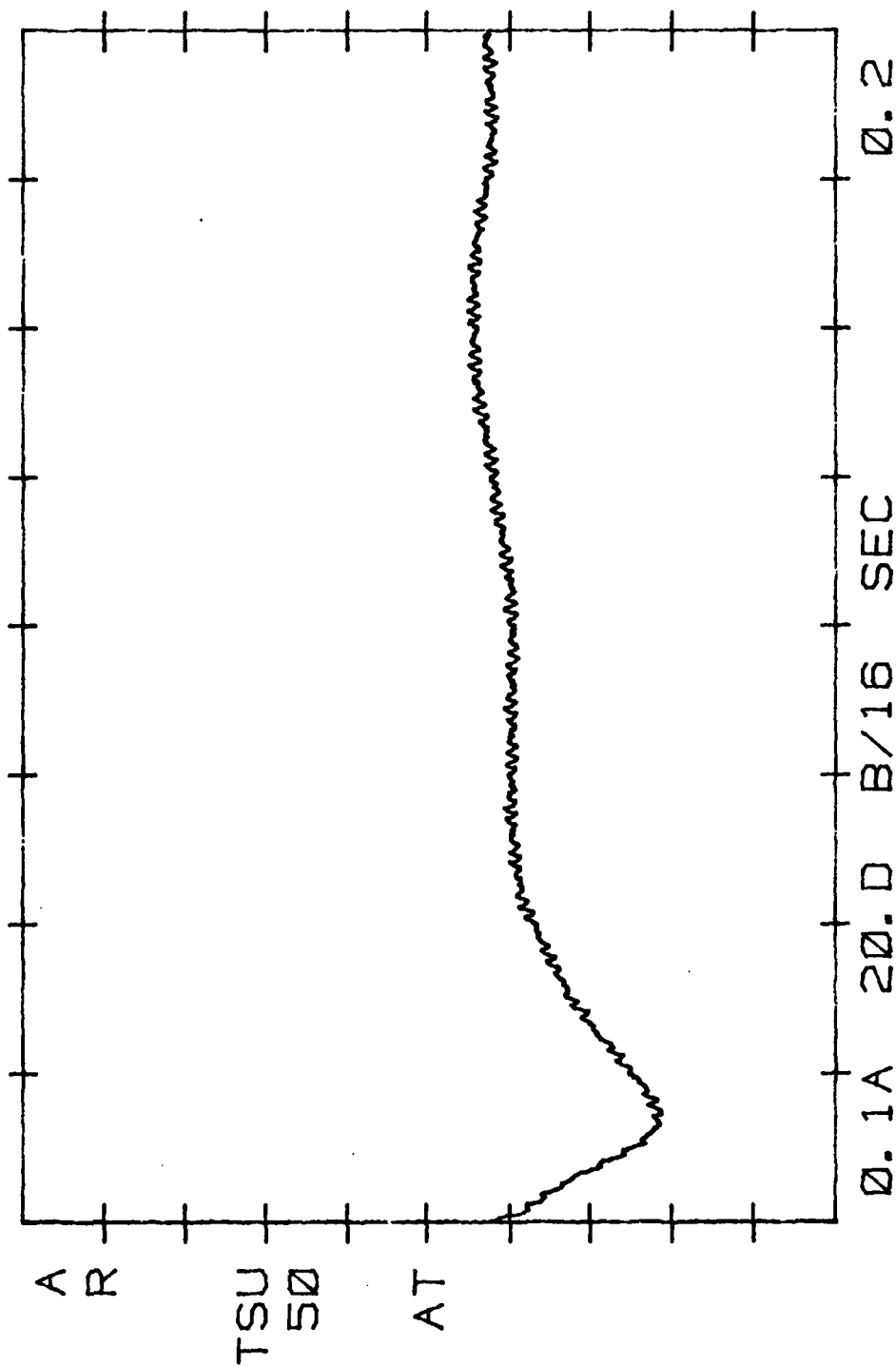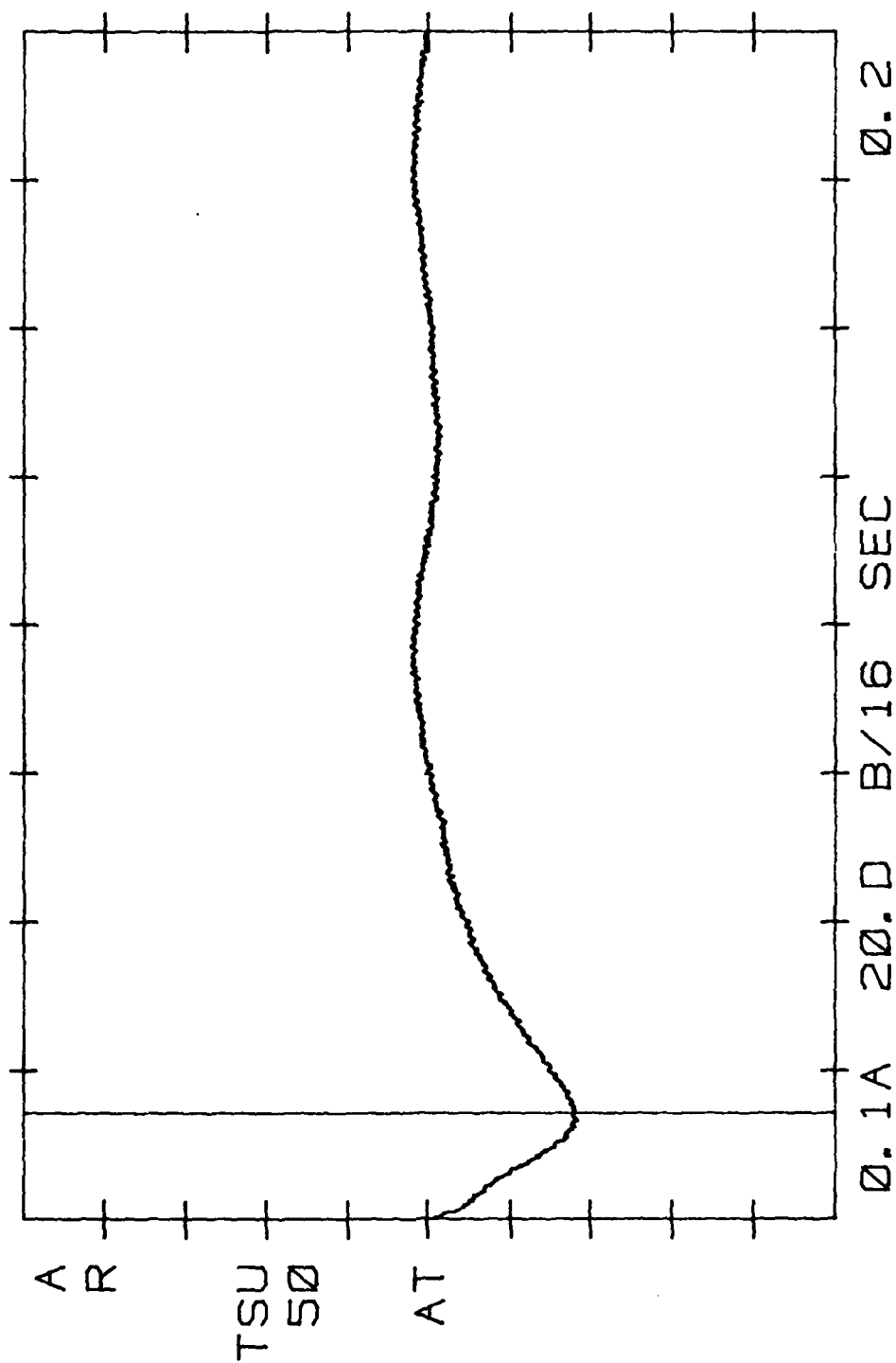
RICKY MEG.061 LT-FR-SAME LIGHT-OFF
10CPS AND NOTCH FILTERS_185.-06 V VLN
20-OCT-83 STROBE T
0.00000 SEC

A
R

TSU
50

AT

0.1A 20.D B/16 SEC 0.2

0.2
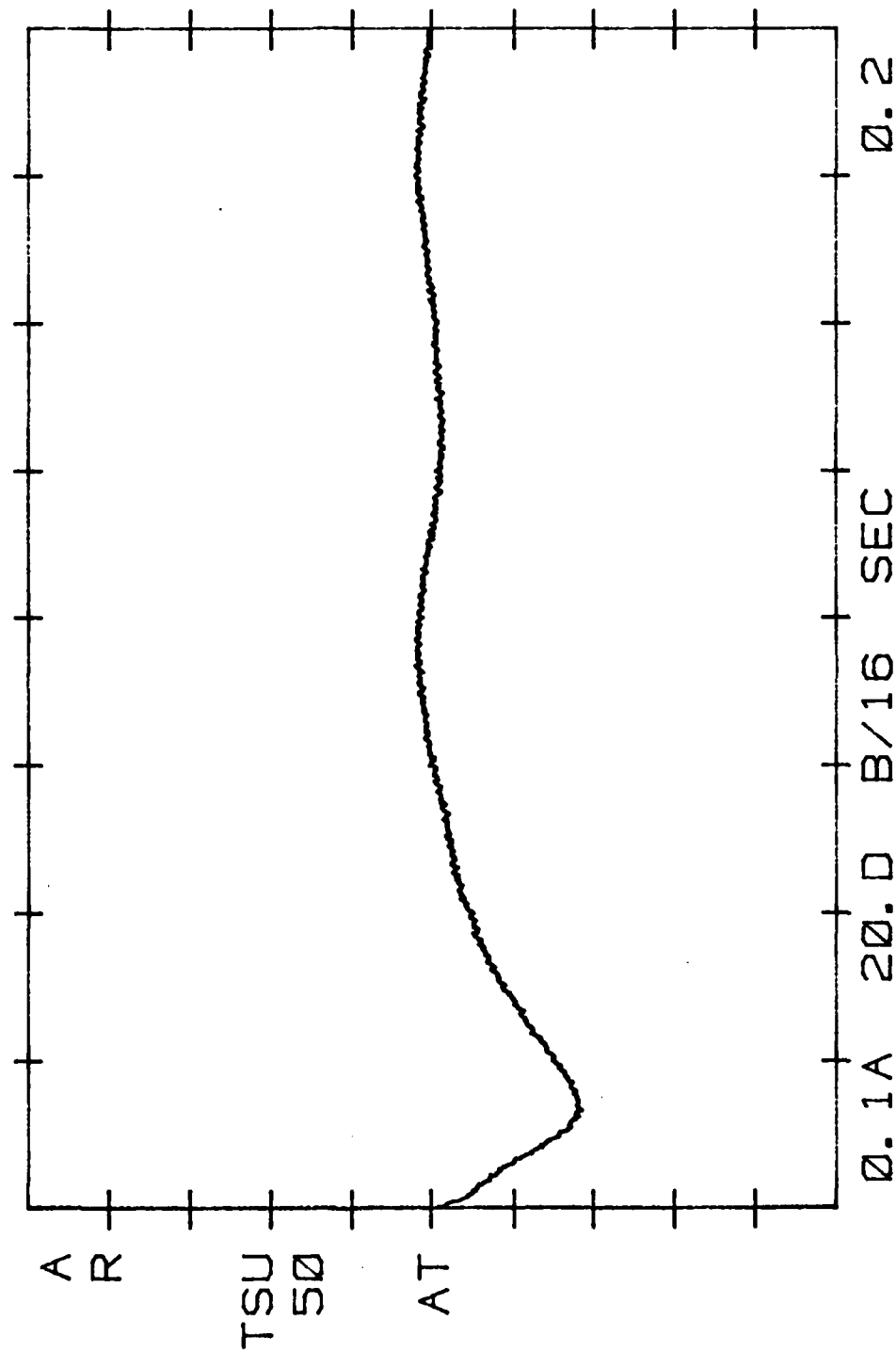
RICKY   MEG.062 LT-FR-NEW LIGHT-OFF
10CPS AND NOTCH FILTERS 2.54-03 V   VLN
20-OCT-83 STROBE   T
           0.01758 SEC

A
R

TSU
50

AT

0.2   20.D B/16 SEC   0.2
0.1A   20.D
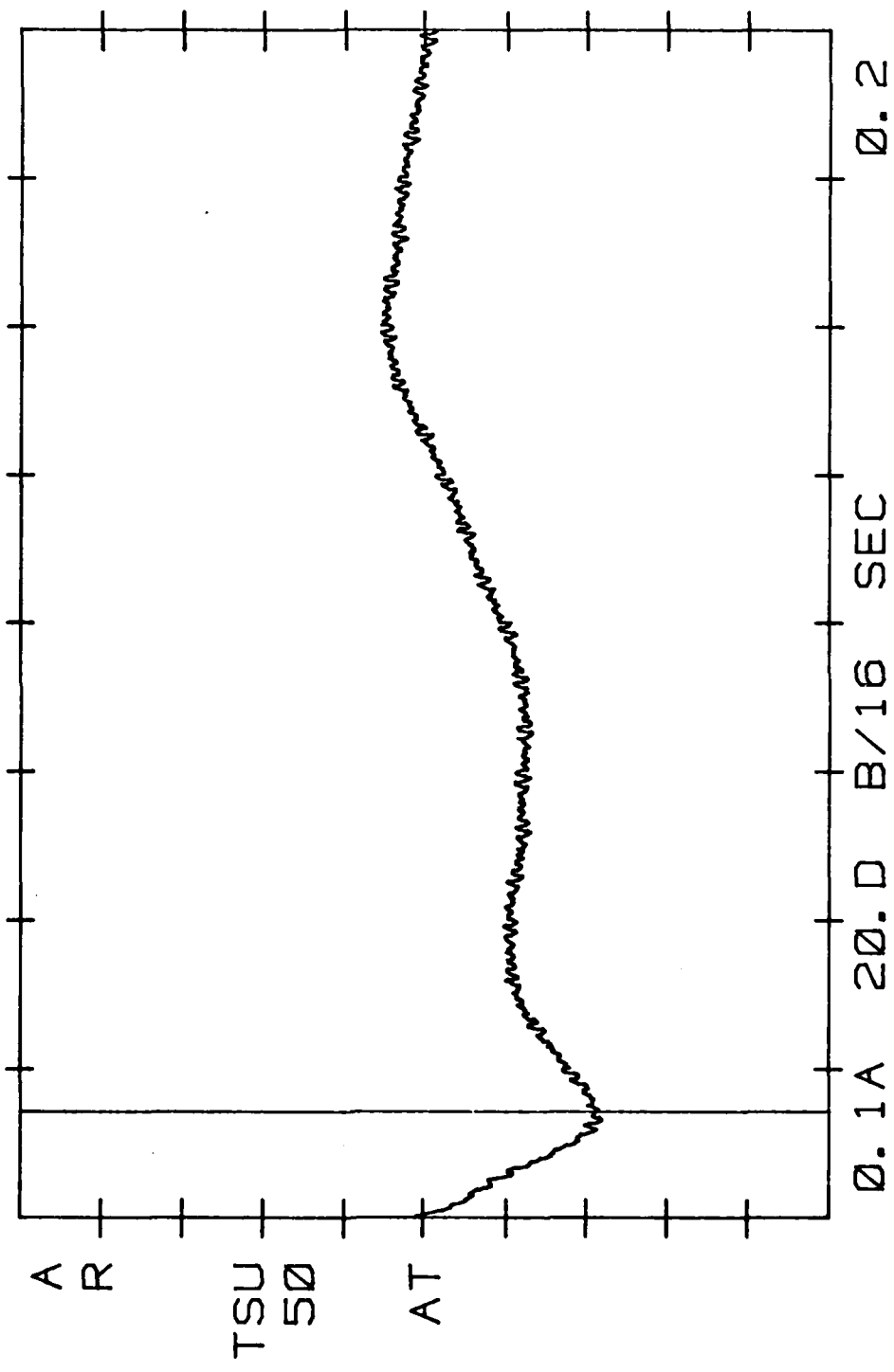
RICKY   MEG.062 LT-FR-NEW LIGHT-OFF
10CPS AND NOTCH FILTERS 121.-06 V   VLN
20-OCT-83 STROBE   T
             0.00000 SEC

A
R
TSU
50
AT

0.1A   20.D B/16 SEC   0.2

0.2
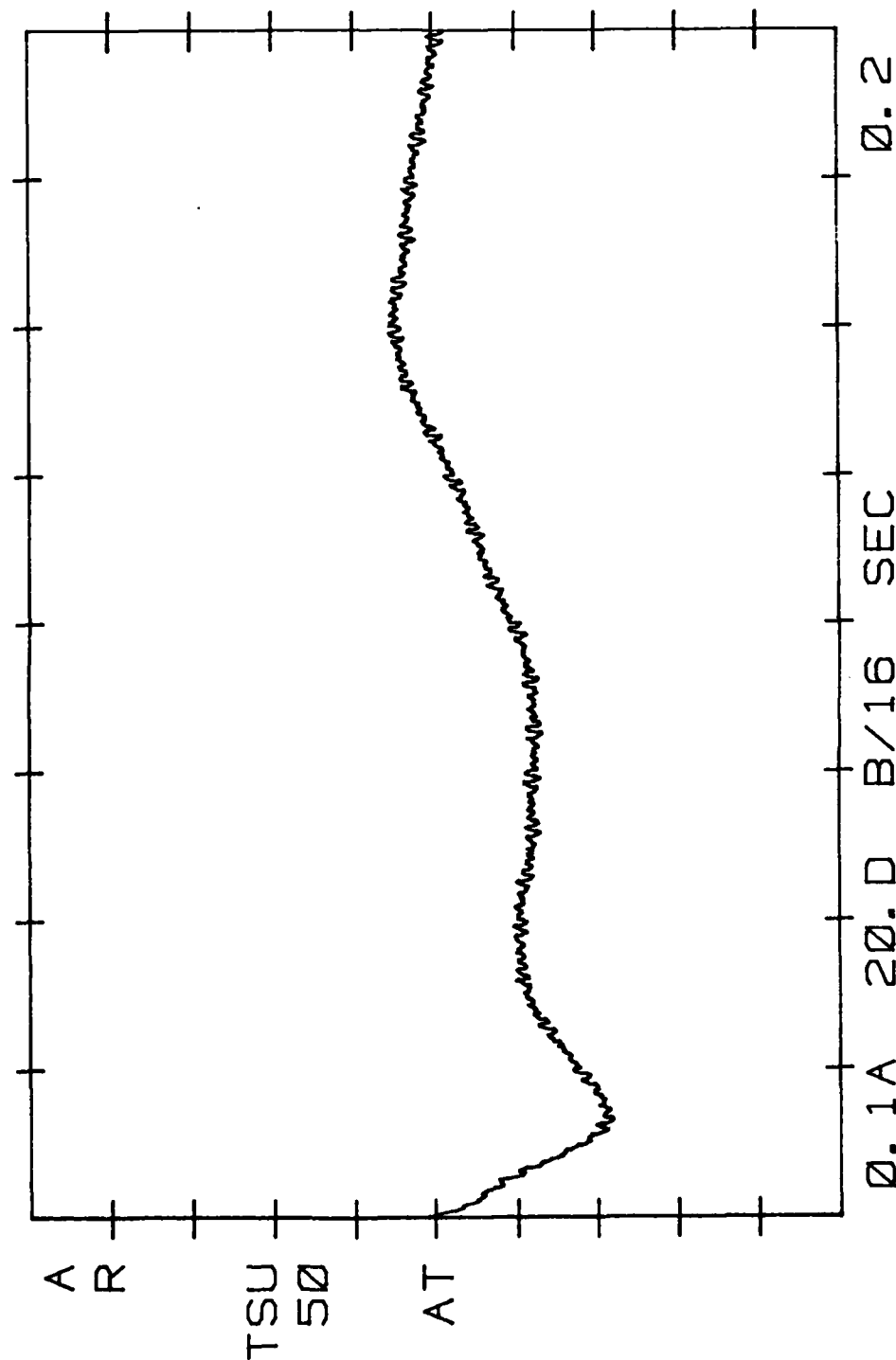
RICKY MEG.063 LT-OC-NEW LIGHT-OFF
10CPS AND NOTCH FILTERS 3.79-03 V VLN
20-OCT-83 STROBE 0.01680 SEC

A
R

TSU
50

AT

0.1A   20.0 B/16 SEC   0.2
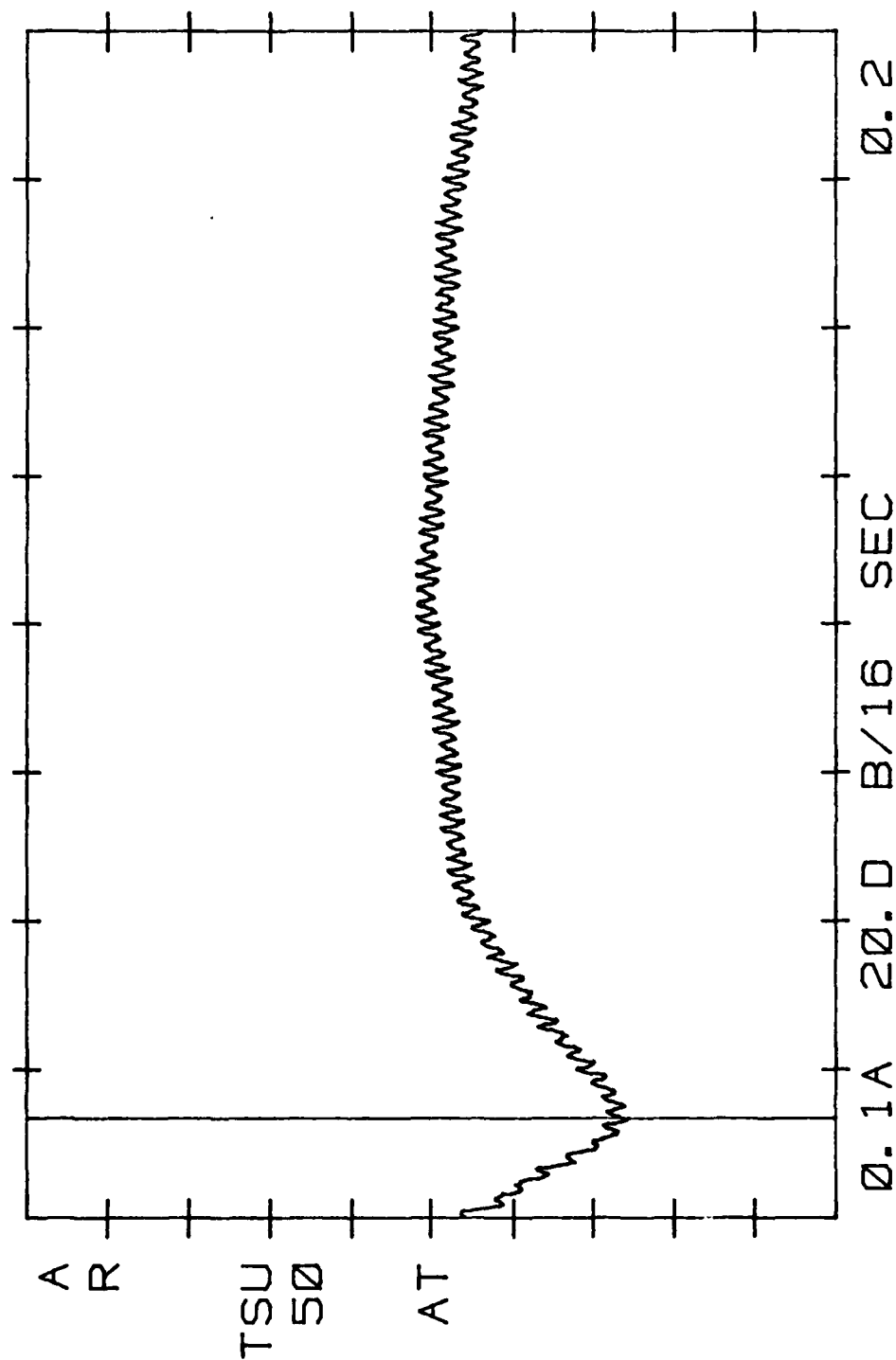
RICKY MEG.063 LT-OC-NEW LIGHT-OFF
10CPS AND NOTCH FILTERS_626.-06 V VLN
20-OCT-83 STROBE 0.00000 SEC T
0.00000 SEC

A
R

TSU
50

AT

0.1A 20.D B/16 SEC 0.2
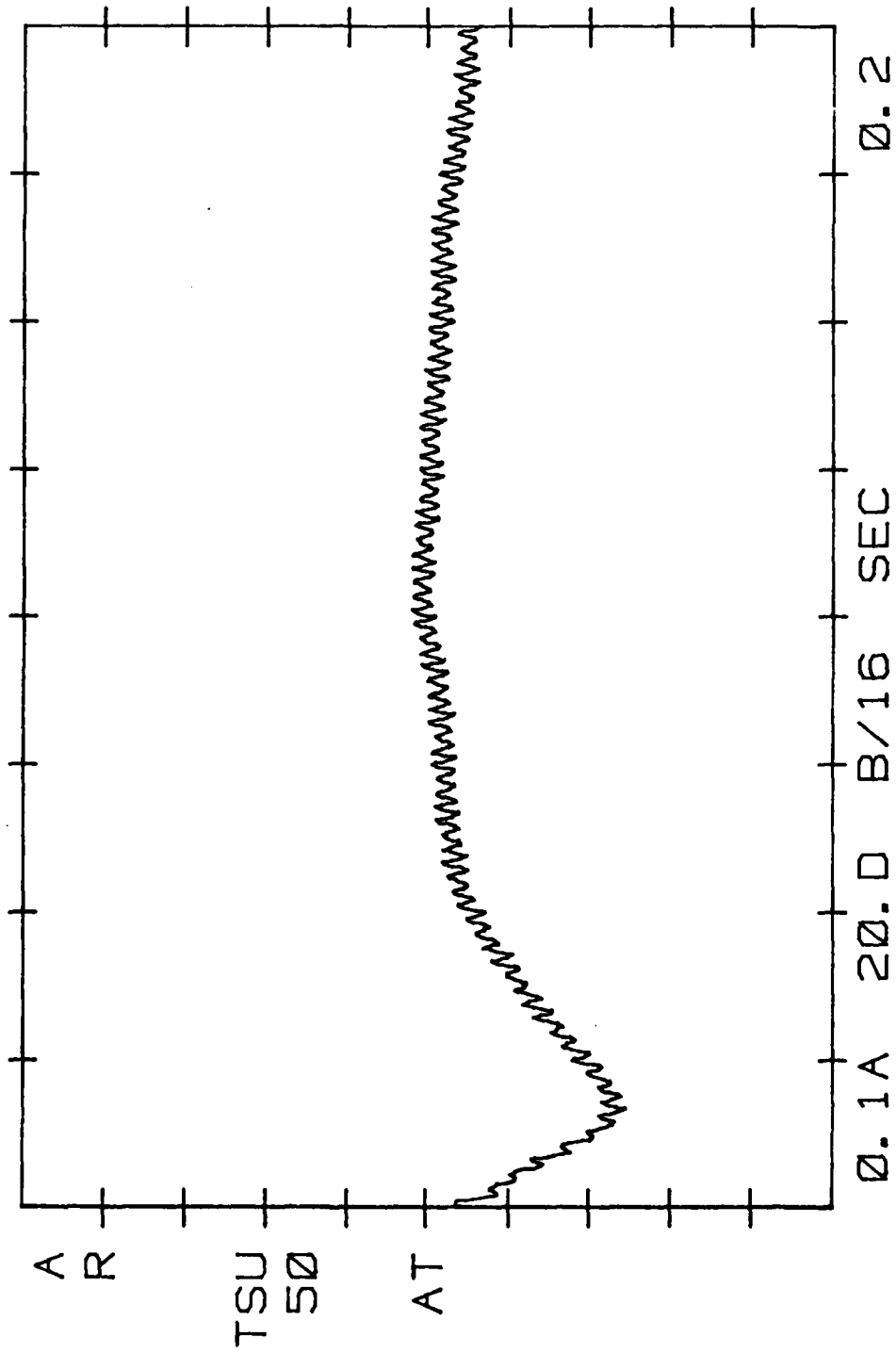
APPENDIX E

DOG AUDITORY EVOKED RESPONSE PLOTS

DOG AUDITORY EVOKED RESPONSES

On the last day we collected data from Ricky, the laboratory beagle, we were able to setup an auditory evoked response (AER) experiment. We used two signal generators and a pseudo-random noise generator to generate a short tone at random interstimulus intervals. This tone was coupled to the dog with air filled earphones. The rest of the setup was the same as for the visual evoked response experiment, that is, the SQUID gradiometer was positioned at different locations over the beagles head too get the best response. The output of the SQUID gradiometer was once again sent to the Nicolet 660B FFT Analyzer, so that, 50 trails could be averaged. That average was then sent out of the Nicolet 660B FFT Analyzer to an Intel 80/20 computer so that it could be stored on a 8 inch disk.

Figure E-1 shows an auditory evoked response taken from a human by electroencephalographic means, as compared to an auditory evoked response taken from a human by magnetoencephalographic means, which is shown in Figure E-2. In my literature search, I was unable to find an auditory evoked response for a dog which had been taken by electroencephalographic means, but was able to find an auditory evoked response for a cat which had been taken by electroencephalographic means. This auditory evoked response of the cat is shown in Figure E-3. The cat's brain is

physically smaller than the brain of a beagle, so I would expect the latencies measured from the cat to be shorter than the latencies we would measure from the beagle. The plots MEG.066 thru MEG.071, which are at the end of this appendix, shows the auditory evoked responses taken from the beagle by magnetoencephalographic means.

LATE AUDITORY EVOKED RESPONSE
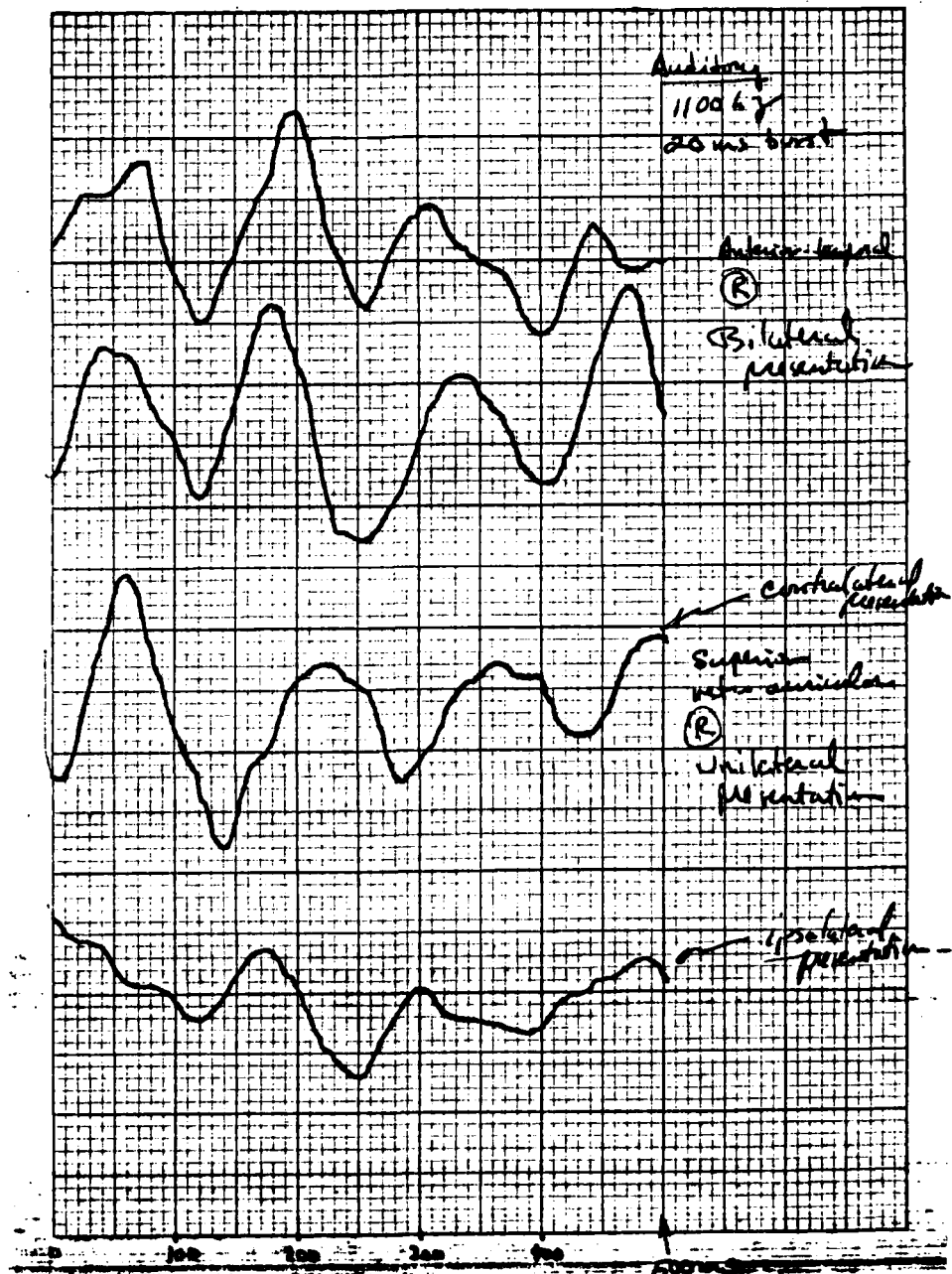
PROCESSING IN PRIMARY AUDITORY PROJECTION AREAS
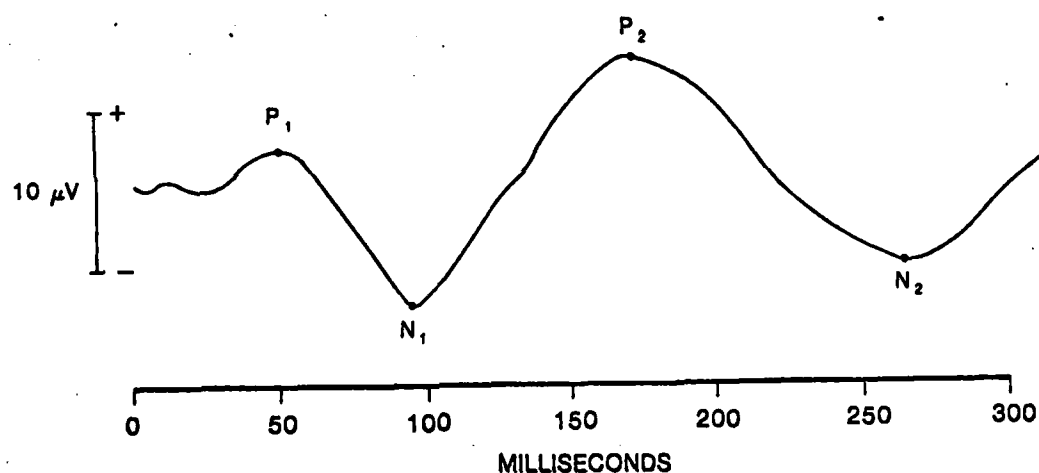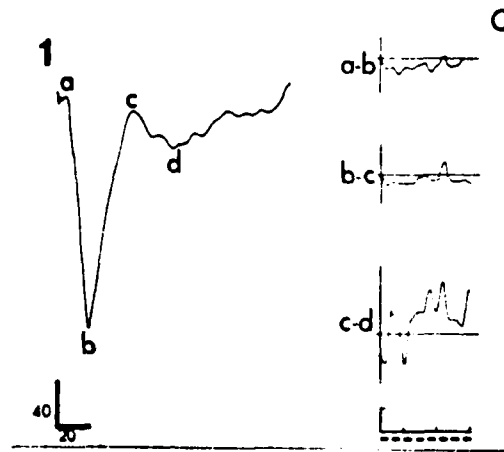

FROM: BRADFORD, 1975

HE-76-2-12

FIGURE E-1

HUMAN ELECTROENCEPHALOHRAPHIC AUDITORY EVOKED RESPONSE

FIGURE E-2

HUMAN MAGNETOENCEPHALOGRAPHIC AUDITORY EVOKED RESPONSE

## FIGURE E-3

CAT'S ELECTROENCEPHALOGRAPHIC AUDITORY EVOKED RESPONSE

In the case of the human auditory evoked response data, we see that both the electroencephalographic auditory evoked response and the magnetoencephalographic auditory evoked response have peaks at latencies of approximately 50 milliseconds and 180 milliseconds.
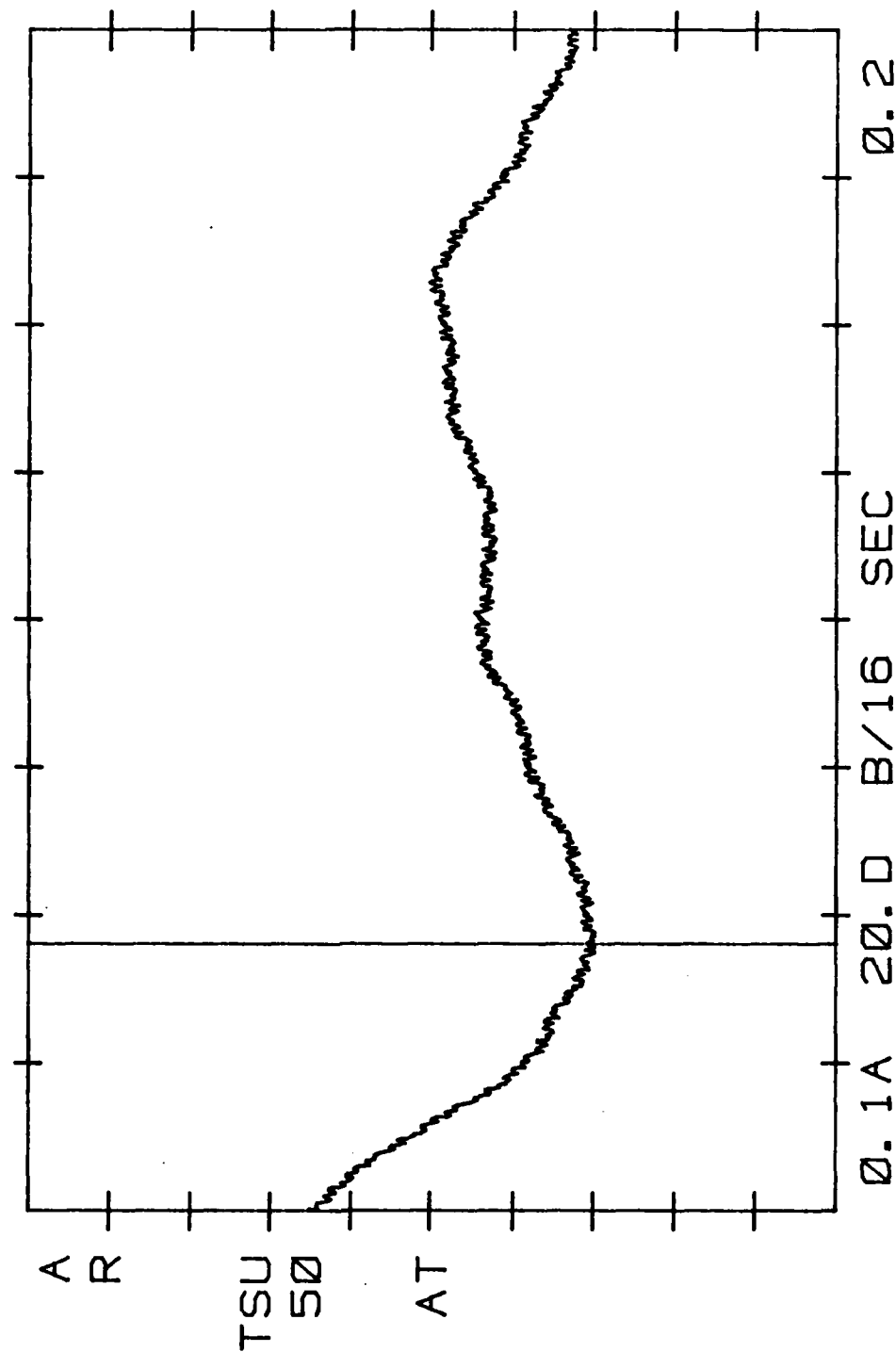
For the cat versus the beagle case, we first see that the cat has a negative going waveform during the first 20 milliseconds of its response. As expected, the beagles waveform is going negative out to 40 milliseconds.

RICKY   MEG.064 LT-OC   LIGHT-OFF
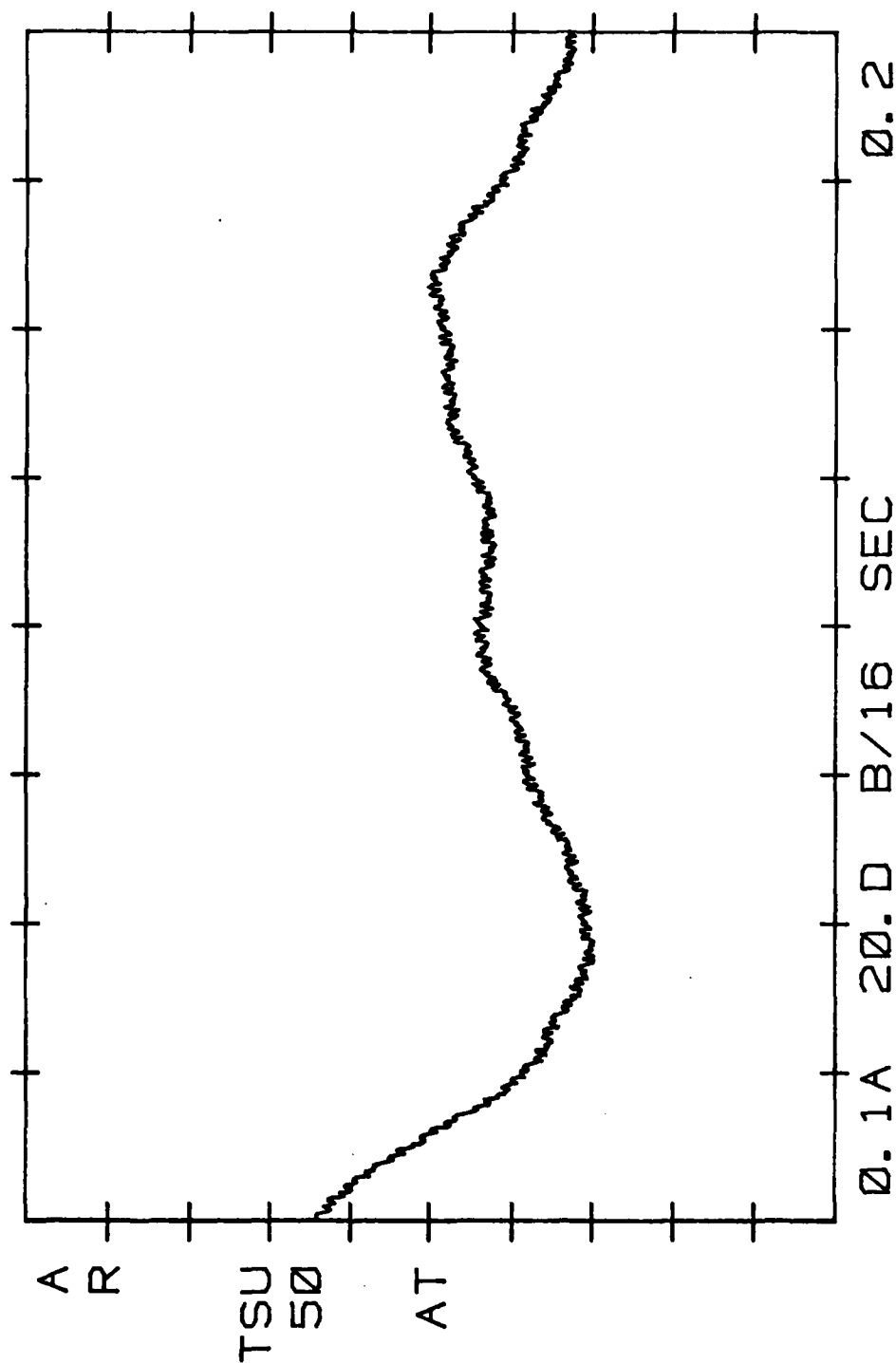10CPS AND NOTCH FILTERS 2.00-03 V VLN
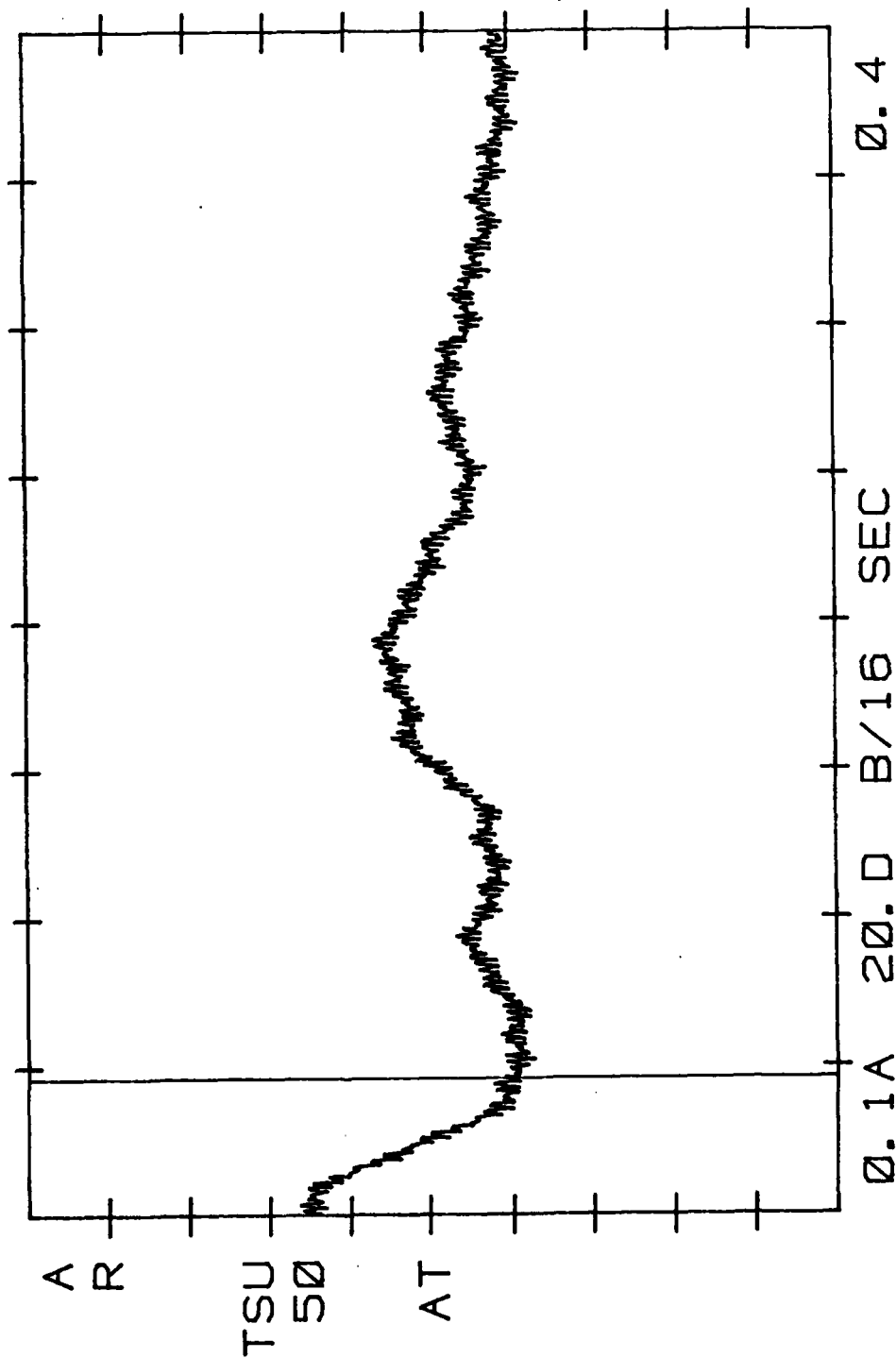20-OCT-83 AUDIO 2K   T

A
R

TSU
50

AT

0.1A   20.0   20.D B/16 SEC   0.2
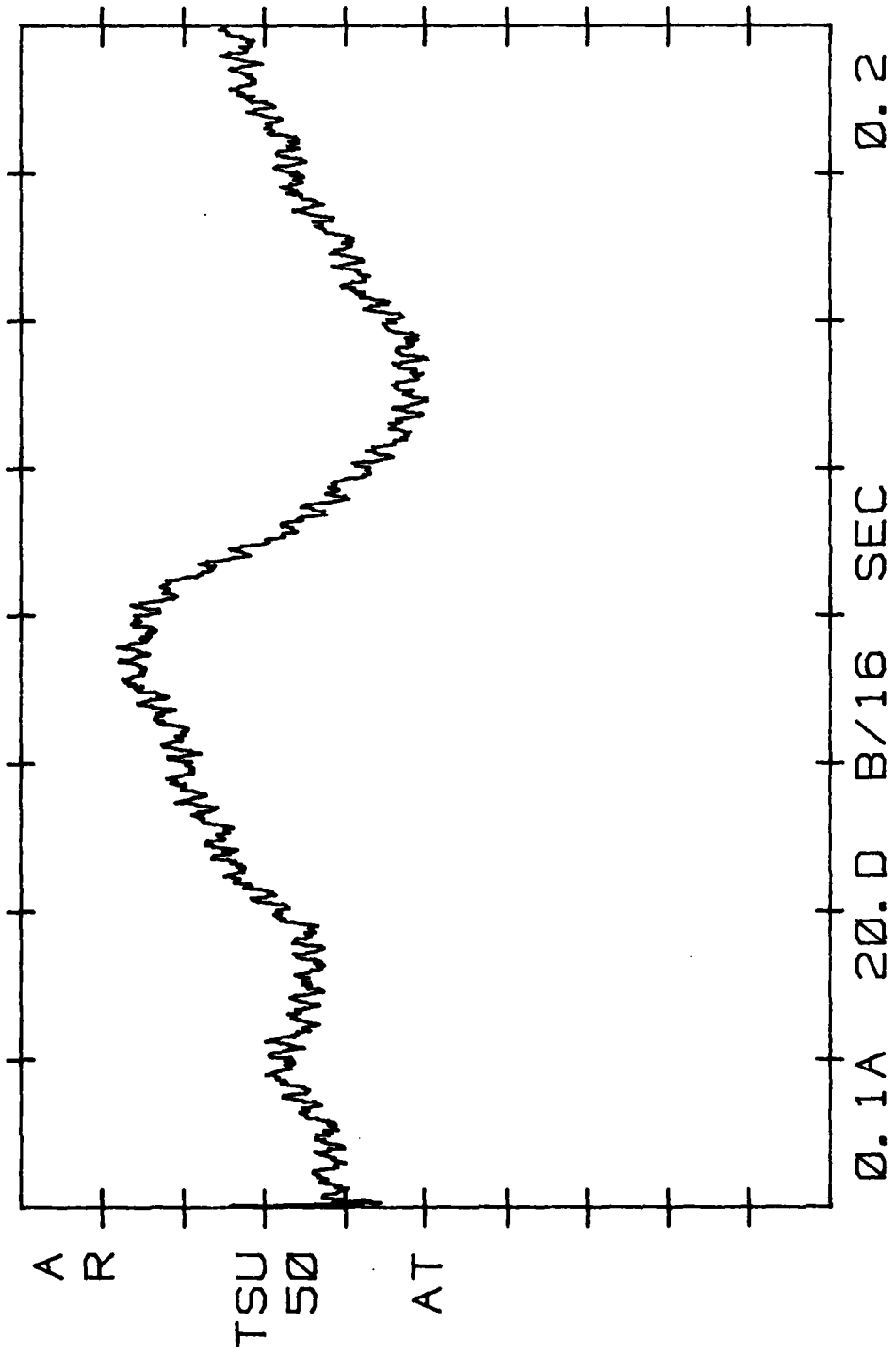
RICKY MEG.065 LT-LAT-NEW LIGHT-OFF
10CPS AND NOTCH FILTERS 2.30-03 V VLN
20-OCT-83 AUDIO 2k V T
0.04512 SEC

A
R

TSU
50

AT

0.1A 20.0 B/16 SEC 0.2

0.2

RICKY MEG.065 LT-LAT-NEW LIGHT-OFF
10CPS AND NOTCH FILTERS 2K 1.81-03 V VLN
20-OCT-83 AUDIO SEC T
0.00000 SEC

A
R

TSU
50

AT

0.1A 20.D B/16 SEC 0.2

0.2

RICKY   MEG.066   LT-LAT-SAME LIGHT-OFF
10CPS AND NOTCH FILTERS 729.-06 V   VLN
20-OCT-83   AUDIO 2k   T
          0.04570 SEC

A
R

TSU
50

AT

0.1A   20.D   B/16 SEC   0.4

E-9

RICKY MEG.066 LT-LAT-SAME LIGHT-OFF
10CPS AND NOTCH FILTERS 1.19-03 V VLN
20-OCT-83 AUDIO 2k V T
0.00000 SEC

A
R

TSU
50

AT

0.1A 20.D B/16 SEC 0.4

RICKY   MEG.067   RT-LAT-NEW   LIGHT-OFF
10CPS AND NOTCH FILTERS 373.-06 V   VLN
20-OCT-83 AUDIO 2k   T
0.04609 SEC

A
R

TSU
50

AT

0.1A   20.0   B/16   SEC

0.4
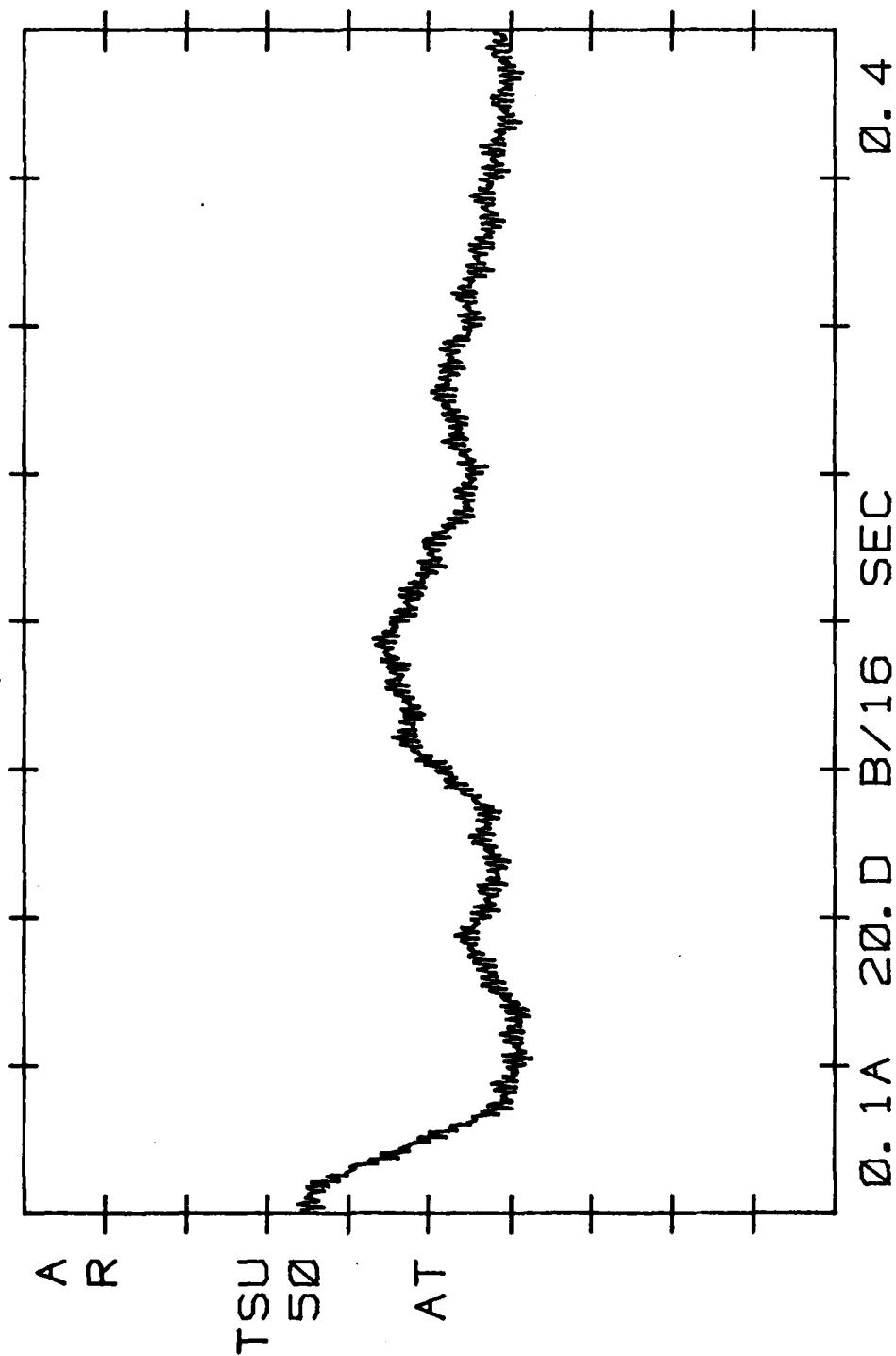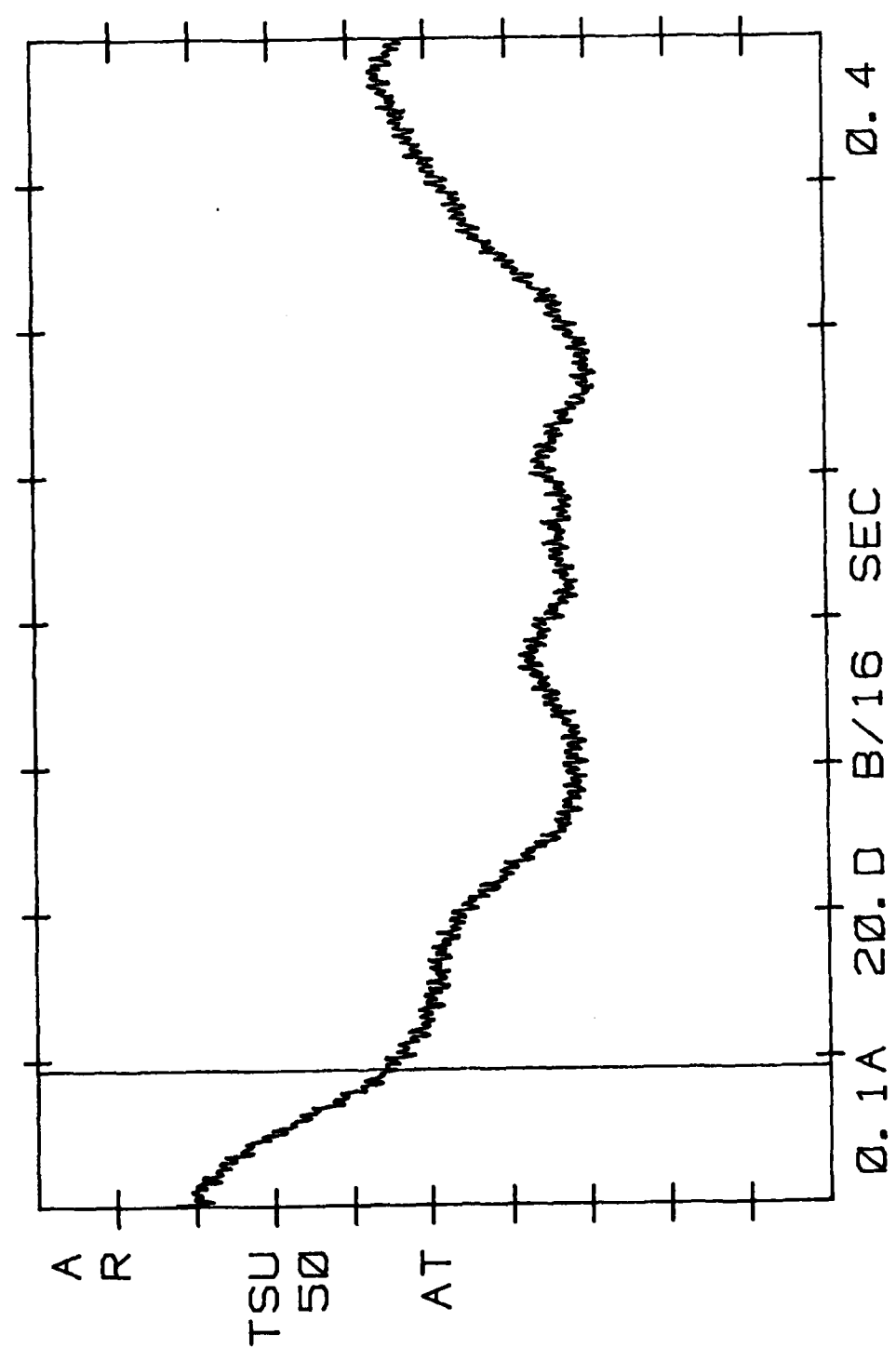
RICKY   MEG.067   RT-LAT-NEW   LIGHT-OFF
10CPS AND NOTCH FILTERS 2.59-03 V   VLN
20-OCT-83   AUDIO 2k   V   T
             0.00000 SEC

A
R
TSU
50
AT

0.1A   20.0   B/16   SEC
0.4   20.0   B/16   SEC
                      0.4
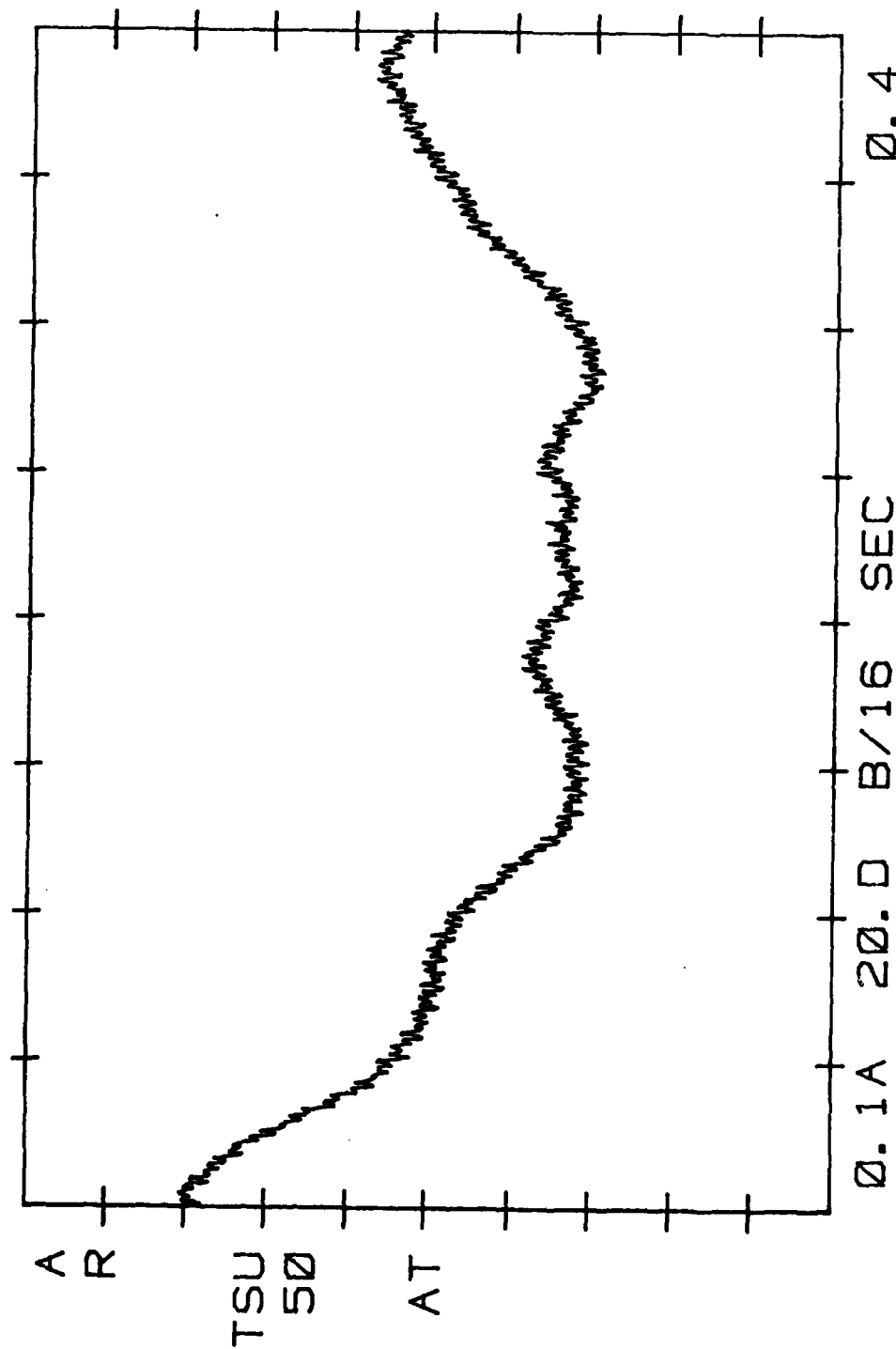
RICKY MEG.068 RT-LAT-SAME LIGHT-OFF
10CPS AND NOTCH FILTERS 1.80-03 V VLN
20-OCT-83 AUDIO 2k T
0.04688 SEC

A
R

TSU
50

AT

0.1A 20.0 20.D B/16 SEC 2

E-13
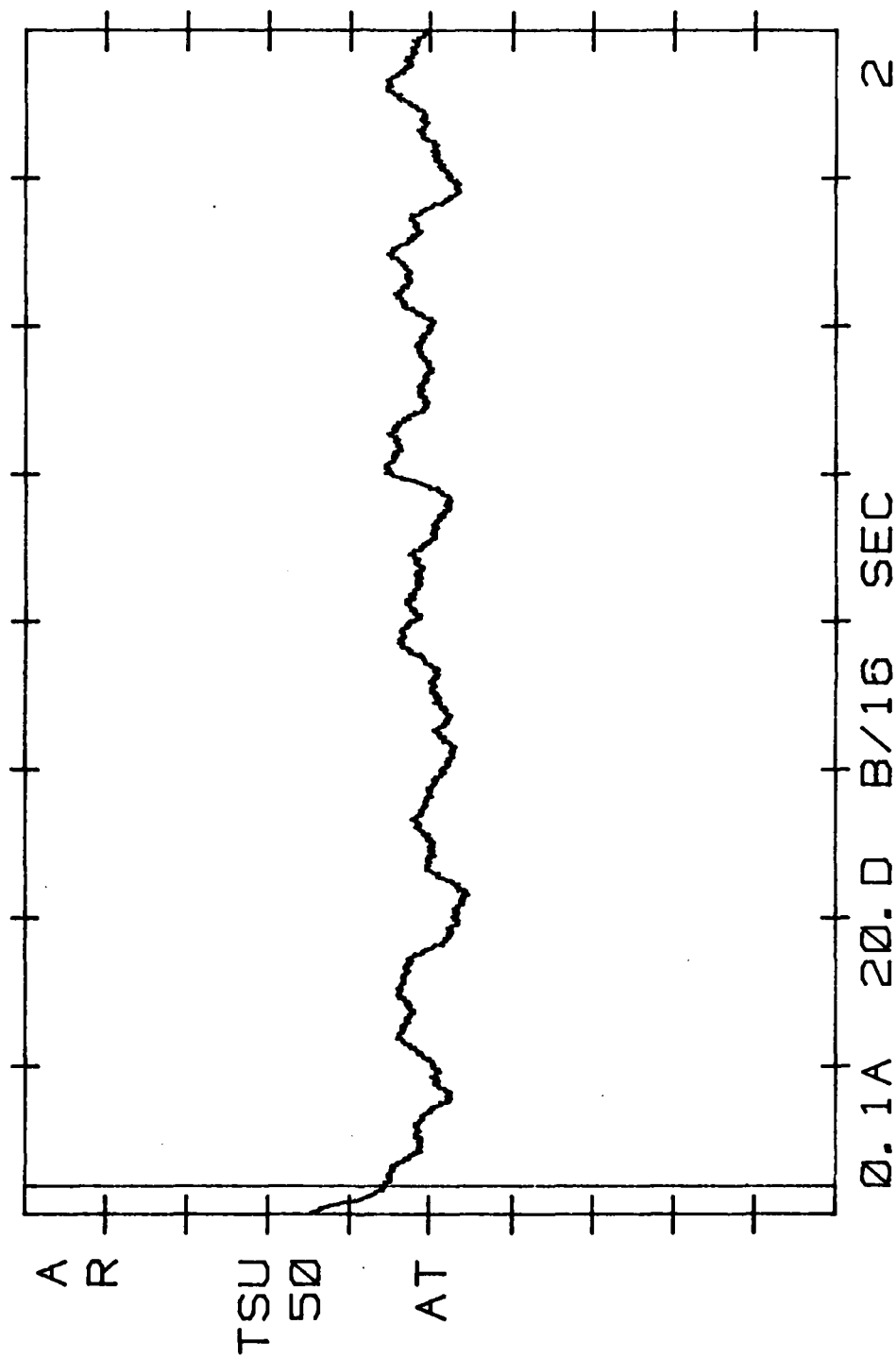
RICKY   MEG.068   RT-LAT-SAME LIGHT-OFF
CPS AND NOTCH FILTERS 4.27-03 V   VLN
20-OCT-83   AUDIO 2k   T
0.00000 SEC
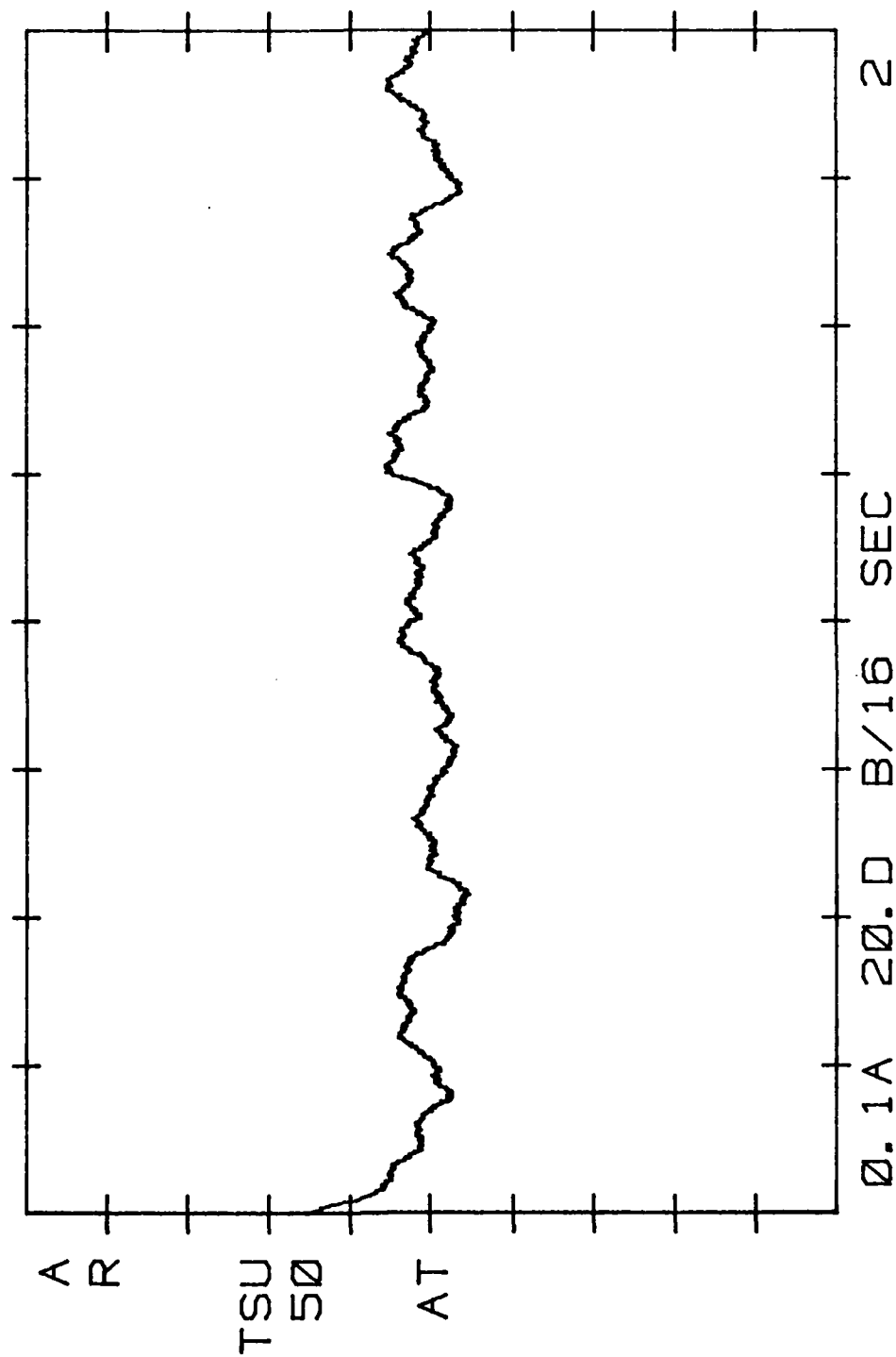
A
R

TSU
50

AT

0.1A   20.0   20.0 B/16 SEC   2

RICKY   MEG.069   RT-LAT-SAME LIGHT-OFF
10 CPS AND NOTCH FILTERS -749.-06 V   VLN
20-OCT-83 AUDIO 2k   T
           0.04297 SEC

A
R

TSU
50

AT

0.1A   20.0 B/16 SEC   2

RICKY   MEG.069   RT-LAT-SAME LIGHT-OFF
10CPS AND NOTCH FILTERS 1.66-03 V   VLN
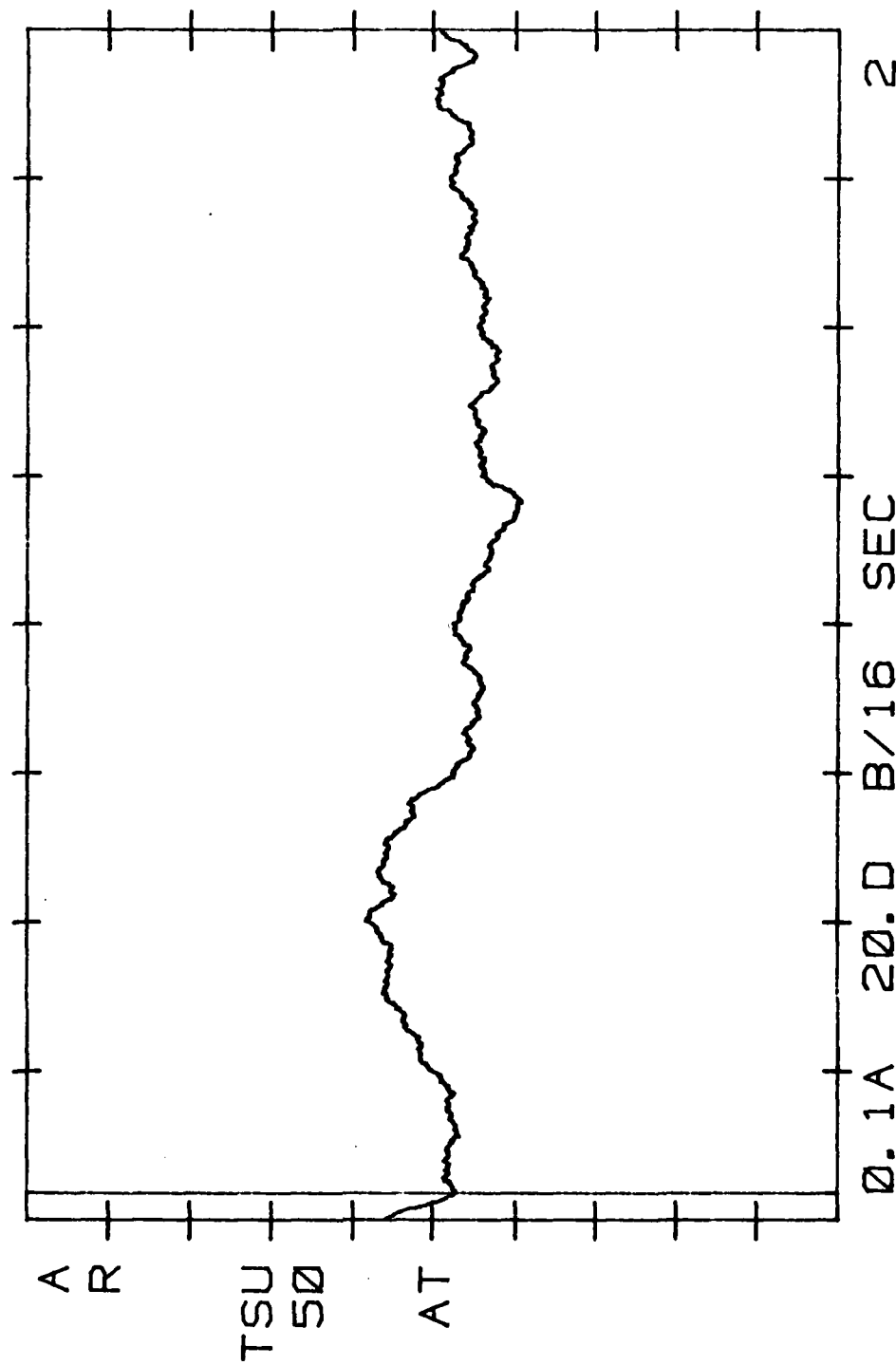20-OCT-83   AUDIO 2k   T
            0.00000 SEC

0.1A   20.D   B/16   SEC   2
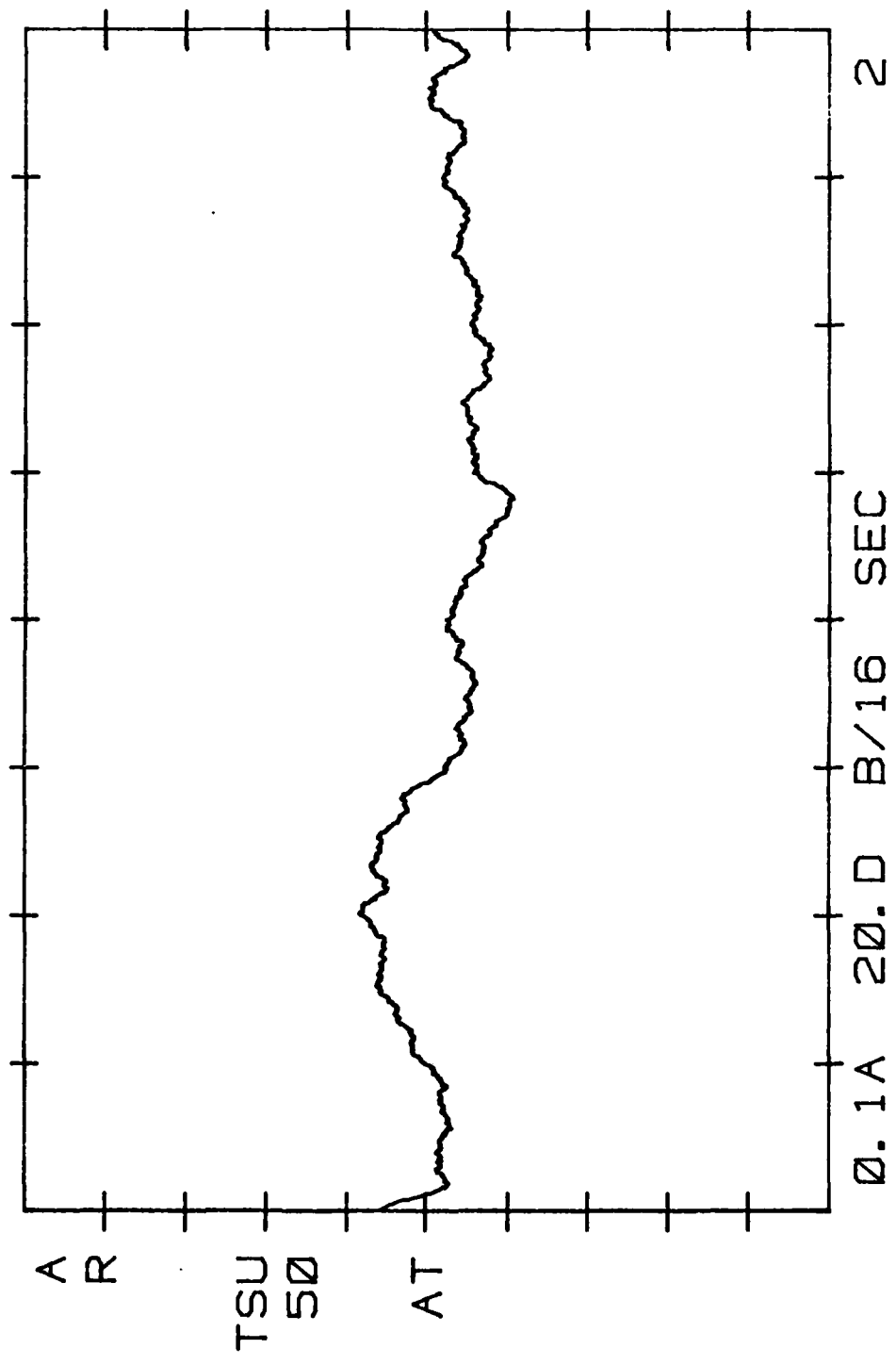
RICKY   MEG.070 RT-LAT-SAME LIGHT-OFF
10CPS AND NOTCH FILTERS 15.0-03 V VLN
20-OCT-83 AUDIO 2k T

A
R

TSU
50

AT

0.1A   20.D   B/16 SEC
0.04
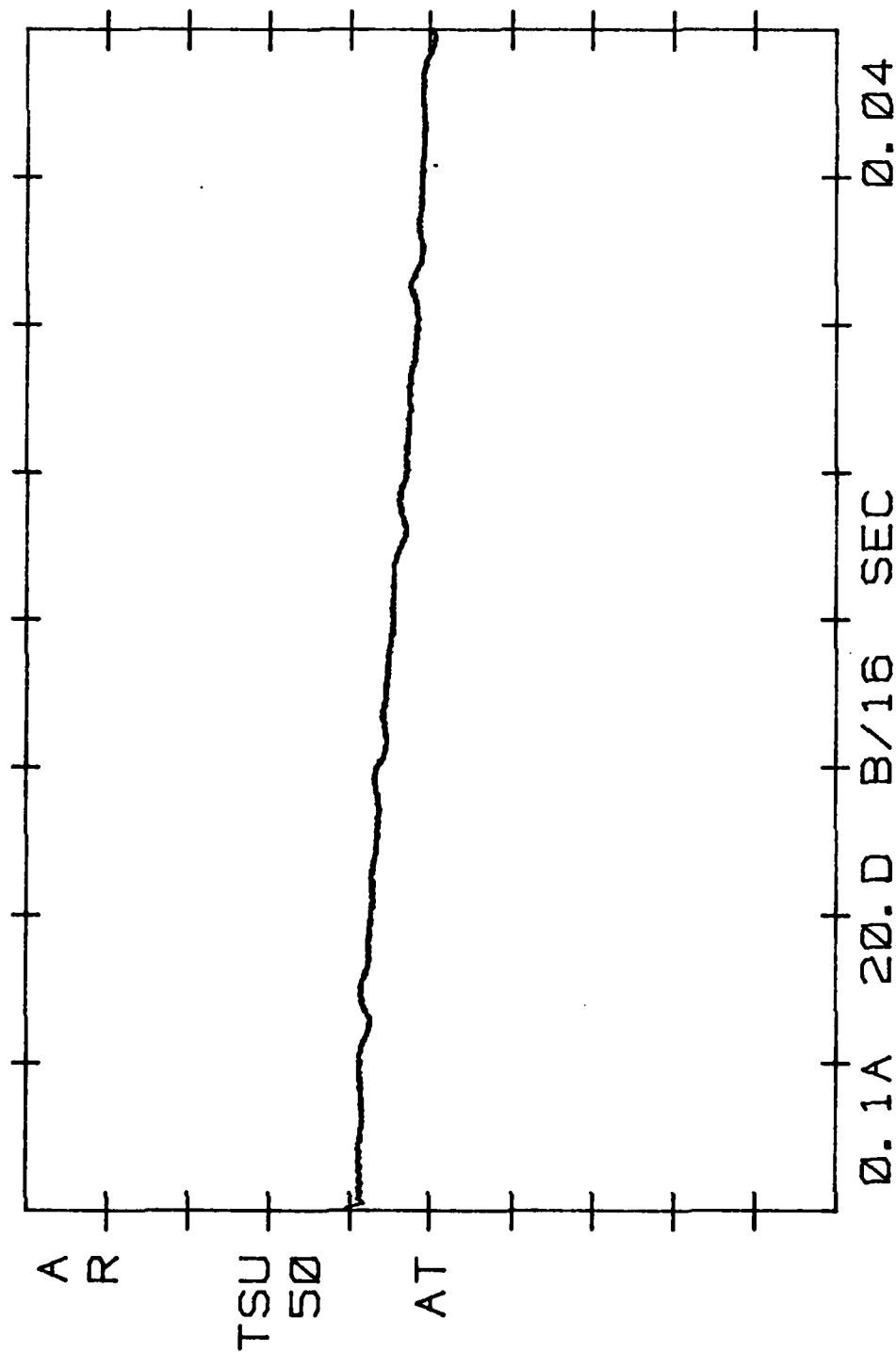
RICKY-BR MEG.071 RT-LAT-SAME LIGHT-OFF
10CPS AND NOTCH FILTERS 1.6D-03 V VLN
20-OCT-83 AUDIO 2k T
0.00000 SEC

A
R

TSU
50

AT

0.1A   20.D   B/16 SEC
        2

E-18
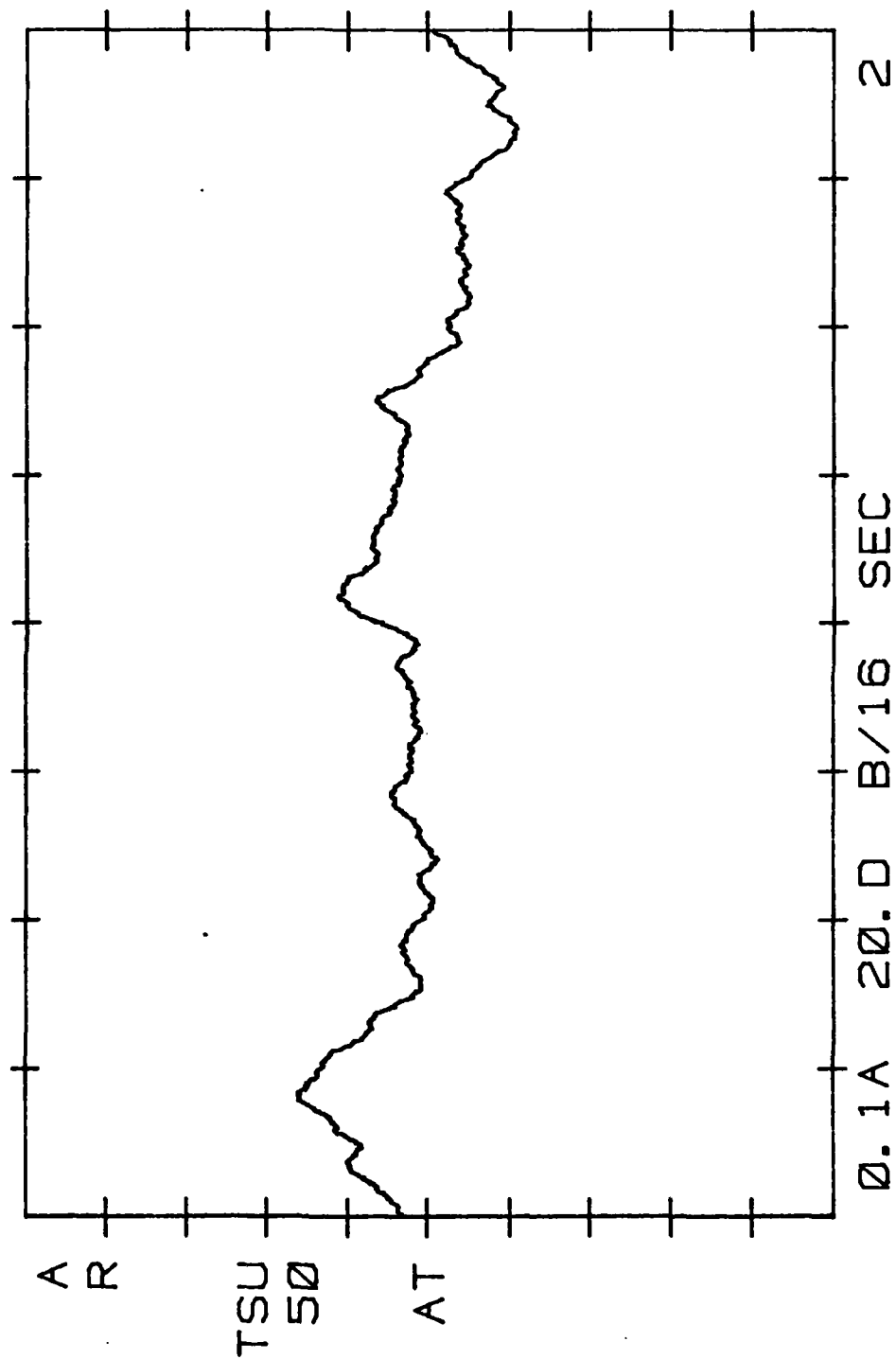
VITA

Robert D. Murray was born the son of Meredith N. and Emma F. Murray on 7 June 1952 in Elyria, Ohio. He graduated from West High School in Cleveland, Ohio in 1970. After one year at Hope College in Holland, Michigan, he entered the United States Air Force. He worked as a Computer Repairman in the Combat Headquarters of NORAD in Colorado Springs, Colorado until his selection for the Airmen's Educational and Commissioning Program in 1973. He received the degree Bachelor of Science in Electrical Engineering from the University of Arizona, Tucson, Arizona in 1975. After receiving his commission from Officer Training School in April 1976, he went to Navigator School where he earn his navigator's wings in January of 1977. From Navigator School he went to Navigator Bombardier Training (NBT), still at Sacremento, California. After NBT, he went to F-4 RTU at MacDill AFB, Florida. In the next four years, he flew as a Weapons Systems Officer in F-4D and E models at Eglin AFB, Florida, Osan AB, Korea, Nellis AFB, Nevada, and Seymour-Johnson AFB, North Carolina. At Osan AB and Nellis AFB, he was Squadron Plans Officer. At Seymour-Johnson AFB, he was Assistant Chief of Squadron Computer Operations, Assistant Chief of Squadron Standardization and Evaluation Shop, and Chief of Squadron Training for the Digital Modular Avionics System (DMAS). He entered the School of Engineering, Air Force Institute of Technology in June 1982.

Permanent Address: 1144 Oakhill Ave.

Fairborn, Ohio 45324

REPORT DOCUMENTATION PAGE

1a. REPORT SECURITY CLASSIFICATION UNCLASSIFIED	1b. RESTRICTIVE MARKINGS
2a. SECURITY CLASSIFICATION AUTHORITY	3. DISTRIBUTION/AVAILABILITY OF REPORT
2b. DECLASSIFICATION/DOWNGRADING SCHEDULE	Approved for public release; distribution unlimited

4. PERFORMING ORGANIZATION REPORT NUMBER(S) AFIT/GE/EE/83D-50	5. MONITORING ORGANIZATION REPORT NUMBER(S)

6a. NAME OF PERFORMING ORGANIZATION School of Engineering	6b. OFFICE SYMBOL (If applicable) AFIT/ENG	7a. NAME OF MONITORING ORGANIZATION

6c. ADDRESS (City, State and ZIP Code) Air Force Institute of Technology Wright-Patterson AFB, Ohio 45433	7b. ADDRESS (City, State and ZIP Code)

8a. NAME OF FUNDING/SPONSORING ORGANIZATION	8b. OFFICE SYMBOL (If applicable)	9. PROCUREMENT INSTRUMENT IDENTIFICATION NUMBER

8c. ADDRESS (City, State and ZIP Code)	10. SOURCE OF FUNDING NOS.			
	PROGRAM ELEMENT NO.	PROJECT NO.	TASK NO.	WORK UNIT NO.

11. TITLE (Include Security Classification) See Box 19

12. PERSONAL AUTHOR(S) Robert D. Murray, B.S., Capt, USAF

13a. TYPE OF REPORT MS Thesis	13b. TIME COVERED FROM _____ TO _____	14. DATE OF REPORT (Yr., Mo., Day) 1983 December	15. PAGE COUNT 169

16. SUPPLEMENTARY NOTATION

Approved for public release: IAW AFR 190-17.

LYNN E. WOLAVER
Dean for Research and Professional Development
Air Force Institute of Technology (ATC)
Wright-Patterson AFB OH 45433

7 Feb 84

17. COSATI CODES			18. SUBJECT TERMS (Continue on reverse if necessary and identify by block number)
FIELD	GROUP	SUB. GR.	SQUID gradiometer, magnetometer, electromagnetics, brain, visual evoked response, superconductivity, magnetoencephalogram
20	03		
08	14		

19. ABSTRACT (Continue on reverse if necessary and identify by block number)

Title: The Application of a Superconducting Quantum Interference Device Second-Order Gradiometer to Measure Visual Evoked Responses

Thesis Chairman: Charles P. Hatsell, Lt. Col., USAF

20. DISTRIBUTION/AVAILABILITY OF ABSTRACT UNCLASSIFIED/UNLIMITED ☒ SAME AS RPT. ☐ DTIC USERS ☐	21. ABSTRACT SECURITY CLASSIFICATION UNCLASSIFIED	
22a. NAME OF RESPONSIBLE INDIVIDUAL Charles P. Hatsell, Lt. Col., USAF	22b. TELEPHONE NUMBER (Include Area Code) (513) 255-4649	22c. OFFICE SYMBOL AMRL/CV

DD FORM 1473, 83 APR   EDITION OF 1 JAN 73 IS OBSOLETE

        The acquisition of a Superconducting Quantum
Interference Device (SQUID) gradiometer by the Air
Force Aerospace Medical Research Laboratory, along
with the previous research conducted   at the Air
Force Institute of Technology which led to the
first   cortical   implant   of   a   multiplexed
multi-electrode semiconductor   brain   electrode,
motivated   the   use   of   the   SQUID second-order
gradiometer   to measure visual evoked responses
(VER) from humans, and from the canine which had
previously had the AFIT brain electrode implanted
and removed. Some discussion of the current dipole
model for the fields measured from the brain is
presented.   The   human   visual   evoked   responses
picked up by gradiometer were compared to previous
human   electroencephalograph   visual   evoked
responses,   and   were   found   to   have   similar
latencies.   The   canine   visual   evoked   responses
which were measured by the gradiometer had similar
initial waveform and latencies, but then dampen
out more rapidly than the waveforms measured by
the AFIT brain chip. Conclusions about the use of
a SQUID gradiometer   in measuring visual evoked
reponses, along with comparisons been the EEG and
AFIT brain chip data versus the SQUID data is
discussed.   Recommendations for further research
with the SQUID gradiometer by itself, and it in
conjuction with the AFIT brain chip are discussed.

FILM
4-8